Modulation of ageing characteristics with an anti-ageing compound

Nicola Hall

Hertford College

University of Oxford

A thesis submitted for the degree of

Doctor of Philosophy

Trinity Term 2016

Abstract

Modulation of ageing characteristics with an anti-ageing compound

Nicola Hall, Hertford College Submitted for the degree of D.Phil, Trinity Term 2016

Investigating the cellular processes anti-ageing compounds interact with can identify genes and pathways involved in ageing. The macrolide lactone FK506 was identified in a phenotypic screen as extending lifespan in yeast and *C. elegans* through an unknown mechanism. FK506 also ameliorates neurodegeneration and age-related weight gain in rodents. Here, the mechanism of action of FK506 has been investigated in two experimental systems: *C. elegans* and 3T3-L1 mouse adipocytes.

As the general mechanisms of ageing are well conserved between *C. elegans* and mammals, *C. elegans* has been used to understand how FK506 acts at an organismal level. Firstly, the result of the phenotypic screen was confirmed. FK506 treatment induced lifespan extension in *C. elegans* in the presence of population crowding stress, but not in the absence of crowding. FK506 treatment inhibited neither *E. coli* OP50 growth nor *C. elegans* pharyngeal pumping, demonstrating that FK506 did not induce dietary restriction to extend lifespan. FK506 treatment increased *C. elegans* thrashing and pharynx pumping rates in early adulthood and delayed accumulation of gut bacteria, showing that FK506 extended healthspan. A transcriptome analysis of FK506-treated *C. elegans* allowed the identification of transcripts whose levels change and potential pathways by which FK506 manifests its effect. To explore this and to identify potential targets of FK506, the cellular functions required for FK506 to extend *C. elegans* lifespan and healthspan were investigated using RNA-seq, RNAi, genetic mutation and co-treatment with small molecule inhibitors and inducers. Interestingly, FK506 was found to have different mechanisms of action on lifespan and healthspan. The mechanism of FK506 on *C. elegans* thrashing rate was DAF-16 dependent, did not require population crowding stress, had a partial interaction with FUdR and autophagy, and may involve Ca^{2+} flux. The mechanism of FK506-induced *C. elegans* lifespan extension overlapped with dietary restriction and was dependent on calcineurin, TOR-independent regulation of autophagy and the presence of population crowding stress.

FK506 may modulate body weight by influencing metabolism and/or acting on adipocytes directly. FK506-treated aged 3T3-L1 adipocytes accumulated significantly less lipid, indicating that FK506 acts directly on adipocytes. RNA-seq of FK506-treated adipocytes found that translation-associated RNAs were upregulated whilst RNAs associated with lipid metabolism were downregulated. An ER-localised FK506-binding protein was up regulated in both *C. elegans* and 3T3-L1 adipocytes, *fkb-4* and Fkbp2 respectively.

In conclusion, FK506 has been confirmed as a potential anti-ageing treatment, through its ability to extend lifespan and healthspan in *C. elegans*. In addition, FK506 has also been shown to act directly on mouse adipocytes, resulting in a reduction in lipid accumulation. This action could explain how FK506 caused weight loss in obese aged rats, restoring body mass to a healthy adult weight.

Acknowledgements

Firstly, I would like to thank my supervisor, Prof. Jane Mellor, for giving me the opportunity to work in her lab and for all the help and guidance she has given me. I would also like to thank our collaborator, Dr. Katja Dettmer-Wilde in the lab of Prof. Peter Oefner, and also Dr. Harry Fischl, Dr. Simon Haenni and Hannah Street, whose work has contributed to this thesis.

This thesis could not have been completed without the support and guidance of the other members of the Mellor lab, particularly Ronja, Françoise and Anitha. For the *C. elegans* work, the advice and help Prof. Alison Woollard and Prof. Jonathan Hodgkin and all the members of their labs has been invaluable. In particular I would like to thank Hayley, Karolina, Maria, Sophie and Sara. For assistance with the tissue culture work, I would like to thank Prof. Lynne Cox, Penny and Sylwia.

My thanks go to the many people whose friendship has not only supported me through my D.Phil, but also made it a joy. I am lucky to have too many wonderful friends to name them all, but Rosanna, Hayley, Emma and my sister Claire have all gone above and beyond in their care and kindness.

Most of all, I would like to thank my parents. Without their love and the help they have provided in countless ways I would not have completed this thesis.

List of abbreviations

3-MA	3-methyladenine
AD	Alzheimer's disease
BAT	Brown adipose tissue
bp	Base pair
Ca^{2+}	Calcium ion
CN	Calcineurin
CNS	Central nervous system
CsA	Cyclosporin A
DMSO	Dimethyl sulfoxide
DNA	Deoxyribonucleic acid
DR	Dietary restriction
ER	Endoplasmic reticulum
FKBP	FK506-binding protein
FUdR	5-fluoro-2'-deoxyuridine
GC	Glucocorticoid
gDNA	Genomic DNA
GR	Glucocorticoid receptor
HDAC	Histone deacetylase
HFD	High fat diet
HPA axis	Hypothalamic–pituitary–adrenal axis
IBMX	3-isobutyl-1-methylxanthine
IIS	Insulin/insulin-like signalling
Li^{+}	Lithium ion
L-VGCC	L-type voltage gated calcium channel
NGM	Nematode growth medium
NODAT	New-onset diabetes after transplant
ORO	Oil-red-O stain
PCR	Polymerase chain reaction
PPIase	Peptidylprolyl isomerase
PTSD	Post-traumatic stress disorder
rDNA	Ribosomal DNA
RNA	Ribonucleic acid
RNAi	RNA interference
ROS	Reactive oxygen species
RT	Reverse-transcription
RyR	Ryanodine receptor calcium channel
SASP	Senescence-associated secretory phenotype
TAG	Triacylglyceride
TF	Transcription factor
TOR	Target of rapamycin
UCP	Uncoupling protein
WAT	White adipose tissue
WT	Wild-type

List of figures

Figure 1.1 The insulin/insulin-like signalling pathway in *C. elegans* and humans 27

Figure 1.2 TOR signalling is downstream of nutrient signalling and regulates the balance between protein synthesis and degradation 28

Figure 1.3 The process of autophagy 29

Figure 1.4 Longevity-regulating interactions of the lysosome with other cellular components 30

Figure 1.5 Some of the pathways through which DR acts to extend lifespan are conserved across *C. elegans*, flies and mice 31

Figure 1.6 The structure of FK506 33

Figure 1.7 Some of the cellular functions downstream of calcineurin 34

Figure 1.8 FK506 extends *C. elegans bus-5* lifespan.....40

Figure 1.9 FK506 delays lipid accumulation in *C. elegans bus-5* 41

Figure 1.10 FK506 causes aged rats to maintain a healthy body weight.....41

Figure 1.11 The protein folding pathway 44

Figure 1.12 Ion channels and transporters involved in Ca^{2+} homeostasis.....45

Figure 1.13 Stress response pathways and their interaction with ageing 54

Figure 1.14 *C. elegans* lifecycle.....59

Figure 1.15 PPARγ and C/EBPα are the major transcription factors controlling adipogenesis 63

Figure 3.1 FK506 did not extend *C. elegans bus-5* lifespan.....83

Figure 3.2 FK506 extended *C. elegans bus-5* lifespan under crowded conditions 84

Figure 3.3 FK506 did not extend *C. elegans bus-5* lifespan with 63 worms per plate 84

Figure 3.4 FK506 did not extend *C. elegans bus-8* lifespan in uncrowded conditions.....85

Figure 3.5 FK506 extended *C. elegans bus-8* lifespan in crowded conditions 86

Figure 3.6 FK506 did not extend *C. elegans* N2 lifespan in uncrowded conditions.....87

Figure 3.7 FK506 extended *C. elegans* N2 lifespan under crowded conditions.....88

Figure 3.8 *C. elegans bus-5* and *C. elegans* N2 did not have significantly different lifespans when treated with 0.5% DMSO 89

Figure 3.9 DMSO extended *C. elegans* N2 and *bus-5* lifespan, but not *bus-8* lifespan.....90

Figure 3.10 FK506 did not inhibit growth of *E. coli* OP50.....92

Figure 3.11 Light microscope image of *C. elegans bus-5* head, with the pharynx labelled 93

Figure 3.12 With arrest at L1 stage by starvation, FK506 increased *C. elegans bus-5* pharynx pumping rate at day 3 of adulthood, but not day 6 94

Figure 3.13 Without L1 stage arrest, FK506 increased or had no effect on *C. elegans bus-5* pharynx pumping rate 95

Figure 3.14 With arrest at L1 stage by starvation, FK506 increased or had no effect *C. elegans bus-8* pharynx pumping rate 96

Figure 3.15 FK506 decreased *C. elegans bus-5* lifespan (with population crowding) in combination with dietary restriction 98

Figure 3.16 FK506 increased *C. elegans bus-5* thrashing rate at days 1 and 3 of adulthood 100

Figure 3.17 FK506 increased *C. elegans* N2 thrashing rate or had no effect across three biological repeats 101

Figure 3.18 *C. elegans bus-5* and N2 worms had similar thrashing rates 102

Figure 3.19 The age of the NGM plates altered *C. elegans bus-5* thrashing rate 104

Figure 3.20 FK506 delayed the accumulation of gut bacteria in *C. elegans bus-5* and *bus-8* 105

Figure 3.21 FK506 had an acute effect on *C. elegans bus-5* thrashing rate.....107

Figure 3.22 *C. elegans bus-5* required continual FK506 treatment to cause lifespan extension 108

Figure 3.23 FUdR reduced the effect of FK506 on *C. elegans bus-5* thrashing rate 110

Figure 3.24 FUdR increased *C. elegans bus-5* lifespan 112

Figure 4.1 FK506 was unable to consistently increase *C. elegans bus-5* thrashing rate in the presence of *E. coli* HT115 123

Figure 4.2 FK506 had no effect on *C. elegans bus-5* lifespan in the presence of *E. coli* HT115.....124

Figure 4.3 Metabolites detected by mass spectrometry in *E. coli* OP50 and *E. coli* HT115 treated with either DMSO or 50 µg/ml FK506 127

Figure 4.4 Genetic crossing strategy to obtain *bus-5(br19); daf-16(mu86)* strain of *C. elegans*.....129

Figure 4.5 PCR to genotype *daf-16(mu86)* or WT alleles. 130

Figure 4.6 Three-primer PCR to genotype *daf-16* wild type and *mu86* alleles.....131

Figure 4.7 FK506 was unable to increase *C. elegans daf-16(mu86)* thrashing rate.....133

Figure 4.8 50 µg/ml FK506 had no significant effect on the lifespan of *C. elegans daf-16(mu86)* under conditions of population crowding 134

Figure 4.9 Some of the cellular pathways and components associated with ageing, including interactions with *C. elegans* FKBPs 135

Figure 4.10 Rapamycin dose response of *C. elegans bus-5* thrashing rate.....137

Figure 4.11 FK506 was unable to increase *C. elegans bus-5* thrashing rate in the presence of rapamycin 139

Figure 4.12 FK506 was unable to increase *C. elegans bus-5* lifespan (with population crowding) in the presence of rapamycin 140

Figure 4.13 At concentrations above the optimum dose FK506 lost the ability to extend lifespan 141

Figure 4.14 FK506 was unable to increase *C. elegans* N2 thrashing rate in the presence of rapamycin 142

Figure 4.15 FK506 and rapamycin did not have an additive effect on *C. elegans* N2 lifespan 143

Figure 4.16 FK506 increased *C. elegans bus-5* thrashing rate in the presence of CsA 145

Figure 4.17 FK506 was unable to increase *C. elegans bus-5* lifespan (with population crowding) in the presence of CsA 146

Figure 4.18 FK506 increased *C. elegans bus-5* thrashing rate in the presence of dantrolene 148

Figure 4.19 FK506 increased *C. elegans bus-5* lifespan (with population crowding) in the presence of dantrolene 149

Figure 4.20 FK506 inconsistently increased *C. elegans bus-5* thrashing rate in the presence of 3-MA and trehalose 151

Figure 4.21 FK506 increased *C. elegans bus-5* lifespan (with population crowding) in the presence of 3-MA, but not in the presence of trehalose 153

Figure 4.22 FK506 increased *C. elegans bus-5* thrashing rate in the presence of serotonin 154

Figure 4.23 FK506 increased *C. elegans bus-5* lifespan (with population crowding) in the presence of serotonin.....155
Figure 4.24 FK506 increased *C. elegans bus-5* thrashing rate in the presence of nicotinamide.....157
Figure 4.25 Finding the optimal dose of Li^+ on *C. elegans bus-5* 159
Figure 4.26 FK506 partially increased *C. elegans bus-5* thrashing rate in the presence of Li^+ 160
Figure 4.27 FK506 increased *C. elegans bus-5* thrashing rate in the presence of metformin 162
Figure 4.28 FK506 had variable action on *C. elegans bus-5* thrashing rate in the presence of caffeine.....163
Figure 5.1 Differentiation changed 3T3-L1 cell morphology from long, thin pre-adipocytes to rounded adipocytes containing lipid droplets 168
Figure 5.2 The experimental protocol used to differentiate 3T3-L1 into adipocytes and the harvesting of cells.....169
Figure 5.3 3T3-L1 treated with 1% DMSO 171
Figure 5.4 3T3-L1 treated with 0.1% DMSO at day 5 contained fewer black inclusions than 1% treated cells 171
Figure 5.5 Untreated 3T3-L1 and 1.25% ethanol-treated 3T3-L1 at day 5 had similar appearances, containing almost no inclusions.....172
Figure 5.6 Methylene blue stained 3T3-L1 fixed at day 20 (1% DMSO-treated) 173
Figure 5.7 PCR amplification of β-actin from cDNA derived from RNA purified from 3T3-L1 adipocytes using the phenol-chloroform protocol 175

Figure 5.8 PCR amplification of β-actin from cDNA derived from RNA purified using the RNeasy kit without DNase 175
Figure 5.9 PCR amplification of β-actin from cDNA derived from RNA purified using the RNeasy kit with DNase.....176
Figure 5.10 Amplification of a 270 bp fragment of mycoplasma 16 S rDNA using EZ-PCR Mycoplasma Test Kit.....177
Figure 5.11 Two of the three samples of conditioned 3T3-L1 medium tested positive for the presence of mycoplasma metabolites 177
Figure 5.12 Amplification of a 425 bp fragment of mycoplasma 16 S rDNA using universal primers.....178
Figure 5.13 ORO staining of TAG in 3T3-L1 adipocytes.....179
Figure 5.14 FK506 decreased TAG accumulation in 3T3-L1 adipocytes.....181
Figure 5.15 FK506 treatment of 3T3-L1 adipocytes did not significantly affect the percentage of viable cells, total number of viable cells or mean cell diameter 183
Figure 6.1 A possible mechanism of action of FK506.....191
Figure 6.2 Summary of the mechanism of action of FK506 on *C. elegans* thrashing rate 198
Figure 6.3 Summary of the mechanism of action of FK506 on *C. elegans* lifespan 200

List of tables

Table 1.1 Ill health and diseases associated with ageing have a negative impact on quality of life 22

Table 2.1 *C. elegans* strains 66

Table 2.2 *daf-16* genotyping PCR primers 71

Table 2.3 Mycoplasma 16 S rDNA intergenic spacer region amplification primers 75

Table 2.4 Primers to amplify 219 bp fragment of mouse β-actin 78

Table 3.1 Summary of the effects of FK506 on *C. elegans* lifespan and healthspan 113

Table 4.1 Overrepresented cellular processes and pathways associated with RNAs differentially regulated by FK506 in *C. elegans bus-8* day 1 adults 119

Table 4.2 The dependence of FK506 action on different cellular functions and proteins 164

Table 5.1 GO-terms associated with genes whose expression is increased in 3T3-L1 adipocytes by FK506 treatment at day 5 post-induction 185

Table 5.2 GO-terms associated with genes whose expression was increased in 3T3-L1 adipocytes by FK506 treatment at day 10 post-induction 185

Table 5.3 GO-terms associated with genes whose expression is decreased in 3T3-L1 adipocytes by FK506 treatment at day 5 post-induction 186

Table 5.4 GO-terms associated with genes whose expression is decreased in 3T3-L1 adipocytes by FK506 treatment at day 10 post-induction 187

Table of contents

Abstract 2

Acknowledgements 3

List of abbreviations 4

List of figures 5

List of tables 11

Table of contents 12

1 Introduction 22

1.1 Ageing 22

1.1.1 What is ageing? 22

1.1.2 The importance of ageing research 22

1.1.3 Theories of ageing 24

1.1.4 Mechanisms of ageing 26

1.1.5 Ageing interventions 30

1.2 FK506 32

1.2.1 Protein binding targets of FK506 33

1.2.2 FK506 inhibits calcineurin 34

1.2.3 FK506 has immunosuppressive activity 36

1.2.4 The effect of FK506 on metabolism 37

1.2.5 FK506 is neuroprotective and influences protein folding 38

1.2.6 Chronos Therapeutics data....39

1.3 FKBPs....42

1.3.1 Protein folding/chaperoning....43

1.3.2 Calcium flux....45

1.3.3 Transcription regulation....47

1.3.4 Neurodegeneration and neurogenesis....47

1.3.5 Brain development and mental health....48

1.3.6 Adipogenesis, obesity and metabolism....50

1.3.7 Cancer and apoptosis....51

1.3.8 Steroid receptors....52

1.3.9 Stress response....53

1.3.10 TOR....54

1.3.11 Autophagy....55

1.3.12 Insulin signalling pathway....55

1.3.13 RNA silencing....55

1.3.14 Immune system....55

1.3.15 TGF-β signalling....56

1.3.16 Bones/BMP....56

1.3.17 Sonic hedgehog signalling....56

1.3.18 Circadian rhythm....56

1.3.19 Microbiome 56

1.3.20 Clostridium botulinum C2 toxin 57

1.3.21 Malaria and other mosquito-borne diseases 57

1.4 *C. elegans* 57

1.4.1 *C. elegans* lifecycle 58

1.4.2 Measurement of ageing in *C. elegans* 59

1.4.3 Drug-sensitive mutants 60

1.5 Adipose tissue 60

1.5.1 Adipose tissue and adipocytes 60

1.5.2 Ageing in adipose tissue 63

1.5.3 3T3-L1 cells as a model of adipose tissue 64

1.6 Aims 65

2 Methods and materials 66

2.1 *C. elegans* 66

2.1.1 *C. elegans* strains 66

2.1.2 Maintenance 66

2.1.3 Population synchronisation 67

2.1.4 Drug-treating plates 67

2.1.5 Thrashing assay 68

2.1.6 Pharyngeal pumping 68

2.1.7 Lifespan assay 68
2.1.8 Dietary restriction (DR) 69
2.1.9 Genetic crosses 69
2.1.10 *daf-16(mu86)* genotyping PCR 70
2.1.11 Phenotyping *bus-5(br19)* – acridine orange staining 71
2.1.12 Gut bacteria accumulation 71
2.1.13 RNAi 72
2.1.14 *E. coli* growth on FK506 72
2.1.15 Metabolomics 72
2.2 3T3-L1 adipocytes 73
2.2.1 Culture of preadipocytes 73
2.2.2 Mycoplasma testing 73
2.2.3 Differentiation and FK506 treatment 75
2.2.4 Formaldehyde fixing of cells and quantifying TAG content (oil red O staining) 75
2.2.5 Quantifying total cell mass (methylene blue staining) 76
2.2.6 Harvesting cells and medium 76
2.2.7 RNA extraction 77
2.2.8 Reverse transcription and PCR 77
2.2.9 RNA-seq 78
2.2.10 RNA-seq data analysis 78

3 Results – FK506 altered the rate of *C. elegans* ageing 80

3.1 Introduction 80

3.2 FK506 increased *C. elegans* lifespan under crowded conditions 82

3.2.1 FK506 increased *C. elegans bus-5* lifespan under conditions of population crowding, but had no effect in uncrowded conditions 82

3.2.2 FK506 increased *C. elegans bus-8* lifespan under conditions of population crowding, but had no effect in uncrowded conditions 85

3.2.3 FK506 increased *C. elegans* N2 lifespan under conditions of population crowding, but had no effect in uncrowded conditions 86

3.2.4 DMSO increased lifespan of *C. elegans bus-5* and N2, but not *bus-8* 89

3.3 The effect of FK506 on *C. elegans* lifespan was not due to dietary restriction....90

3.3.1 FK506 did not inhibit growth of *E. coli* strain OP50 91

3.3.2 FK506 did not inhibit pharyngeal pumping 92

3.3.3 FK506 and dietary restriction did not have an additive effect on lifespan ...96

3.4 FK506 increased *C. elegans* thrashing rate 98

3.4.1 FK506 increased *C. elegans bus-5* thrashing rate 99

3.4.2 FK506 increased *C. elegans* N2 thrashing rate inconsistently.....101

3.4.3 *C. elegans bus-5* and N2 had comparable thrashing rates.....102

3.4.4 FK506 lost the ability to increase *C. elegans bus-5* thrashing rate over time 103

3.5 FK506 delayed accumulation of gut bacteria in *C. elegans bus-5* and *bus-8* 104

3.6 Continual treatment with FK506 gave the largest increase in *C. elegans bus-5* thrashing rate and lifespan 106

3.6.1 FK506 had an acute effect on *C. elegans bus-5* thrashing rate 106

3.6.2 *C. elegans bus-5* required continual treated with FK506 to extend lifespan 107

3.7 An interaction between the anti-ageing mechanisms of FK506 and FUdR in *C. elegans bus-5* 109

3.7.1 FUdR decreased the ability of FK506 to increase *C. elegans bus-5* thrashing rate 109

3.7.2 The interaction between FUdR and FK506 on *C. elegans bus-5* lifespan is unknown 111

3.8 Summary 113

3.9 Discussion 114

3.9.1 Validation of the lifespan assay 114

3.9.2 FK506 extended *C. elegans* lifespan under conditions of population crowding stress 114

3.9.3 FK506 extended *C. elegans* healthspan 114

3.9.4 FK506 did not extend *C. elegans* lifespan by creating DR conditions, but did not have an additive effect with DR on lifespan 115

3.9.5 FK506 had different mechanisms of action on *C. elegans* lifespan and healthspan 115

3.9.6 FK506 lost biological activity over time 116

4 Results – FK506 mechanism of action 117

4.1 Introduction 117

4.2 RNA-seq identified cellular processes altered by FK506 treatment in *C. elegans bus-8* 118

4.2.1 Lipid metabolism 119

4.2.2 Uncoupling proteins 120

4.2.3 Calcium ion homeostasis 120

4.2.4 Translation and response to stress 121

4.3 The impact of the RNAi bacteria strain, *E. coli* HT115, on the action of FK506 .122

4.3.1 The effect of FK506 on *C. elegans bus-5* thrashing rate was inconsistent in the presence of *E. coli* HT115 122

4.3.2 FK506 had no effect on *C. elegans bus-5* lifespan in the presence of *E. coli* HT115 124

4.3.3 *E. coli* OP50 and *E. coli* HT115 metabolomics 125

4.4 FK506 activity was DAF-16 dependent 128

4.4.1 Crossing *daf-16(mu86)* into the *bus-5(br19)* background 128

4.4.2 The FK506-induced thrashing rate increase was DAF-16 dependent 132

4.4.3 The DAF-16 dependence of FK506-induced lifespan extension is uncertain 133

4.5 Co-treatment with small molecule drugs 134

4.5.1 FK506 had no additive effect with rapamycin 135

4.5.2 FK506-induced lifespan extension was calcineurin dependent, but thrashing rate increase was calcineurin independent 143

4.5.3 FK506 action was independent of RyR 146

4.5.4 FK506 action interacted with autophagy 149

4.5.5 FK506 action was serotonin signalling independent 153

4.5.6 The effect of FK506 on thrashing rate was sirtuin-independent 156

4.5.7 FK506 and Li^+ had separate but over lapping mechanisms 157

4.5.8 FK506 and metformin acted independently on *C. elegans bus-5* thrashing rate 161

4.5.9 FK506 and caffeine had overlapping mechanisms on *C. elegans bus-5* thrashing rate 162

4.5.10 Summary 164

4.6 Discussion 164

5 Results – adipocyte cell culture 167

5.1 Introduction 167

5.2 Method optimisation 169

5.2.1 Ethanol instead of DMSO was selected as FK506 vehicle 170

5.2.2 Methylene blue stain concentration was optimised to quantify total cell mass 172

5.2.3 RNA purification method was optimised to prevent gDNA contamination 174

5.3 Mycoplasma testing 176

5.4 FK506 decreased lipid accumulation in 3T3-L1 adipocytes 179

5.5 FK506 did not measurably affect cell viability 182

5.6 FK506 significantly altered RNA levels in 3T3-L1 adipocytes 183

5.6.1 FK506 increased levels of RNAs associated with translation and the ribosome 184

5.6.2 FK506 decreased levels of RNAs associated with lipid transport and metabolism 186

5.6.3 FK506 had no effect on the RNA levels of uncoupling proteins 187

5.6.4 FK506 upregulated an ER-localised FKBP in both 3T3-L1 adipocytes and *C. elegans* 187

5.7 Discussion 188

6 Discussion 190

6.1 FK506 extended *C. elegans* lifespan and healthspan 191

6.1.1 FK506 extended *C. elegans* lifespan 191

6.1.2 FK506 did not create dietary restriction conditions 193

6.1.3 FK506 extended *C. elegans* healthspan 194

6.2 The mechanism of action of FK506 on C. elegans 194

6.2.1 FK506 had separate mechanisms of action on *C. elegans* lifespan and healthspan 194

6.2.2 The mechanism of FK506-induced *C. elegans* thrashing rate increase 196

6.2.3 The mechanism of FK506-induced *C. elegans* lifespan extension 198

6.2.4 FK506 altered *E. coli* HT115 metabolites....201
6.3 FK506 decreased lipid accumulation in mouse adipocytes....202
6.4 FK506 had similar effects in *C. elegans* and mouse adipocytes....204
6.5 FK506 and rapamycin have different anti-ageing mechanisms....205
6.6 Criticisms of methods....205
6.6.1 The instability of FK506 complicates interpretation of results....205
6.6.2 The suitability of *C. elegans* as a model organism....206
6.6.3 The suitability of 3T3-L1 adipocytes as a model of adipose tissue....207
6.7 Further work....208
7 Appendix....210
7.1 RNA-seq: *C. elegans bus-8* RNAs upregulated by FK506 treatment....210
7.2 RNA-seq: *C. elegans bus-8* RNAs downregulated by FK506 treatment....215
7.3 RNA-seq: 3T3-L1 adipocyte RNAs altered by FK506....216
7.3.1 Day 5 – increased by FK506....216
7.3.2 Day 5 – decreased by FK506....217
7.3.3 Day 10 – increased by FK506....218
7.3.4 Day 10 – decreased by FK506....219
7.3.5 Day 15 – decreased by FK506 (none increased)....219
Bibliography....220

1 Introduction

1.1 Ageing

1.1.1 What is ageing?

Ageing is the gradual impairment of normal biological function that increases in a stochastic manner with age, often with deleterious consequences. Ageing and age-related disorders (see Table 1.1) pose huge social and economic challenges to our society as the world's population ages.

Health issues associated with old age
Cardiovascular disease
Dementia and Alzheimer's disease (neurodegeneration)
Type II diabetes
Neoplasms
Sight impairment – cataracts and macular degeneration
Osteoporosis
Auditory impairment
Physiological frailty – e.g. reduced effectiveness of immune system after physical or psychological trauma

Table 1.1 Ill health and diseases associated with ageing have a negative impact on quality of life (Cox & Faragher 2007).

1.1.2 The importance of ageing research

In the UK, the Office for National Statistics (ONS) has projected that between 2011 and 2021 the number of people aged 65+ will increase by 24% and people aged 85+ by 39%. It has been predicted that 50% of people born in 2007 will live to 103 or beyond (House of Lords Select Committee on Public Service and Demographic Change 2013).

Unfortunately, there is a gap between life expectancy and healthy life expectancy (i.e. healthspan). In the UK, the healthspan of women is increasing at the same rate as

lifespan, but the lifespan of men is increasing faster than healthspan, increasing the amount of time spent in ill-health at the end of life (House of Lords Select Committee on Public Service and Demographic Change 2013). The number of people aged 65+ with diabetes will increase by over 45% from 2010 to 2030, arthritis, coronary heart disease and stroke all by over 50%, and dementia by over 80% (House of Lords Select Committee on Public Service and Demographic Change 2013). This rise in the number of people with long-term health conditions will need to be matched by increases in social and health care provision.

Currently 67% of men and 84% of women aged 65 will need social care before death (House of Lords Select Committee on Public Service and Demographic Change 2013). The number of people aged 65+ needing daily assistance (e.g. to wash, get dressed or get in and out of bed) is projected to rise by 90% from 2010 to 2030. This ageing population means the public cost of social and health care for older people will need to rise from £9.3 billion in 2010 to £12.7 billion by 2022 (House of Lords Select Committee on Public Service and Demographic Change 2013).

Even as the demand for care in old age increases, the number of working age people to fund the costs and provide informal care is decreasing. In 2015 there were 3.22 working age people per person of pension age, but this old age support ratio will decline to 2.87 in 2035, and by 2017 there will be more elderly people needing care than there are working-age family members able to provide that care (House of Lords Select Committee on Public Service and Demographic Change 2013).

The social, economic and human costs of ill-health and the associated poor quality of life in later life mean it is essential to research the causes of ageing in order to develop

treatments to prevent and alleviate age-associated disorders. As all these seemingly very different disorders are caused by the same underlying pathways of ageing, it is much more efficient (in terms of both cost and time) to focus research on ageing itself than each individual disorder.

1.1.3 Theories of ageing

There are environmental, genetic and stochastic elements to ageing. The rate of ageing can be altered by environmental factors, such as diet, and is highly heritable so must have a genetic component. However, because ageing is stochastic lifespan is not consistent within an isogenic population living in the same environment, instead while most individuals will have a lifespan close to the average, some will be short-lived and some long-lived. The genetic element of ageing is a highly evolutionarily conserved process, from yeast to humans (Fontana et al. 2010; Gems & Partridge 2013), and common pathways link different age-related disorders.

Attempts to formulate an overarching theory of why animals age started with the idea of programmed ageing, in which ageing is specifically selected for by evolution. Weismann suggested ageing benefits the population by removing elderly animals to increase the resources available for younger, fitter individuals (Weismann et al. 1891). However, in wild populations very few animals reach old age, instead being killed much earlier by predation or disease, so there is very little selection pressure on ageing characteristics. Selection pressure is strongest before and during the reproductively active stages of life, whilst most ageing characteristics appear post-reproduction, again meaning that there is little to no selection pressure on ageing.

Another theory of ageing is that it is an inevitable consequence of damage accumulated over an individual's lifetime, such as that from reactive oxygen species (ROS) generated as a side product of metabolism. However, ROS can both decrease and increase mouse lifespan (Balaban et al. 2005; Pinton et al. 2007; Howes 2006; Lapointe et al. 2009) and seemingly similar species can have hugely different lifespans, such as mice (2-3 years) and naked mole rats (around 30 years). The disposable soma theory of ageing (Kirkwood 1977) sought to resolve these problems, suggesting that there is a trade-off when allocating resources between repairing damage and reproducing. Somatic maintenance is only worthwhile up to the end of reproduction, so efficient use of resources to maximise reproductive success results in ageing. This would suggest reproduction and ageing are tied to one another, but these processes can be uncoupled (Gems & Partridge 2013; Kenyon 2010).

Medawar's evolutionary theory of ageing (Medawar 1952), that the lack of selection pressure after reproduction prevents the elimination or selection for mutations, suggests that ageing is a by-product of the accumulation of damaging mutations. Following from this, Williams proposed the antagonistic pleiotropy theory (Williams 1957) that mutations that are beneficial in early life will be selected for, even if they have negative effects in later life. For example, cellular senescence is an essential anti-cancer process, preventing proliferation of damaged cells. However, the accumulation of senescent cells with age becomes harmful through reduced tissue function and the pro-inflammatory senescence-associated secretory phenotype (SASP).

1.1.4 Mechanisms of ageing

At a cellular and molecular basis, there are many known mechanisms of ageing, including the insulin/insulin-like signalling (IIS) pathway, TOR signalling, senescence and autophagy.

1.1.4.1 The IIS pathway

Inhibition of the IIS pathway (shown in Figure 1.1) through mutation of the insulin/IGF receptor or its substrate extends lifespan. This is highly conserved across evolution – *C. elegans daf-2* (Kenyon et al. 1993), *Drosophila* CHICO (Clancy et al. 2001) and mouse Irs1 (Selman et al. 2008) mutants all have increased lifespan and/or delayed onset of age-related disorders. Alleles of certain IIS components are correlated with longevity in human studies (Suh et al. 2008; Kojima et al. 2004; Pawlikowska et al. 2009). IIS is the convergence point for many age-altering inputs, including diet and stress.

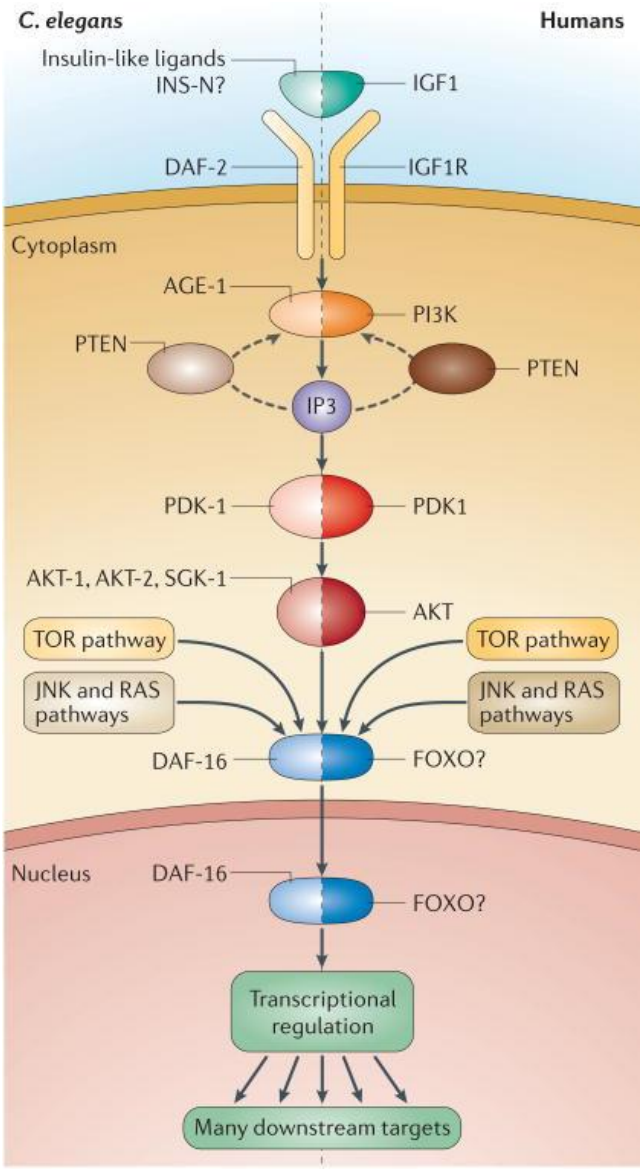

Figure 1.1 The insulin/insulin-like signalling pathway in C. elegans and humans. Mutation of daf-2 extends C. elegans lifespan whilst mutation of daf-16 shortens lifespan. Figure taken from (Christensen et al. 2006).

1.1.4.2 TOR signalling

Another well-conserved pathway is TOR signalling. TOR is downstream of nutrient signalling, and regulates cell growth, metabolism, autophagy and translation (Figure 1.2). Inhibition of TOR signalling, by rapamycin or genetic mutation, increases lifespan.

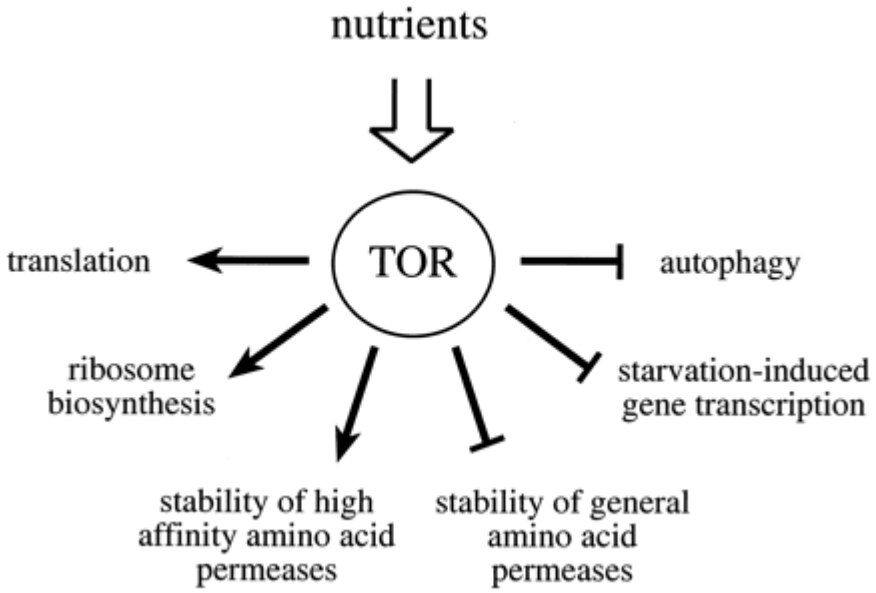

Figure 1.2 TOR signalling is downstream of nutrient signalling and regulates the balance between protein synthesis and degradation. Figure from (Raught et al. 2001).

1.1.4.3 Senescence

Cells with DNA damage, or cells that have reached their limit of number of divisions (Hayflick 1965) enter a state of senescence, in which they irreversibly stop dividing. This prevents aged cells and cells with irreparable DNA damage uncontrollably proliferating and becoming cancerous. However, there are negative phenotypes of senescent cells including loss of tissue-specific function and the senescence-associated secretory phenotype (SASP), which promotes inflammation. Senescent cells accumulate with age (Jeyapalan et al. 2007; C. Wang et al. 2009) and their removal extends lifespan and delays ageing (Baker et al. 2008; Baker et al. 2011; Baker et al. 2016).

1.1.4.4 Autophagy

Accumulation and aggregation of misfolded proteins is associated with several ageing disorders, including cataracts and neurodegeneration. One of the main cellular mechanisms to clear aggregated proteins is autophagy, the process of which is shown in

Figure 1.3. Autophagy is linked to many ageing pathways (Figure 1.4), and upregulation of autophagy promotes lifespan extension. Induction of autophagy by spermidine increases lifespan of yeast, *C. elegans*, *Drosophila* and human immune cells (Eisenberg et al. 2009; Morselli et al. 2011), and dietary restriction and inhibition of IIS and TOR all act to extend lifespan at least partially via activation of autophagy (Antebi 2007; Hansen et al. 2008).

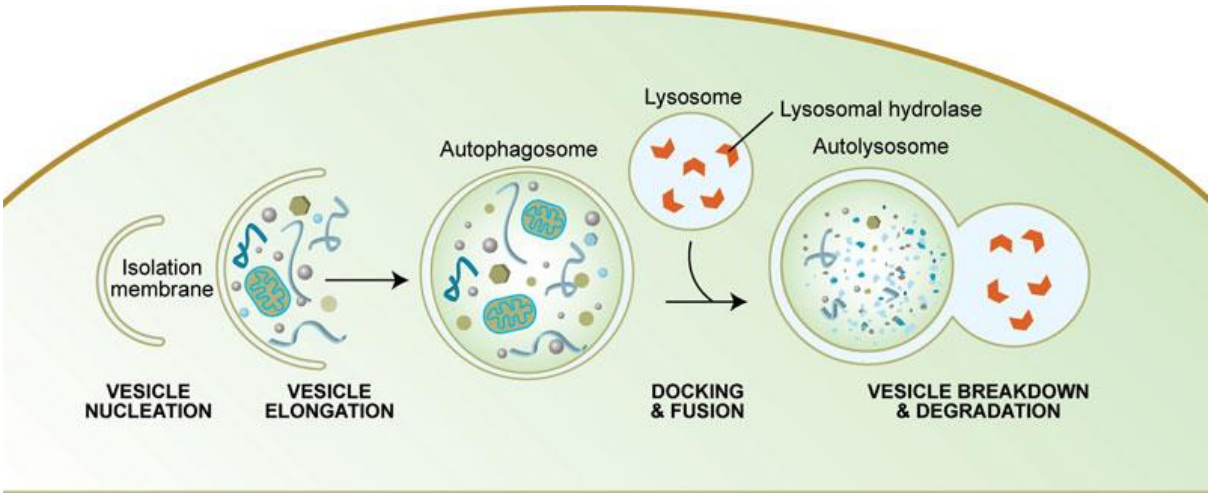

Figure 1.3 The process of autophagy. The autophagosome forms, engulfing the material to be degraded, then fuses with the lysosome. The material is degraded and the components recycled by the autolysosome. Figure from Wormbook (http://www.wormbook.org/chapters/www_autophagy/autophagy.html).

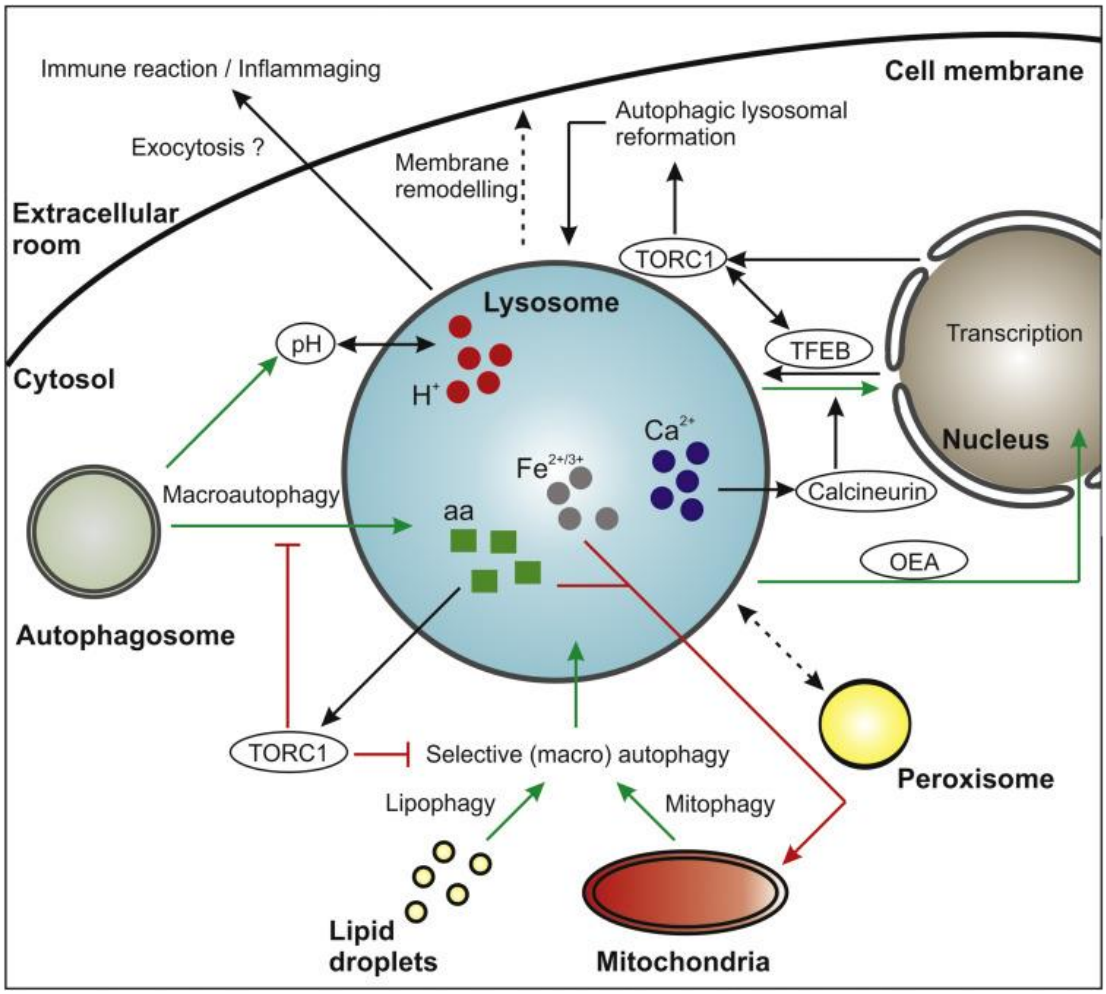

Figure 1.4 Longevity-regulating interactions of the lysosome with other cellular components. Lysosomes are required for and also regulate autophagy. Green arrows = positive effects, red arrows = negative effects on lifespan. Figure from (Carmona-Gutierrez et al. 2016).

1.1.5 Ageing interventions

The rate of ageing can be modulated with genetic, diet and small molecule interventions. Investigating the cellular processes these interventions interact with can elucidate mechanisms of ageing.

1.1.5.1 Dietary restriction

Dietary restriction (DR) extends lifespan and delays the onset of age-related disorders across evolution, from yeast and *C. elegans* (Greer & Brunet 2009), through to rhesus monkeys (Colman et al. 2014). DR acts on lifespan via many nutrient signalling pathways

(Figure 1.5), including IIS (Honjoh et al. 2009), TOR (Kapahi et al. 2004), sirtuins (Rogina & Helfand 2004) and AMPK (Greer et al. 2007). In *C. elegans* the mechanism of DR depends of the method of causing DR and the genetic background (Greer & Brunet 2009).

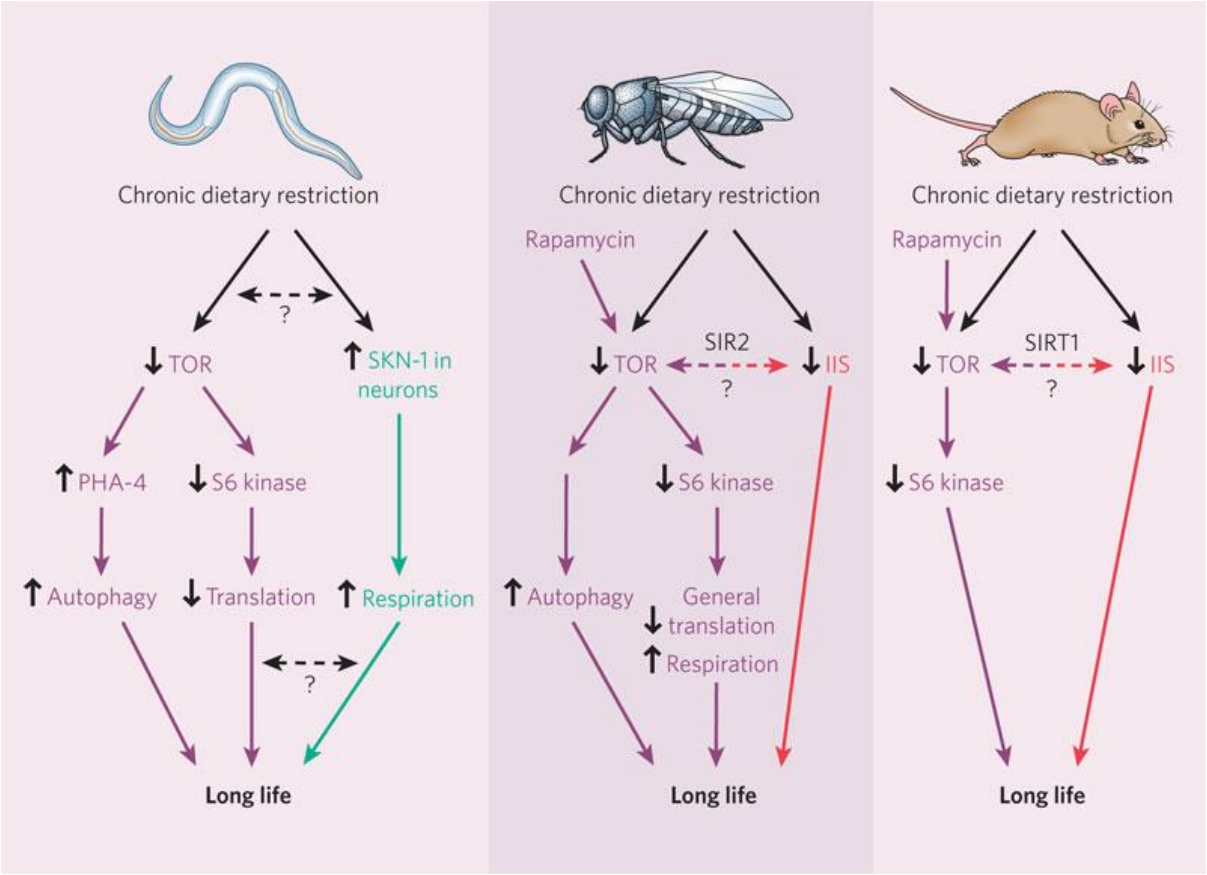

Figure 1.5 Some of the pathways through which DR acts to extend lifespan are conserved across C. elegans, flies and mice. These pathways include the TOR and IIS pathways. Figure from (Kenyon 2010).

1.1.5.2 Genetic mutations

Despite ageing being a highly complicated, multi-faceted process, single gene mutations can alter the rate of ageing in humans and other organisms. The human premature ageing conditions Werner's syndrome and Hutchinson–Gilford progeria syndrome are both caused by mutation of single genes (WRN and LMNA respectively), and IIS mutation can alter the rate of ageing and significantly change lifespan in several organisms (section 1.1.4.1).

1.1.5.3 Small molecule drugs

Many compounds with anti-ageing activity have been discovered, targeting a variety of ageing pathways. Rapamycin binds FKBP12 and this complex inhibits TOR, which at high doses causes immunosuppression but at low doses has anti-ageing activity. Spermidine increases lifespan by inducing autophagy (Eisenberg et al. 2009; Morselli et al. 2011). Metformin extends *C. elegans* lifespan not by directly acting on the worm, but by altering folate metabolism in the bacterial food source of the worms (Cabreiro et al. 2013). Small molecule interventions tend to cause much smaller increases in lifespan than those seen in mutants or DR treatment, possibly because only one component in a complex network of ageing pathways is targeted, or only partial inhibition is achieved, or the compound also has negative side effects.

Here, a potential new anti-ageing compound was investigated: FK506.

1.2 FK506

FK506 is a high molecular weight (804 g/mol) macrolide lactone (Figure 1.6). FK506 was isolated from the fungus *Streptomyces tsukubaenis*, in a screen of bacterial fermentation broths for immunosuppressive activity (Kino et al. 1987). FK506 binds FKBP12 to prevent T cell activation via inhibition of calcineurin (Ho et al. 1996) and is used in humans mainly after organ transplants, and also to treat the inflammatory skin disorder atopic dermatitis and the autoimmune disorder vitiligo. FK506 also has antifungal activity against certain species (Lamoth et al. 2015; Kino et al. 1987), but has not been found to inhibit growth of bacteria or yeast (Kino et al. 1987).

Despite its high molecular weight, FK506 can cross blood-brain barrier (Caraveo et al. 2014). FK506 is not water soluble, but is soluble in many other solvents, including DMSO and ethanol (Kino et al. 1987). FK506 is highly temperature sensitive and degrades into inactive impurities (Subasranjan et al. 2010). FK506 has seven rotatable bonds, and reaches an equilibrium of three tautomers (Akashi et al. 1996). *Cis-trans* epimerisation is associated with immunosuppressive activity (Lhoest et al. 1995).

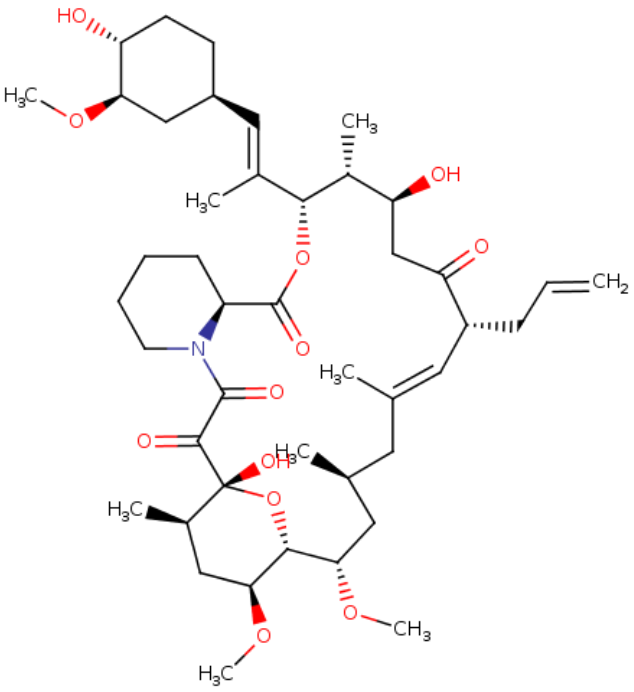

Figure 1.6 The structure of FK506. FK506, also known as tacrolimus, has molecular weight of 804. Figure from (http://www.drugbank.ca/drugs/DB00864).

1.2.1 Protein binding targets of FK506

The main targets of FK506 are the FK506-binding protein (FKBP) family of proteins, of which there are 8 in *C. elegans* (*fkb-1 – 8*) and many more in mammals. FK506 binds the FKBPs within their peptidylprolyl isomerase (PPIase) active site (Rossetto et al. 2015), but in FKBPs where the key binding residues are not conserved, such as FKBP38, FK506 is

unable to bind (Kang et al. 2008). *C. elegans fkb-1* to *-6* are able to bind FK506 (Zlotkowski et al. 2013). Binding FK506 inhibits the PPIase activity of the FKBPs, but does not inhibit their protein chaperone activity (Kang et al. 2008) and confers the ability to bind and inhibit calcineurin.

1.2.2 FK506 inhibits calcineurin

Via binding to FKBP12, FK506 inhibits calcineurin (CN) (Liu et al. 1991), a calcium-dependent regulator of many cellular functions, such as immune response (further detail in section 1.2.3), apoptosis (Thomson et al. 1995) and others shown in Figure 1.7. In *C. elegans*, CN signalling shortens lifespan by promoting dephosphorylation and inactivation (by blocking nuclear localisation) of DAF-16 (FOXO transcription factor in the IIS pathway) (Tao et al. 2013). FKBP12 also interacts with CN without FK506 binding, influencing CN activity by altering the NFAT transcription factor binding site with peptidyl-prolyl isomerisation (Guasch et al. 2015).

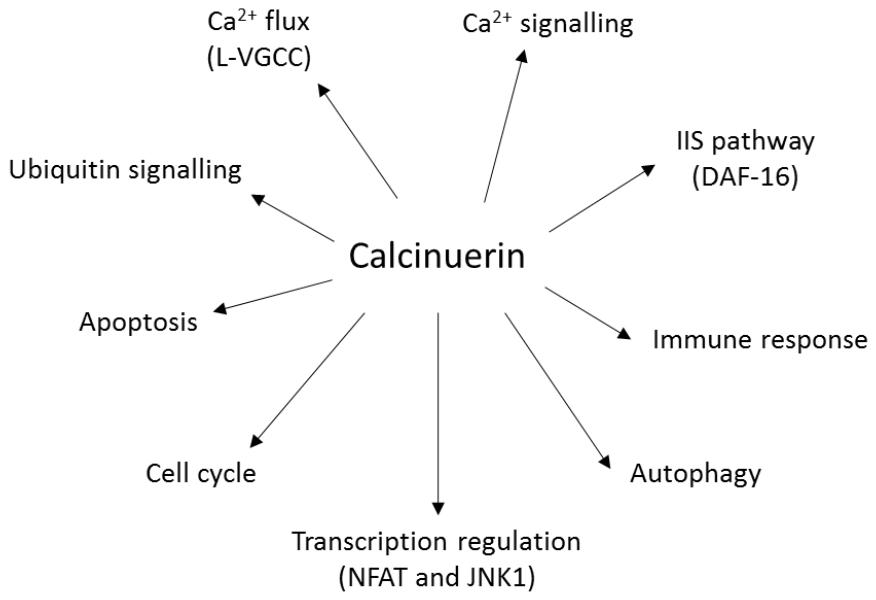

Figure 1.7 Some of the cellular functions downstream of calcineurin. Adapted from (Yu et al. 2015).

FK506 reduces Ca^{2+} flux. Via CN inhibition, FK506 inhibits L-type voltage gated Ca^{2+} channel (L-VGCC) activity (Norris et al. 2002). L-VGCC activity increases with age in hippocampal neurons in culture and *in vivo*, and FK506 treatment of aged rat neurons reduces L-VGCC activity to the level seen in younger rat neurons (Norris et al. 2010). FK506 also ameliorates the effects of calcium stress, reducing changes to the metabolome (Jenkins et al. 2013).

Through inhibition of CN, FK506 is able to alter gene expression. CN dephosphorylates NFAT, allowing this transcription factor to translocate to the nucleus to activate expression of target genes, and as FK506 inhibits CN, it also inhibits NFAT. FK506 reduces osteoblast differentiation via inhibition of expression of NFAT target gene Tβ4 (Lee et al. 2015), but FK506 promotes increased bone density by inhibiting RANKL expression (NFAT target gene) in osteoblasts, as RANKL promotes bone resorption by osteoclasts (Park et al. 2015). Inhibition of NFAT gives FK506 the ability to retard prostate and bladder cancer tumour growth (Kawahara, Kashiwagi, Ide, Li, Zheng, Ishiguro, et al. 2015; Kawahara, Kashiwagi, Ide, Li, Zheng, Miyamoto, et al. 2015; Kawahara et al. 2016) and FK506 reduces expression of Wnt-related genes associated with NFAT and nuclear β-catenin (Lee et al. 2015). FK506 also influences gene expression through inhibition of JNK1. CN is an activator of JNK1, so FK506 treatment prevents JNK1 from phosphorylating several transcription factors involved in T cell proliferation, apoptosis, autophagy and cell differentiation (Klettner et al. 2001).

1.2.3 FK506 has immunosuppressive activity

At high doses, FK506 is an immunosuppressant used after organ transplant and to treat other inflammatory disorders, such as rheumatoid arthritis (Miyata et al. 2005) and membranous nephropathy (Peng et al. 2014). Whilst FK506 and rapamycin are structurally similar and both bind FKBPs, they cause immunosuppression by inhibiting different T lymphocyte signalling pathways (Bierer et al. 1990). As the CYP3A5 allele genotype of patients affects the optimal immunosuppresive dose of FK506 (Hesselink et al. 2014), this protein is likely to be involved in FK506 metabolism.

FK506 has immunosuppressive activity independent of PPIase inhibition (Nath & Isakov 2015). FK506 (in complex with FKBP12) inhibits T cell proliferation via inhibition of calcineurin (Ho et al. 1996), part of the NFAT signalling pathway that promotes IL-2 expression, required for T cell proliferation (Nath & Isakov 2015; Matsuda et al. 2000). FK506 also acts independently of CN, inhibiting (in complex with an FKBP) the JNK-p38 signalling pathway (Nath & Isakov 2015; Matsuda et al. 2000; Vafadari et al. 2012) and suppressing T cell migration by inhibiting association of CrkII and C3G (Nath & Isakov 2015).

The negative side effects of FK506 immunosuppressive treatment include nephrotoxicity (Wallemacq & Reding 1993; Benedetti et al. 2013) and cardiotoxicity (Atkison et al. 1995; Dollinger et al. 1995; Chang et al. 2001; Cox & Freese 1996; Földes et al. 2014; Nakata et al. 2000; Nishimura et al. 2002; Nomoto et al. 1994; Turska-Kmieć et al. 2007). Immunosuppressive FK506-treatment can also cause new-onset diabetes after transplantation (NODAT) by damaging pancreatic islets (Jin et al. 2014), and is more likely to cause NODAT than cyclosporin A (CsA, another CN-inhibiting immunosuppressant)

(Borda et al. 2014). However, FK506 is less likely than CsA to have negative side effects on lipid metabolism (Bonthuis et al. 2013; Perrea et al. 2008). FK506 has also been reported to cause calcineurin-inhibitor induced pain syndrome (CIPS) (Malat et al. 2002), and anxiety and akathisia (DiMartini et al. 1996). Treatment with a low FK506 dose is less likely to cause negative side effects, and was found to promote macrophage polarisation towards the M2 phenotype, giving protection against atherosclerosis. High doses of FK506 did not skew macrophage polarisation so did not give protection against atherosclerosis, instead causing hypercholesterolaemia (Bai et al. 2010).

1.2.4 The effect of FK506 on metabolism

There is evidence in the literature that FK506 influences lipid metabolism. FK506 increases lipolysis and reduces fat storage in human subcutaneous adipocytes (Pereira et al. 2013). FK506 also reduces body weight and fat mass in mice treated with I mg/kg/day FK506 for 7 days, after feeding on a high fat diet (HFD) for 20 weeks (most likely due to the effect of CN inhibition in skeletal muscle) (Pfluger et al. 2015).

In mouse 3T3-L1 adipocytes FK506 does not alter lipid droplet accumulation or levels of C/EBPα protein (TF required for adipocyte differentiation) 6 days after induction of differentiation, unlike rapamycin which inhibits differentiation. A 100-fold excess of FK506 was able to reverse the inhibitory effect of rapamycin (Yeh, Bierer, et al. 1995). However, whilst FK506 has no effect on 3T3-L1 differentiation under optimal conditions, FK506 increases 3T3-L1 differentiation under suboptimal conditions by blocking the calcineurin-mediated calcium dependent inhibition of adipogenesis (Neal & Clipstone

2002). Over several hours of treatment, FK506 does not alter glucose breakdown in confluent 3T3-L1 cells (Takahashi et al. 2009).

FK506 binds spartin (a protein associated with neurological disorders) at much lower affinity than FKBP12. FK506 inhibits the localisation of spartin and its binding partner AIP4 (E3 ubiquitin ligase) to lipid droplets, preventing the ubiquitination and degradation of ADRP, a protein involved in lipid homeostasis whose expression level decreases in differentiated adipocytes (Tokunaga et al. 2013).

Immunosuppressive treatment with FK506 in human transplant patients can also influence metabolism. FK506-based treatment after kidney transplantation increases the levels of serum lipid metabolites (Kim et al. 2010) and alters levels of sugars and inositol in urine (Diémé et al. 2014). FK506-based immunosuppressive treatment of rats alters expression of glucose, amino acid and lipid metabolism proteins, redox/respiratory chain proteins and cytoskeletal proteins in the kidneys (Kędzierska et al. 2014).

1.2.5 FK506 is neuroprotective and influences protein folding

FK506 promotes nerve regeneration (Gold et al. 1994; Kang et al. 2008) and is neuroprotective (Kang et al. 2008). FK506 is able to promote nerve regeneration at sub-immunosuppressive doses (0.5 and 1 mg/kg/day) (Yang et al. 2003). 1 mg/kg/day FK506 was also able to increase lifespan and reduce neurodegeneration in a mouse model of Tau aggregation (Yoshiyama et al. 2007). This activity may come through inhibition of FKBP51, which promotes neurite outgrowth (Hausch 2015), or via inhibition of CN. CN is up-regulated in the central nervous system (CNS) of a mouse model of Alzheimer's disease with overproduction of Aβ protein, and FK506-treatment improves memory

function in this model (Dineley et al. 2007). FK506 was also able to improve memory function and restore dendritic spine density in transgenic mice expressing Aβ-precursor protein, most likely through inhibition of CN (Cavallucci et al. 2013). In Neuro2A and PC12 cells, FK506 protects against H_2O_2-induced cell death, not via inhibition of CN, but by inducing expression of anti-apoptotic genes (Klettner et al. 2001).

The FKBPs are protein-folding chaperones with PPIase activity. The PPIase activity of FKBPs may promote Tau protein misfolding, and therefore aggregation, so inhibition of PPIase activity is another possible neuroprotective mechanism of FK506 (Sulistio & Heese 2015). Despite the PPIase activity of FKBPs being involved in folding collagen and other proteins, in Ito liver cells FK506 did not affect synthesis of collagen or other proteins, but did inhibit cell proliferation (Ikeda & Fujiwara 1995).

FK506-treatment increases survival in mice infected with prion protein, and reduces accumulation of abnormal prion protein in cell culture. These treated cell have increased levels of autophagy proteins, increasing autolysosome formation (Nakagaki et al. 2013), so FK506 may protect against prion protein accumulation by inducing autophagy. However, FK506 does not induce autophagy in neuroblastoma cells (Sulistio & Heese 2015).

1.2.6 Chronos Therapeutics data

Through a phenotypic screen of out-of-patent drugs, FK506 was found to extend lifespan in *S. cerevisiae* and the drug-sensitive strain *C. elegans bus-5* (Figure 1.8) and is being repositioned as a treatment for age-related conditions by Chronos Therapeutics Ltd. FK506 treatment ameliorated neurodegeneration in rodent models, and was also able to

reduce protein aggregation in transgenic yeast and *C. elegans*. FK506 delayed age-related fat accumulation in *C. elegans* (Figure 1.9), and also maintained a healthy adult weight in elderly Fischer rats (Figure 1.10). Between 18 and 24 months, rat body weight increases greatly. Upon starting FK506 treatment at 18 months (week 3) this weight gain was reversed and a healthy weight maintained until death (i.e. continual treatment with FK506 did not cause continued weight loss below a healthy adult weight). A six-week trial in C57BL/6 mice (data not shown) showed the beginnings of a similar trend. Analysis of blood markers in the rats showed no negative side effects such as metabolic syndrome (glucose) or immunosuppression (IL-6 and IL-2), and a decreased level of TAG.

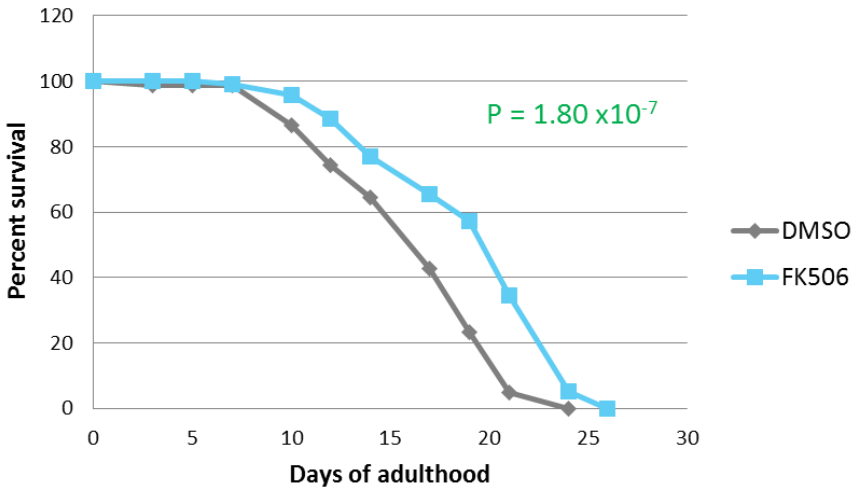

Figure 1.8 FK506 extends C. elegans bus-5 lifespan. Lifespan assay performed under crowded conditions (100 worms/plate) at a dose of 50 µg/ml FK506, vs. DMSO vehicle control. n = 100, P value calculated using OASIS log-rank test.

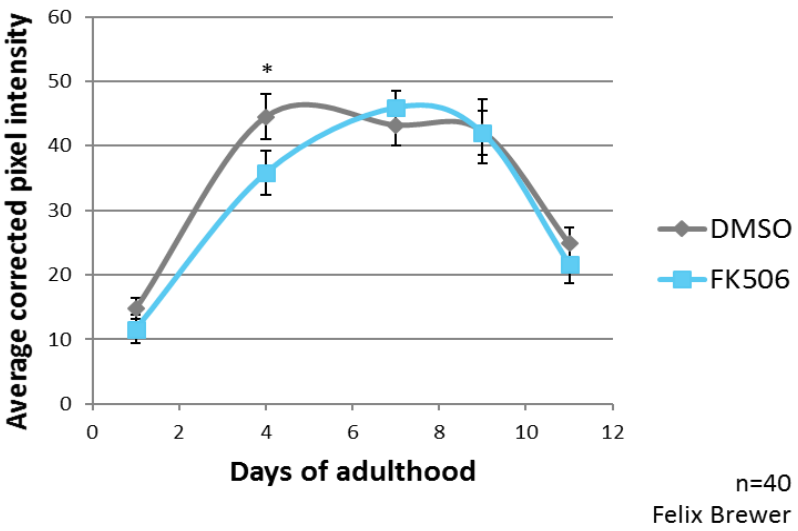

Figure 1.9 FK506 delays lipid accumulation in C. elegans bus-5. Worms were stained with oil-red-O and images taken with a light microscope. The amount of lipid stained was quantified using ImageJ.

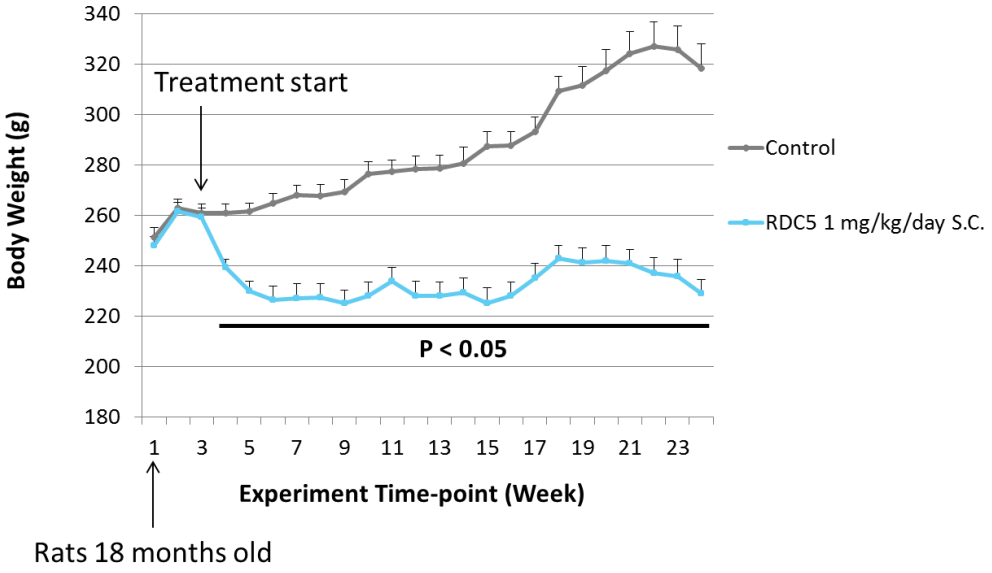

Chronos Therapeutics

Figure 1.10 FK506 causes aged rats to maintain a healthy body weight. Elderly rats (from 18 months) gain a large amount of weight (control rats, grey line), but when treated with 1 mg/kg/day FK506 the beginning of this weight gain is reversed and the rats maintain a healthy adult weight (~230 g) until sacrificed at 24 months of age.

The mechanism of FK506 action against age-related weight gain and other ageing characteristics is unknown. Currently, FK506 is used as an immunosuppressant (Kino et al. 1987), however the anti-ageing dose in rodents is sub-immunosuppressive and does not inhibit production of immune system markers, including IL-6 and IL-2 (unpublished data, Chronos Therapeutics). The anti-ageing mechanism of action could be through alternative downstream effects of binding FKBP12, or other binding targets, including the other FKBPs.

1.3 FKBPs

FKBPs are the main protein binding targets of FK506, which binds the same site as rapamycin (Bianchin et al. 2015) within the PPIase domain of FKBPs. FKBPs are found in bacteria (Ünal & Steinert 2015) and eukaryotes, including yeast (four FKBPs) (Monneau et al. 2013), *C. elegans* (8 FKBPs) and humans, and also plants (Leng et al. 2013; Niu et al. 2013), and are well conserved across species (Galat 2003). The FKBP active site is very open (Wang et al. 2013) and has many hydrophobic residues, meaning weak hydrogen bonds are important in protein and FK506 binding (Rajan et al. 2013). The residues required for PPIase activity and FK506 binding are well conserved across most FKBPs, but the residues of the loop above this site often differ, altering binding specificity (Romano et al. 2015).

FKBPs have well studied roles in protein folding, and regulation of steroid receptor signalling and ryanodine receptor function, but are also linked to adipogenesis, neurodegeneration, apoptosis and many other processes.

1.3.1 Protein folding/chaperoning

FKBPs assist in the folding of collagen and other proteins (Ikeda & Fujiwara 1995) by acting as chaperones (often in complex with Hsp90) and by altering protein conformation as peptidyl-proline isomerases (PPIases) (Figure 1.11). PPIase activity is inhibited by FK506 binding (Ikeda & Fujiwara 1995). The NMR structure of FKBP12 shows that the loop important in binding proteins partners has alternative conformations, allowing specific binding to many different proteins (Mustafi et al. 2013). However, only FKBPs containing a TPR domain bind Hsp90, and the identity of the FKBP bound influences Hsp90 activity (Romano et al. 2015). The only *C. elegans* FKBP containing a TPR domain is FKB-6 (most similar to human FKBP51 and FKBP52), which can interact with DAF-21 (of the Hsp90 family) and is expressed throughout life, particularly in the adult dorsal and ventral nerve cords (Richardson et al. 2007).

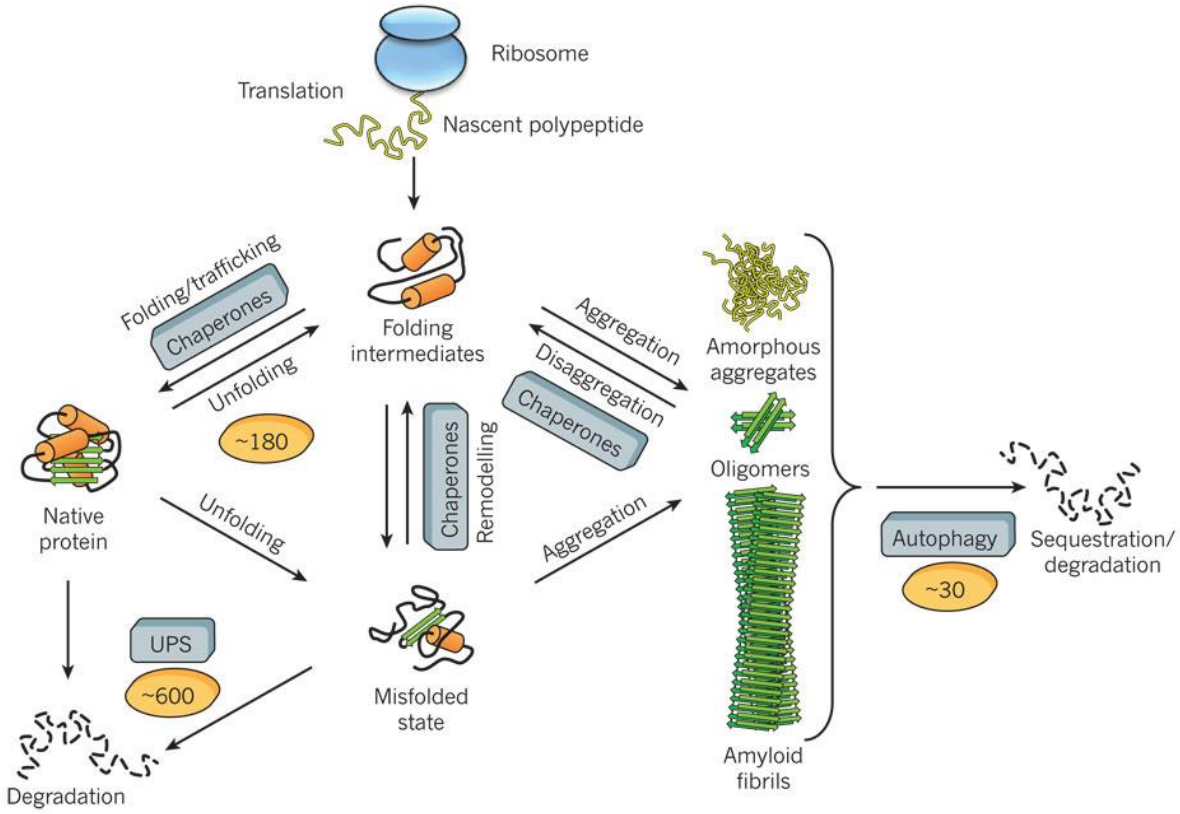

Figure 1.11 The protein folding pathway. FKBPs are involved in protein folding through their chaperone and PPIase activities. Proteins that fail to fold correctly are targeted for degradation by the proteasome or autophagy. Figure from (Hartl et al. 2011).

Collagen proteins contain many proline residues that must be isomerised by FKBPs localised to the ER (human FKBP65, *C. elegans fkb-3*, *-4* and *-5*) for correct folding, and loss of these ER-localised FKBPs can cause collagen-deformation diseases (Romano et al. 2015). *fkb-3*, *-4* and *-5* are required in *C. elegans* for normal development as well as collagen synthesis, and whilst there is redundancy between the three genes, the triple mutant and *fkb-4;fkb-5* double mutant have cold-sensitive lethality (Winter et al. 2007). The role of FKBPs in collagen folding is most well-known, but FKBPs also have other targets. For example, yeast Fpr4 catalyses isomerisation of proline residues in the tail of histone H3 (Monneau et al. 2013).

1.3.2 Calcium flux

There are many calcium channels and transporters that regulate calcium homeostasis (Figure 1.12), and FK506 influences calcium flux through regulation of the ryanodine receptor (RyR), L-VGCC and TRPC6 channels.

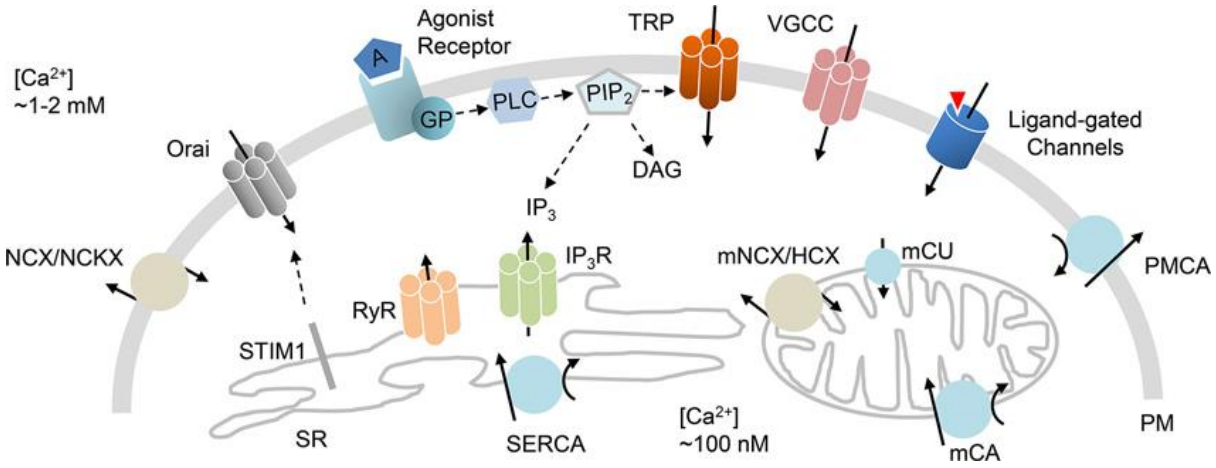

Figure 1.12 Ion channels and transporters involved in Ca^{2+} homeostasis. FK506 alters function of the RyR, L-VGCC and TRPC6 channels. Figure from (Harraz & Altier 2014).

Calcium flux through RyRs regulates several cell processes, including mitochondrial calcium levels, ATP levels and expression of metabolism and apoptosis genes (Bround et al. 2013). FKBP12 and FKBP12.6 competitively bind (in the absence of FK506 (Kang et al. 2008)) and regulate activity of the RyR1 (Eltit et al. 2010) and RyR2 calcium channel with opposite effect – FKBP12 binds RyR2 and increases Ca^{2+} release (Galfré et al. 2012; Kang et al. 2008) whilst FKBP12.6 binds RyR2 and inhibits Ca^{2+} release (Gant et al. 2011). However, Xiao *et al*. found FKBP12.6 had no significant effect on RyR2 activity (Xiao et al. 2007) and Zalk *et al*. suggest that in muscle both FKBP12 and FKBP12.6 bind and stabilise the closed state of RyR, creating clusters of RyR channels for coupled gating (Zalk et al. 2007). The binding of RyR to FKBPs is regulated by phosphorylation of RyR2 by PKA,

downstream of β-adrenergic signalling (reduces binding), and also by the oxidation state of RyR1 cysteine residues (Zalk et al. 2007).

The FKBP12.6-RyR interaction regulates insulin secretion (Chen et al. 2010), may influence heart arrhythmias in diabetics (Liu et al. 2014), and loss of FKBP12.6-RyR2 binding is linked to heart disorders (Zalk et al. 2007). Statins reduce anoxia-induced Ca^{2+} flux dysregulation by inhibiting the mevalonate pathway, causing increased expression of FKBP12.6, which stabilises the closed state of RyR2 (Yang et al. 2015).

FKBP12.6 gene expression declines with age, causing a loss of RyR2 inhibition that contributes to the dysregulation of Ca^{2+} flux with age. This dysregulation is associated with Alzheimer's disease (AD), and FKBP12.6 expression is decreased in the brains of AD patients (Gant et al. 2015). The age-related decline in FKBP12.6 causes increased Ca^{2+} release through RyR and L-VGCC, impairing neural and cognitive function (Gant et al. 2011; Gant et al. 2014; Gant et al. 2015). Overexpression of FKBP12.6 in the hippocampus of aged rats rescues the regulation of Ca^{2+} flux to levels seen in young rats and reverses the decline in memory (Gant et al. 2015). Ageing also causes a loss in FKBP12-RyR binding, again leading to Ca^{2+} flux dysregulation, which causes chronic metabolic stress and cellular damage (Breckner et al. 2013).

FK506 inhibits Ca^{2+} release (whilst rapamycin increases flux) (Gant et al. 2014), but this may be independent of FKBP12.6 (Xiao et al. 2007). FK506 causes dissociation of FKBP12 and RyR (Breckner et al. 2013; Kang et al. 2008) which would be expected to increase Ca^{2+} flux dysregulation, so the mechanism by which FK506 inhibits Ca^{2+} release may be dependent on the inhibition of L-VGCC via CN (see 1.2.2). Also, FKBP25 and FKBP38

regulate non-capacitive calcium entry through the TRPC6 channel, downstream of GPCR signalling (Lopez et al. 2015).

1.3.3 Transcription regulation

FKBP25 localises to the nucleus (Gudavicius et al. 2013) and associates with histone deacetylases (HDACs) so may have a role in chromatin regulation, and promotes binding of the transcriptional repressor YY1 to DNA (Romano et al. 2015). FKBP25 increases activity of the transcription factor p53 (cell cycle regulator and tumour suppressor), by promoting auto-ubiquitination and degradation of its inhibitor MDM2 (Romano et al. 2015). FKBP51 may also have a role in chromatin regulation, as it binds p300 (histone acetyltransferase and transcriptional co-activator), giving FKBP51 a possible pro-cancer role (Romano et al. 2015).

The PPIase activity of the FKBPs can influence gene expression. Yeast Fpr4 isomerises the protein tail of histone H3, potentially influencing chromatin structure (Monneau et al. 2013) and FKBP52 isomerises IFR-4 (a T and B lymphocyte transcription factor), regulating the protein-binding interactions of IFR-4 to influence immune response-linked gene expression in lymphocytes (Nath & Isakov 2015).

1.3.4 Neurodegeneration and neurogenesis

FKBP51 and FKBP52 have opposite effects on neurogenesis. FKBP51 inhibits, and FKBP52 promotes neurite outgrowth (Hausch 2015). In relation to neurodegeneration, FKBPs have both positive and negative effects on protein aggregation, including Tau protein and

therefore Alzheimer's disease (AD) (Blair et al. 2015). The PPIase activity of FKBPs may promote protein misfolding (see section 1.2.5) and the binding of hyperphosphorylated Tau by FKBP14 may prevent ubiquitination and degradation (Sulistio & Heese 2015). FKBP51 (associated with Hsp90) also blocks degradation of Tau, promoting aggregation, and increased levels of FKBP51 are associated with AD and ageing (expression increases due to demethylation of regulatory regions) (Blair et al. 2013). FKBP52 binds Tau (Chambraud et al. 2010; Zheng et al. 2015), but has the opposite effect to FKBP51, decreasing Tau protein (Sulistio & Heese 2015). RNAi of *fkb-6* in *C. elegans* increases Tau toxicity (Kraemer et al. 2006). However, FKBP52 and also FKBP12 increase levels of α-synuclein protein, promoting Parkinson's Disease (Sulistio & Heese 2015), though FKBP12 has been found to have both positive and negative effects on protein aggregation (Hausch 2015).

1.3.5 Brain development and mental health

The FKBP5 gene (FKBP51 protein), through either gene polymorphisms or altered expression is associated with:

- Memory in elderly people (Fujii, Ota, Hori, Hattori, Teraishi, Matsuo, et al. 2014)
- Brain structure (Fujii, Ota, Hori, Hattori, Teraishi, Sasayama, et al. 2014)
- Attention deficit hyperactivity disorder (ADHD) (Isaksson et al. 2015)
- Sensitivity to stress and post-traumatic stress disorder (PTSD) (Hartmann et al. 2015; Hartmann et al. 2012; Jochems et al. 2015; Klengel et al. 2013; Laukova et al. 2014; Lessard & Holman 2014; Nedelcovych et al. 2015; Sabbagh et al. 2014;

Sanchez 2012; Tozzi et al. 2015; Wilker et al. 2014; Yehuda et al. 2015; Zannas et al. 2015)

- Depression (Lukic et al. 2014; Owens et al. 2015; Sabbagh et al. 2014; Suzuki et al. 2014; Tozzi et al. 2015)
- Anxiety disorders (Hartmann et al. 2015; Zannas & Binder 2013)

Signalling through the glucocorticoid receptor (GR) is important in the physiological response to stress, via downregulation of the hypothalamic–pituitary–adrenal axis (HPA axis) (Isaksson et al. 2015; Suzuki et al. 2014). FKBP51 inhibits the GR (Hartmann et al. 2012) by inhibiting ligand binding, preventing translocation to the nucleus (Lukic et al. 2014). Overexpression of FKBP51 in specific regions of the brain in mice increases anxiety behaviour (Hartmann et al. 2015). Inhibiting FKBP51 reduces these behaviours (Hartmann et al. 2015) and FKBP51 knock-out mice are less sensitive to psychological stress (Hartmann et al. 2012; Sanchez 2012). Despite FKBP51 knock-out altering glucocorticoid (GC) signalling, the mice have normal longevity, glucose tolerance and cytokine profiles (phenotypes associated with GC signalling) (Sabbagh et al. 2014).

FKBP51 is also a target of GR signalling, creating a feedback loop (Fries et al. 2015). FKBP51 expression increases in rats exposed to prolonged stress (Laukova et al. 2014), whereas social stress decreases FKBP52 expression (in macrophages), removing competition for FKBP51 binding and promoting GC signalling inhibition. Repeated social stress causes GC resistance in immune cells, associated with inflammatory diseases (Jung et al. 2015).

DNA methylation on the FKBP5 gene within the glucocorticoid response element is influenced by allele type (alleles with decreased methylation have increased expression

and increased PTSD risk (Sabbagh et al. 2014)) and also exposure to trauma to determine response to stress (Klengel et al. 2013). In particular, the C/T SNP in intron two influences cortisol secretion (Suzuki et al. 2014) and depressive symptoms (Tozzi et al. 2015). DNA methylation on FKBP5 may also be inherited across generations, as the methylation pattern on FKBP5 is altered in both survivors of the Holocaust and their children (Yehuda et al. 2015). In mice, FKBP5 methylation decreases with age, increasing FKBP51 levels and inhibiting GC signalling, increasing sensitivity to psychological stress (Sabbagh et al. 2014).

1.3.6 Adipogenesis, obesity and metabolism

Adipogenesis is often studied using the 3T3-L1 mouse cell line of embryonically-derived preadipocytes in which adipogenesis can be chemically induced. After induction of differentiation, there is a burst of proliferation termed 'clonal expansion', after which the adipocytes no longer divide. It is unknown whether differentiating adipocytes undergo clonal expansion *in vivo*. FKBP51 and FKBP52 have opposite effects on lipid storage, as FKBP51(-/-) mice are resistant to weight gain on a high-fat diet, whilst FKBP52(+/-) mice are more susceptible (Sanchez 2012). Knockdown of FKBP51 increases, and ectopic expression inhibits, adipogenesis (Toneatto et al. 2013). This influence on adipogenesis is independent of PPIase activity (L. a Stechschulte et al. 2014), and has components both dependent (Toneatto et al. 2013) and independent (Sanchez 2012) of GR binding.

During the clonal expansion phase in 3T3-L1, FKBP51 expression increases (Toneatto et al. 2013; Yeh, Li, et al. 1995; Yeh, Bierer, et al. 1995) and FKBP52 expression decreases (Toneatto et al. 2013). Dependent on PKA signalling, FKBP51 translocates to and is retained (for 48 hours) in the nucleus, where it interacts with chromatin and the nuclear

matrix. As adipocyte differentiation increases FKBP51 and GR interaction, this translocation may alter transcription of GR target genes (Toneatto et al. 2013). FKBP51 can also promote adipogenesis through binding of PHLPP to inhibit the Akt-p38 signalling pathway, preventing phosphorylation of GR and PPARγ. Loss of the activatory phosphorylation of GR inhibits GR signalling, relieving adipogenesis inhibition, and loss of the inhibitory phosphorylation of PPARγ allows this transcription factor to activate transcription of genes required for adipogenesis (L. A. Stechschulte et al. 2014).

FKBP51 has also been linked to insulin resistance (Castro et al. 2013) and type 2 diabetes (Pereira et al. 2014; Gragnoli 2014). FKBP51 regulates GC signalling and therefore the HPA axis, which regulates cortisol levels, known to be linked to metabolic syndrome and depression (Gragnoli 2014), so FKBP51 may be the mechanism of the link between chronic stress and metabolism (Balsevich et al. 2014).

As well as regulating adipogenesis, FKBP52 and GR regulate gluconeogenesis. Loss of FKBP52 causes dysregulation of gluconeogenesis and promotes liver steatosis (unwanted accumulation of fat within cells) under high fat diet conditions, as metabolism shifts from gluconeogenesis to lipogenesis (Warrier et al. 2010).

1.3.7 Cancer and apoptosis

Several FKBPs have roles is apoptosis, and as such are linked to cancer since apoptosis-resistance is an important characteristic of cancerous cells. FKBP12 may have pro-cancer activity by blocking apoptotic TGF-β signalling, whilst FKBP52 and FKBP65 are overexpressed in breast and prostate cancer cells respectively (Romano et al. 2015). DNA methylation of the FKBP4 gene encoding FKBP52 is altered in breast cancer (Ostrow et al.

2009). FKBP51 also has pro-cancer (Sanchez 2012; D'Angelillo et al. 2015) and anti-apoptotic activities (via NF-κB transcription factors) (Romano et al. 2015).

FKBP38 binds Bcl-2 to regulate its localisation, and in different situations has either pro- or anti-apoptotic activity (Romano et al. 2015; Salminen et al. 2013). The amount of FKBP38 protein is linked to cancer aggressiveness (Romano et al. 2015). FKBP25 and FKBP37 also regulate apoptosis, and FKBP37 is a tumour suppressor gene (Romano et al. 2015). FKBP25 has nuclear localisation, associating with HDACs, and forms a regulatory feedback loop with p53 (Romano et al. 2015).

1.3.8 Steroid receptors

FKBP51 and FKBP52, in complex with Hsp90, each bind and regulate the steroid hormone receptors: glucocorticoid (GR), androgen (AR) and progesterone (PR) (Guy et al. 2015; Kang et al. 2008; LeMaster et al. 2015). In combination with ligand binding, the FKBP/Hsp90 complex regulates the translocation of the receptor from the cytoplasm to the nucleus, where the receptor activates transcription of target genes (Kang et al. 2008; Nath & Isakov 2015; Romano et al. 2015). FKBP52 regulation of AR signalling is important in male genitalia development and FKBP52 regulation of PR signalling is required for the correct development of the uterus (Sanchez 2012).

GR signalling regulates the HPA axis, the neuroendocrine system that responds to stress, producing cortisol, and also regulates processes including metabolism and the immune response. Polymorphisms in the FKBP5 gene which alter expression levels of FKBP51 cause changes in the regulation of GR signalling and the HPA axis (Binder et al. 2004). FKBP51 inhibits GR signalling (Jochems et al. 2015; Hartmann et al. 2012) and is also a

target gene of cortisol (Nath & Isakov 2015), creating a negative feedback loop (Suzuki et al. 2014). Acetylation of Hsp90 promotes binding to FKBP51 over FKBP52, inhibiting GR signalling and increasing psychological stress resistance in mice (Jochems et al. 2015).

1.3.9 Stress response

FKBP51 and FKBP52 protect against oxidative stress (Sanchez 2012; Gallo et al. 2011; Romano et al. 2015). As part of the oxidative stress response, FKBP51 binds Hsp90 and other mitochondrial proteins (Gallo et al. 2011). FKBP51 is involved in ER stress (Castro et al. 2013) and FKBPs may have a role in the temperature stress response (Fasseas et al. 2012). *C. elegans fkb-4* responds to metabolic stress, and is required for DR-induced lifespan extension (Ludewig et al. 2014). Cellular stress response pathways are summarised in Figure 1.13, highlighting pathways in which FKBPs may be involved.

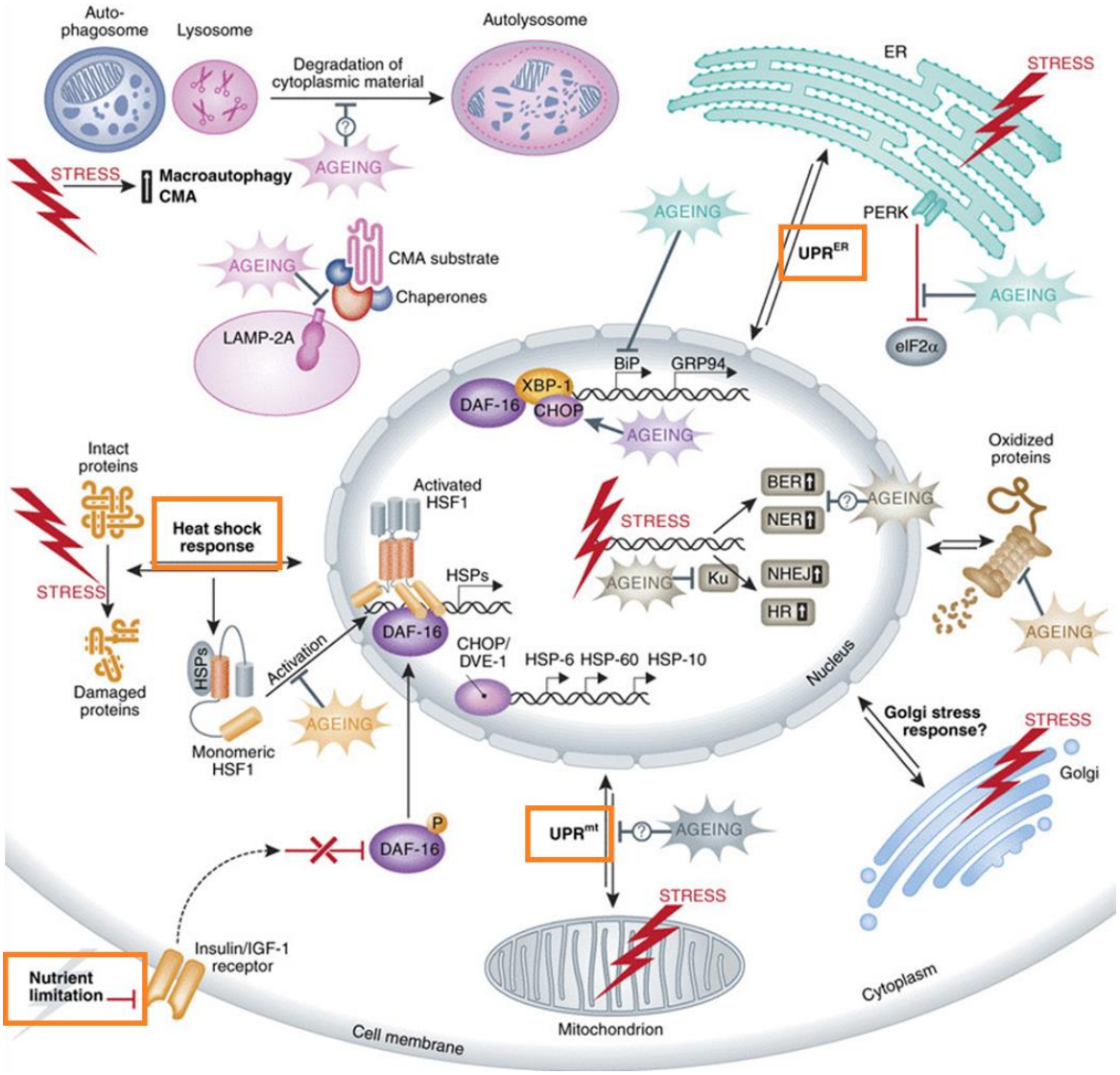

Figure 1.13 Stress response pathways and their interaction with ageing. FKBPs have roles in the response to oxidative, temperature and metabolic stress responses. Some of the pathways FKBPs may have a role in are highlighted by orange boxes. Oxidative stress can damage many different cellular components, including DNA and proteins, in multiple organelles. The main damage caused by heat shock is protein unfolding. UPR = unfolded protein response. Figure from (Kourtis & Tavernarakis 2011).

1.3.10 TOR

As well as FKBP12 binding rapamycin to inhibit TOR, FKBP38 also binds and inhibits mTOR

(Fu et al. 2015; Yoon et al. 2011).

1.3.11 Autophagy

Several FKBPs are linked to regulation of autophagy. FKBP51 associates with BECN1 and is required for the effect of anti-depressants on autophagy (Gassen et al. 2015; Gassen et al. 2014). FKBP12 and FKBP38 bind mTOR (Ge et al. 2014; Yoon et al. 2011), a regulator of autophagy, and FKBP38 also binds Bcl-2, which has a role in autophagy in the ER (Salminen et al. 2013).

1.3.12 Insulin signalling pathway

FKBPs interact with the IIS pathway in mammals (Yu & Larsen 2001) and also in *C. elegans*. Reduced IIS increases lifespan and decreases expression of *fkb-3*, *fkb-4* and *fkb-5* (Yu & Larsen 2001; Honda et al. 2011). The positive regulation of *fkb-3* and *fkb-5* by IIS is mediated by DAF-16, whereas IIS regulation of *fkb-4* is only partially DAF-16 dependent (Yu & Larsen 2001).

1.3.13 RNA silencing

FKBP51 and FKBP52 are required for efficient RNAi as part of the complex that regulates Ago2 chaperoning (Pare et al. 2013). FK506 inhibits the interaction of FKBP51 and FKBP52 with Ago2, causing decreased levels of Ago2 protein and miRNA, both unstable when unloaded from each other (Martinez et al. 2013).

1.3.14 Immune system

FKBPs have many different roles in the immune system. FKBP12 has a role in T cell differentiation and interacts with CrkII, which signals to receptors including TCRs (Nath & Isakov 2015). FKBP12 is also a cytokine secreted by mast cells to activate neutrophils (Nath & Isakov 2015). FKBP52 regulates gene expression in lymphocytes (see 1.3.3).

FKBPs are also involved in inflammation. Activated monocytes differentiating into macrophages have increased FKBP133 expression, which has a role in gut inflammation (Romano et al. 2015). FKBP15 is also linked to gut inflammation (Harbour et al. 2012). FKBP51 is a target gene of cortisol, which inhibits inflammation (Nath & Isakov 2015) and is the end product of the HPA axis, regulated by FKBPs via GR (see 1.3.8).

1.3.15 TGF-β signalling

FKBP12 binds TGF-βR1, an interaction inhibited by FK506 (Kang et al. 2008).

1.3.16 Bones/BMP

FKBPs are involved in BMP (bone morphogenetic protein) signalling and bone formation. FKBP12 represses BMP signalling (Spiekerkoetter et al. 2013), whilst BMP2 may be upstream of FKBPs and the Wnt signalling pathway (Lee et al. 2007). Mutations in FKBP65 (ER localised) cause osteogenesis imperfecta (brittle bone disease) (Romano et al. 2015).

1.3.17 Sonic hedgehog signalling

FKBP38 suppresses sonic hedgehog signalling, a secreted morphogen that controls the patterning and growth of various tissues in the developing vertebrate embryo, including the central nervous system (Saita et al. 2014).

1.3.18 Circadian rhythm

Drosophila protein BRIDE OF DOUBLETIME is a non-canonical FKBP with an inactive PPIase domain and is involved in regulation of the circadian clock (Fan et al. 2013).

1.3.19 Microbiome

FKBP51 expression (a marker of steroid responsiveness) is correlated with Actinobacteria in the bronchial microbiome of severe asthma patients (Huang et al. 2015).

1.3.20 Clostridium botulinum C2 toxin

Clostridial binary actin-ADP-ribosylating toxins share a specific FKBP-dependent translocation mechanism during their uptake into mammalian cells, and FKBP51 binds C2 toxin *in vitro*. FK506 protected cultured mammalian cells from C2 toxin and delayed translocation of the C2I component of the C2 toxin across the membrane into the cytosol (Kaiser et al. 2012).

1.3.21 Malaria and other mosquito-borne diseases

Both host and parasite FKBPs are involved in disease. FKBPs are a target for potential anti-malaria treatments (MacDonald & Boyd 2015), as modulation of PPIase activity of the *Plasmodium* FKBP35 inhibits parasite growth (Harikishore et al. 2013). FKBPs are host resistance factors, which reduce dengue and West Nile virus infection in HeLa cells (Rider et al. 2013), and O'nyong-nyong virus infection alters FKBP expression in the midgut of mosquitoes (Rider et al. 2013).

1.4 *C. elegans*

The nematode worm *C. elegans* was established as a model organism in the 1960s by Sydney Brenner, and since then 6 Nobel prizes have been awarded for research done in this organism. *C. elegans* is well suited to research as it is easy and cheap to culture in high numbers, has short lifespan and generation times, and is amenable to many experimental techniques – including genetic manipulation, RNAi and fluorescence microscopy. Using a well-established model organism is useful as *C. elegans* has a fully sequenced genome, there are well-developed protocols for maintenance and

experimentation, and there is a wealth of literature available. RNAi is easily performed in *C. elegans* by providing a food source of *E. coli* containing a plasmid from which expression of double-stranded RNA can be induced. A library of bacterial clones has been constructed of the RNase-deficient *E. coli* HT115 strain transformed with these plasmids (vector L4440) covering most *C. elegans* genes (Fraser et al. 2000).

C. elegans is particularly well suited as a whole-organism model of ageing due to its short lifespan, making lifespan assays possible, and the availability of methods to quantify the health of individuals, so the rate of ageing can be measured (Lees et al. 2016). The mechanisms and pathways of ageing such as the insulin signalling pathway, TOR signalling and dietary restriction are highly conserved between *C. elegans* and humans (Fontana et al. 2010).

1.4.1 *C. elegans* lifecycle

The majority of nematodes in a population are self-fertilising hermaphrodites, with a small number of males (~0.1%). They have a lifespan of approximately three weeks and reach maturity in about three days, passing through four larval stages (L1-4) before reaching adulthood (Figure 1.14). There is also an alternative dauer developmental pathway, triggered by environmental stresses such as starvation. A population can be synchronised by bleaching, which kills all worms but not the eggs, or picking L4 worms, which can be identified by the characteristic white semi-circle on the side of their body.

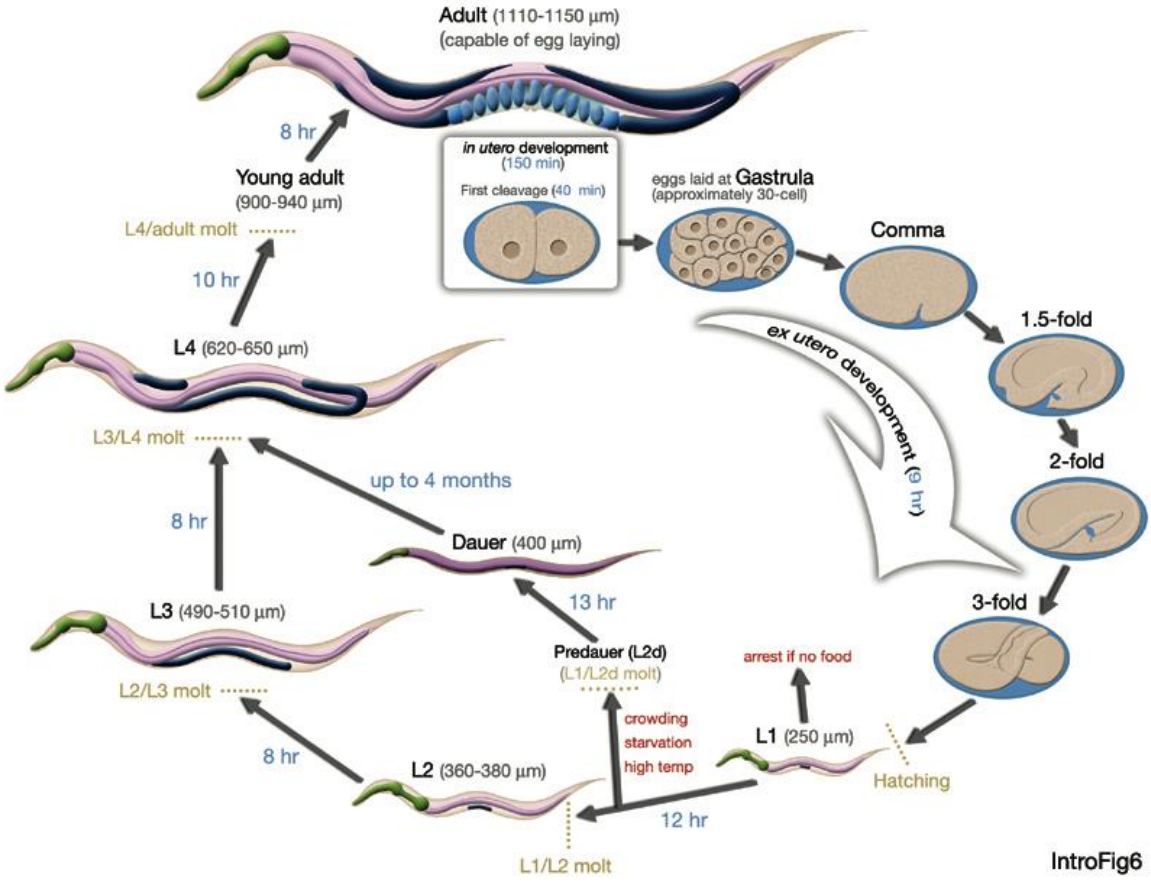

Figure 1.14 C. elegans lifecycle. Figure from http://www.wormatlas.org/ver1/handbook/anatomyintro/anatomyintro.htm.

1.4.2 Measurement of ageing in *C. elegans*

The simplest measurement of ageing in *C. elegans* is lifespan – there is a high correlation between the rate of ageing and age at death. To assay lifespan, an age-synchronised population of worms are cultured together (10 or fewer worms per plate to avoid noticeable crowding effects) and the number of dead worms counted every 2-3 days. However, this does not directly measure health, and therefore the rate of ageing.

Movement can be used to assay the health of a worm. In a thrashing assay a single worm is placed in a droplet of M9 buffer, and the number of thrashes from one side and back to its original position are counted. As *C. elegans* ages, the thrashing rate declines. The

onset of this decline is stochastic, so the thrashing rate varies within a homogenous population (Augustin & Partridge 2009). The decline in muscle function can also be measured by counting the rate of pharynx pumping, the contraction and release of the muscle within the head that allows *C. elegans* to feed. Due to the stochastic nature of ageing, population variation increases with age so these assays are best performed in early adulthood.

The appearance of nematodes changes with age, but this is less quantifiable. Inspection by light microscopy shows a disintegration of tissue structure with age, and fluorescent microscopy shows the accumulation of auto-fluorescent granules (lipofuscin) (Klass 1977).

1.4.3 Drug-sensitive mutants

The thick cuticle of *C. elegans* can prevent larger compounds from being absorbed through the surface of the worm, instead requiring very high doses to ensure sufficient uptake with food (Lees et al. 2016). To allow absorption of compounds through the surface of the worm, *bus* mutants with defective cuticle formation are used, most commonly *bus-8* and *bus-5* strains (Gravato-Nobre et al. 2005).

1.5 Adipose tissue

1.5.1 Adipose tissue and adipocytes

Adipose tissue dysfunction is both a characteristic of ageing and a contributing factor to several age-related disorders. Adipose tissue senses (via nervous and hormonal signals

(Lafontan 2012)) and regulates organismal metabolic state. It is an endocrine organ that secretes hormones such as adiponectin and leptin (Yu & Zhu 2004), pro-inflammatory cytokines (including IL-6 (Cartwright et al. 2007)), and many other proteins that regulate haemostasis, blood pressure, immune function, angiogenesis and energy balance (Rosen & MacDougald 2006).

There are two types of adipose tissue – white and brown fat, both insulin-sensitive, but brown adipose tissue (BAT) is specialised in thermogenesis (Klein et al. 2002) whilst white adipose tissue (WAT) is the major site of lipid storage. Adults have only small amounts of BAT (Rosen & MacDougald 2006), so WAT is the focus of this study. Most WAT differentiation occurs in the postnatal period in mice (Rosen & MacDougald 2006) and fat tissue growth involves both increases in the size and number of adipocytes (Cartwright et al. 2007). There is constant turnover of adipocytes throughout life, and preadipocytes (which have mesenchymal origin) make up 15-50% of cells in adipose tissues (Cartwright et al. 2007).

Fat depot sizes peak by middle or early old age (human 40-70 years), followed by a substantial decline in size with fat tissue dysfunction and redistribution in advanced old age (human >70 years) (Cartwright et al. 2007). This age-related decline in adipose tissue mass is due to a decrease in cell size, not cell number, and is accompanied by the accumulation of ectopic fat in the bone marrow, liver, muscle and other sites (Cartwright et al. 2007). Deposits in different locations have different molecular and physiological properties (Rosen & MacDougald 2006), including that peripheral subcutaneous fat tends to be lost first whilst visceral fat is preserved (Cartwright et al. 2007). Differences in gene expression are maintained in preadipocytes from different depots even after many

population doublings in cell culture (Cartwright et al. 2007). Both the accumulation of ectopic fat, and this change in the ratio of peripheral to central fat with age, are associated with insulin resistance, type II diabetes and atherosclerosis (Cartwright et al. 2007).

Adipogenesis is triggered in preadipocytes by pro-adipogenic signals (Figure 1.15), including nutrients, hormones (including insulin and IGF-1) and paracrine and autocrine effectors (e.g. free fatty acids and cAMP). These signals activate pathways that alter the expression and activity of transcription factors (TFs) that regulate expression of 1000s of differentiation-dependent genes (Cartwright et al. 2007), including those involved in cell growth, lipid transport and the extra cellular matrix (Birzele et al. 2012). PPARγ is the major transcription factor regulating adipocyte differentiation as it is both necessary (Rosen et al. 1999; Gurnell et al. 2000) and sufficient (Hu et al. 1995) for adipogenesis (reviewed by Rosen *et al*. (Rosen et al. 2000)). PPARγ is also required to maintain the adipocyte phenotype (Tamori et al. 2002). PPARγ and C/EBPα, another important TF, transcriptionally transactivate adipose-specific genes including adiponectin, leptin and GLUT4 (Cartwright et al. 2007). Other proteins with regulatory roles include C/EBP family members, KLF family members, HDACs (anti-adipogenic) and several cell cycle checkpoint control proteins (Rosen & MacDougald 2006). Many major signalling pathways are also involved in adipogenesis, such as Wnt, Hedgehog and Notch signalling (Rosen & MacDougald 2006). The most easily observed change that occurs during adipogenesis is the accumulation of lipids, stored in a droplet in the cell cytoplasm (Hosono et al. 2005; Yu & Zhu 2004; Horii et al. 2009; Dzitoyeva & Manev 2013; Mikkelsen et al. 2010; Birzele et al. 2012).

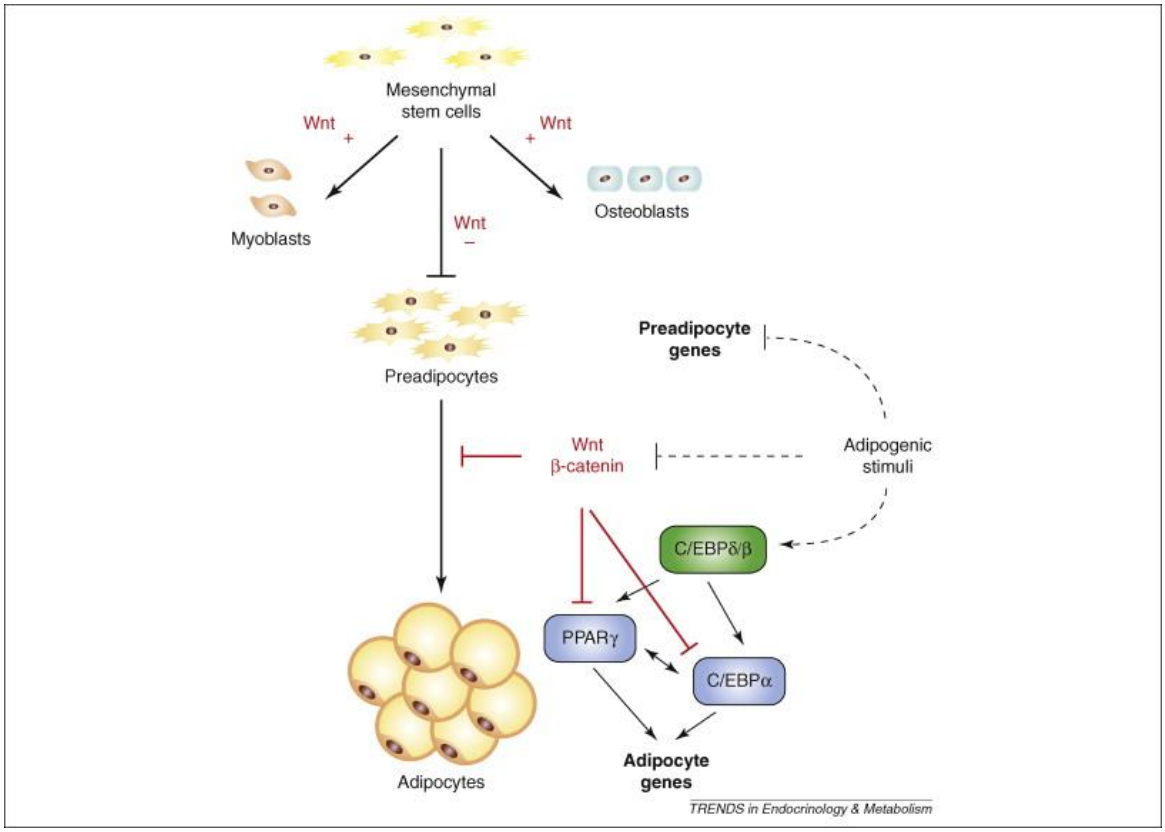

Figure 1.15 PPARγ and C/EBPα are the major transcription factors controlling adipogenesis. Figure from (Christodoulides et al. 2009).

1.5.2 Ageing in adipose tissue

Preadipocytes lose the ability to proliferate and differentiate with age, both in cell culture and *in vivo* (Cartwright et al. 2007). In comparison to preadipocytes from young rats, those taken from old rats have lower expression of pro-adipogenic PPARγ and C/EBPα and higher expression of anti-adipogenic C/EBPβ-LIP and CHOP (Karagiannides et al. 2001; Karagiannides et al. 2006). The pro-inflammatory adipokine TNFα is secreted by preadipocytes and increases in adipose tissue with age (Cartwright et al. 2007). TNFα inhibits PPARγ and C/EBPα expression, reduces insulin sensitivity and increases expression of anti-adipogenic C/EBPβ-LIP and CUGBP1 (Cartwright et al. 2007).

Aged adipocytes have decreased expression of PPARγ, C/EBPα, GLUT4 and IRS-1 (Zoico et al. 2010), decreased expression (Yu & Zhu 2004) and secretion (Zoico et al. 2010) of adiponectin, and reduced insulin sensitivity, triglyceride turnover and fatty acid re-esterification (Yu & Zhu 2004). The decline in preadipocyte and adipocyte function with age contributes to the dysfunction of adipose tissue in old age and the increased risk of age-related disorders, including insulin resistance and metabolic disorder.

1.5.3 3T3-L1 cells as a model of adipose tissue

3T3-L1 is a mouse embryonically-derived preadipocyte cell line that can be induced to undergo adipogenesis to form adipocytes, which can be aged in culture. 3T3-L1 is the standard mammalian cell line model of adipocytes and adipogenesis, and has been widely studied. Whilst much is known about differentiation of 3T3-L1 cells into adipocytes, less is known about how these adipocytes age.

In cultures of mouse 3T3-L1 cells, differentiated adipocytes appear to have three metabolically and functionally distinct stages: (1) overlaps with differentiation, characterised by small, immature adipocytes (days 0-5), (2) fully mature adipocytes at peak overall metabolic activity (days 5-10) and (3) aged cells (>10 days) with decline in every major cell function except net energy storage, as triglyceride content increases in a near linear manner throughout all stages (Yu & Zhu 2004).

1.6 Aims

This study aims to first confirm the result of the phenotypic screen indicating that FK506 extends *C. elegans* lifespan, and then to examine whether FK506 extends lifespan and healthspan in different strains of *C. elegans*. The effect of FK506 on *C. elegans* healthspan will be characterised by assaying thrashing rate, gut bacteria accumulation and pharynx pumping rate, as healthspan and lifespan are correlated.

Second, the mechanism of lifespan and healthspan extension by FK506 will be assessed. Trivial explanations for lifespan extension by FK506 will be examined, including induction of dietary restriction. Genes and cellular functions required for lifespan and healthspan extension by FK506 will be investigated using RNA-seq, RNAi, genetic mutation and co-treatment with small molecule inhibitors and inducers.

Third, the mechanism of action of FK506 in mammalian cells will be examined, focussing on the ability of FK506 to decrease the weight of elderly rats to within the normal healthy adult range. This study will investigate whether FK506 acts directly on adipocytes to reduce lipid accumulation and improve cell viability, using the mouse pre-adipocyte cell line 3T3-L1. RNA-seq will be used to investigate which cellular processes are altered by FK506 as the adipocytes age in culture.

2 Methods and materials

2.1 *C. elegans*

2.1.1 *C. elegans* strains

Strains used were: *bus-5(br19)*, *bus-8(e2885)*, N2 Bristol wild-type, CF1038 *daf-16(mu86)*, B6917 *bus-5(br19)*; *him-1(e879)*.

Name in thesis	**Genotype**	**Phenotype**	**Origin**
bus-5	*bus-5(br19)*	Cuticle mutant, drug sensitive	Prof. JA Hodgkin (Gravato-Nobre et al. 2005)
bus-8	*bus-8(e2885)*	Cuticle mutant, drug sensitive	Prof. JA Hodgkin
N2 Bristol	Wild-type	Wild-type	-
CF1038	*daf-16(mu86)*	Insulin/insulin-like signalling pathway mutant, short-lived	*C. elegans* Genetic Centre
B6917	*bus-5(br19)*; *him-1(e879)*	Drug sensitive cuticle mutant and has high incidence of males	Crossed by Chronos Therapeutics

Table 2.1 C. elegans strains

2.1.2 Maintenance

C. elegans were maintained and cultured at 20°C on NGM plates using standard techniques (WormBook n.d.), fed with an excess of *E. coli* OP50. If worm stocks starved they were passed through two generations before being used in an experiment. Stocks were stored in liquid nitrogen in freezing solution (30% glycerol, 0.1 M sodium chloride, 50 mM potassium phosphate, 0.3 mM magnesium sulphate). If required, vials were thawed at room temperature and poured onto an NGM plate seeded with *E. coli* OP50, stocks were then put through at least two generations before use in experiments.

2.1.3 Population synchronisation

Populations were synchronised by bleaching to leave only eggs alive, then seeded on NGM plates with *E. coli* OP50. After 2.5-3 days, L4 worms were picked to new plates.

Bleaching protocol: worms and eggs were washed off the NMG plate using M9 into a 15 ml tube, then centrifuged for 5 min at 3000 rpm. The supernatant was discarded to <0.5 ml and the pellet of worms transferred to a 2 ml tube, with extra M9 added if required to bring the volume to 0.5 ml. 1 ml bleach (55% H_2O, 25% sodium hydroxide, 20% sodium hypochlorite) was added to the pellet of worms, and vortexed for 3-4.5 min depending on *C. elegans* strain (N2 = 4.5 min, *bus-5(br19)* = 3.5 min, *bus-8(e2885)* = 3 min). Immediately after vortexing, the worms were centrifuged for 30 s at 13,200 rpm. The supernatant was removed and 2 ml M9 added to the tube before centrifuging again with the tube orientation altered to move the pellet to the opposite side of the tube, then repeated. After the third centrifuge, the pellet of eggs was resuspended in the required M9 to seed 50 µl/55 mm plate and 100 µl/85 mm plate.

2.1.4 Drug-treating plates

All drugs were dissolved in DMSO or H_2O. A total of 300 µl H_2O and 15 µl DMSO (0.5%), plus 50 µl 10 mg/ml FUdR in H_2O for lifespan experiments only, was applied to each 55 mm plate (3 ml surface volume), with the exception of metformin, which required a larger volume of H_2O to be dissolved. A master mix (x number of plates plus 5%) for each treatment was prepared, then applied evenly to the surface of each 55 mm NGM plate. Once dry, 100 µl *E. coli* OP50 was added to the centre of each plate and allowed to dry. The plates were stored at room temperature in the dark. All plates for each experiment

were treated with drug and seeded with *E. coli* the day before the worms were synchronised by bleaching.

2.1.5 Thrashing assay

The worm population was synchronised by bleaching, and the eggs seeded on drug- or control-treated plates (described in 2.1.4), so each worm was treated from hatching. After 2.5-3 days, 20 L4 worms per treatment were picked onto a new plate (day 0). Thrashing rate was assayed on days 1 and 3 of adulthood. To assay thrashing rate each worm was picked into a droplet of M9 (3 g/l KH_2PO_4, 6 g/l Na_2HPO_4, 5 g/l NaCl, 1 mM $MgSO_4$), allowed to acclimatise, and the number of body bends with return to original position counted for 3x 30 s, then the worm was picked onto a new plate.

2.1.6 Pharyngeal pumping

The worm population was synchronised by bleaching, and the eggs seeded on drug- or control-treated plates (described in 2.1.4), so each worm was treated from hatching. After 2.5-3 days, 20 L4 worms per treatment were picked onto a new plate (day 0). Worms were transferred to new plates away from offspring every two days after pharyngeal pumping rate was assayed on days 2-6, depending on experiment. To assay pharyngeal pumping rate the number of pharynx pumps was counted for 30 s, then the worm transferred to a new plate.

2.1.7 Lifespan assay

The worm population was synchronised by bleaching, and the eggs seeded on drug- or control-treated plates (described in 2.1.4), so each worm was treated from hatching. After 2.5-3 days, L4 worms were picked onto new plates containing FUdR (day 0) – 100/plate for crowded conditions (one plate per treatment), 5 or 10 per plate for non-

crowded conditions (12 plates per treatment). Every two days the number of dead worms was counted. A worm was counted as dead if it was not moving, even after 3 prods with a platinum wire.

For the lifespan assay without FUdR, NGM plates were treated with drug the same as for thrashing assays and adult worms were picked regularly onto new plates (without transferring any offspring) until no more eggs were laid (days 2, 4, 6, 8 and 15). The worms on the with-FUdR DMSO- and FK506-treated plates were also picked to new plates to control for the effects of picking and fresh plates of drug.

Lifespan data was analysed using OASIS (Online Application for Survival Analysis) (Yang et al. 2011), which uses the log-rank test to give P values for significance.

2.1.8 Dietary restriction (DR)

Lifespan was assayed under dietary restriction conditions: the lifespan assay was started as normal (see 2.1.7), but on day 2 of adulthood the DR worms were transferred onto DMSO- or FK506-treated plates with no *E. coli* OP50, where they remained for the rest of the experiment.

2.1.9 Genetic crosses

To cross *daf-16(mu86)* mutation into the *bus-5(br19)* genetic background, the double mutant B6917 *bus-5(br19)*; *him-1* was used to obtain sufficient numbers of males. Two *daf-16* L4 hermaphrodites and 5-11 L4/young adult B6917 males were placed on an NGM plate seeded with *E. coli* OP50 and incubated at 20°C. After ~5 days the offspring were examined to check for males – if the cross was successful there would be ~50% male offspring (only ~0.01% males if hermaphrodite self-fertilises). If the cross was successful, 10 L4 hermaphrodites (younger than the males present, F1 generation, all heterozygous)

were transferred onto individual plates and allowed to self-fertilise. 50 of the offspring (F2 generation, 1/16 should be double mutants) were transferred to individual plates and left to lay eggs. After 2 days the F2 mother was removed from the plate for genotyping (*daf-16(mu86)* mutation, see 2.1.10). The F3 offspring were phenotype-tested for the *bus-5(br19)* mutation (see 2.1.11).

2.1.10 *daf-16(mu86)* genotyping PCR

DNA extraction (single worm lysis): A single worm was picked into 2.5 µl lysis mix (50 µM KCl, 2.5 µM $MgCl_2$, 10 µM Tris HCl pH 8.3, 0.45% NP40, 0.45% Tween-20, 0.01% gelatine, 0.1 mg/ml proteinase K) then frozen at -80°C for >20 min, then incubated at 60°C for 1 hour, followed by 95°C for 15 min. If required, the lysed worm was stored at -20°C.

PCR: A master mix containing all reagents except DNA template was made for the number of reactions plus 10%, then aliquoted before adding template. Per reaction in 0.2 ml DNase-free PCR tubes was mixed: 1X GC buffer (NEB), 0.2 mM dNTPs, 2.4 pmol/µl each of the three primers (see Table 2.2), 0.5 units Phusion HF DNA polymerase (NEB) and 1 µl lysed worm template (MQ H_2O for negative control), plus MQ H_2O up to a final volume of 25 µl. The reactions then underwent the following thermal cycle: first, 98°C for 5 min, then 25 cycles of 98°C for 30 s (denaturing), 57°C for 30 s (annealing) and 72°C for 2 min (elongation), finishing with 72°C for 10 min and then hold at 4°C.

Primer sequences:

Name	Description	Sequence	Melting temperature
Daf16 WT F	Forward primer for wild type *daf-16*	GTGTCTATGTTGCTCGAAATG	~60°C
Daf16(mu86) F	Forward primer for *daf-16(mu86)* (gift of Sara Maxwell)	CGTATTCTCGTGGGAAAGTG	~62°C
Daf16 R	Reverse primer for both genotypes (gift of Sara Maxwell)	CGTTATCAAATGCTCCTTGC	~62°C

Table 2.2 daf-16 genotyping PCR primers

Gel electrophoresis: 5 µl PCR product mixed with 1 µl 6X blue loading dyes (Thermo or NEB) and 1 µl DNA ladder (100 bp plus, Thermo) were loaded onto a 1% agarose/TBE/ethidium bromide gel and ran at 110 V for about 25 min, until the ladder bands were separated. The gel was imaged on a UV transilluminator (Syngene) and images captured by digital camera (Kodak EDAS 290).

2.1.11 Phenotyping *bus-5(br19)* – acridine orange staining

In a 96-well plate, at least 6 adult *C. elegans* were placed in 0.1 mg/ml acridine orange in M9 buffer and incubated for >10 min at room temperature. The worms were inspected under light microscope for absorption of the stain. Strains with a correctly formed cuticle (N2 and *daf-16(mu86)*) remained clear, whereas homozygous cuticle mutants (*bus-5* and *bus-8*) absorbed the stain and appeared orange.

2.1.12 Gut bacteria accumulation

Synchronised populations of day 2 adult *bus-5* and *bus-8* were transferred to GFP-*E. coli* (OP50:pFVP25.1, gift of Dr. M. Gravato-Nobre) NGM plates for 24 h. Individual worms were washed in M9 buffer to remove surface bacteria and presence of gut bacteria and shape of gut assayed using a fluorescent microscope (Leica MZFLIII).

2.1.13 RNAi

Thrashing rate and lifespan were assayed as before (sections 2.1.5 and 2.1.7 respectively), but using NGM plates containing IPTG to induced expression from the L4440 vector, and the RNAi bacterial strain *E. coli* HT115 containing the empty vector.

2.1.14 *E. coli* growth on FK506

FK506 (Invitrogen) dissolved in DMSO (Sigma) was added to molten LB agar. *E. coli* OP50 in LB medium (overnight culture at 37°C with shaking) was spread on each plate (LB only for negative control) and incubated overnight at 37°C. The volume of *E. coli* OP50 culture per plate was optimised to form 100-150 colonies. The number of colonies formed was counted.

2.1.15 Metabolomics

NGM plates were treated with DMSO or 50 μg/ml FK506 and seeded with either *E. coli* OP50 or *E. coli* HT115 (empty L4440), as previously. Plates were incubated at room temperature overnight, then at 20°C for four days (as they would be during a thrashing rate or lifespan assay, to the equivalent of day 1 of *C. elegans* adulthood). The bacteria were washed off each plate with 1 ml M9 buffer and centrifuged at 5000 rpm for 1 min. The supernatant was removed and the pellet resuspended in 1 ml 80% ethanol, then stored at -80°C.

Metabolites were measured by mass spectrometry by Dr. Katja Dettmer-Wilde (Institute of Functional Genomics, University of Regensburg) using the methods outlined in (Timischl et al. 2008).

2.2 3T3-L1 adipocytes

2.2.1 Culture of preadipocytes

Mouse embryonic 3T3-L1 preadipocytes (Public Health England) were cultured and differentiated according to standard methods in the literature (Yu & Zhu 2004; Zoico et al. 2010; Eguchi et al. 2008; Helledie et al. 2002). In brief: 3T3-L1 preadipocytes were grown at 37°C in 5% CO_2 in Gibco DMEM (high glucose, Life Technologies) containing 10% calf serum (Sigma), 1X penicillin-streptomycin (Sigma), 8 mg/ml pantothenic acid and 8 mg/ml biotin.

2.2.2 Mycoplasma testing

2.2.2.1 EZ-PCR Mycoplasma Test Kit

Conditioned medium was tested for the presence of mycoplasma DNA using the EZ-PCR Mycoplasma Test Kit (Biological Industries) according to the manufacturer's protocol. The PCR products were analysed by gel electrophoresis on a 1% agarose/TBE/EtBr gel at 110 V for 30 min. The gel was imaged on a UV transilluminator (Syngene) and images captured by digital camera (Kodak EDAS 290) with 0.5 s exposure.

2.2.2.2 Chemical-based assay

Conditioned medium was tested for the presence of mycoplasma metabolites using the Mycoplasma Detection Kit – Quick Test (Biotool) according to the manufacturer's protocol.

2.2.2.3 PCR with universal mycoplasma primers

Using DNA extracted from conditioned medium as template, a 425 bp section was amplified from the 16 S rDNA intergenic region which is conserved between mycoplasma using universal primers (Molla Kazemiha et al. 2009).

DNA extraction: Conditioned medium was centrifuged for 1 min at 13,200 rpm. The pellet was incubated in equal proportions of extraction buffer (2 % Triton, 1 % SDS, 100 mM NaCl, 10 mM Tris-Cl pH 8.0, 1 mM EDTA) and phenol:chloroform:isoamyl alcohol with vortexing for 10 min, then centrifuged at 13,000 rpm and 4°C for 10 min. The upper phase was transferred into EtOH: Ammonium acetate (7.5 M) 6:1, then centrifuged at 13,000 rpm and 4°C for 15 min and the supernatant removed. The pellet was dried at 65°C for 5 min then resuspended in MQ H_2O (shook then incubated at 65°C for 5 min).

PCR: A master mix containing all reagents except DNA template was made for the number of reactions plus 10%, then aliquoted before adding template. Per reaction in 0.2 ml DNase-free PCR tubes was mixed: 1X GC buffer (NEB), 0.2 mM dNTPs, 2.4 pmol/µl each of the two primers (see Table 2.3), 0.5 units Phusion HF DNA polymerase (NEB) and 1 µl extracted DNA template (MQ H_2O for negative control), plus MQ H_2O up to a final volume of 25 µl. The reactions then underwent the following thermal cycle: first, 98°C for 5 min, then 35 cycles of 98°C for 30 s (denaturing), 55°C for 30 s (annealing) and 72°C for 1 min (elongation), finishing with 72°C for 10 min and then hold at 4°C.

Primer sequences:

Name	Description	Sequence	Melting temperature
Mycoplasma F	Forward primer to amplify mycoplasma 16 S rDNA	GTGGGGAGCAAAYAGGATTAGA	59°C
Mycoplasma R	Reverse primer to amplify mycoplasma 16 S rDNA	GGCATGATGATTTGACGTCRT	57°C

Table 2.3 Mycoplasma 16 S rDNA intergenic spacer region amplification primers

Gel electrophoresis: 5 µl PCR product mixed with 1 µl 6X blue loading dyes (NEB) and 1 µl DNA ladder (100 bp plus, Thermo) were loaded onto a 2% agarose/TBE/ethidium bromide gel and ran at 100 V for 40 min. The gel was imaged on a UV transilluminator (Syngene) and images captured by digital camera (Kodak EDAS 290) with 2 s exposure.

2.2.3 Differentiation and FK506 treatment

Differentiation: $1x10^5$ 3T3-L1 pre-adipocytes were seeded per well in 6-well plates and grown to confluence. Two days post-confluence (day 0) differentiation was induced in DMEM with 10% foetal bovine serum (FBS, Life Technologies) supplemented with 1 µg/ml insulin (Sigma), 0.5 mM 3-isobutyl-1-methylxanthine (IBMX, Sigma), 0.25 µM dexamethasone (Sigma) and DMSO (Sigma)/ethanol or FK506 (in DMSO/ethanol, Sigma). On day 2 fresh medium supplemented with insulin and DMSO/ethanol or FK506 only was applied. From day 4 cells were incubated in DMEM with 10% FBS, which was changed every 2 days.

2.2.4 Formaldehyde fixing of cells and quantifying TAG content (oil red O staining)

Fixed cells were washed 3 times in PBS and incubated in formaldehyde (Sigma) for 50-60 min. The cells were washed 6 times in PBS and incubated in 90 mg/ml oil red O (ORO) in 60% isopropanol. After 6 washes in water, the cells were photographed (EVOS XL

Core), then incubated in isopropanol for 10 min to extract the stain and absorbance measured at wavelength 520 nm (Shimadzu UV mini 1240 spectrophotometer) (Dzitoyeva & Manev 2013).

2.2.5 Quantifying total cell mass (methylene blue staining)

Adapted from (Oliver et al. 1989). Fixed cells were washed 3 times in MQ H_2O and incubated in 800 µl 0.01% methylene blue in 0.01 M borate buffer (volume and concentration varied as specified in figure legend during method optimisation) for 30 min at room temperature. After 4 washes in 0.01 M borate buffer, the cells were photographed (EVOS XL Core) and scanned (Epsom Perfection 3170 Photo), then incubated in 400 µl extraction buffer (1:1 ethanol:0.1 M HCl) for 5 min at room temperature with shaking at 75 rpm. The extracted stain was diluted 1/50 and absorbance measured at wavelength 650 nm (Shimadzu UV mini 1240 spectrophotometer).

2.2.6 Harvesting cells and medium

Cells were harvested on days 0 (immediately before applying differentiation medium), 5, 10, 15 and 20. Medium was collected from each well and immediately frozen at -80°C. Cells were then incubated for minimum 2 h in DMEM, without FBS. Cells were released from the surface of the plate by trypsinisation with TrypLE Express (Life Technologies), viable cell number counted (Cellometer), washed in PBS (Sigma) and centrifuged. The cell pellets (two per well) were stored at -80°C.

2.2.7 RNA extraction

2.2.7.1 Phenol-chloroform extraction

Cell pellets were incubated in equal volumes TES buffer and acid phenol at 65°C with agitation at 1400 rpm for 30 s every 5 min for a total of 20 min in the thermomixer (Eppendorf). The sample was centrifuged at 13,000 rpm and 4°C for 10 min and the upper phase transferred into 5.5% v/v 3 M NaOAc /EtOH. The sample was incubated at -80°C for 30 min and centrifuged at 13,000 rpm and 4°C for 15 min. The supernatant was discarded and the pellet air dried at room temperature then resuspended in milli-q water (Millipore). DNase, DNase buffer (Roche) and RNase out (Invitrogen) were added and the sample incubated at 37°C for 30 min. An equal volume of acid phenol was added and the sample vortexed for 1 min then centrifuged at 13,000 rpm and 4°C for 15 min. The upper phase was transferred into 5.5% v/v 3 M NaOAc/EtOH and the sample incubated at -80°C for 30 min then centrifuged at 13,000 rpm and 4°C for 15 min. The supernatant was discarded and the pellet air dried at room temperature then resuspended in milli-q water (Millipore).

2.2.7.2 RNeasy lipid tissue kit

RNA was purified using the RNeasy lipid tissue kit (Qiagen) according to the manufacturer's protocol, either with or without the optional DNase step.

2.2.8 Reverse transcription and PCR

cDNA was synthesised from purified RNA using oligo dT primer and SuperScript III Reverse Transcriptase (Invitrogen) according to the manufacturer's protocol. β-actin cDNA fragments were PCR amplified using Phusion Taq (NEB) using a 52°C annealing temperature, 1 min extension time and 50 cycles. PCR products were separated by gel

electrophoresis on a 1% agarose/TBE/EtBr gel and identified by molecular weight. Image taken under UV light (Kodac EDAS 290).

Primer sequences:

Name	Description	Sequence	Melting temperature
B-actin(M)170_F	Forward primer to amplify β-actin DNA fragment	AGGCCCAGAGCAAGAGAG	58°C
B-actin(M)388_R	Reverse primer to amplify β-actin DNA fragment	GGGTGTTGAAGGTCTCAAAC	57°C

Table 2.4 Primers to amplify 219 bp fragment of mouse β-actin

2.2.9 RNA-seq

Purified RNA was diluted to 54 ng/µl and 4 µl was mixed with 1 µl 1/250 diluted ExFold RNA spike in mix 1 or 2 (ERCC). Libraries were prepared for RNA-seq using the 3' mRNA-seq library preparation kit for Ion Torrent (Lexogen) according to the manufacturer's protocol. Library concentration was measured using a High Sensitivity DNA chip (Agilent) on the Agilent 2100 Bioanalyzer according to the manufacturer's protocol.

RNA-seq was performed using the Ion PI Hi-Q kit on the Ion Chef System and Proton Semiconductor Sequencer (Ion Torrent by Life Technologies), according to the manufacturer's protocol.

2.2.10 RNA-seq data analysis

Base calls were generated by the Torrent Server analysis and aligned to the mm10 mouse reference genome using the Torrent Mapping Alignment Program (TMAP), which combines three alignment algorithms (BWA-short, BWA-long and SSAHA). The absolute reads were analysed by Dr. H. Fischl using the DESeq algorithm from the DESeq2 package (Love et al. 2014) within R/Bioconductor. This was applied to the read counts for all three

biological replicates across the two conditions being compared. RNAs were identified as significantly differentially expressed if $p < 0.05$, after adjustment for multiple testing using the Benjamini-Hochberg method. I analysed these lists of differentially regulated RNAs using the PANTHER overrepresentation test (Mi & Thomas 2009; Mi et al. 2016) to identify GO-terms and PANTHER pathways associated with these genes.

3 Results – FK506 altered the rate of *C. elegans* ageing

3.1 Introduction

FK506 was identified in a phenotypic screen as able to extend *C. elegans bus-5* lifespan, with an optimum dose of 50 μg/ml (section 1.2.6). In this study, the results of the screen were confirmed in *C. elegans bus-5* and *bus-8*. The *bus-5* and particularly *bus-8* cuticle-formation mutations affect the health of the worms, with *bus-5* mutants having skiddy movement and *bus-8* mutants having greatly reduced mobility and a shortened lifespan. Therefore, the effect of FK506 on the wild-type strain *C. elegans* N2 lifespan was assayed to investigate whether FK506 interacts with the genotype of the *bus-5* and *bus-8* strains rather than normal *C. elegans* ageing.

Whilst the phenotypic screen is useful for identifying lifespan-extending compounds, it offers no insight into the mechanism of action of these compounds. Potentially, FK506 may not be acting directly on *C. elegans* ageing, but could instead be creating dietary restriction (DR) conditions that have an anti-ageing effect. DR extends lifespan and delays ageing in many organisms, including *C. elegans* (section 1.1.5.1). The main mechanisms of DR in *C. elegans* are limiting *E. coli* food intake by inhibiting *E. coli* growth or *C. elegans* pharyngeal pumping, so the effect of FK506 on these characteristics was tested.

The effect of FK506 on the rate of *C. elegans* ageing was characterised by assaying healthspan. Does FK506 delay ageing, extending the time spent in good health, or does FK506 just delay death, prolonging only the latter stages of life? Lifespan and healthspan are correlated, but this relationship is not fixed. There are several methods to measure healthspan (section 1.4.2), including pharynx pumping rate and thrashing rate, which measure muscle function, and the accumulation of lipofuscin, gut bacteria and tissue degradation, which indicate a decline in organismal maintenance. As pharynx pumping and thrashing rate are most easily quantified, these are the methods used here. Healthspan can be measured in early adulthood, whilst population survival is >95%.

FK506 treatment timing requirement was also tested – is constant treatment required, or is treatment during a specific life stage, for example during development or adulthood, most important (Rangaraju et al. 2015)? For example, if FK506 altered the rate of ageing by influencing development, then treatment solely during the larval stages would be sufficient to extend lifespan.

FK506 is known to be temperature sensitive and degrade over time (section 1.2). As such, FK506 is unlikely to be stable and remain fully active for the entire duration of these experiments. FK506 will also be metabolised by *E. coli* OP50, further reducing activity over time. Here, thrashing was assayed on plates that had been treated with FK506 and stored at room temperature for a week compared to the normal freshly prepared plates, to test how quickly FK506 loses activity.

Also investigated here was the effect of FUdR, used to prevent growth of offspring and known to extend *C. elegans* lifespan. Does FUdR, routinely used in lifespan experiments, interact with the mechanism of action of FK506? If so, the pathways targeted by FK506

may overlap with the pathways involved with the ageing mechanism of reproduction. Blocking reproduction, either with FUdR, laser ablation of the gonad or gonadless-mutants like *glp-1*, extends lifespan.

3.2 FK506 increased *C. elegans* lifespan under crowded conditions

To confirm the result of the phenotypic screen, the effect of FK506 on *C. elegans* lifespan was assayed in the *bus-5*, *bus-8* and wild-type N2 strains. Lifespan assays are normally performed in uncrowded conditions (up to 10 worms per plate), as the degree of crowding can impact on lifespan (Barna et al. 2012). However, the phenotypic screen was conducted with a high density of worms. The crowding stress response may be triggered through two mechanisms: mechano-sensation of collisions with other worms or chemo-sensation of the molecules secreted by other worms.

3.2.1 FK506 increased *C. elegans bus-5* lifespan under conditions of population crowding, but had no effect in uncrowded conditions

The effect of FK506 on *C. elegans bus-5* lifespan was tested under uncrowded and crowded conditions.

3.2.1.1 FK506 had no effect on *C. elegans bus-5* lifespan in uncrowded conditions

In uncrowded conditions, with 5 or 10 worms per plate, FK506 did not extend *C. elegans bus-5* lifespan at concentrations up to 75 µg/ml (Figure 3.1 A). As FK506 is a highly unstable compound, suboptimal conditions during manufacturing or shipping could reduce biological activity, so FK506 from a different supplier was tested. However, FK506

supplied by Tocris, compared to previous batches obtained from Abcam (Figure 3.1 A), showed no effect on *C. elegans bus-5* lifespan at a dose of 50 µg/ml (Figure 3.1 B).

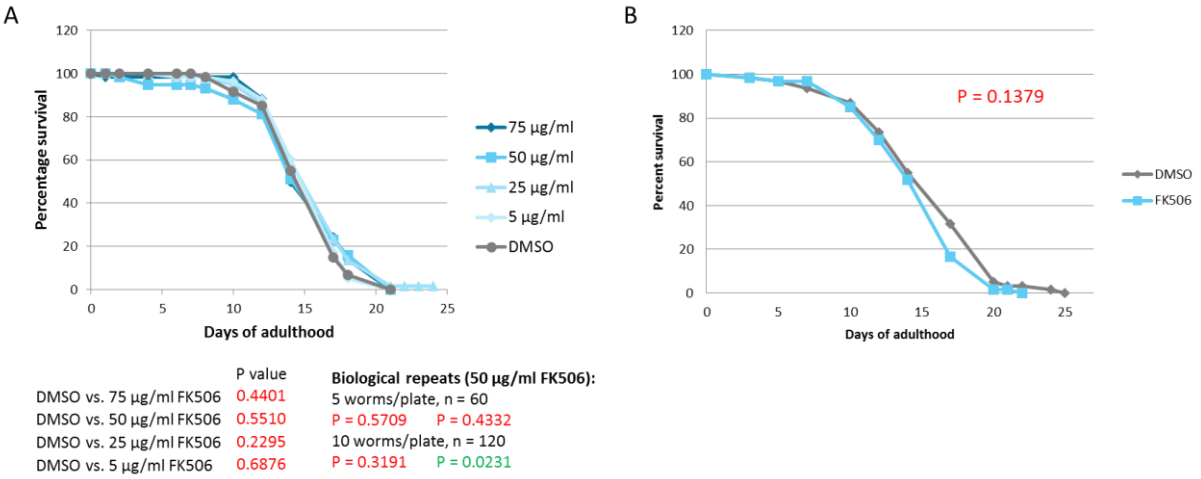

Figure 3.1 FK506 did not extend C. elegans bus-5 lifespan. (A) C. elegans bus-5 dose response to FK506 (manufacturer Abcam). 5-75 µg/ml FK506 had no significant effect on C. elegans bus-5 lifespan (5 worms/plate, n = 60). In two biological repeats 50 µg/ml FK506 had no effect on bus-5 lifespan with 5 worms/plate (n = 60). With 10 worms/plate (n = 120), in one biological repeat 50 µg/ml FK506 had no effect, but in another repeat significantly increased bus-5 lifespan. (B) After changing FK506 supplier to Tocris, 50 µg/ml FK506 still had no significant effect on C. elegans bus-5 lifespan (5 worms/plate, n = 60). P values calculated using OASIS Log-Rank Test.

3.2.1.2 FK506 increased *C. elegans bus-5* lifespan under crowded conditions

As the phenotypic screen was performed with a high population density, *C. elegans bus*-5 lifespan was assayed under conditions of population crowding. With 100 worms per plate, FK506 extended *bus-5* lifespan (Figure 3.2), and was able to do so in most biological repeats. Due to the highly unstable state of FK506, and the highly sensitive nature of lifespan assays, the degree of lifespan extension caused by FK506 was variable and occasionally there was no significant difference (<1/3 of experiments). Therefore, the lifespan-extending effect of FK506 required the crowding stress response to be active.

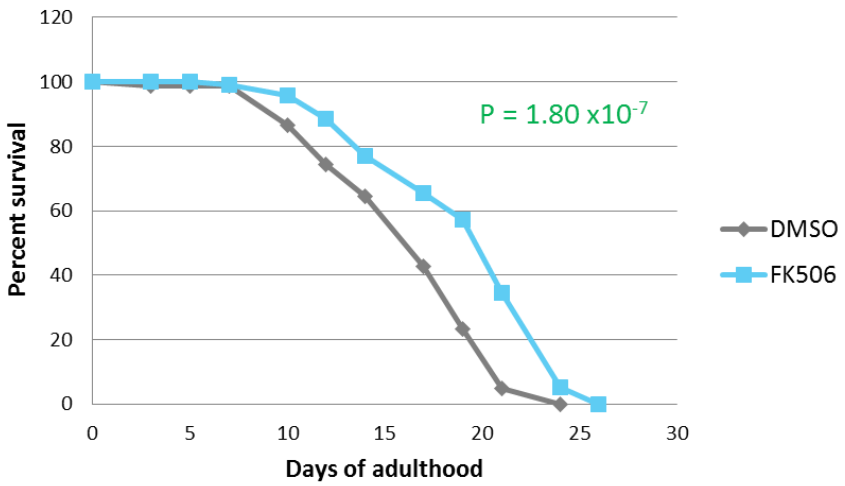

Figure 3.2 FK506 extended C. elegans bus-5 lifespan under crowded conditions. 50 µg/ml FK506 significantly extended bus-5 lifespan (P = 1.80x10^{-7}) with 100 worms per plate, and did so in most biological repeats. N = 100, P values calculated by OASIS using log-rank test.

When the lifespan of *C. elegans bus-5* was assayed under crowded conditions of 63 worms per plate, FK506 caused a non-significant increase in *bus-5* lifespan (Figure 3.3). Therefore the action of FK506 is proportional to the degree of crowding and how active the population crowding stress response is.

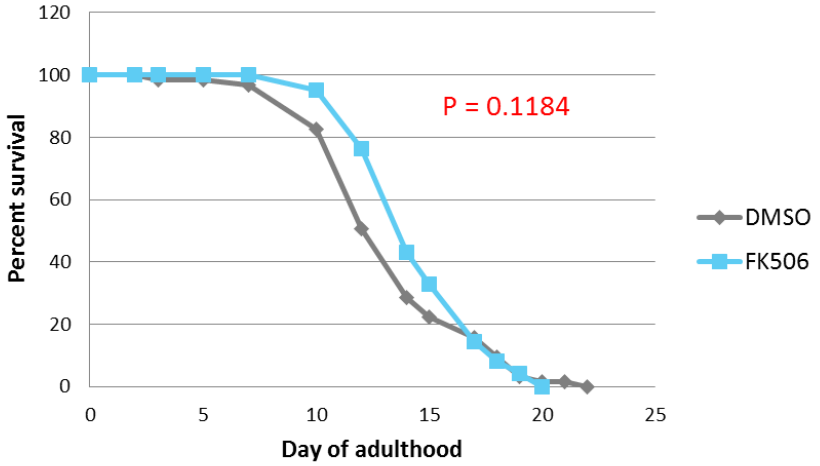

Figure 3.3 FK506 did not extend C. elegans bus-5 lifespan with 63 worms per plate. 50 µg/ml FK506 did not significantly extend bus-5 lifespan (P = 0.1184) with 63 worms per plate. N = 63, P values calculated by OASIS using log-rank test.

3.2.2 FK506 increased *C. elegans bus-8* lifespan under conditions of population crowding, but had no effect in uncrowded conditions

Whilst the *bus-8* strain is the more commonly used drug-sensitive strain in the literature, the *bus-8* worms are much less healthy (decreased movement around the plate) and have a shorter lifespan than *C. elegans* N2 and *bus-5* (maximum lifespan roughly 15-17 days of adulthood, rather than >20), due to the more severe cuticle mutation. Previous work in the lab found that 10 µg/ml FK506 was the optimum dose for *C. elegans bus-8* (rather than 50 µg/ml for *C. elegans bus-5*). In common with the effect observed in *C. elegans bus-5*, FK506 did not extend *bus-8* lifespan in uncrowded conditions of five worms per plate (Figure 3.4), but did significantly increase lifespan in crowded conditions of 100 worms per plate (Figure 3.5). Therefore the lifespan-extending effect of FK506 in *C. elegans bus-8* also requires activation of the crowding stress response.

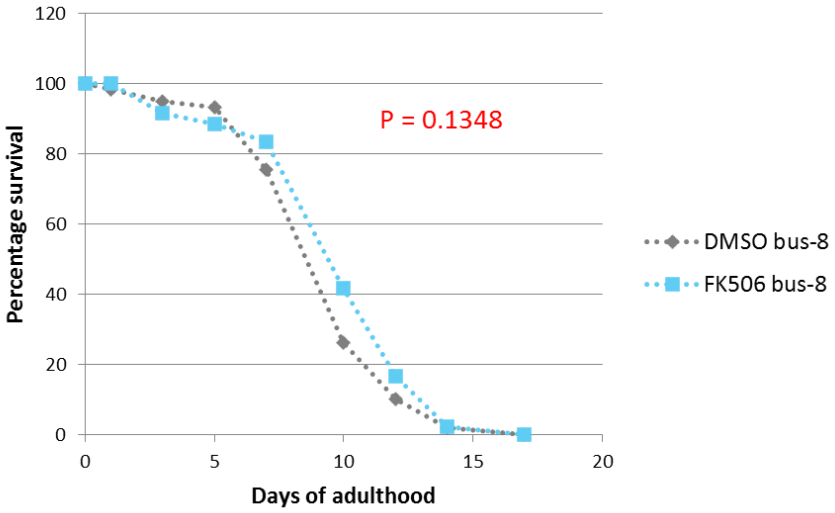

Figure 3.4 FK506 did not extend C. elegans bus-8 lifespan in uncrowded conditions. 10 µg/ml FK506 had no significant effect on bus-8 lifespan (P = 0.1348). 5 worms/plate, n = 60, P values calculated by OASIS using log-rank test.

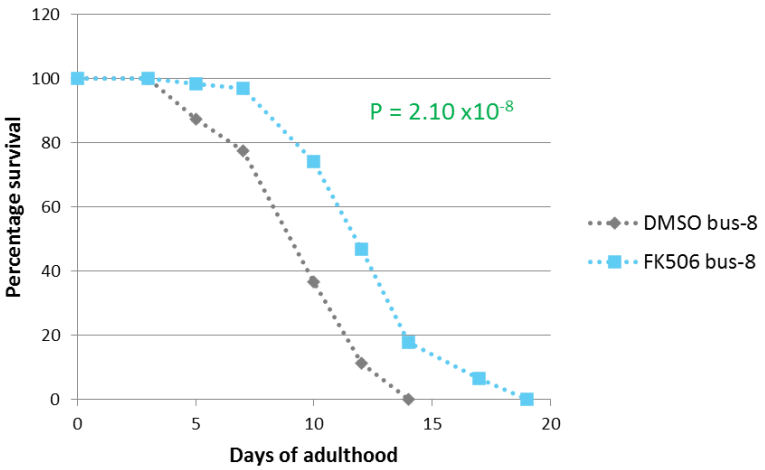

Figure 3.5 FK506 extended C. elegans bus-8 lifespan in crowded conditions. 10 µg/ml FK506 significantly increased bus-8 lifespan (P = 2.10x10^{-8}). 100 worms/plate, n = 100, P values calculated by OASIS using log-rank test.

3.2.3 FK506 increased *C. elegans* N2 lifespan under conditions of population crowding, but had no effect in uncrowded conditions

The drug sensitive *C. elegans bus-5* and *bus-8* strains were used in the phenotypic screen to ensure biologically active compounds that were unable to cross the *C. elegans* cuticle were not missed, as only a limited amount of compound will be ingested orally by the worms. However, using these strains carries the risk that the compounds do not target normal *C. elegans* ageing and instead interact with the genotype. Rapamycin, structurally related to FK506 and with a similar molecular weight, is biologically active in *C. elegans* N2 so in theory FK506 should also be able to extend lifespan in *C. elegans* N2. Therefore the effect of FK506 on the lifespan of the wild-type strain *C. elegans* N2 was tested in uncrowded and crowded conditions.

3.2.3.1 FK506 had no effect on *C. elegans* N2 lifespan in uncrowded conditions

The effect of FK506 on *C. elegans* N2 lifespan was tested in uncrowded conditions of five worms per plate. FK506 had no significant effect on *C. elegans* N2 lifespan in uncrowded

conditions at 50 µg/ml, with either 1.5% or 0.5% DMSO (Figure 3.6 A and B respectively). This lack of effect was not caused by too low a dose, as higher doses had either no effect or decreased lifespan.

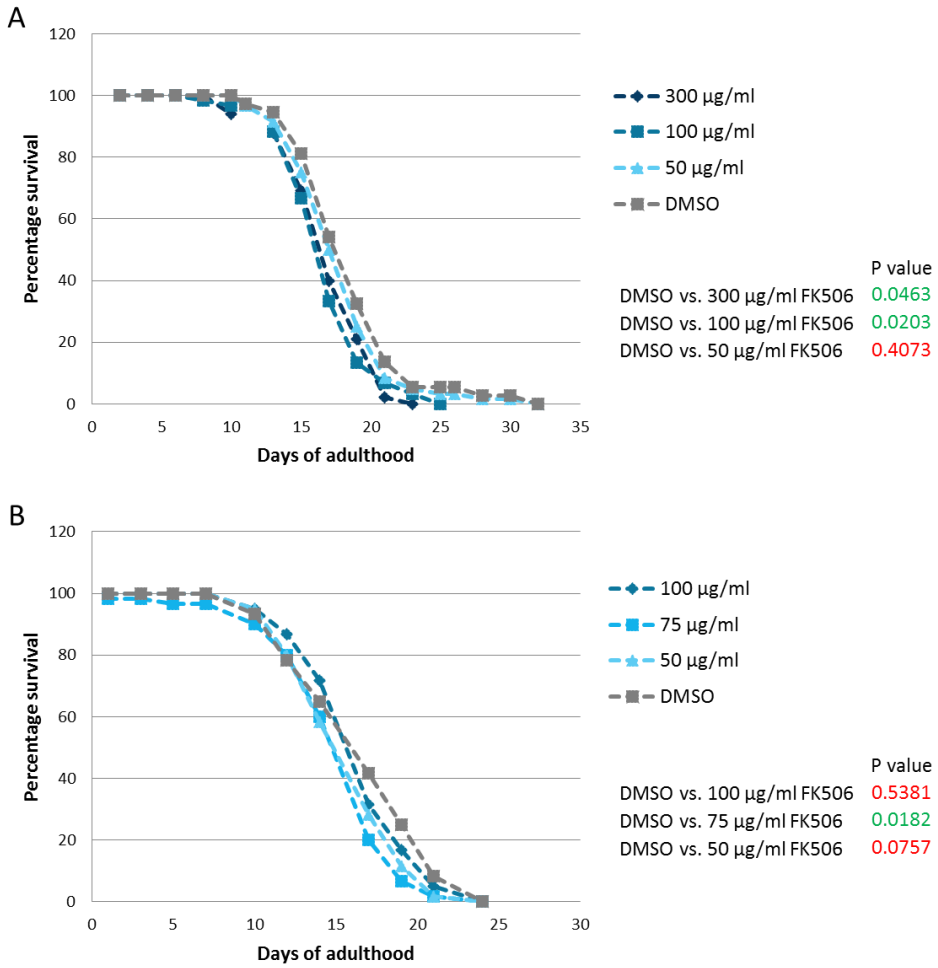

Figure 3.6 FK506 did not extend C. elegans N2 lifespan in uncrowded conditions. (A) With 1.5% DMSO, 100 and 300 µg/ml FK506 decreased N2 lifespan whilst 50 µg/ml FK506 had no significant effect. (B) With 0.5% DMSO, 75 µg/ml FK506 decreased N2 lifespan whilst 50 and 100 µg/ml FK506 had no significant effect. 5 worms/plate, n = 60, P values calculated using OASIS Log-Rank Test.

3.2.3.2 FK506 increased *C. elegans* N2 lifespan under crowded conditions

FK506 was able to increase *C. elegans bus-5* and *bus-8* lifespans under conditions of population crowding stress, so the effect of FK506 on *C. elegans* N2 lifespan was tested

under crowded conditions. With crowded conditions of 100 worms per plate, 50 µg/ml FK506 increased *C. elegans* N2 lifespan in two of three biological repeats (Figure 3.7).

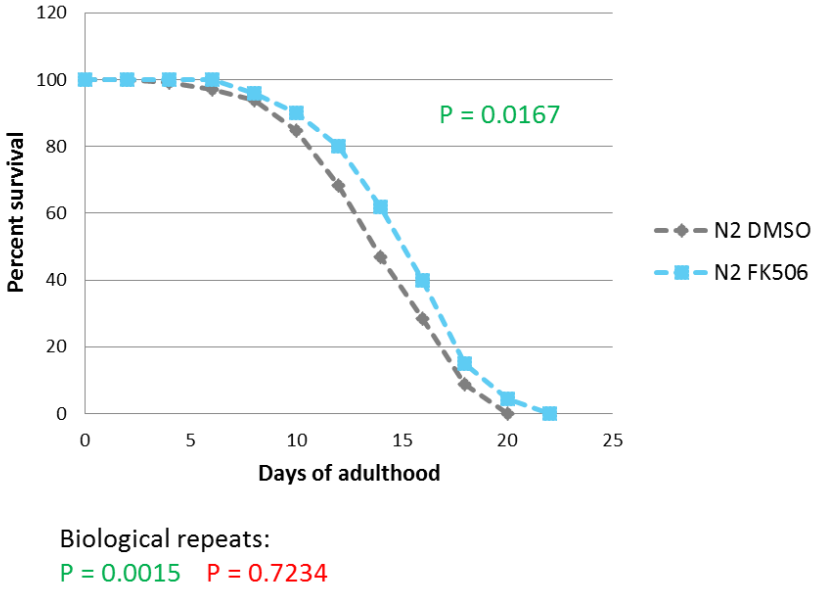

Figure 3.7 FK506 extended C. elegans N2 lifespan under crowded conditions. 50 µg/ml FK506 increased N2 lifespan (P = 0.0167). In one biological repeat FK506 increased lifespan (P = 0.0015) whilst in another FK506 had no effect (P = 0.7234). 100 worms/plate, n = 100, P values calculated using OASIS Log-Rank Test.

FK506 was able to extend lifespan in *C. elegans bus-5*, *bus-8* and N2 strains, so the lifespan extending effect is not a result of an interaction with the cuticle mutation genotypes and instead FK506 must influence normal *C. elegans* ageing. The interaction with crowding stress was seen in all three strains as well, suggesting that this is important to the mechanism of action of FK506.

3.2.3.3 *C. elegans bus-5* and N2 had similar lifespans

FK506 was able to extend lifespan in both *C. elegans bus-5* and N2 under crowded conditions. However, this effect was more reliable in *bus-5* than N2, possibly because FK506 is more bioavailable in the *C. elegans bus-5* strain, as the cuticle does not impede

uptake. The lifespan of *C. elegans bus-5* was not significantly different to the lifespan of *C. elegans* N2 in two biological repeats (Figure 3.8), suggesting *C. elegans bus-5* ages normally. Therefore, *C. elegans bus-5* is a suitable model of normal ageing.

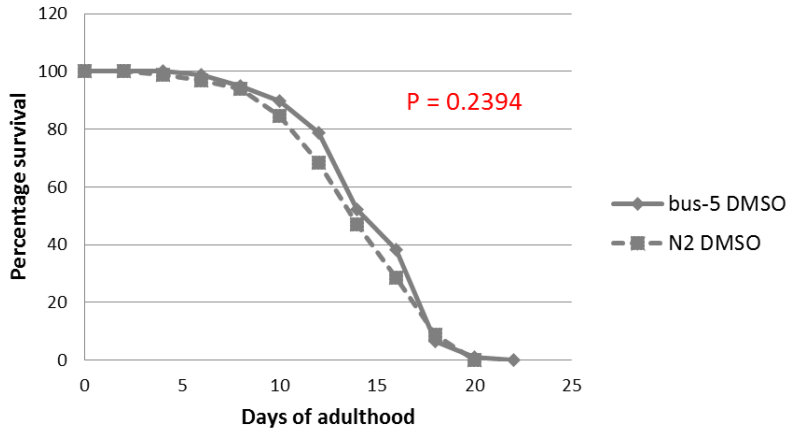

Biological repeat: P = 0.0839

Figure 3.8 C. elegans bus-5 and C. elegans N2 did not have significantly different lifespans when treated with 0.5% DMSO. 100 worms/plate, n = 100, P values calculated using OASIS Log-Rank Test.

3.2.4 DMSO increased lifespan of *C. elegans bus-5* and N2, but not *bus-8*

FK506 is not water-soluble, so must be dissolved in a non-polar solvent, such as ethanol or DMSO. Chronic ethanol treatment has a positive effect on *C. elegans* lifespan during larval stages but a negative effect during adulthood (Davis et al. 2008), whereas 1% DMSO extends lifespan in a DR and IIS independent manner, potentially by preventing protein aggregation (Frankowski et al. 2013). As both solvents effect lifespan, both could interact with FK506.

A final volume of 0.5% DMSO was used in all experiments to dissolve FK506 (and other non-water soluble compounds), as this is the minimum volume required to dissolve the desired concentrations of both FK506 and rapamycin together (section 4.5.1).

0.5% DMSO extended lifespan in *C. elegans* N2 and *bus-5*, but not *bus-8* (Figure 3.9 B, C

and D respectively). 1.5% DMSO caused an even more significant increase in N2 lifespan (Figure 3.9 A). Although the concentration of DMSO used did increase lifespan, alternative solvents also effect lifespan and could potentially interact with FK506, so it was decided to use DMSO to provide continuity with the work of previous lab members.

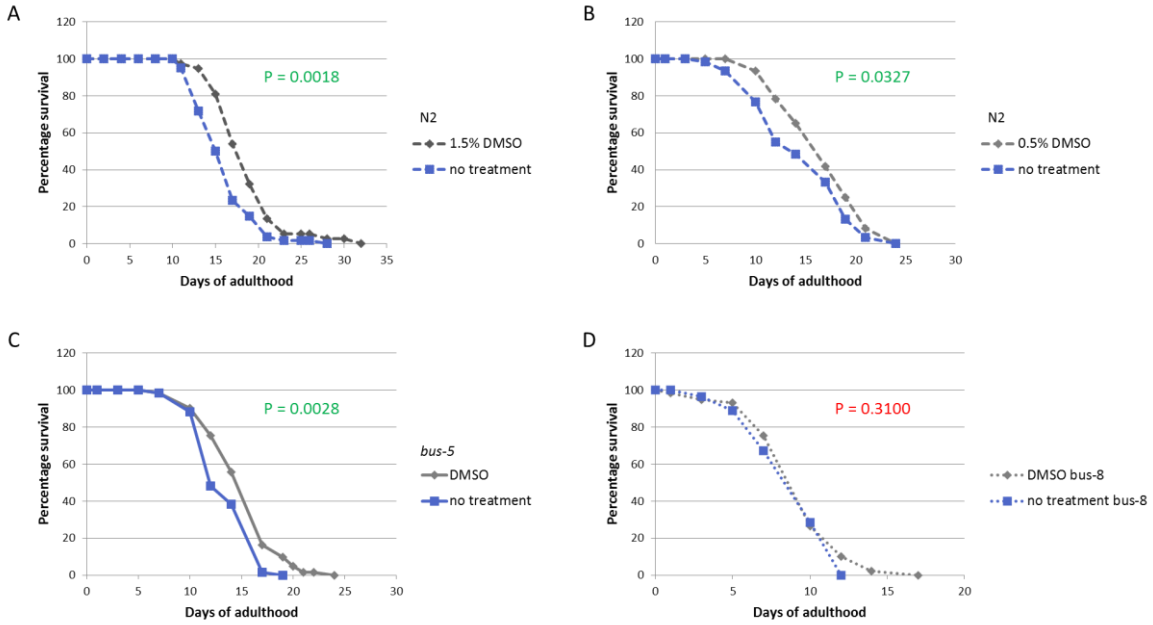

Figure 3.9 DMSO extended C. elegans N2 and bus-5 lifespan, but not bus-8 lifespan. 1.5% (A) and 0.5% (B) DMSO significantly extended C. elegans N2 lifespan (P = 0.0018 and 0.0327 respectively). 0.5% DMSO significantly extended C. elegans bus-5 lifespan (C, P = 0.0028) and also extended bus-5 lifespan in a second biological repeat (P = 0.0013, 10 worms/plate, n = 120). 0.5% DMSO had no effect on C. elegans bus-8 lifespan (D, P = 0.3100). (A, B, C, D) 5 worms/plate, n = 60, P values calculated using OASIS Log-Rank Test.

3.3 The effect of FK506 on *C. elegans* lifespan was not due to dietary restriction

Dietary restriction (DR) requires limited caloric intake, whilst maintaining optimum nutrition levels. DR extends lifespan in all organisms it has been tested in, from yeast and *C. elegans*, to mice and rhesus monkeys (Colman et al. 2014; Colman et al. 2009; Greer & Brunet 2009). DR also delays the onset of various age-related disorders, including diabetes, cancer and cardiovascular disease in rhesus monkeys (Colman et al. 2009). If

FK506 limited food intake, either by inhibiting *E. coli* growth or by decreasing pharynx pumping (contraction of the head muscle), this would create DR conditions and FK506 would be only indirectly causing lifespan extension.

3.3.1 FK506 did not inhibit growth of *E. coli* strain OP50

Limiting the availability of bacteria, either by supplying a reduced volume or providing dead bacteria, causes DR and extends *C. elegans* lifespan (Greer & Brunet 2009). FK506 inhibits growth of certain funguses, but has no known anti-bacterial activity (Kino et al. 1987; Lamoth et al. 2015). If FK506 inhibited *E. coli* growth, this would limit the food intake of the worms, creating DR conditions, and therefore indirectly cause lifespan extension.

FK506 did not significantly reduce the number of *E. coli* OP50 colonies grown at up to 50 µg/ml (Figure 3.10), the concentration used to treat *C. elegans bus-5*. Therefore FK506 did not inhibit *E. coli* OP50 growth, so does not cause DR via this mechanism.

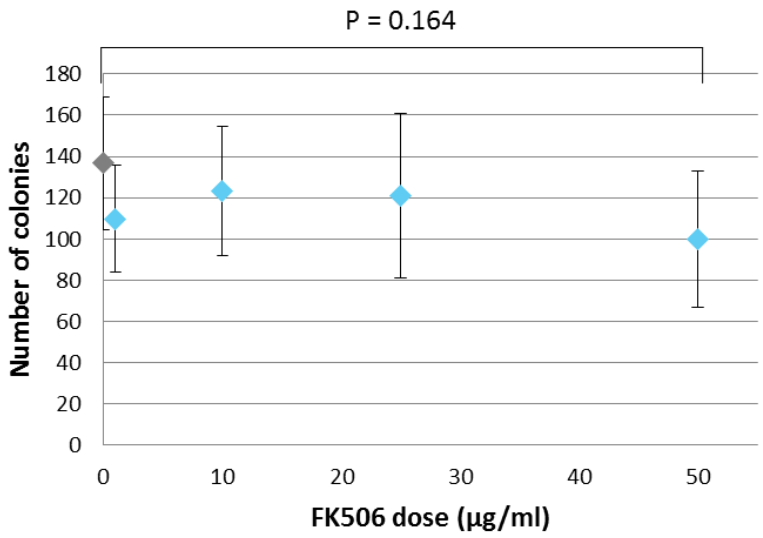

Figure 3.10 FK506 did not inhibit growth of E. coli OP50 at concentrations up to 50 µg/ml, the dose used to treat C. elegans bus-5. P=0.164 (T test), n=6, error bars = SEM.

3.3.2 FK506 did not inhibit pharyngeal pumping

Pumping of the pharyngeal muscle within the head of *C. elegans*, shown in Figure 3.11, allows intake of food. Inhibition of pharyngeal pumping limits food intake, causing DR, and extends worm lifespan. Mutation of the *C. elegans eat-2* gene, required for normal pharynx muscle function, causes an increase in lifespan via DR (Lakowski & Hekimi 1998). If FK506 inhibited pharyngeal pumping, this would decrease food intake, causing DR and indirect lifespan extension.

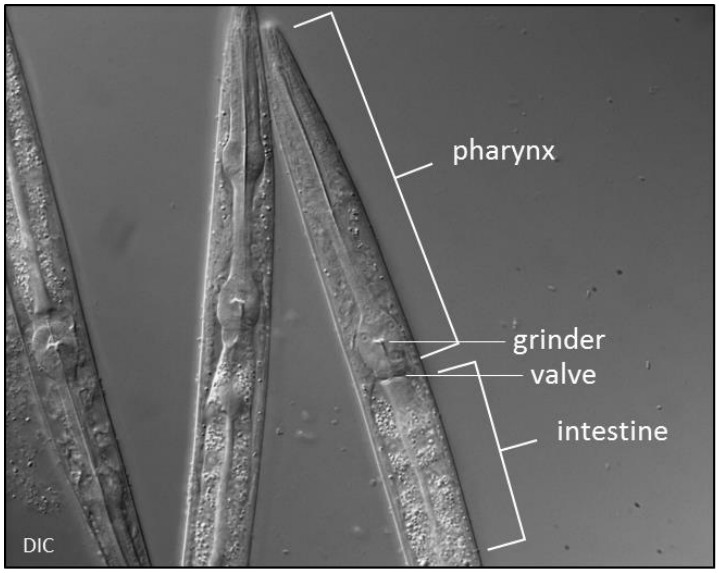

Figure 3.11 Light microscope image of C. elegans bus-5 head, with the pharynx labelled. Pumping of the pharyngeal muscle causes intake of food, so inhibition of pharynx pumping would cause dietary restriction. 0.5% DMSO treatment, day 5 of adulthood. Assisted by Dr. M. Gravato-Nobre.

Pharynx pumping was measured during early adulthood, at days 2 to 6 of adulthood. Earlier than this pharynx pumping is too quick to count accurately and later than this natural population variation becomes too large to be able to see significant differences between treatment groups. Pharyngeal pumping was assayed with 20 worms per plate from L4 stage, instead of the 100 worms per plate used in lifespan experiments, as only n = 10 was required.

3.3.2.1 FK506 increased or had no effect on *C. elegans bus-5* pharynx pumping rate

Pharyngeal pumping rate was assayed with an additional population synchronisation step at L1 stage by starvation, and also without this step as starvation during development may alter ageing.

50 µg/ml FK506 did not inhibit pharynx pumping during the early adulthood of *C. elegans bus-5* worms, with or without an additional step of population synchronisation by

arresting at the L1 stage by starvation. With arrest at L1, FK506 increased the rate of pumping at day 3 and had no significant effect at day 6, mainly due to increased population variation (Figure 3.12). Without starvation the increase in pumping rate was seen less consistently, but FK506 either had no effect or increased pumping rate at day 3 or 4 of adulthood (Figure 3.13).

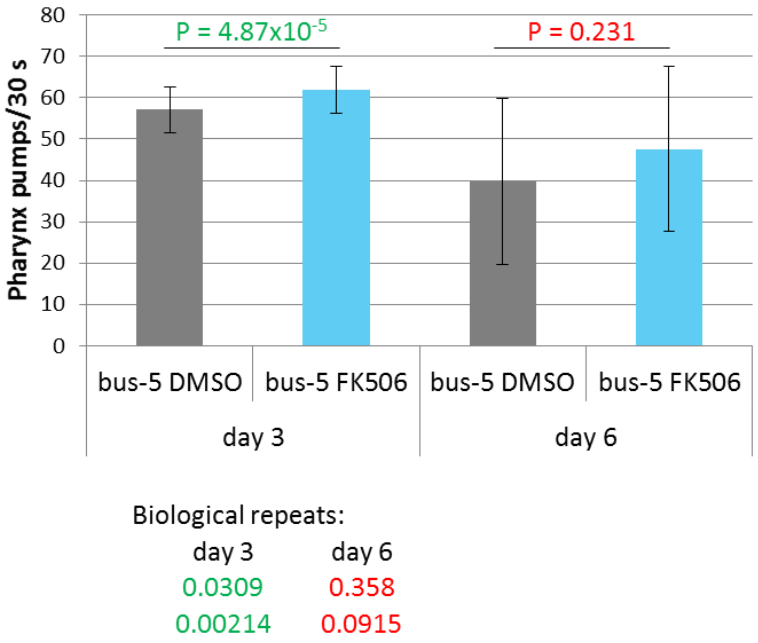

Figure 3.12 With arrest at L1 stage by starvation, FK506 increased C. elegans bus-5 pharynx pumping rate at day 3 of adulthood, but not day 6. 50 µg/ml FK506 significantly increased bus-5 pharynx pumping rate at day 3 of adulthood but had no significant effect at day 6 of adulthood. Error bars = SD, n = 10, P values calculated using T Test.

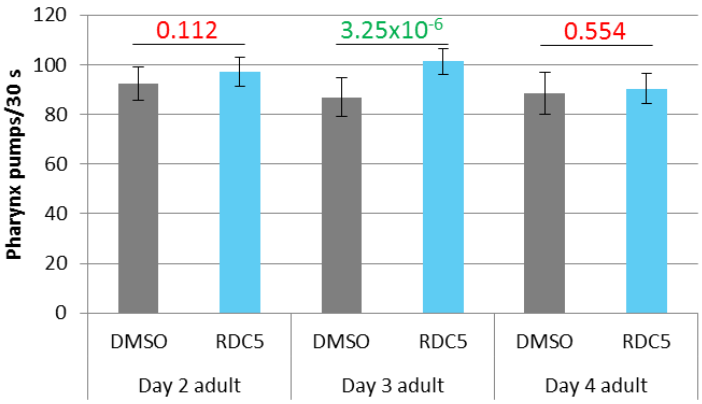

Biological repeats:

	Day 2	Day 3	Day 4
DMSO vs. FK506	0.90018	0.945451	0.018146

	Day 3	Day 5
DMSO vs. FK506	0.64158	0.184666

	Day 3	Day 6
DMSO vs. FK506	0.014264	0.508259

Figure 3.13 Without L1 stage arrest, FK506 increased or had no effect on C. elegans bus-5 pharynx pumping rate. 50 µg/ml FK506 mainly had no significant effect on bus-5 pharynx pumping rate at days 2 to 6 of adulthood. In two biological repeats FK506 significantly increased pumping rate at day 3 of adulthood, and in one repeat at day 4. Error bars = SEM, n = 10, P values calculated using T Test.

FK506 did not inhibit *C. elegans bus-5* pharynx pumping, so did not cause DR by limiting food intake. Instead FK506 tended towards an increased pumping rate. As pharynx pumping naturally declines with age, this suggests FK506 increases healthspan as well as lifespan.

3.3.2.2 FK506 increased or had no effect on *C. elegans bus-8* pharynx pumping rate

The effect of 10 µg/ml FK506 on *bus-8* pharyngeal pumping was measured in early adulthood after arrest at the L1 stage by starvation (Figure 3.14). FK506 did not inhibit pumping rate, so (as in *C. elegans bus-5*) FK506 did not cause DR via this mechanism in *C. elegans bus-8*. FK506 increased the rate of thrashing at day 3 of adulthood, albeit less

consistently than the effect on *C. elegans bus-5*, again suggesting an increased healthspan.

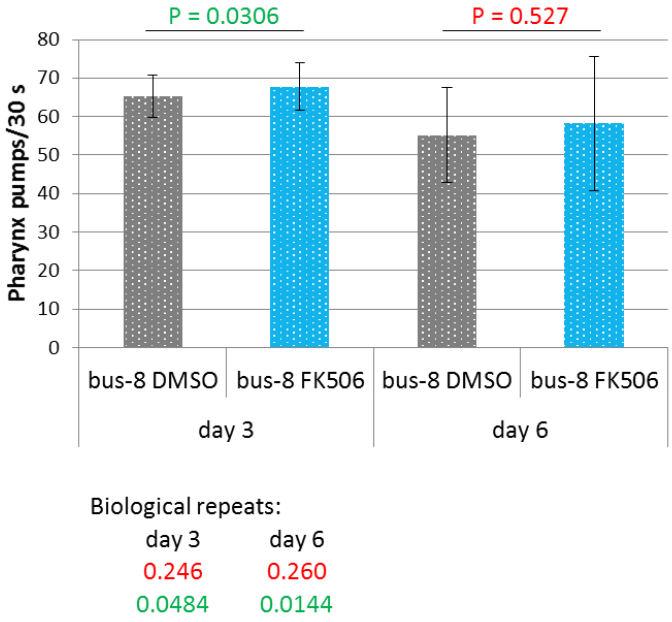

Figure 3.14 With arrest at L1 stage by starvation, FK506 increased or had no effect C. elegans bus-8 pharynx pumping rate. 10 µg/ml FK506 significantly increased bus-5 pharynx pumping rate at day 3 of adulthood in two biological repeats, but had no effect in a third repeat. At day 6 of adulthood, FK506 had no significant effect in two repeats, but increased pharynx pumping in one repeat. Error bars = SD, n = 10, P values calculated using T Test.

FK506 did not inhibit *E. coli* OP50 growth and did not inhibit pharyngeal pumping. This suggests that FK506 does not cause DR conditions, and instead has a direct anti-ageing effect on *C. elegans*.

3.3.3 FK506 and dietary restriction did not have an additive effect on lifespan

Dietary restriction extends lifespan and delays ageing in every organism it has been tried in (section 1.1.5.1). To test whether FK506 is a DR-mimetic, targeting the same ageing pathways that DR affects, *C. elegans bus-5* were treated with FK506 in the presence of DR conditions. There are many different methods of DR in *C. elegans*, so the method of

withdrawing all *E. coli* OP50 at day 2 of adulthood was selected as it is frequently used in the literature (Greer & Brunet 2009; Kaeberlein et al. 2006).

C. elegans bus-5 were treated with 50 µg/ml FK506 from hatching in the presence of DR conditions from day 2 of adulthood, and lifespan with population crowding was assayed (Figure 3.15). As expected, DR conditions significantly increased *bus-5* lifespan, almost doubling maximum lifespan from 21 days of adulthood (DMSO) to 39 days of adulthood (DMSO + DR). Under normal feeding conditions of an excess of *E. coli* OP50 throughout life, FK506 treatment significantly extended lifespan, but under DR conditions FK506 significantly decreased lifespan. This negative effect of FK506 occurred from 50% population mortality onwards. At 25% mortality there was no significant difference between DMSO-treated and FK506-treated *bus-5* under DR conditions, but at 50%, 75% and 90% mortality FK506 treatment significantly decreased lifespan. This suggests that FK506 does target the same pathways as DR, and in later life has an additional negative effect.

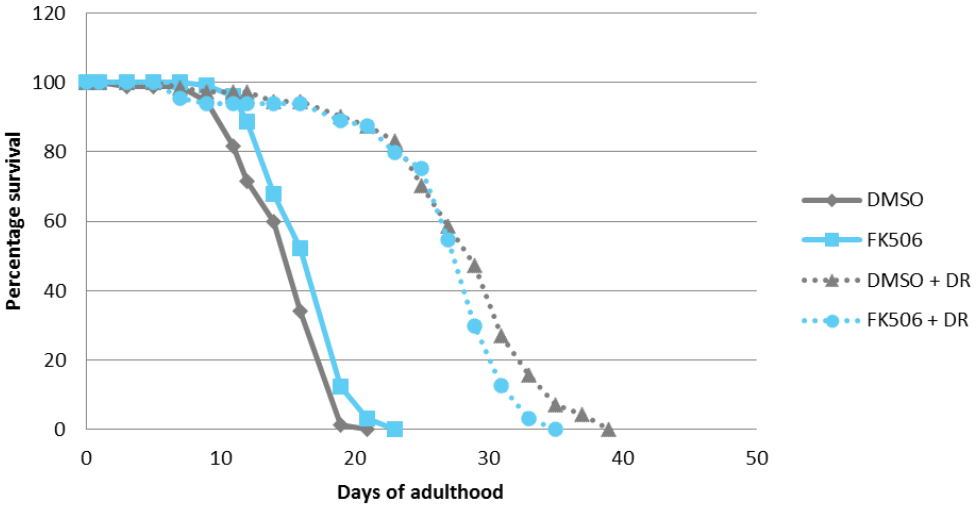

Log-Rank Test	P value
DMSO vs. FK506	0.0012
DMSO vs. DMSO + DR	0.0
DMSO + DR vs. FK506 + DR	0.0238

Fisher's Exact Test	
DMSO + DR vs. FK506 + DR	
Population mortality	**P value**
25%	0.7039
50%	0.0265
75%	0.0188
90%	0.0082

Figure 3.15 FK506 decreased C. elegans bus-5 lifespan (with population crowding) in combination with dietary restriction. DR conditions were created by transferring the worms to NGM plates without E. coli OP50 at day 2 of adulthood. With continual E. coli OP50 feeding, 50 µg/ml FK506 extended bus-5 lifespan compared to the DMSO vehicle-treated control, but in the presence of DR FK506 decreased bus-5 lifespan. DR conditions significantly extended lifespan, almost doubling the maximum lifespan of the DMSO-treated controls. 100 worms/plate, n = 100, P values calculated using OASIS Log-Rank Test and Fisher's Exact Test.

3.4 FK506 increased *C. elegans* thrashing rate

FK506 increased *C. elegans bus-5* and *bus-8* pharynx pumping rate, suggesting an increased healthspan as well as lifespan. Thrashing rate, the speed of body bends by a worm in liquid, is another measure of healthspan. Thrashing rate decreases with age, and is correlated with lifespan (though this rate can be slowed by egg laying). If FK506 increases healthspan as well as lifespan this increase in health should be detectable in early adulthood, so thrashing rate was measured at days 1 and 3 of adulthood. Later in adulthood, stochastic differences in ageing rate between individual worms means the

intra-population variation is too high to see statistically significant differences between treatment groups.

Worms do not move at a constant pace – they turn and move backwards, occasionally curl tightly before releasing and sometimes pause movement, all of which decrease the thrashing rate. To account for these variations in movement, the number of thrashes per 30 s was counted three times for each worm and averaged, and individual counts outside two standard deviations were censored to remove anomalies.

3.4.1 FK506 increased *C. elegans bus-5* thrashing rate

The effect of FK506 on thrashing rate was tested in *C. elegans bus-5*. FK506 significantly increased *C. elegans bus-5* thrashing rate at doses of 25-100 μg/ml at days 1 and 3 of adulthood (Figure 3.16). 5 μg/ml FK506 increased *C. elegans bus-5* thrashing rate at day 1, but not day 3 of adulthood, possibly because this low amount of FK506 could be fully metabolised and degraded by this time. There was no consistent significant difference in thrashing rates between 50 μg/ml FK506 and higher doses, so to provide continuity with previous work 50 μg/ml was used.

The ability of FK506 to increase thrashing rate suggests that FK506 increases *C. elegans bus-5* healthspan. From L4 stage, the worms in thrashing experiments were incubated with 20 worms per plate, rather than the 100 worms per plate required to give significant lifespan extension (section 3.2). This means that crowding stress is not required for the FK506-induced increase in thrashing rate, and suggests that FK506 may have different mechanisms of action on lifespan and thrashing rate.

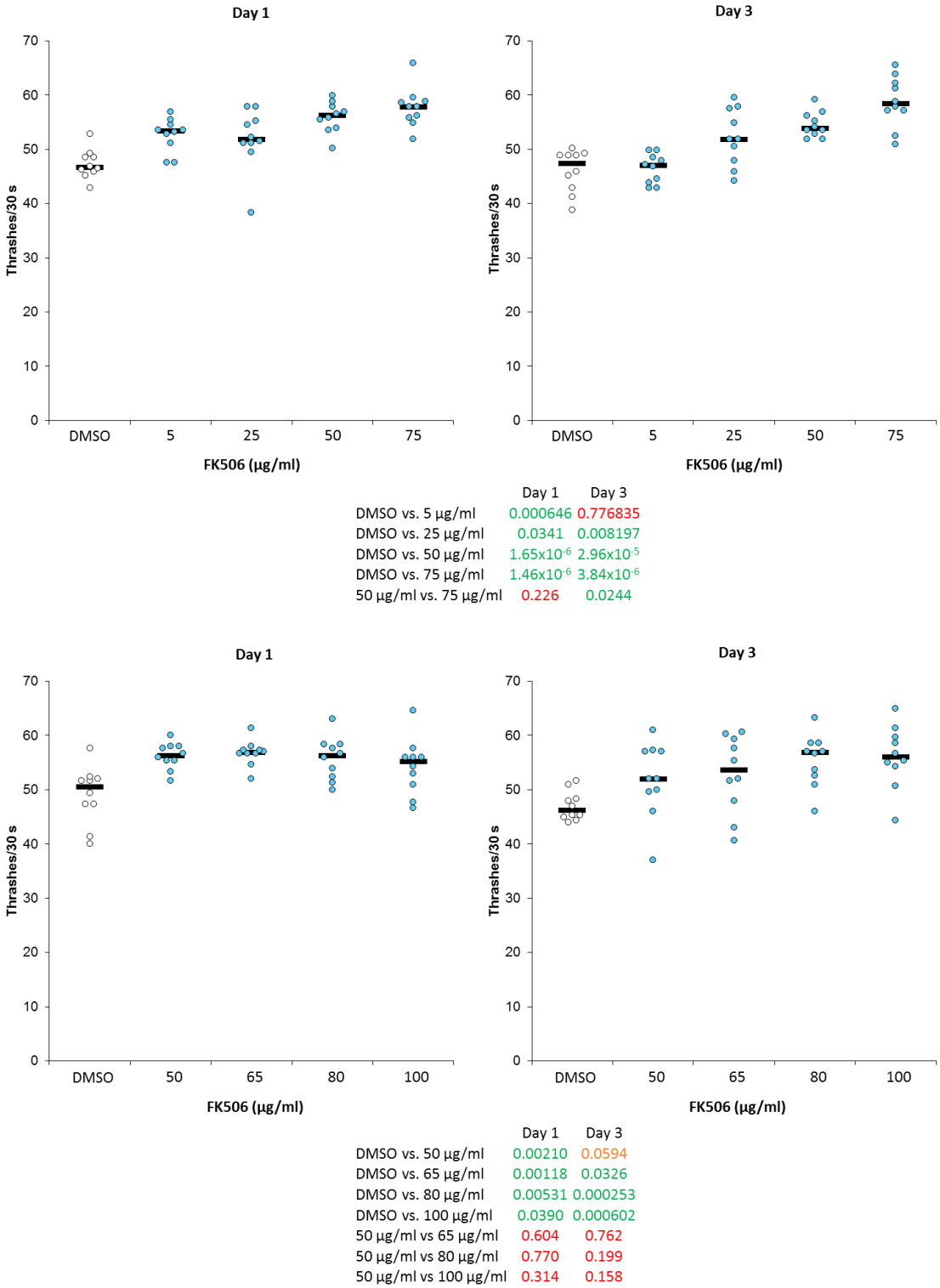

Figure 3.16 FK506 increased C. elegans bus-5 thrashing rate at days 1 and 3 of adulthood. 5 µg/ml FK506 increased bus-5 thrashing rate at day 1 but not day 3 of adulthood. 25-100 µg/ml FK506 significantly increased bus-5 thrashing rate at days 1 and 3. 65-100 µg/ml FK506 did not significantly increase bus-5 thrashing rate over 50 µg/ml FK506. Bar = median, n = 10, P values calculated using T Test.

3.4.2 FK506 increased *C. elegans* N2 thrashing rate inconsistently

Next, the effect of FK506 on *C. elegans* N2 thrashing rate was tested to find out whether the increased rate in *C. elegans bus-5* was due to a genotype interaction. The effect of FK506 on *C. elegans* N2 thrashing rate was less consistent than the effect seen on that of *C. elegans bus-5* (Figure 3.17). In one biological repeat 50 µg/ml FK506 increased *C. elegans* N2 thrashing rate at days 1 and 3 of adulthood, in another repeat FK506 had no effect at either day, and in a third repeat FK506 had no effect on N2 thrashing rate at day 1 of adulthood, but increased thrashing rate at day 3 with near significance (P=0.06). This suggests that FK506 did slightly increase *C. elegans* N2 healthspan, but interacted with the *C. elegans* genotype to have a larger effect in *C. elegans bus-5*, possibly due to higher bioavailability in the drug-sensitive cuticle mutant.

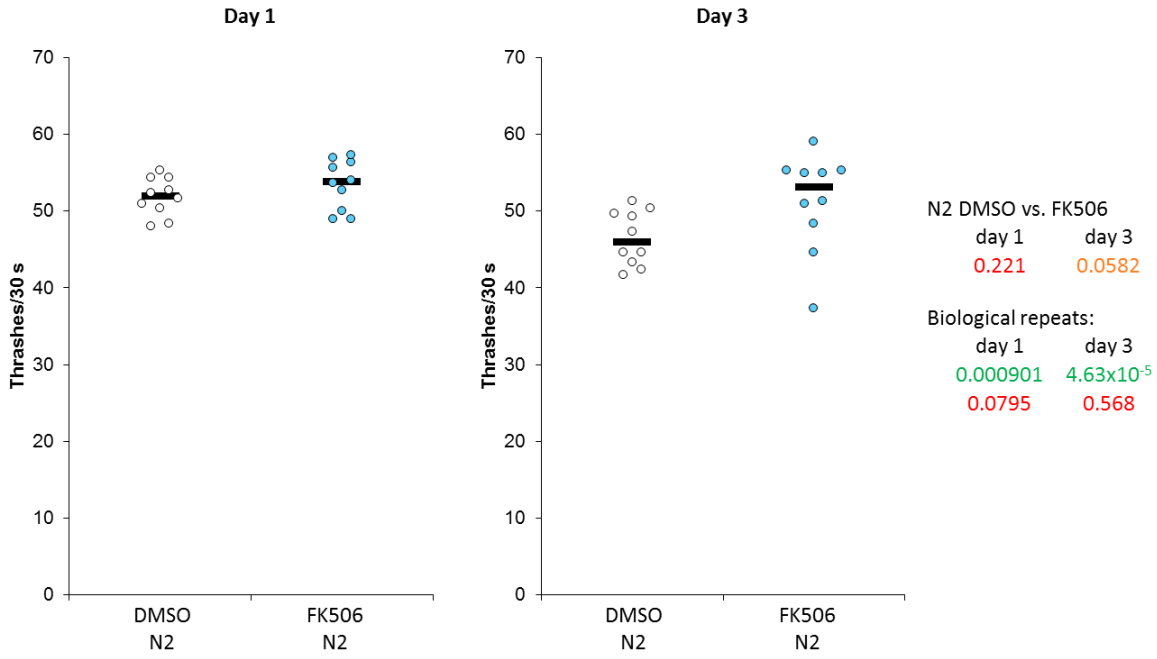

Figure 3.17 FK506 increased C. elegans N2 thrashing rate or had no effect across three biological repeats. In one repeat, 50 µg/ml FK506 increased N2 thrashing rate at days 1 and 3 of adulthood, in another repeat FK506 had no effect at either day and lastly FK506 had no effect at day 1 but increased thrashing rate with near significance at day 3. Bar = median, n = 10, P values calculated using T Test.

3.4.3 *C. elegans bus-5* and N2 had comparable thrashing rates

C. elegans bus-5 and N2 did not have significantly different lifespans, suggesting *C. elegans bus-5* can be used to model normal ageing despite abnormal cuticle formation. The thrashing rate of *C. elegans bus-5* and N2 were compared to investigate whether the *bus-5* mutation affects healthspan. *C. elegans bus-5* and N2 did not consistently have significantly different thrashing rates at days 1 and 3 of adulthood (Figure 3.18). In three biological repeats *C. elegans bus-5* had significantly slower thrashing rates than N2 at day 1 but not day 3, and in two repeats there was no difference between *C. elegans bus-5* and N2 thrashing rates at either day. When there was a significant difference, this difference was small, showing *C. elegans bus-5* are similar in health to *C. elegans* N2 and therefore are a good model of normal ageing. However, this slight difference may be why FK506 more consistently increased the thrashing rate of *C. elegans bus-5* than N2.

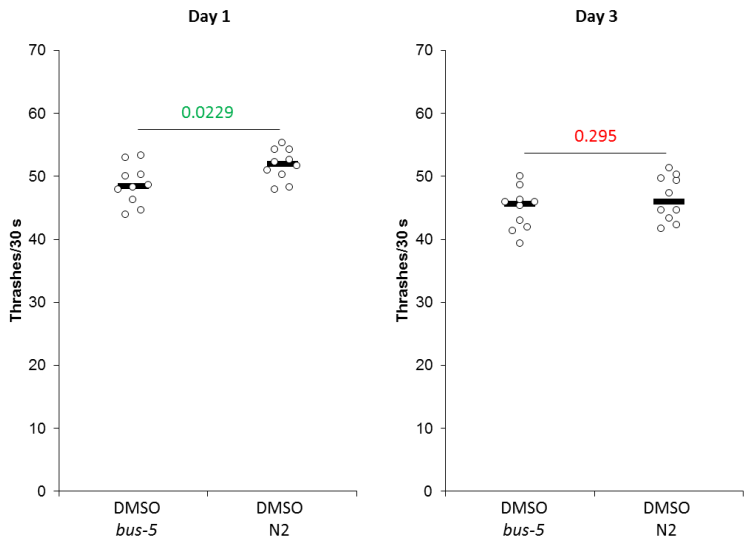

Biological repeat	N2 vs. *bus-5* (DMSO) P value	
	Day 1	Day 3
1	0.061003	0.959848
2	0.002548	0.093761
3	0.000731	0.565
4	0.709	0.371

Figure 3.18 C. elegans bus-5 and N2 worms had similar thrashing rates. N2 had a significantly higher rate of thrashing than bus-5 or there was no difference at days 1 and 3 of adulthood, with 0.5% DMSO. Bar = median, n = 10, P values calculated using T Test.

3.4.4 FK506 lost the ability to increase *C. elegans bus-5* thrashing rate over time

FK506 is unstable, and epimerisation and degradation of the compound affect biological activity (section 1.2), as well as metabolism of FK506 by *E. coli* and *C. elegans*. How quickly FK506 becomes inactive may affect lifespan and healthspan assays differently due to the differences in experiment length. To test the change in FK506 activity over time, *C. elegans bus-5* thrashing rate was assayed using NGM plates that had been FK506-treated and seeded with *E. coli* OP50 then incubated at room temperature for 8 days (old plates), in comparison to the usual one-day incubation (fresh plates) (Figure 3.19).

At days 1 and 3 of adulthood, FK506 was able to increase *C. elegans bus-5* thrashing rate on the fresh plates. However, on the old plates FK506 had no significant effect on *bus-5* thrashing rate at either day, suggesting FK506 has lost biological activity. This would mean FK506 was not fully active for the duration of lifespan assays, and degradation products may be present that could affect *C. elegans* lifespan or health.

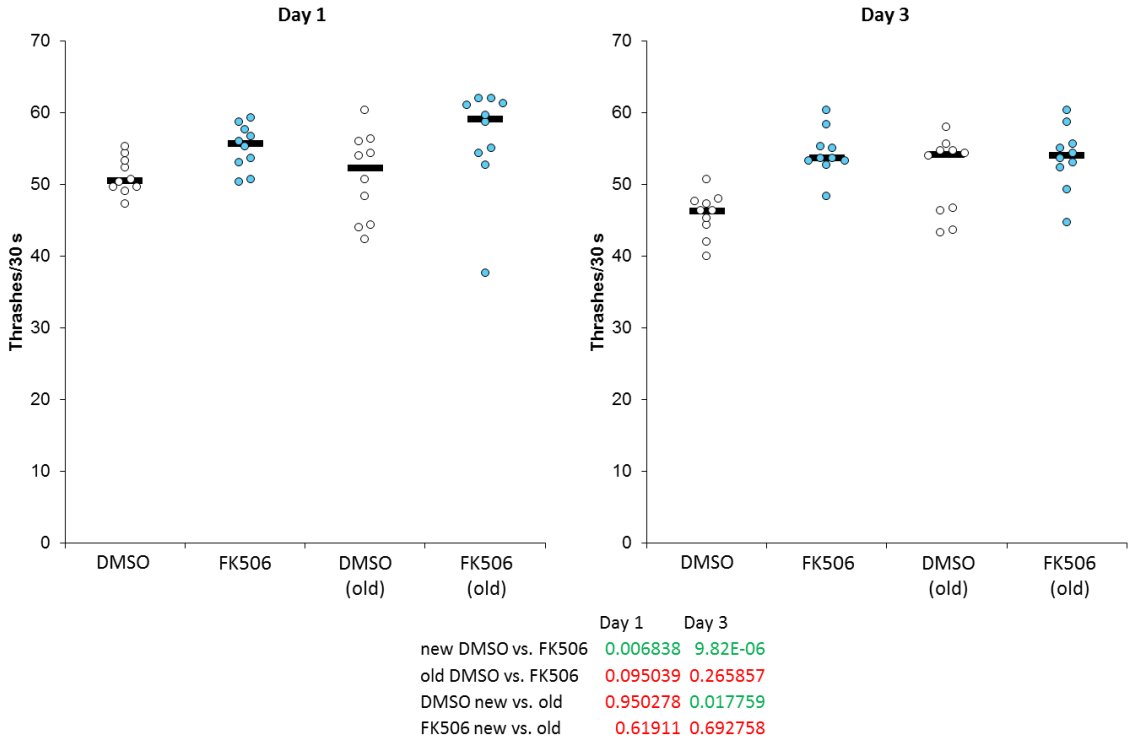

Figure 3.19 The age of the NGM plates altered C. elegans bus-5 thrashing rate. NGM plates treated with 50 µg/ml FK506 or DMSO and seeded with E. coli OP50 the day before C. elegans population synchronisation (normal method) were compared to plates treated and seeded 8 days before synchronisation (and stored at room temperature). On the fresh plates, FK506 increased bus-5 thrashing rate at days 1 and 3 of adulthood (compared to DMSO treatment). On the old plates FK506 was unable to increase thrashing rate at days 1 and 3 of adulthood. Bar = median, n = 10, P values calculated using T Test.

3.5 FK506 delayed accumulation of gut bacteria in *C. elegans bus-5* and *bus-8*

As *C. elegans* age, they accumulate bacteria in their guts, causing the gut to become distended and the eventual constipation contributes to the death of the worm (Cabreiro & Gems 2013). In young worms, the grinder breaks down all the consumed *E. coli*, and if any bacteria escape the grinder they are killed by the worm's immune system. However, as the worm ages, the efficiency of the grinder and immune system decline and increasingly live bacteria reach the intestine and replicate, resulting in the accumulation

of bacteria in the intestine of the worm. This means the accumulation of gut bacteria can be used as a measure of healthspan.

To assay the rate of accumulation of bacteria, the worms were fed *E. coli* OP50 expressing GFP. In early adulthood (days 3 and 4), FK506 treatment decreased the number of *bus-5* and *bus-8* worms containing bacteria within their intestine (Figure 3.20). This suggests that FK506 increased the length of time *C. elegans* were able to control bacterial accumulation. In combination with the results that FK506 increased *C. elegans* pharynx pumping and thrashing rates, this strongly suggests that FK506 extends *C. elegans* healthspan as well as lifespan.

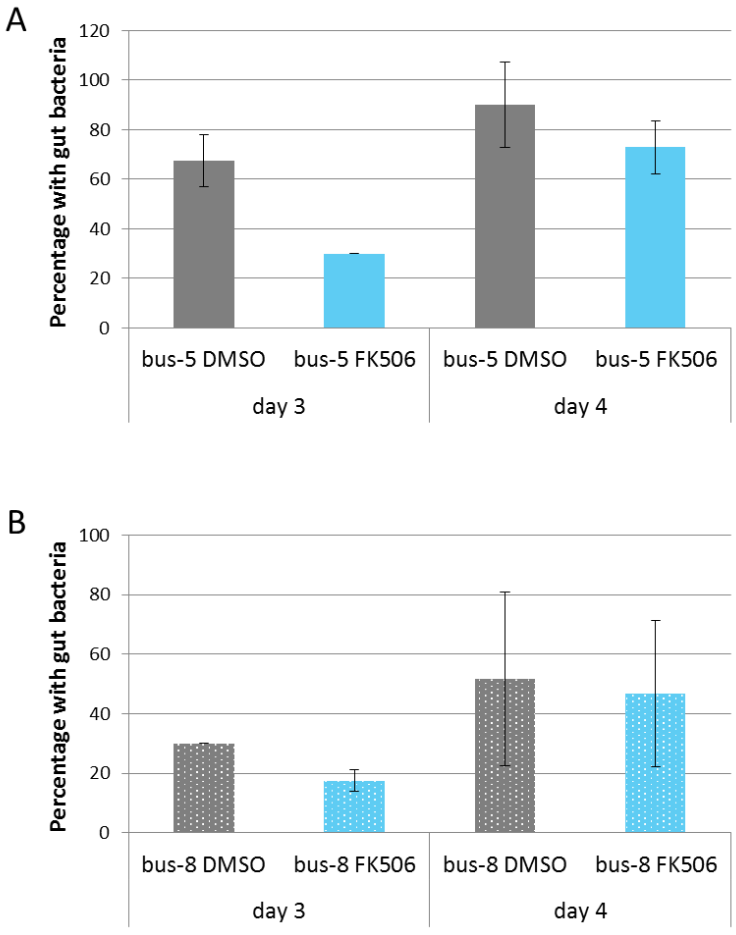

Figure 3.20 FK506 delayed the accumulation of gut bacteria in C. elegans bus-5 (A) and bus-8 (B). Fewer FK506-treated bus-5 and bus-8 worms contained gut bacteria at day 3 than DMSO-treated worms, but this gap had decreased at day 4. Error bars = SD, day 3 n = 2 biological repeats, day 4 n = 3 (20 worms per repeat).

3.6 Continual treatment with FK506 gave the largest increase in *C. elegans bus-5* thrashing rate and lifespan

Not all ageing interventions require constant treatment – some are only required during a specific life stage (Rangaraju et al. 2015), whilst others have opposite effects at different stages (Davis et al. 2008). Here, the timing of FK506 treatment was varied to find when in the *C. elegans* lifecycle FK506 has its lifespan-extending effect. *C. elegans bus-5* were either continually treated with FK506, treated up to the L4 stage (then transferred to DMSO treatment), treated from the L4 stage (previously DMSO-treated), and for the lifespan experiment only, treated with FK506 between only L4 and day 10 of adulthood (DMSO-treated before and after).

3.6.1 FK506 had an acute effect on *C. elegans bus-5* thrashing rate

These different dosing regimens were tested on *C. elegans bus-5* thrashing rate. The largest effect of FK506 on *C. elegans bus-5* thrashing rate was achieved by continual treatment (Figure 3.21). At day 1 of adulthood, both treating up to L4 and from L4 caused a near-significant or significant increase in thrashing rate respectively, but both were significantly lower than continual treatment. This suggests that the effect of FK506-treatment is quickly gained and lost – only one day after FK506 treatment was removed, the worms treated up to L4 had a thrashing rate significantly lower than the continually treated worms, whilst only one day of FK506 treatment significantly increased the thrashing rate of the worms treated from L4 compared to the DMSO-treated worms.

This is supported by the results seen at day 3 of adulthood. In day 3 adults, the FK506-treated up to L4 worms had no significant difference in thrashing rate to control DMSO-treated worms, indicating that the effect of FK506 on thrashing rate was lost after

removal from FK506 treatment and that FK506 treatment during development does not 'program' an increase in thrashing rate during adulthood.

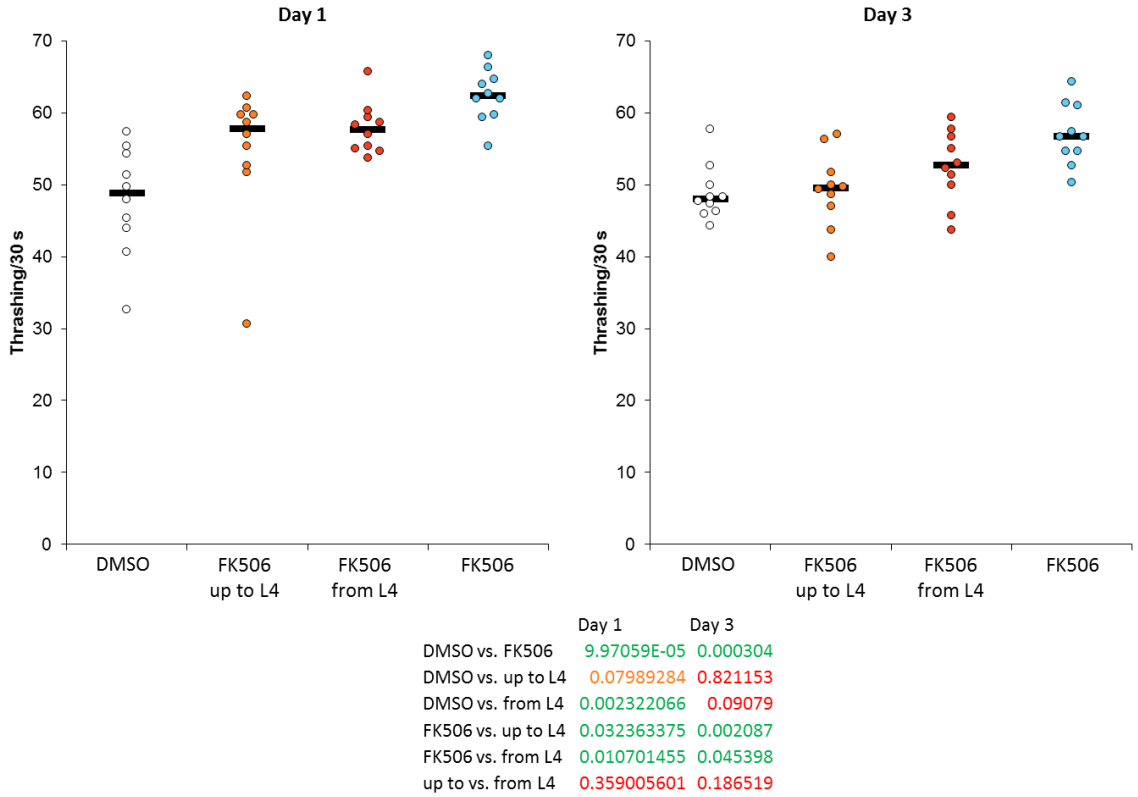

Figure 3.21 FK506 had an acute effect on C. elegans bus-5 thrashing rate. Continuous 50 µg/ml FK506 treatment caused the largest increase in bus-5 thrashing rate at both days 1 and 3 of adulthood. bus-5 treated with FK506 from hatching up to L4 stage (then moving to DMSO treatment) had near-significantly increased thrashing rate compared to DMSO-treated bus-5 at day 1 of adulthood, but had significantly lower thrashing rate than bus-5 continually treated with FK506. By day 3 of adulthood, bus-5 treated with FK506 up to L4 stage had thrashing rate not significantly different to DMSO-treated bus-5. bus-5 treated with FK506 from L4 stage (DMSO-treated during larval stages) had significantly increased thrashing rate compared to DMSO-treated bus-5 at day 1 of adulthood, but were significantly slower than continually FK506-treated bus-5 at both days. Bar = median, n = 10, P values calculated using T Test.

3.6.2 *C. elegans bus-5* required continual treated with FK506 to extend lifespan

Next, the effect of these different FK506 dosing regimens was tested on *C. elegans bus-5* lifespan (Figure 3.22). Constant treatment with FK506 was required to significantly increase *C. elegans bus-5* lifespan. All three partial treatment regimens had no significant effect on *bus-5* lifespan in comparison to DMSO treatment and had significantly reduced

lifespans compared to continual FK506 treatment. However, the lifespan curves of all three partial FK506 treatments were in between that of DMSO treatment and continual FK506 treatment, suggesting partial treatment with FK506 does have a small effect.

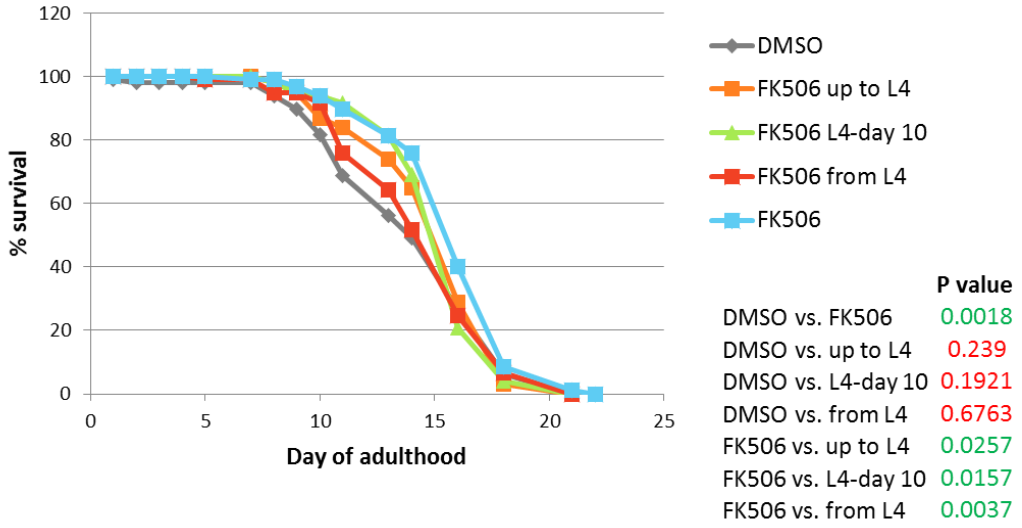

Figure 3.22 C. elegans bus-5 required continual FK506 treatment to cause significant lifespan extension. Continual 50 µg/ml FK506 treatment significantly increased bus-5 lifespan over DMSO treatment. Treatment with FK506 up to L4 stage (then moving to DMSO), treatment with FK506 between L4 stage and day 10 of adulthood (DMSO treated before and after), and treatment with FK506 from L4 stage (DMSO treated from hatching), caused lifespan curves intermediate between the continual DMSO and FK506 treatment curves, but not significantly different to DMSO treatment and significantly lower than continual FK506 treatment. 100 worms/plate, n = 100, P values calculated using OASIS Log-Rank Test.

In summary, *C. elegans bus-5* required constant FK506 treatment to increase lifespan, but treatment with FK506 starting at L4 stage was sufficient to significantly increase *bus-5* thrashing rate. Along with the result that the FK506-induced extension of *C. elegans* lifespan required crowding stress, but that healthspan extension (increased pharynx pumping and thrashing rate) did not require crowding, this suggests that FK506 has different mechanisms of action on *C. elegans* lifespan and healthspan.

3.7 An interaction between the anti-ageing mechanisms of FK506 and FUdR in *C. elegans bus-5*

FUdR (5-fluorodeoxyuridine) is often used in *C. elegans* lifespan assays because it prevents growth of the offspring, meaning the adult worms being assayed do not need to be regularly separated from their offspring (Hosono 1978; Gandhi et al. 1980; Mitchell et al. 1979). The assayed worms are transferred onto plates containing FUdR at the L4 stage, and because adult *C. elegans* are post-mitotic, FUdR does not harm the adult worms. Reducing or preventing reproduction, for example by laser-ablation of the gonads (Hsin & Kenyon 1999) or using germline-less mutants such as *glp-1* (Alper et al. 2010), extends lifespan in *C. elegans*. In line with this, FUdR extends lifespan in *C. elegans* and may interact with ageing interventions (Aitlhadj & Stürzenbaum 2010).

3.7.1 FUdR decreased the ability of FK506 to increase *C. elegans bus-5* thrashing rate

Thrashing assays were usually performed without FUdR, as the experiment is over only a short time period and with 20 worms per plate (rather than the 100 used in lifespan assays), so the worms are easily transferred to a new plate away from offspring once thrashing rate has been counted on day 1 of adulthood. To determine whether FUdR and FK506 interact to influence healthspan, *C. elegans bus-5* thrashing rate was assayed in the presence and absence of FUdR (Figure 3.23).

FUdR had no effect on *C. elegans bus-5* thrashing rate at day 1 of adulthood, but decreased thrashing rate at day 3 (with 0.5% DMSO, Figure 3.23). FUdR treatment

interfered with the ability of FK506 to increase *bus-5* worm thrashing rate. In the presence of FUdR, FK506 had no effect on *bus-5* thrashing rate at day 1 of adulthood, but increased thrashing rate at day 3 (Figure 3.23). In a biological repeat FK506 had no effect on *C. elegans bus-5* thrashing rate in the presence of FUdR at days 1 and 3. This suggests that there is overlap between the mechanisms of action of FK506 and FUdR on thrashing rate.

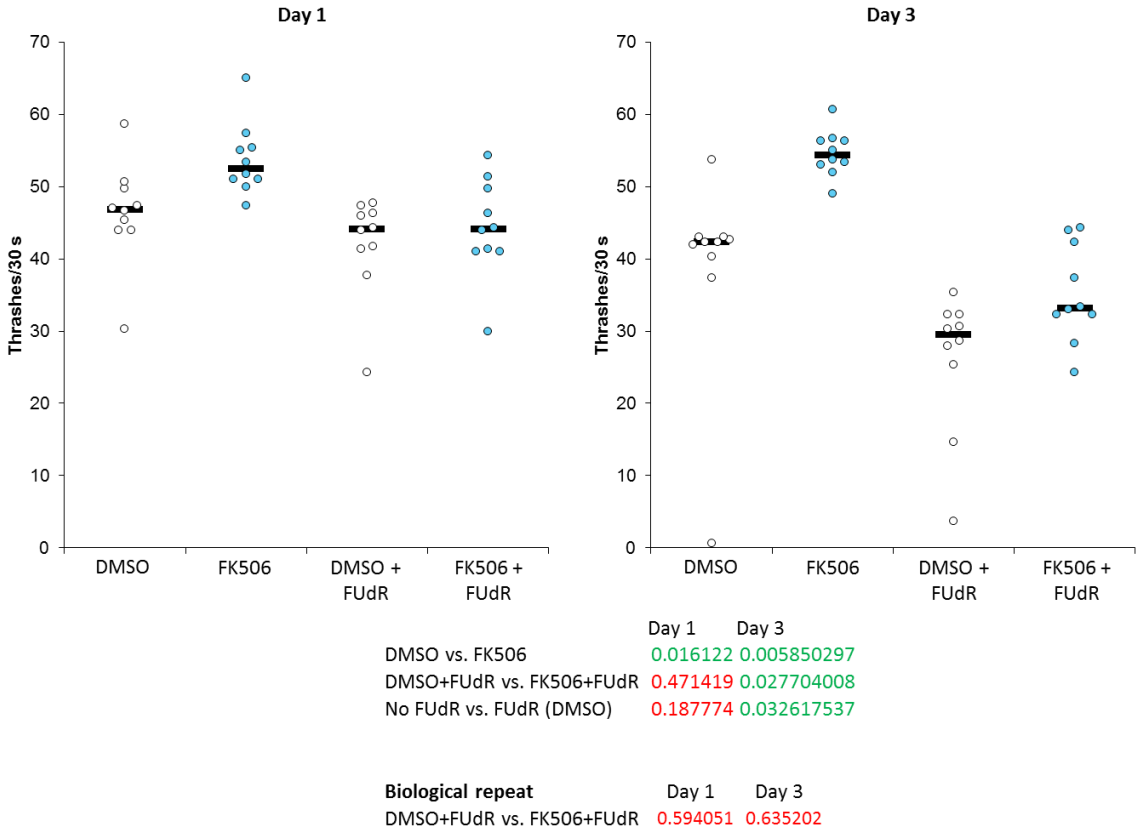

Figure 3.23 FUdR reduced the effect of FK506 on C. elegans bus-5 thrashing rate. Without FUdR, 50 µg/ml FK506 treatment increased bus-5 thrashing rate at days 1 and 3 of adulthood, compared to DMSO treatment. FUdR treatment (with DMSO) had no effect on thrashing rate at day 1, but decreased thrashing rate at day 3. In the presence of FUdR, FK506 had no effect at day 1, but increased thrashing rate at day 3. However, in a biological repeat FK506 had no effect on bus-5 thrashing rate at day 1 or 3 of adulthood. Bar = median, n = 10, P values calculated using T Test.

3.7.2 The interaction between FUdR and FK506 on *C. elegans bus-5* lifespan is unknown

Without FUdR to prevent growth of offspring, the synchronised adult worms must be transferred onto new plates every two days away from the offspring during the egg-laying period (about the first 10 days of adulthood). All plates were FK506/DMSO-treated and seeded with *E. coli* OP50 on the same day, then incubated at room temperature until required. Here, both without FUdR- and with FUdR-treated *C. elegans bus-5* were transferred to new plates every other day to control for the stress of being moved and also the lack of accumulation of *C. elegans* secreted products, such as ascarosides which are involved in population density signalling (Kaplan et al. 2011; Srinivasan et al. 2012).

Without FUdR 50 µg/ml FK506 had no effect on *C. elegans bus-5* lifespan, but FK506 did not extend lifespan in the FUdR-treated *bus-5* either (Figure 3.24). This suggests that the stress of being transferred interacts with the action of FK506, or the accumulation of *C. elegans* secreted products is required, or the way the drug is metabolised on the plate is important. When the worms are kept on the same plate, the worms and bacteria will metabolise FK506, reducing the concentration over time, and potentially causing the accumulation of metabolite products. When the worms are transferred to new plates every two days, only the bacteria will have been metabolising the FK506 and this will alter the decline in concentration of FK506 during the experiment, and also alter the rate of accumulation of metabolite products and which metabolites are produced.

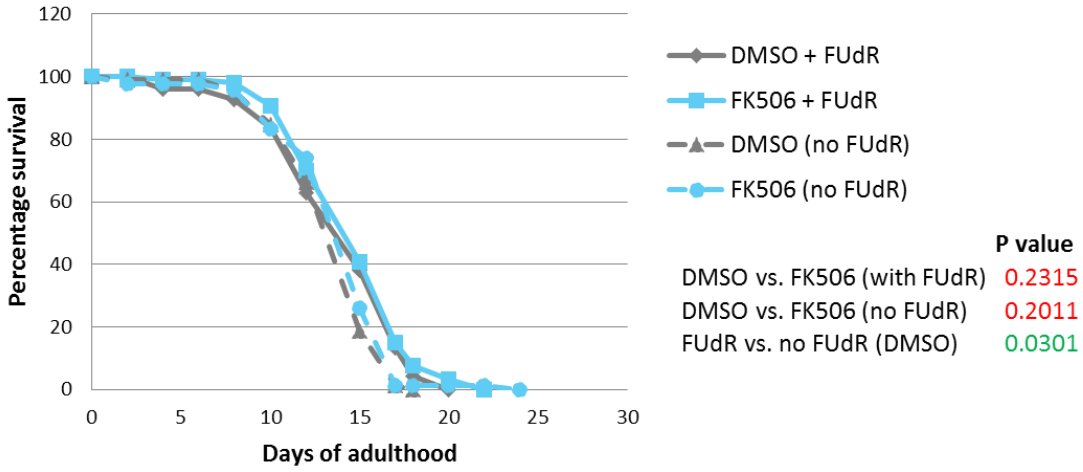

Figure 3.24 FUdR increased C. elegans bus-5 lifespan. 50 µg/ml FK506 had no effect on bus-5 lifespan either with or without FUdR treatment. 167 µg/ml FUdR significantly increased bus-5 lifespan (in the presence of 0.5% DMSO). 100 worms/plate, n = 100, P values calculated using OASIS Log-Rank Test.

3.8 Summary

Experiment	Strain	Result
Lifespan, uncrowded	*C. elegans bus-5*, *bus-8*, N2	FK506 had no effect
Lifespan, crowded	*C. elegans bus-5*, *bus-8*, N2	FK506 significantly extended lifespan
Growth of *E. coli*	*E. coli* OP50	FK506 had no significant effect on number of colonies formed
Pharynx pumping	*C. elegans bus-5* and *bus-8*	FK506 increased or had no effect on pumping rate (FK506 did not inhibit pharyngeal pumping)
Dietary restriction (lifespan)	*C. elegans bus-5*	In combination with DR, FK506 decreased lifespan compared to DR alone
Thrashing rate	*C. elegans bus-5*	FK506 significantly increased thrashing rate
	C. elegans N2	FK506 inconsistently increased or had no effect on N2 thrashing rate
Thrashing rate on plates drug-treated and seeded with *E. coli* OP50 a week prior to use	*C. elegans bus-5*	FK506 lost the ability to increase thrashing rate (FK506 activity lost over time)
Gut bacteria accumulation	*C. elegans bus-5* and *bus-8*	FK506 delayed accumulation of gut bacteria
FK506 dose timing – thrashing rate assay	*C. elegans bus-5*	FK506-induced increase of thrashing rate did not require continual treatment
FK506 dose timing – lifespan	*C. elegans bus-5*	Continual treatment with FK506 was required to significantly increase lifespan
Interaction between FK506 and FUdR activities	*C. elegans bus-5*	FUdR decreased the ability of FK506 to increase thrashing rate The interaction between FUdR and FK506 on lifespan is unknown

Table 3.1 Summary of the effects of FK506 on C. elegans lifespan and healthspan

3.9 Discussion

3.9.1 Validation of the lifespan assay

DMSO and FUdR both increased *C. elegans* lifespan, effects previously reported in the literature (Frankowski et al. 2013; Aitlhadj & Stürzenbaum 2010). By replicating the effects of known anti-ageing compounds here, the method of the lifespan assay is validated.

3.9.2 FK506 extended *C. elegans* lifespan under conditions of population crowding stress

FK506 did not extend lifespan in uncrowded conditions, but did extend lifespan with population crowding stress conditions of 100 worms per plate in *C. elegans* strains *bus-5*, *bus-8* and wild-type N2. This suggests that the mechanism of action of FK506 on *C. elegans* lifespan involves the crowding stress response pathway.

3.9.3 FK506 extended *C. elegans* healthspan

FK506 had a small, positive effect on *C. elegans bus-5* and *bus-8* pharynx pumping rate, increased thrashing rate in *C. elegans bus-5* and N2, and delayed accumulation of gut bacteria in *C. elegans bus-5* and *bus-8*. These results strongly suggest that FK506 extends *C. elegans* healthspan as well as lifespan, reducing the rate of ageing in early life and not just delaying death by prolonging the latter stages of life.

FK506 was less effective increasing *C. elegans* N2 than *bus-5* thrashing rate, suggesting a possible genotype interaction with the mechanism of action of FK506 on thrashing rate.

FUdR treatment reduced the ability of FK506 to increase *C. elegans bus-5* thrashing rate, suggesting an overlap in the mechanisms of action of FK506 and FUdR on *C. elegans*.

3.9.4 FK506 did not extend *C. elegans* lifespan by creating DR conditions, but did not have an additive effect with DR on lifespan

FK506 did not inhibit *E. coli* OP50 growth or pharynx pumping, so did not limit *C. elegans* food intake. This means FK506 did not create DR conditions and most likely caused lifespan extension by a direct effect.

However, there was no additive effect of FK506 and DR on *C. elegans bus-5* lifespan, suggesting FK506 targets some of the pathways influenced by DR. In the presence of DR conditions, from 50% population survival onwards FK506 had a negative effect on lifespan. This may be due to the accumulation of FK506 metabolites that have a negative effect on *C. elegans* lifespan. In the absence of DR, the positive effect of FK506 on lifespan outweighs these negative side effects, but when lifespan is extended by DR through the same pathways the negative effects become apparent.

3.9.5 FK506 had different mechanisms of action on *C. elegans* lifespan and healthspan

FK506 extended *C. elegans* lifespan only in the presence of population crowding conditions (100 worms/plate from L4 stage), but FK506 was able to increase healthspan in *C. elegans* incubated without crowding stress (20 worms/plate from L4 stage for pharynx pumping, thrashing rate and gut bacteria accumulation assays). *C. elegans bus-5* required continual FK506 treatment throughout life to significantly increase lifespan, but starting FK506 treatment at the L4 stage was sufficient to increase thrashing rate. These results suggest that FK506 has different mechanisms of action on lifespan and healthspan.

3.9.6 FK506 lost biological activity over time

FK506 is likely to remain biologically active for the duration of the healthspan assays, but not for the full duration of the lifespan assays. With time degradation products will accumulate which may also have an effect on *C. elegans* healthspan and lifespan.

Now it has been established that FK506 extends *C. elegans* lifespan (under crowded conditions) and healthspan, the mechanism of action of FK506 can be investigated.

4 Results – FK506 mechanism of action

4.1 Introduction

FK506 extended *C. elegans* lifespan (under population crowding stress) and healthspan, but the mechanism of action is unknown. FK506 did not have an additive effect with dietary restriction, but as DR acts through many pathways this does not specify a mechanism. The differing requirements for dosing timing and crowding stress between the effects of FK506 on lifespan and healthspan suggest that FK506 may have multiple cellular targets.

There are many methods that can be used to elucidate the mechanism of action of a compound. Here, RNA-seq was used to identify altered cellular processes and therefore potential targets in an unbiased way. Once potential targets were identified, knockdown of these processes was used to test whether that protein/process was required for the mechanism of action of FK506.

There are multiple methods that can be used to knockdown gene function. Specific genes can be knocked down using genomic mutation or RNAi, and small molecule inhibitors/inducers can be used to target certain proteins or processes (although often with side effects). These methods have been used here to identify the protein activities

and cellular processes required for FK506 to increase *C. elegans* thrashing rate and lifespan.

As shown previously, *C. elegans bus-5* is a good model of normal ageing, and the effect of FK506 on lifespan and thrashing rate was seen more reliably than in *C. elegans* N2. *C. elegans bus-5* is also more amenable to treatment with small molecule inhibitors/inducers, so was used here to investigate the mechanism of action of FK506.

4.2 RNA-seq identified cellular processes altered by FK506 treatment in *C. elegans bus-8*

To search for cellular processes that may be targeted by FK506, RNA-seq was performed to identify changes in RNA expression. The RNA-seq data was collected by Simon Haenni on *C. elegans bus-8* at day 1 of adulthood with three repeats. The aligned read counts were analysed here, firstly by calculating P value (with significance threshold adjusted for multiple testing) and then the genes with significantly altered RNA level were inputted to the PANTHER overrepresentation test (Mi & Thomas 2009; Mi et al. 2016). A selection of the GO-terms and PANTHER pathways associated with these differentially expressed RNAs are shown in Table 4.1.

GO-term/PANTHER pathway	Fold enrichment	Bonferroni P value
Biosynthetic process	>5	6.02 E-23
Translation	4.64	4.34 E-16
Response to stress	4.35	2.38 E-14
Lipid metabolic process	+ 3.19	6.48 E-14
RNA splicing	>5	6.05 E-10
Fatty acid metabolic process	+ 3.74	0.000289
Wnt signalling pathway	+ 4.89	0.000626
Cellular calcium ion homeostasis	>5	0.00476
Pyruvate metabolism	>5	0.0153
p53 pathway	>5	0.0195

Table 4.1 Overrepresented cellular processes and pathways associated with RNAs differentially regulated by FK506 in C. elegans bus-8 day 1 adults. RNA-seq data collected by Simon Haenni. Genes with significantly different RNA level after FK506 treatment (with P value correct for multiple testing) analysed using PANTHER overrepresentation test (Mi & Thomas 2009; Mi et al. 2016).

Interestingly, RNA of an FKBP that binds FK506 (Zlotkowski et al. 2013) and is localised to the endoplasmic reticulum (Winter et al. 2007; Bell et al. 2006), *fkb-4*, was increased by FK506. Expression of *fkb-4* is regulated by the IIS pathway, partially mediated by DAF-16 (Yu & Larsen 2001).

4.2.1 Lipid metabolism

Within the RNAs whose levels were significantly altered by FK506 treatment, RNAs associated with lipid and fatty acid metabolic processes were overrepresented. Previous work in the lab and by Chronos Therapeutics found that FK506 prevented age-related weight gain in rats and delayed lipid accumulation in *C. elegans* (section 1.2.6). The RNA-seq results suggest FK506 at least partially influences lipid metabolism by altering gene expression.

There are many pathways that regulate lipid metabolism, including serotonin signalling, which upregulates lipid metabolism and also affects lifespan (Watanabe et al. 2010; Lucanic et al. 2013; Sze et al. 2000). To investigate whether FK506 acts via the serotonin signalling pathway, *C. elegans* will be co-treated with FK506 and serotonin to test whether FK506 is able to increase lifespan when the serotonin signalling pathway is constitutively active.

4.2.2 Uncoupling proteins

The Chronos Therapeutics trial of FK506 in rats found that FK506 reversed age-related weight gain and caused the rats to maintain a healthy adult weight, whilst control-treated rats gained weight in old age (Figure 1.10). Potentially this weight loss could be caused by activation of uncoupling proteins, which convert energy to heat. Uncoupling proteins are found in brown fat and are used to maintain body temperature, but this process can be dangerous if over-activated. However, it is unlikely that FK506 activates uncoupling proteins because the rats did not continue to lose weight once a healthy weight was reached and they then maintained this healthy weight for the remaining 20 weeks of the trial whilst receiving daily FK506 treatment.

C. elegans have one uncoupling protein, *ucp-4*. The RNA level of *ucp-4* was unchanged by FK506 treatment ($p = 0.65$), suggesting the effect of FK506 on body weight is not through increased expression of uncoupling protein. However, an effect on protein synthesis or activity cannot be ruled out.

4.2.3 Calcium ion homeostasis

RNAs associated with cellular calcium ion homeostasis were also overrepresented. FK506 interacts with calcineurin (section 1.2.2), and the calcium ion channels RyR and (via

calcineurin) L-VGCC, proteins associated with calcium ion flux. This suggests that calcium ion flux may be involved in the FK506 anti-ageing mechanism of action, and the requirement of FK506 action for calcineurin and RyR activities will be tested.

4.2.4 Translation and response to stress

The terms translation and response to stress were identified, processes known to be altered by rapamycin, the anti-ageing compound structurally related to FK506. This suggests that FK506 and rapamycin target the same proteins to alter ageing. *C. elegans* will be co-treated with FK506 and rapamycin to test whether these compounds have an additive effect or not.

Whilst RNA-seq can identify the changes in RNA levels caused by FK506 treatment, suggesting potential targets, it cannot reveal whether these altered RNA levels lead to changes in protein levels or activity. Gene expression regulation at the level of translation and protein turnover or regulation of protein activity may be activated to prevent perturbation of the system. Also, FK506 is known to directly bind and regulate proteins (e.g. FK506-FKBP12 inhibits calcineurin). RNA-seq cannot detect these changes in protein activity. Proteomics would be needed to confirm whether changes to RNA levels cause changes in protein levels. To investigate whether FK506 acts via regulating protein activity, these proteins or cellular processes can be inhibited or activated in conjunction with FK506 treatment, to test whether FK506 action is dependent or independent of these functions.

Also, the RNA-seq was performed on *C. elegans bus-8*, which has significantly shorter lifespan than the *C. elegans bus-5* and N2 strains. Potentially FK506 could be having genotype-specific effects that are not relevant to normal ageing.

4.3 The impact of the RNAi bacteria strain, *E. coli* HT115, on the action of FK506

The mechanism of action of FK506 could be investigated using RNAi knockdown of different genes, then testing whether each gene is required for FK506 to increase *C. elegans bus-5* thrashing rate and lifespan. The *C. elegans* RNAi library (using the L4440 vector) is transformed into *E. coli* HT115, an RNase-deficient strain to improve the efficiency of the RNAi (Fraser et al. 2000). Different *E. coli* strains influence *C. elegans* lifespan and metabolism. In comparison to *E. coli* OP50, *E. coli* HT115 alters lipid metabolism (Brooks et al. 2009), so potentially the bacterial strain used could interact with the mechanism of FK506 action. Before RNAi can be used to investigate FK506 mechanism, it is necessary to test whether *E. coli* HT115 influences the ability of FK506 to increase thrashing rate and lifespan.

4.3.1 The effect of FK506 on *C. elegans bus-5* thrashing rate was inconsistent in the presence of *E. coli* HT115

Firstly, the influence of *E. coli* HT115 on the ability of FK506 to increase thrashing rate was tested. *C. elegans bus-5* were treated with 50 µg/ml FK506 with *E. coli* HT115 or OP50 food source from hatching, and thrashing rate was assayed (Figure 4.1). In comparison to control-treated *bus-5* on *E. coli* OP50, control-treated *bus-5* on *E. coli* HT115 had a significantly higher rate of thrashing at day 1 but not day 3 of adulthood, suggesting that the bacterial strain does effect thrashing rate. When grown on OP50, FK506 increased thrashing rate at days 1 and 3 of adulthood. In the presence of *E. coli* HT115, the effect of FK506 on thrashing rate was inconsistent across five biological

repeats, mainly significantly increasing thrashing rate at day 1 of adulthood, but having no significant effect at day 3.

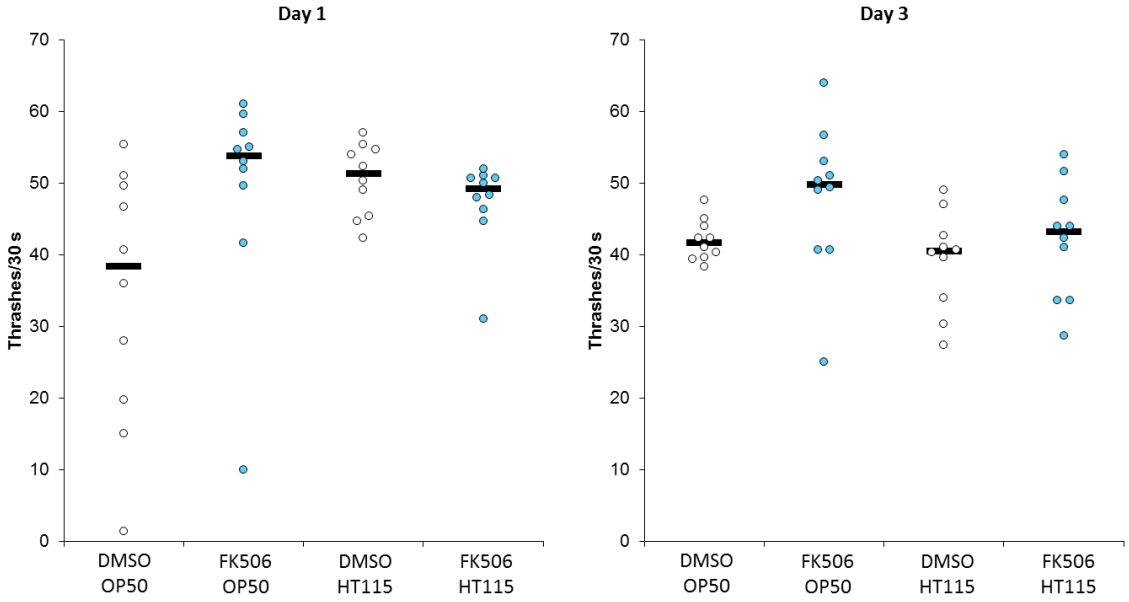

	Day 1	Day 3
OP50 DMSO vs. OP50 FK506	0.056074	0.115484
HT115 DMSO vs. HT115 FK506	0.215441	0.405431
OP50 DMSO vs. HT115 DMSO	0.01953	0.256462

Biological repeats	Day 1	Day 3
HT115 DMSO vs. HT115 FK506 (2)	0.069108	0.5713
(3)	0.014663283	0.3423
(4)	0.076149283	0.6085
(5)	0.010128918	0.0196

Figure 4.1 FK506 was unable to consistently increase C. elegans bus-5 thrashing rate in the presence of E. coli HT115. 50 µg/ml FK506 increased C. elegans bus-5 thrashing rate at days 1 and 3 of adulthood on E. coli OP50 (not significantly due to outliers), but in the presence of E. coli HT115 FK506 treatment inconsistently significantly increased thrashing rate or had no significant effect. Bar = median, n = 10, P values calculated using T Test.

In conclusion, *E. coli* HT115 interacted with the action of FK506 on *C. elegans bus-5* thrashing rate. Using the *E. coli* HT115 strains containing the empty L4440 vector, FK506 inconsistently increased or had no significant effect on *bus-5* thrashing rate at days 1 and 3 of adulthood. This rules out using RNAi as an approach to study the mechanism of action of FK506 on thrashing rate.

4.3.2 FK506 had no effect on *C. elegans bus-5* lifespan in the presence of *E. coli* HT115

The influence of *E. coli* HT115 on the ability of FK506 to increase lifespan was tested. *C. elegans bus-5* were treated with 50 µg/ml FK506 with *E. coli* HT115 or OP50 food source from hatching, and lifespan was assayed (Figure 4.2). There was no significant difference in lifespan in DMSO-treated *C. elegans bus-5* between *E. coli* HT115 and *E. coli* OP50 feeding, as previously found in *C. elegans* N2 (without DMSO treatment) (Brooks et al. 2009). In both biological repeats, FK506 significantly increased *C. elegans bus-5* lifespan on *E. coli* OP50, but had no significant effect on *bus-5* lifespan on *E. coli* HT115. As FK506 had no effect on *C. elegans bus-5* lifespan in the presence of *E. coli* HT115, RNAi could not be used to investigate FK506 mechanism of action on lifespan.

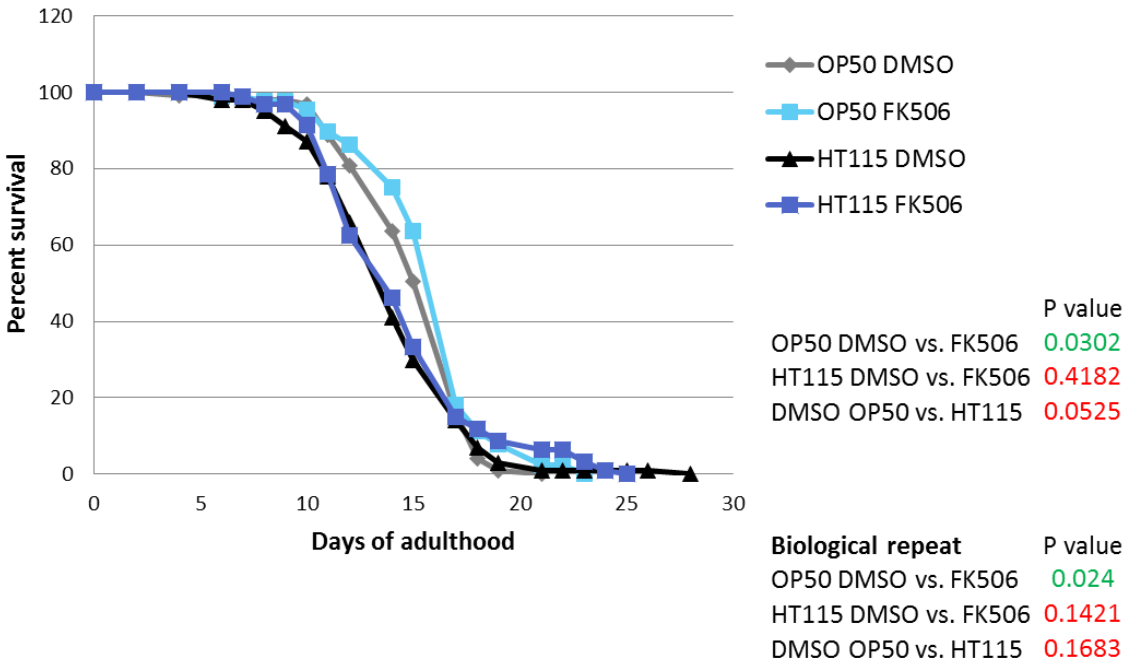

Figure 4.2 FK506 had no effect on C. elegans bus-5 lifespan in the presence of E. coli HT115. In two biological repeats there was no significant difference between C. elegans bus-5 lifespan on E. coli HT115 compared to E. coli OP50 (DMSO-treated). In both repeats, in C. elegans bus-5 fed E. coli OP50 50 µg/ml FK506 significantly increased lifespan in comparison to DMSO treatment. In C. elegans bus-5 fed E. coli HT115, FK506 had no significant effect in both biological repeats. 100 worms/plate, n = 100, P values calculated using OASIS Log-Rank Test.

4.3.3 *E. coli* OP50 and *E. coli* HT115 metabolomics

The strain of bacterial food source has been shown to influence the effect of FK506 on *C. elegans bus-5* lifespan and thrashing rate. Potentially, this influence could be via differences in bacterial metabolites. The anti-ageing drug metformin extends *C. elegans* lifespan not by acting directly on the worm, but by altering bacterial folate metabolism (Cabreiro et al. 2013). In collaboration with Dr. Katja Dettmer-Wilde, mass spectrometry was used to measure the concentrations of amino acids and organic acids in *E. coli* OP50 and *E. coli* HT115 treated with DMSO or 50 µg/ml FK506 (Figure 4.3).

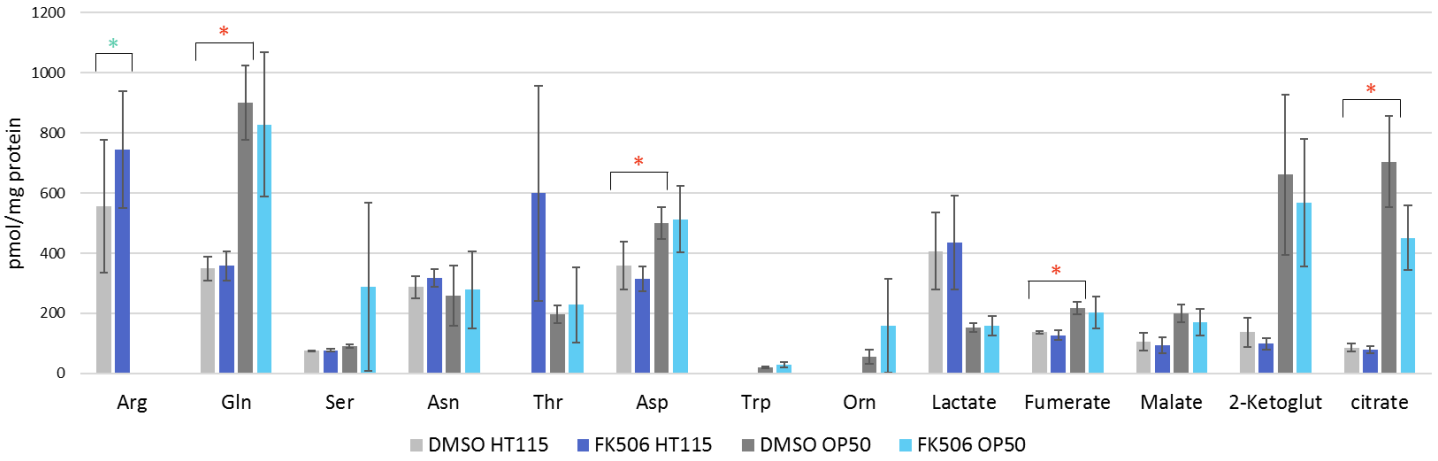

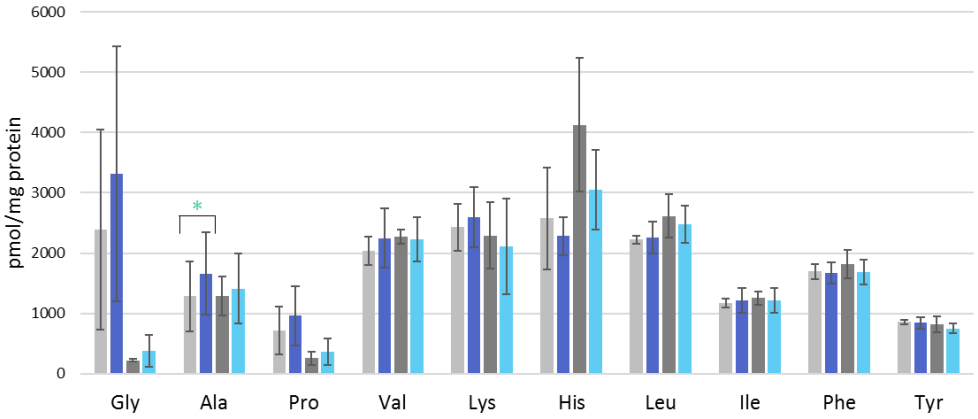

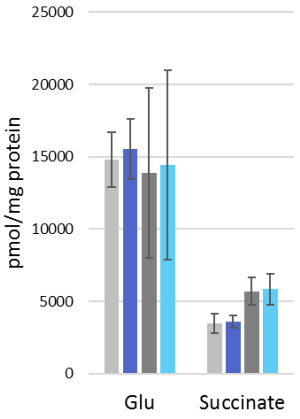

OP50 DMSO vs. FK506
No differences

HT115 DMSO vs. FK506
Arg (arginine) - increased by FK506
Ala (alanine) - increased by FK506

HT115 vs. OP50 DMSO
Gln (glutamine) - increased in OP50
Asp (aspartate) - increased in OP50
Fumerate - increased in OP50
Citrate - increased in OP50

Figure 4.3 Metabolites detected by mass spectrometry in E. coli OP50 and E. coli HT115 treated with either DMSO or 50 µg/ml FK506. No significant differences were detected between DMSO- and FK506-treated E. coli OP50. In E. coli HT115 FK506 increased the amounts of arginine (P = 0.02) and alanine (P = 0.04). In comparison to E. coli HT115 (DMSO), E. coli OP50 (DMSO) has higher amounts of glutamine (P = 0.02), aspartate (P = 0.03), fumerate (P = 0.02) and citrate (P = 0.04). Mass spectrometry performed by Dr. Katja Dettmer-Wilde. P values calculated using T Test.

Comparing control-treated *E. coli* OP50 and *E. coli* HT115, glutamine, aspartate, fumerate and citrate were increased in *E. coli* OP50. This confirms that there are metabolic differences between the two bacterial strains, that potentially impact on the anti-ageing activity of FK506.

FK506 did not alter the concentrations of any of the tested amino acids or organic acids in *E. coli* OP50, but increased the concentrations of arginine and alanine in *E. coli* HT115. Arginine was not detected in two of the three *E. coli* OP50 biological repeats, so could not be compared in this strain. Both alanine and arginine have an anti-ageing effect. Alanine supplementation in aged mice improves skeletal muscle function (Vallejo et al. 2016), prevents obesity, and improves glucose tolerance and insulin secretion (Araujo et al. 2016). Arginine supplementation has a positive effect on muscle protein synthesis in ageing (Riddle et al. 2016) and can reduce obesity (Hu et al. 2016; Araujo et al. 2016). Increasing these amino acids in the *C. elegans* food source could be the mechanism through which FK506 delays lipid accumulation in *C. elegans*, and the effects of alanine and arginine on muscle function could contribute to the increased thrashing rate caused by FK506.

4.4 FK506 activity was DAF-16 dependent

The insulin/insulin-like signalling (IIS) pathway is a major regulator of lifespan and ageing (section 1.1.4.1), and as such many ageing interventions act wholly or partially through this pathway, including dietary restriction. The terminal component of this pathway is the transcription factor DAF-16/FOXO. Deletion or mutation of *daf-16* accelerates ageing and shortens lifespan (Ogg et al. 1997). The dependence of FK506 action on IIS was tested using the *daf-16* null mutant strain CF1038 *daf-16(mu86)*.

4.4.1 Crossing *daf-16(mu86)* into the *bus-5(br19)* background

As the effect of FK506 in the N2 strain was variable, and to provide continuity with other experiments, an attempt was made to cross the *daf-16(mu86)* mutation into the *bus-5* genetic background, using the crossing strategy outlined in Figure 4.4. To obtain sufficient numbers of *bus-5* males to mate with *daf-16(mu86)* hermaphrodites the double mutant strain B6917 *bus-5(br19)*; *him-1* was used.

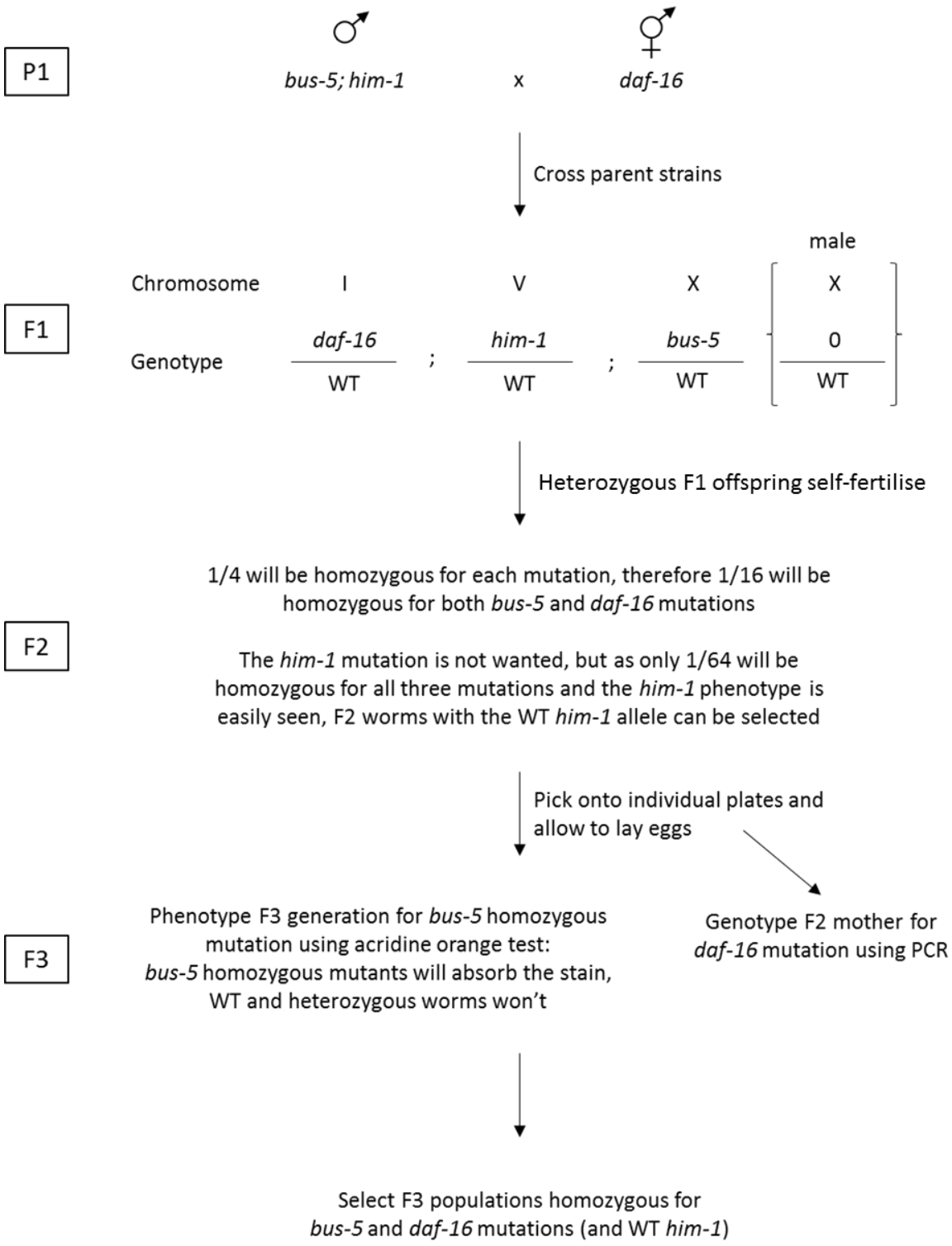

Figure 4.4 Genetic crossing strategy to obtain bus-5(br19); daf-16(mu86) strain of C. elegans.

To genotype the F3 generation in a single PCR reaction, a three-primer PCR was designed (Figure 4.5). Forward and reverse primer sequences to genotype the *daf-16(mu86)* allele were gifted by Dr. S. Maxwell, so a forward primer was designed to amplify the wild type allele, as the same reverse primer could be used for both alleles. The *daf-16(mu86)* allele is a large deletion mutation, so the reverse primer was located after the deletion region, with the wild type forward primer located within the deletion region and the *daf-16(mu86)* forward primer located before the deletion region. PCR cycle extension time was limited to prevent amplification using the *daf-16(mu86)* forward primer from wild type template. The primers were designed to give ~500 bp size separation between the two products to give unambiguous interpretation by gel electrophoresis, shown in Figure 4.6.

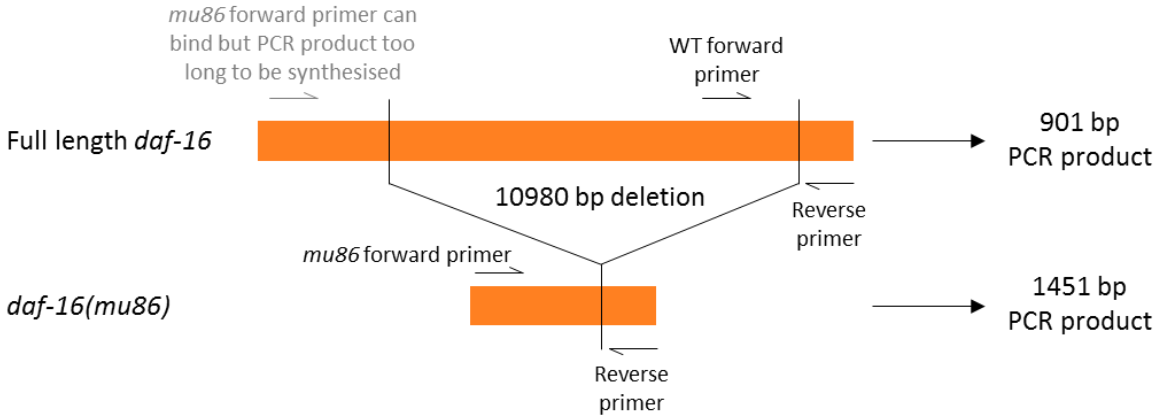

Figure 4.5 PCR to genotype daf-16(mu86) or WT alleles.

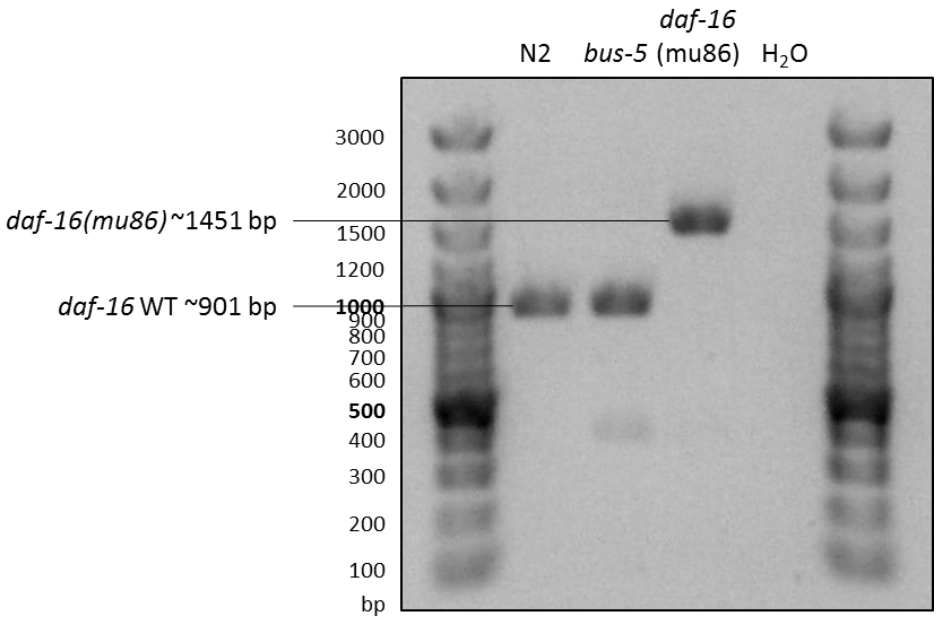

Figure 4.6 Three-primer PCR to genotype daf-16 wild type and mu86 alleles. C. elegans N2 and bus-5 strains both had the ~901 bp PCR product, indicating the wild type daf-16 allele. CF1038 daf-16(mu86) strain had the ~1451 bp PCR product, indicating the daf-16(mu86) deletion allele. 1% agarose/TBE/EtBr gel with TBE buffer. Ran at 110 V for 25 min. Markers: 100 bp plus ladder (Thermo). UV image taken with 2 s exposure.

The F2 and F3 generations of successful mating were *daf-16* genotyped and *bus-5* phenotyped (by acridine orange staining) respectively, but no homozygous *bus-5(br19)*; *daf-16(mu86)* offspring were identified. It would be expected that a quarter of the F2 generation would be *bus-5(br19)* homozygous, but the actual number detected was far lower. The B6917 *bus-5(br19)*; *him-1* strain was *bus-5* phenotyped and was discovered to be less than 50% *bus-5(br19)* homozygous, hugely reducing the chance of obtaining homozygous *bus-5(br19)*; *daf-16(mu86)* offspring, so the attempt at crossing the strains using this method was abandoned. Due to time constraints other methods of obtaining male *bus-5(br19)* could not be tried here, and so the CF1038 *daf-16(mu86)* strain (N2 background) was used.

4.4.2 The FK506-induced thrashing rate increase was DAF-16 dependent

To test whether the ability of FK506 to increase *C. elegans* thrashing rate is DAF-16 dependent, the null mutant strain CF1038 *daf-16(mu86)* strain was treated with FK506. *C. elegans bus-5*, N2 and *daf-16(mu86)* strains were treated with 50 µg/ml FK506 from hatching and thrashing rate was assayed (Figure 4.7). As expected, short-lived *daf-16(mu86)* had a significantly slower rate of thrashing than *bus-5* and N2 at days 1 and 3 of adulthood, confirming that *daf-16* mutation decreases healthspan as well as lifespan. In *C. elegans bus-5* FK506 treatment significantly increased thrashing rate at both days 1 and 3 of adulthood, and in *C. elegans* N2 FK506 treatment increased thrashing rate with near-significance at day 3 but had no effect at day 1. However, in *daf-16(mu86)* FK506 significantly decreased thrashing rate at day 1 of adulthood and had no effect at day 3. This suggests that the effect of FK506 on thrashing rate is DAF-16 dependent, and that in the absence of DAF-16 FK506 has a negative effect in early life.

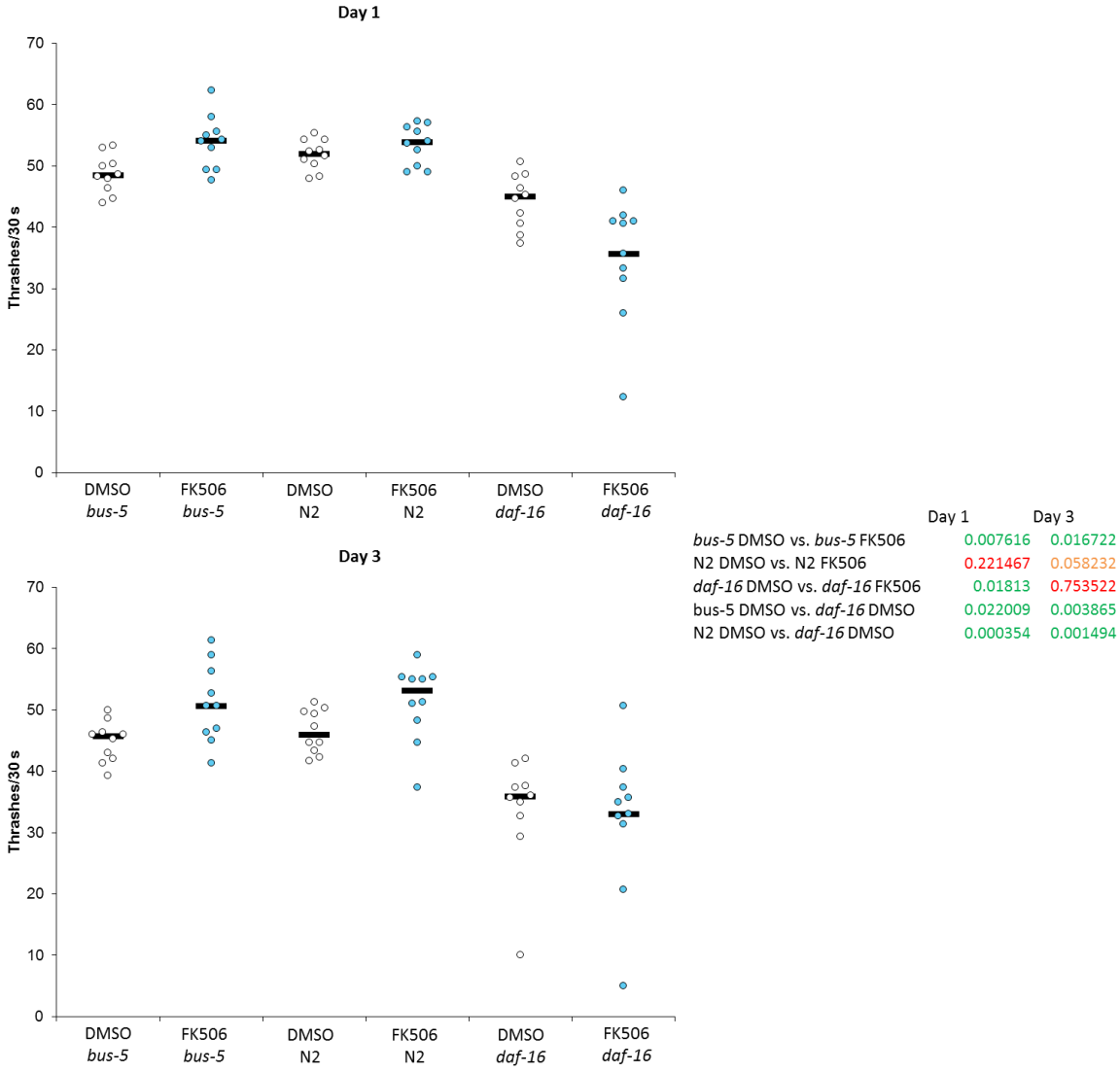

Figure 4.7 FK506 was unable to increase C. elegans daf-16(mu86) thrashing rate. DMSO-treated daf-16(mu86) had a significantly lower rate of thrashing than DMSO-treated bus-5 and N2 at both days. 50 µg/ml FK506 significantly increased C. elegans bus-5 thrashing rate at days 1 and 3 of adulthood, and increased to near-significance thrashing rate at day 3 but not day 1 in C. elegans N2, whilst in C. elegans daf-16(mu86) FK506 treatment significantly decreased thrashing rate at day 1 of adulthood and had no effect at day 3. Bar = median, n = 10, P values calculated using T Test.

4.4.3 The DAF-16 dependence of FK506-induced lifespan extension is uncertain

To test whether the ability of FK506 to increase *C. elegans* lifespan is DAF-16 dependent, the null mutant strain CF1038 *daf-16(mu86)* strain was treated with FK506. *C. elegans* N2 and *daf-16(mu86)* strains were treated with 50 µg/ml FK506 from hatching and lifespan was assayed under population crowding conditions (Figure 4.8). As expected, *daf-*

16(mu86) had a significantly shorter lifespan than *C. elegans* N2. FK506 had no effect on *daf-16(mu86)* lifespan, but also had no effect on N2 lifespan, suggesting FK506 was not active (possibly due to its unstable nature or its less reliable effect on N2). The identical lifespan curves of DMSO- and FK506-treated *daf-16(mu86)* suggest the effect of FK506 on lifespan is DAF-16 dependent, but this needs to be confirmed by repeating this experiment.

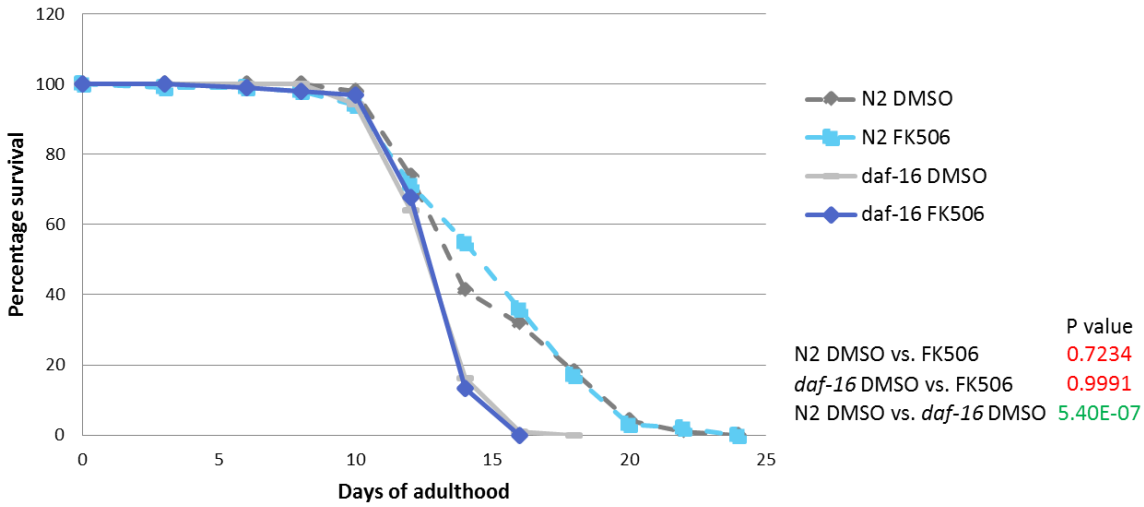

Figure 4.8 50 µg/ml FK506 had no significant effect on the lifespan of C. elegans daf-16(mu86) under conditions of population crowding. However, FK506 also had no effect on the lifespan of C. elegans N2, so the lack of lifespan extension could be due to the instability of FK506. 100 worms/plate, n = 100, P values calculated using OASIS Log-Rank Test.

In conclusion, the effect of FK506 on *C. elegans* thrashing rate is DAF-16 dependent, and the effect of FK506 on lifespan may be DAF-16 dependent, but this is unconfirmed.

4.5 Co-treatment with small molecule drugs

As the RNAi approach cannot be used, and the time required to cross genetic mutants into the *bus-5* background was too long, an alternative approach was considered to

dissect the mechanism of action of FK506. *C. elegans bus-5* were treated with FK506 in combination with small molecule drugs to inhibit or induce specific cellular functions (Figure 4.9), and thrashing rate and lifespan (with population crowding) were assayed. If FK506 lost the ability to increase thrashing rate or lifespan, the mechanism of FK506 must require the inhibited cellular function.

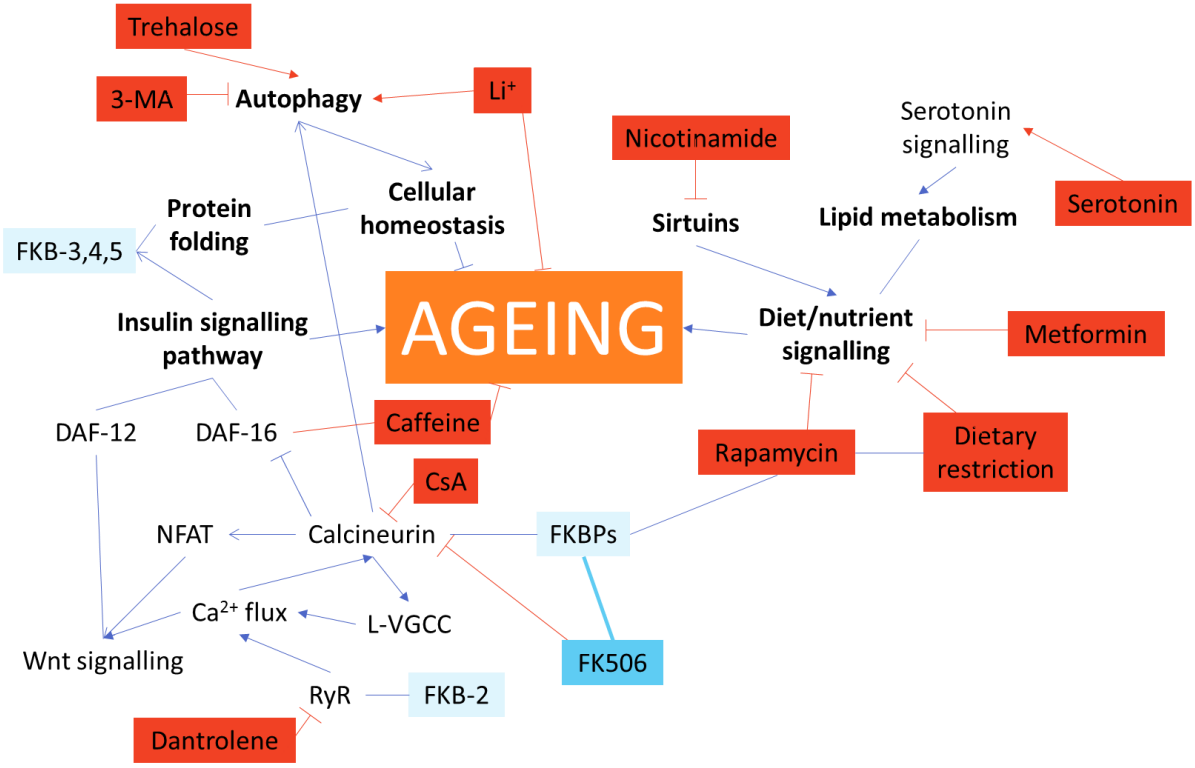

Figure 4.9 Some of the cellular pathways and components associated with ageing, including interactions with C. elegans FKBPs. The small molecule inhibitors and inducers used in this study to investigate the mechanism of action of FK506 are highlighted in red.

4.5.1 FK506 had no additive effect with rapamycin

Rapamycin is an anti-ageing compound that binds the FKBPs. Rapamycin inhibits TOR and the TOR signalling pathways, but unlike FK506, does not inhibit calcineurin. Therefore FK506 and rapamycin might be expected to have distinct mechanisms of action. However, both compounds bind the FKBP family of proteins and in terms of improved thrashing and

lifespan, they could act on a similar target. First it is necessary to establish a suitable dose to test the effect of rapamycin on the *C. elegans bus-5* strain.

4.5.1.1 Finding optimal rapamycin concentration in *C. elegans bus-5*

Rapamycin treatment at 90 μg/ml extends *C. elegans* N2 lifespan (Seo et al. 2013). As *C. elegans bus-5* are drug-sensitive they may require a lower dose. The effect of 1-90 μg/ml rapamycin on *bus-5* thrashing rate was tested to find the optimal dose (Figure 4.10). 1 and 10 μg/ml rapamycin had no effect on *bus-5* thrashing rate, and 50 μg/ml significantly increased thrashing rate at day 1 of adulthood but not day 3. 25, 70 and 90 μg/ml rapamycin all significantly increased *bus-5* thrashing rate at both day 1 and 3 of adulthood (except P=0.07 for 70 μg/ml at day 3). When compared to the DMSO-treated control 90 μg/ml rapamycin had the lowest P values and therefore caused the most significant increase in thrashing rate, so this dose was used.

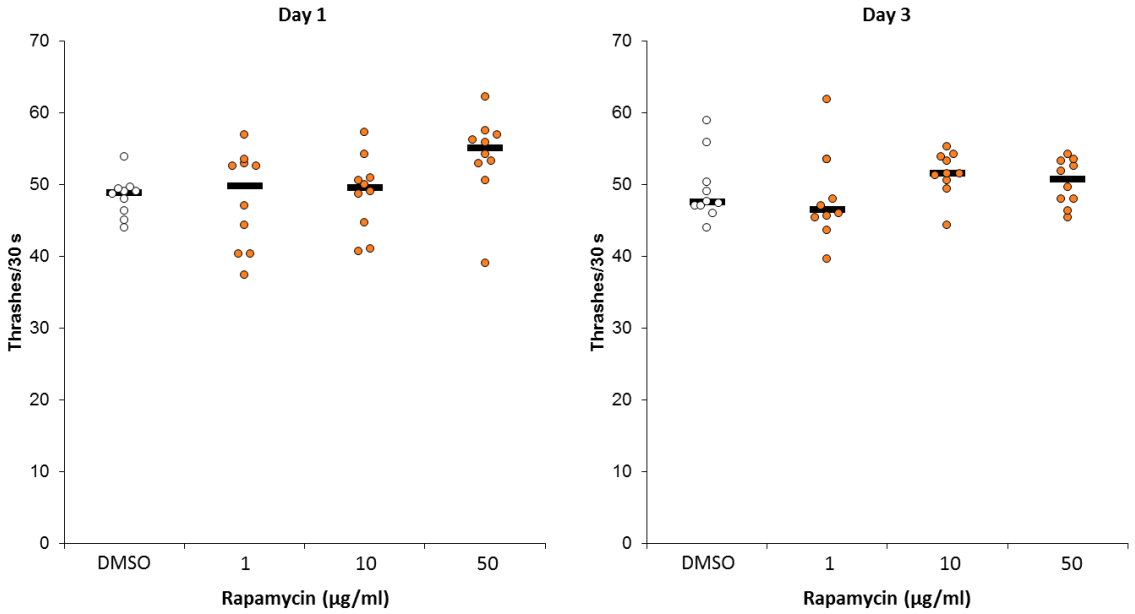

	Day 1	Day 3
DMSO vs. 1 µg/ml	0.845954	0.732658
DMSO vs. 10 µg/ml	0.8236	0.221421
DMSO vs. 50 µg/ml	0.020171	0.586953
10 µg/ml vs. 50 µg/ml	0.057339	0.389562

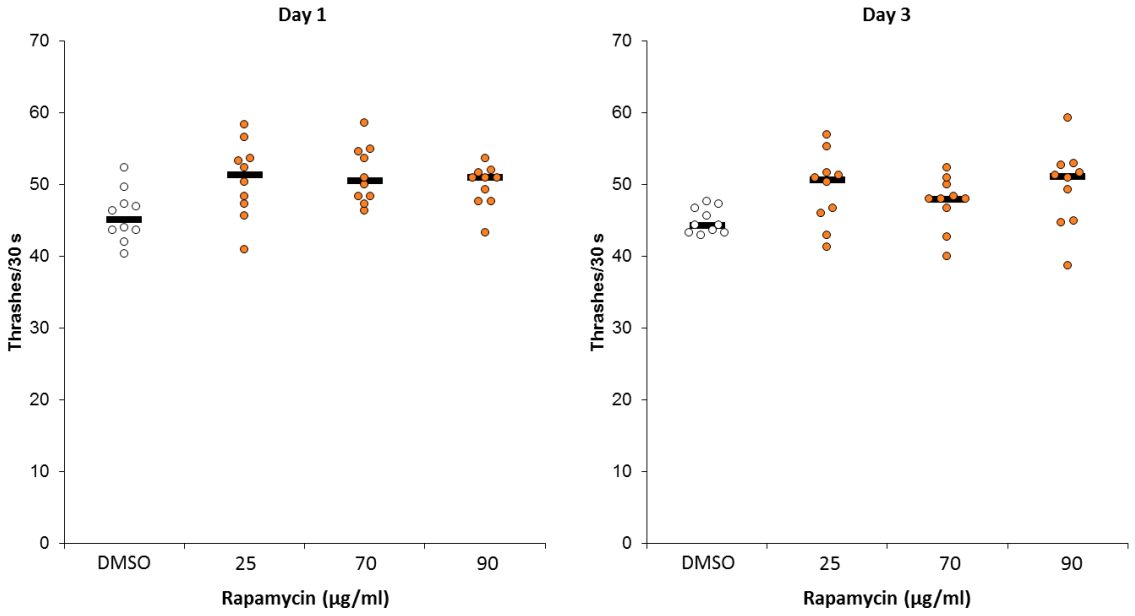

	Day 1	Day 3
DMSO vs. 25 µg/ml	0.023246	0.023715
DMSO vs. 70 µg/ml	0.003719	0.069760
DMSO vs. 90 µg/ml	0.011164	0.029061
70 µg/ml vs. 90 µg/ml	0.354741	0.327691

Figure 4.10 Rapamycin dose response of C. elegans bus-5 thrashing rate. 90 µg/ml rapamycin produced the most significant increase in thrashing rate. Bar = median, n = 10 (20 worms/plate), P value calculated with T Test.

4.5.1.2 Rapamycin and FK506 do not have an additive effect in *C. elegans bus-5*

Now the optimum rapamycin dose was established, the effect of treating with both FK506 and rapamycin was tested to find out whether they act via the same targets, firstly on thrashing rate. *C. elegans bus-5* were co-treated with 50 µg/ml FK506 and 90 µg/ml rapamycin from hatching and thrashing rate was assayed (Figure 4.11). Both FK506 and rapamycin significantly increased thrashing rate at days 1 and 3 of adulthood in two biological repeats, confirming that rapamycin extends *C. elegans* healthspan as well as its known extension of lifespan. Co-treating with FK506 and rapamycin did not have an additive effect – treating with FK506 in combination with rapamycin was not significantly different from rapamycin alone at both days of adulthood, in both biological repeats. As FK506 was unable to increase thrashing rate in the presence of rapamycin, they must have overlapping targets, most likely the FKBPs.

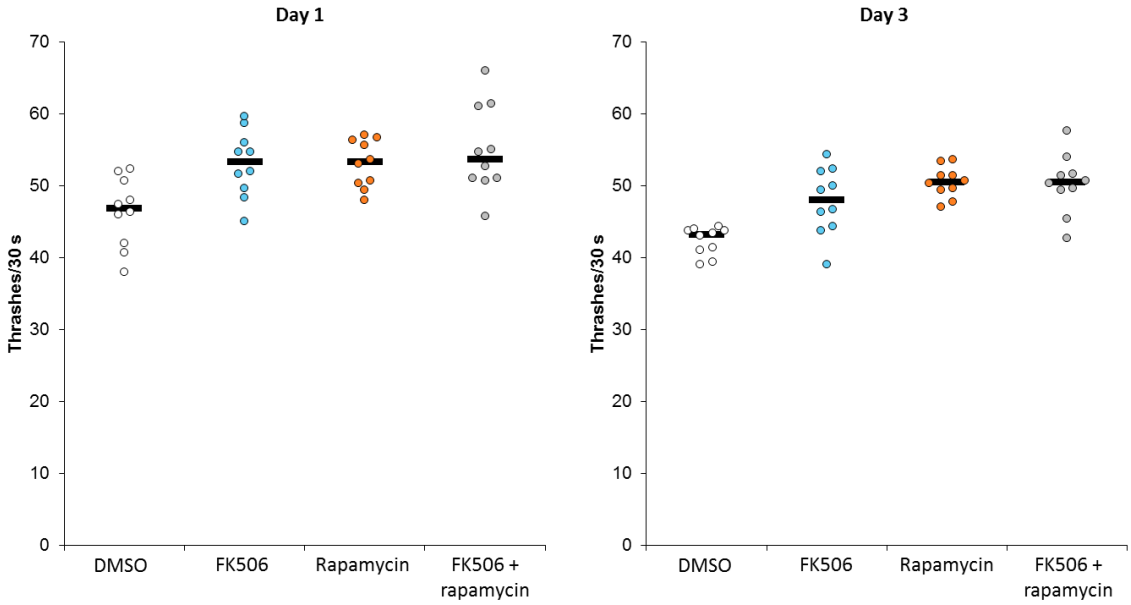

	Day 1	Day 3
DMSO vs. FK506	0.005306	0.004852
DMSO vs. rapamycin	0.002282	5.94E-08
Rapamycin vs. FK506+rapamycin	0.420852	0.91198

Biological repeat	Day 1	Day 3
DMSO vs. FK506	5.37E-05	4.86E-06
DMSO vs. rapamycin	0.03283	0.000183
Rapamycin vs. FK506+rapamycin	0.60260	0.26706

Figure 4.11 FK506 was unable to increase C. elegans bus-5 thrashing rate in the presence of rapamycin. Both 50 µg/ml FK506 and 90 µg/ml rapamycin significantly increased C. elegans bus-5 thrashing rate at days 1 and 3 of adulthood, in both biological repeats. Thrashing rate when co-treating with FK506 and rapamycin was not significantly different than when treating with rapamycin alone, in both biological repeats. Bar = median, n = 10, P values calculated using T Test.

Next, the additive effect of rapamycin and FK506 on lifespan was tested. *C. elegans bus-5* were co-treated with 50 µg/ml FK506 and 90 µg/ml rapamycin from hatching and lifespan with population crowding was assayed (Figure 4.12). Both FK506 and rapamycin individually extended *bus-5* lifespan in two biological repeats, confirming the lifespan extending action of rapamycin. Co-treating with FK506 and rapamycin was not significantly different to treating with rapamycin alone in one repeat, and in the other repeat co-treating significantly decreased lifespan compared to rapamycin treatment.

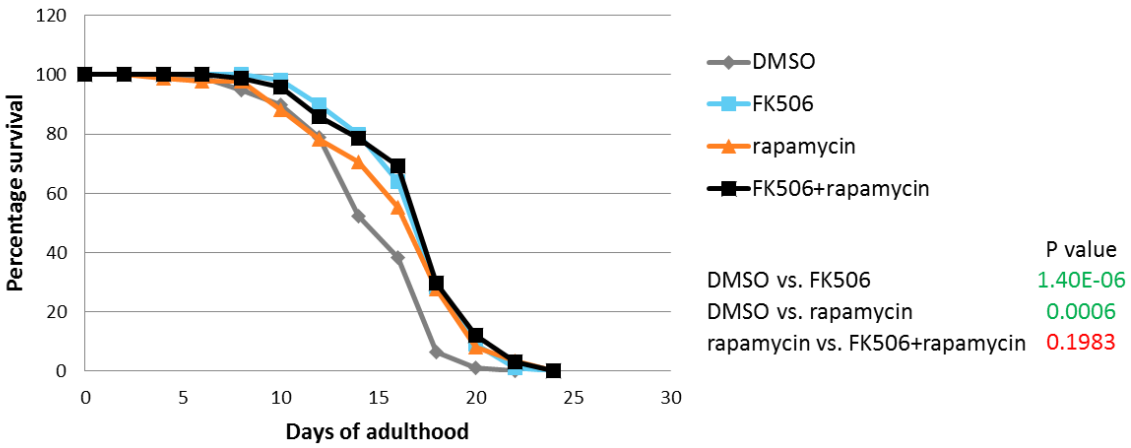

Biological repeat	P value
DMSO vs. FK506	0.0242 (increased)
DMSO vs. rapamycin	0.0236 (increased)
Rapamycin vs. FK506 + rapamycin	0.0323 **(decreased)**

Figure 4.12 FK506 was unable to increase C. elegans bus-5 lifespan (with population crowding) in the presence of rapamycin. Co-treating with FK506 and rapamycin was not significantly different to treating with rapamycin alone, but in a biological repeat co-treating with FK506 and rapamycin significantly decreased lifespan compared to treating with rapamycin alone. Both 50 µg/ml FK506 alone and 90 µg/ml rapamycin alone extended bus-5 lifespan compared to the DMSO vehicle-treated control in both repeats. 100 worms/plate, n = 100, P values calculated using OASIS Log-Rank Test.

Therefore, FK506 and rapamycin do not have an additive effect on lifespan extension, so must have overlapping targets, most likely the FKBPs. As FK506 and rapamycin both bind the FKBPs, during co-treatment there will be competition to bind the FKBPs and weaker binding sites will be bound, which in one repeat had a negative effect. This fits with the response of *C. elegans bus-5* lifespan to FK506, as at concentrations above the optimum dose FK506 loses the ability to extend lifespan (Figure 4.13). Potentially this 'overdose' of FKBP inhibition could be disguising an additive effect of FK506 and rapamycin on lifespan, and optimising lower concentrations of each compound for co-treatment could reveal an additive increase in lifespan.

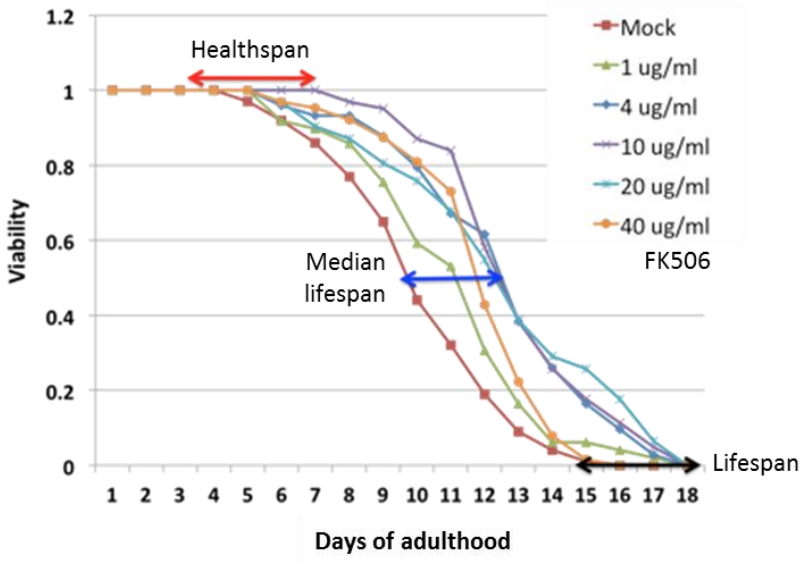

Figure 4.13 At concentrations above the optimum dose FK506 lost the ability to extend lifespan. The optimum lifespan-extending dose of FK506 on C. elegans bus-8 is 10 µg/ml. At concentrations above and below this level lifespan extension by FK506 is reduced. ~150 worms/plate. Data from Chronos Therapeutics.

4.5.1.3 Rapamycin and FK506 do not have an additive effect in *C. elegans* N2

Rapamycin and FK506 had no additive effect on *C. elegans bus-5*, so this was also tested in *C. elegans* N2 to ensure this was not a genotype-specific effect. First, the additive effect of FK506 and rapamycin on thrashing rate was tested.

C. elegans N2 were co-treated with 50 µg/ml FK506 and 90 µg/ml rapamycin from hatching and thrashing rate was assayed (Figure 4.14). FK506 increased thrashing rate at days 1 and 3 of adulthood, but unlike the effect seen in *bus-5*, rapamycin significantly increased N2 thrashing at day 3 only and not day 1, in two biological repeats. Co-treating with FK506 and rapamycin did not significantly increase thrashing rate compared with rapamycin alone at both days of adulthood, matching the result found in *C. elegans bus-5*.

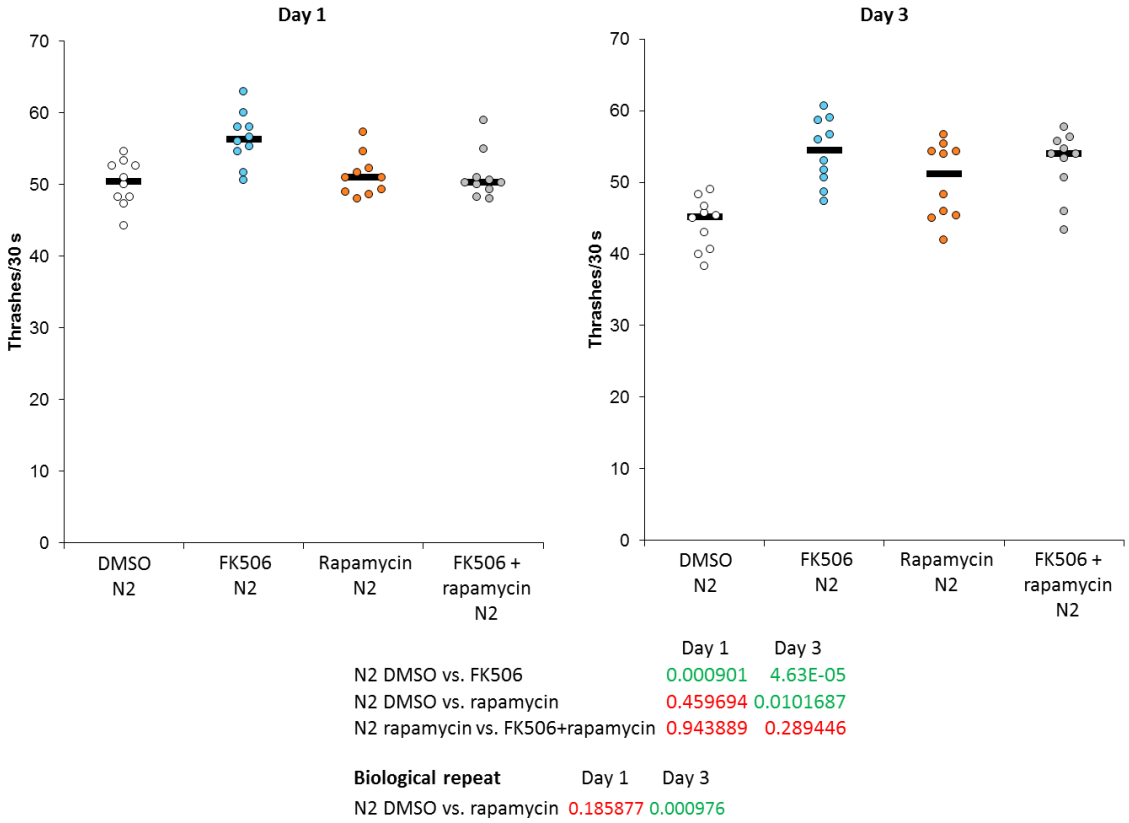

Figure 4.14 FK506 was unable to increase C. elegans N2 thrashing rate in the presence of rapamycin. 50 µg/ml FK506 increased N2 thrashing rate at days 1 and 3 of adulthood. 90 µg/ml rapamycin increased N2 thrashing rate at day 3, but not day 1 of adulthood in two biological repeats. Co-treating with FK506 and rapamycin produced no significant increase in thrashing rate over treating with rapamycin alone at both days 1 and 3 of adulthood. Bar = median, n = 10, P values calculated using T Test.

Next, the additive effect of FK506 and rapamycin on *C. elegans* N2 lifespan was tested. *C. elegans* N2 were co-treated with 50 µg/ml FK506 and 90 µg/ml rapamycin from hatching and lifespan was assayed (Figure 4.15). Treating with FK506 alone significantly increased N2 lifespan, and treating with rapamycin alone also significantly increased lifespan. Co-treating with rapamycin and FK506 was not significantly different to treating with rapamycin. Therefore, FK506 and rapamycin did not have an additive effect on *C. elegans* N2 lifespan, suggesting FK506 and rapamycin both target the FKBPs in *C. elegans* N2.

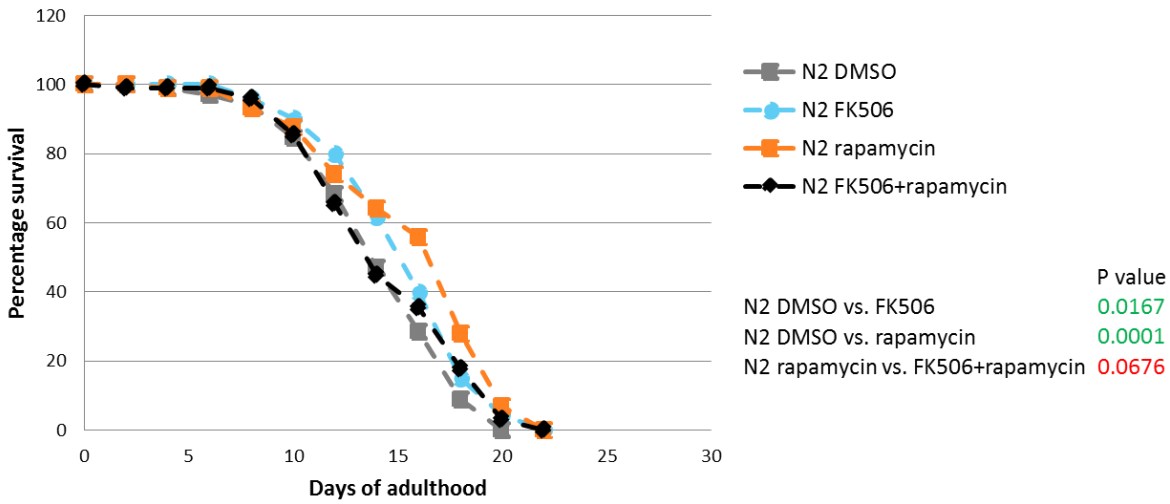

Figure 4.15 FK506 and rapamycin did not have an additive effect on C. elegans N2 lifespan. 50 µg/ml FK506 increased lifespan and 90 µg/ml rapamycin increased lifespan. C. elegans N2 lifespan when co-treating with rapamycin and FK506 was not significantly different to treating with rapamycin alone. 100 worms/plate, n = 100, P values calculated using OASIS Log-Rank Test.

In conclusion, FK506 and rapamycin did not have an additive effect on thrashing rate or lifespan in both *C. elegans bus-5* and N2. This suggests that FK506 targets the FKBPs in the mechanism of thrashing rate increase and lifespan extension, and that FK506 has the same mechanism of action in *C. elegans bus-5* and N2.

4.5.2 FK506-induced lifespan extension was calcineurin dependent, but thrashing rate increase was calcineurin independent

FK506 inhibits calcineurin when in complex with FKBPs. Cyclosporin A (CsA) inhibits calcineurin, but does not bind the FKBP family. To address whether it is the interaction of FK506 with FKBPs and the subsequent inhibition of calcineurin activity that improves healthspan and lifespan, *C. elegans bus-5* was co-treated with both FK506 and CsA.

To test the calcineurin-dependence of FK506-induced thrashing rate increase, *C. elegans bus*-5 were co-treated with 50 µg/ml FK506 and 50 µg/ml CsA (Donohoe et al. 2009) from hatching and thrashing rate was assayed at days 1 and 3 of adulthood (Figure 4.16). When treated with FK506 *C. elegans bus-5* thrashing rate was significantly increased, but the effect of CsA was inconsistent. In one repeat CsA had no significant effect on thrashing rate at both days and in the second repeat CsA significantly increased thrashing rate at day 3 and with near-significance at day 1. Co-treating with FK506 and CsA increased *bus-5* thrashing rate in comparison to CsA alone in both repeats, except at day 1 in the second repeat (the effect of FK506 alone was also insignificant at day 1 in this repeat), suggesting calcineurin activity is not required for FK506 to increase *C. elegans bus-5* thrashing rate.

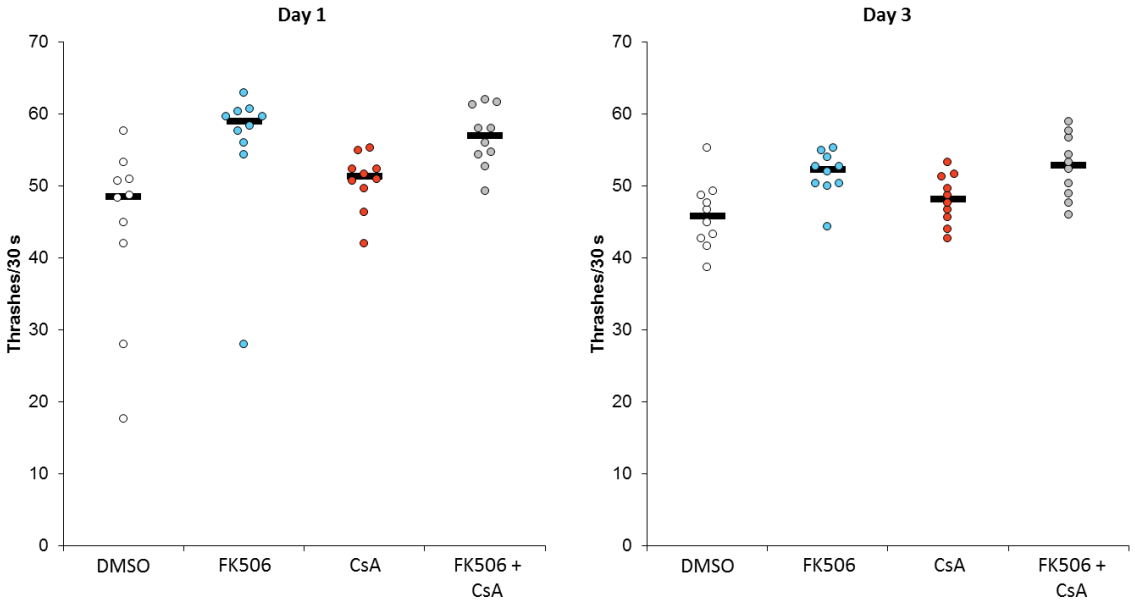

	Day 1	Day 3
DMSO vs. FK506	0.034471	0.005647
DMSO vs. CsA	0.146091	0.244382
CsA vs. FK506+CsA	0.00338	0.020716

Biological repeat	Day 1	Day 3
DMSO vs. FK506	0.084504	0.001272
DMSO vs. CsA	0.078049	0.002710
CsA vs. FK506+CsA	0.72235	0.01152

Figure 4.16 FK506 increased C. elegans bus-5 thrashing rate in the presence of CsA. 50 µg/ml FK506 significantly increased C. elegans bus-5 thrashing rate at days 1 and 3 of adulthood but 50 µg/ml CsA had no effect in one repeat and in the other repeat increased thrashing rate at both days. Co-treating with FK506 and CsA produced a significant increase in thrashing rate over treating with CsA alone in two biological repeats at day 3 of adulthood and at day 1 in one repeat. Bar = median, n = 10, P values calculated using T Test.

Next, the calcineurin dependence of FK506-induced lifespan extension was tested. *C. elegans bus*-5 were co-treated with 50 µg/ml FK506 and 50 µg/ml CsA from hatching and lifespan with population crowding was assayed (Figure 4.17). Treating with either FK506 alone or CsA alone significantly increased *bus-5* lifespan, but there was no additive effect of co-treating with both FK506 and CsA. As the lifespan of co-treated *bus-5* was not significantly different to CsA-treated *bus-5*, this suggests that calcineurin activity is required for the action of FK506 on lifespan.

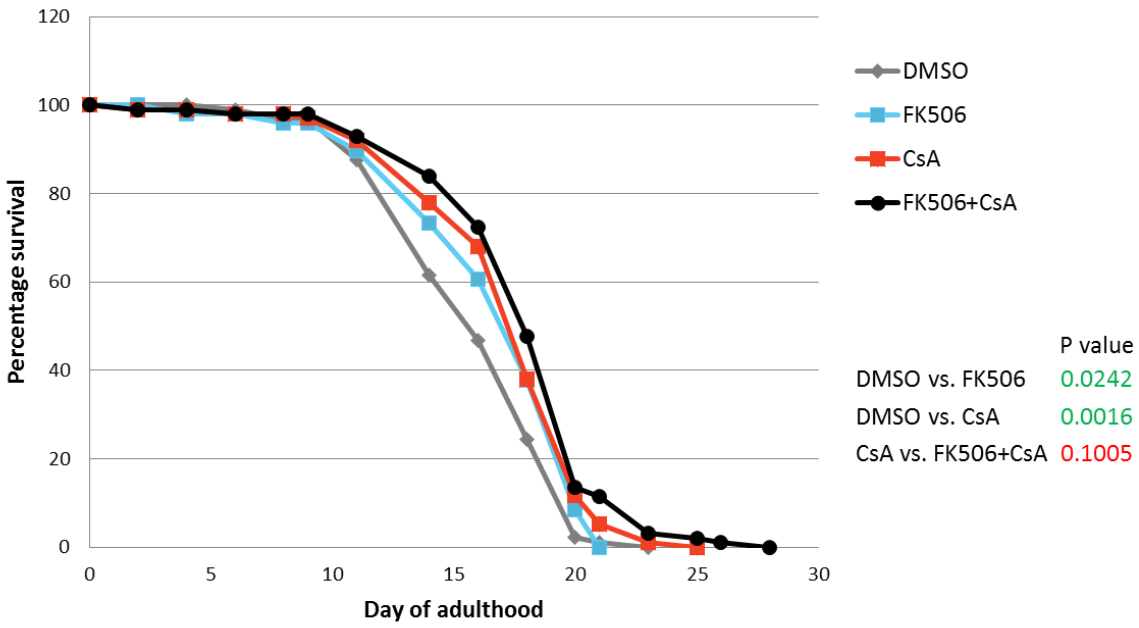

Figure 4.17 FK506 was unable to increase C. elegans bus-5 lifespan (with population crowding) in the presence of CsA. Lifespan when co-treating with FK506 and CsA was not significantly different to treating with CsA alone. Both 50 µg/ml FK506 alone and 50 µg/ml CsA alone extended bus-5 lifespan compared to the DMSO vehicle-treated control. 100 worms/plate, n = 100, P values calculated using OASIS Log-Rank Test.

The action of FK506 on thrashing rate was calcineurin-independent, whilst the effect of FK506 on lifespan was calcineurin-dependent. This suggests that FK506 has separate mechanisms of action on thrashing and lifespan, matching the results in chapter 3 that the effects of FK506 on thrashing and lifespan have different requirements for crowding stress and dosing timing (section 3.8.5).

4.5.3 FK506 action was independent of RyR

FKBP12 and FKBP12.6 bind and regulate activity of the ryanodine receptor (RyR), so by homology *C. elegans* FKB-2 may also bind RyR. FK506 causes FKBP12 to dissociate from RyR (section 1.3.2). Regulation of calcium ion flux through RyR is a possible mechanism of action of FK506. *C. elegans bus-5* were co-treated with FK506 and the RyR inhibitor dantrolene to test whether RyR activity is required for the FK506 anti-ageing effects.

To test the combined effects of FK506 and dantrolene on thrashing rate, *C. elegans bus*-5 were co-treated with 50 µg/ml FK506 and 10 µM dantrolene (Kitagawa et al. 2003; Xu et al. 2001) from hatching and thrashing rate was assayed at days 1 and 3 of adulthood (Figure 4.18). When treated with FK506 *C. elegans bus-5* thrashing rate was significantly increased, but dantrolene treatment had no significant effect on thrashing rate in both biological repeats. Co-treating with FK506 and dantrolene significantly increased *bus-5* thrashing rate in comparison to dantrolene alone at day 3 of adulthood, and with near significance ($p = 0.07$) at day 1. This suggests that RyR activity is not required for FK506 to increase thrashing rate, but that potentially in early life FK506 influences calcium flux, possibly via L-VGCC (section 1.3.2).

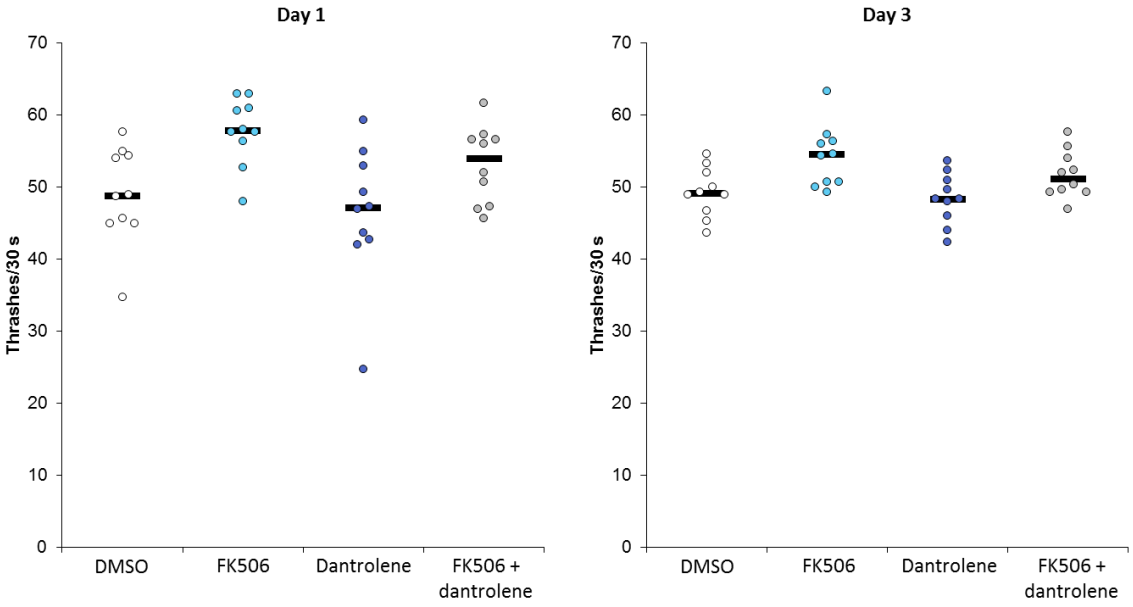

	Day 1	Day 3
DMSO vs. FK506	0.003526	0.011188
DMSO vs. dantrolene	0.506803	0.558935
dantrolene vs. FK506 + dantrolene	0.071564	0.040899

Biological repeat	Day 1	Day 3
DMSO vs. FK506	0.007616	0.016722
DMSO vs. dantrolene	0.217915	0.687856
dantrolene vs. FK506 + dantrolene	0.072221	0.031598

Figure 4.18 FK506 increased C. elegans bus-5 thrashing rate in the presence of dantrolene in two biological repeats. 50 µg/ml FK506 significantly increased C. elegans bus-5 thrashing rate at days 1 and 3 of adulthood, but 10 µM dantrolene had no significant effect. Co-treating with FK506 and dantrolene produced a significant increase in thrashing rate over treating with dantrolene alone at day 3, and increased thrashing rate at day 1 with p = 0.07, in two biological repeats. Bar = median, n = 10, P values calculated using T Test.

To test the combination of FK506 and dantrolene on lifespan, *C. elegans bus*-5 were co-treated with 50 µg/ml FK506 and 10 µM dantrolene from hatching and lifespan with population crowding was assayed (Figure 4.19), in two biological repeats. Treating with FK506 alone significantly increased *bus-5* lifespan, but treating with dantrolene alone had no significant effect. Co-treating with both FK506 and dantrolene significantly increased lifespan compared to dantrolene alone. As FK506 was able to increase lifespan in the presence of RyR inhibition by dantrolene, this suggests RyR activity is not required for FK506 to extend lifespan.

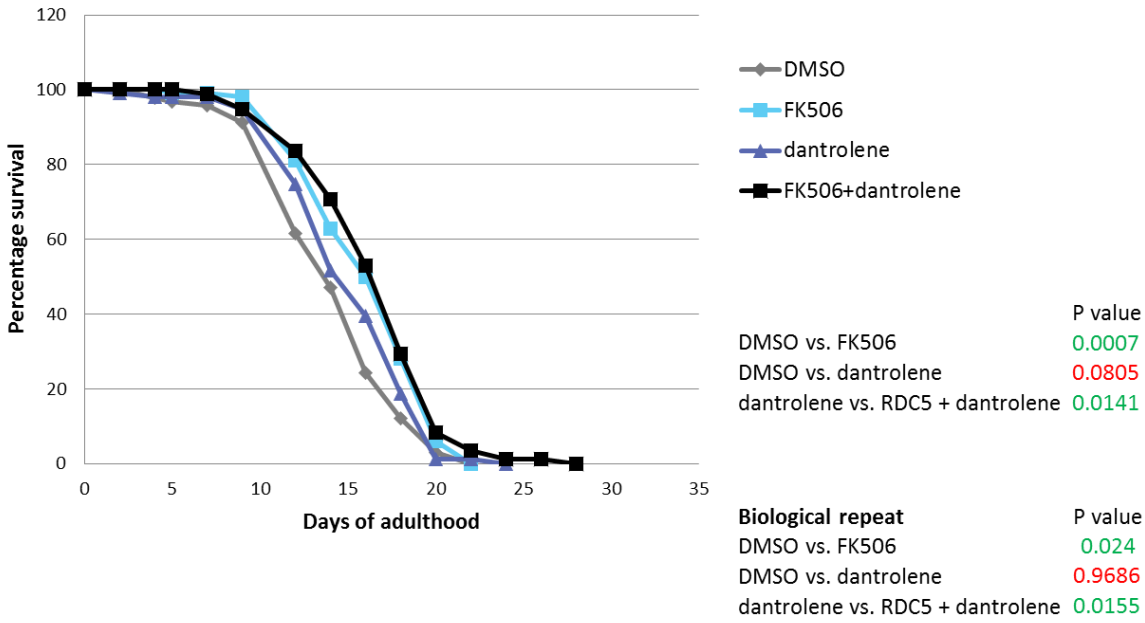

Figure 4.19 FK506 increased C. elegans bus-5 lifespan (with population crowding) in the presence of dantrolene. Co-treating with FK506 and dantrolene significantly increased lifespan compared to treating with dantrolene alone, in two biological repeats. 50 µg/ml FK506 alone extended bus-5 lifespan compared to the DMSO vehicle-treated control but 10 µM dantrolene alone had no significant effect. 100 worms/plate, n = 100, P values calculated using OASIS Log-Rank Test.

Both the thrashing rate and lifespan effects of FK506 were independent of RyR activity, so the mechanism of action of FK506 in not via regulation of RyR activity. However, the slight interaction between FK506 and dantrolene on thrashing rate suggests calcium ion flux may be involved in the mechanism of action of FK506 on thrashing rate, but not lifespan. This could be via regulation of other calcium channels, or an impact on muscle contraction, which requires ion flux.

4.5.4 FK506 action interacted with autophagy

Autophagy can influence ageing, and is regulated by calcineurin (section 1.1.4.4).

C. elegans bus-5 were co-treated with the autophagy inhibitor 3-methyladenine (3-MA)

(Samokhvalov et al. 2008) and inducer trehalose (Depuydt et al. 2016) to investigate whether the mechanism of action of FK506 requires autophagy.

Firstly, the requirement for autophagy was tested on FK506-induced thrashing rate increase. *C. elegans bus*-5 were co-treated with 50 µg/ml FK506 and 1.5 mg/ml 3-MA (Samokhvalov et al. 2008) or 5 mM trehalose (Depuydt et al. 2016) from hatching and thrashing rate was assayed at days 1 and 3 of adulthood (Figure 4.20). When treated with FK506 or 3-MA *C. elegans bus-5* thrashing rate was significantly increased, but trehalose treatment had an inconsistent effect on thrashing rate across the three biological repeats. In one repeat trehalose had no effect on thrashing rate, in a second repeat trehalose significantly increased thrashing rate, and in the third repeat trehalose had no effect at day 1 but significantly increased thrashing rate at day 3. This inconsistency may arise due to the effect of trehalose on *E. coli* OP50 growth. Bacteria can use trehalose as a carbon and energy source (Argüelles 2000), increasing growth rate. The subsequent changes in bacterial metabolism and quantity may influence *C. elegans* ageing and/or thrashing rate.

Co-treating with FK506 and 3-MA significantly increased *bus-5* thrashing rate at day 3 of adulthood but not day 1 in two repeats, and increased thrashing rate at day 1 but not day 3 in one repeat. Therefore, inhibition of autophagy did not prevent FK506 inducing an increase in thrashing rate, but made this effect inconsistent. Co-treating with FK506 and trehalose also had an inconsistent effect compared to treating with trehalose alone. In one repeat FK506 was able to increase thrashing rate at both days in the presence of trehalose, but in another repeat FK506 had no significant effect in the presence of trehalose. In the third repeat FK506 did not increase thrashing rate at day 1 but did at day

3 in the presence of trehalose. Therefore, induction of autophagy prevented FK506 consistently increasing thrashing rate. In conclusion, the mechanism of action of FK506 on thrashing rate interacts with, but does not require autophagy.

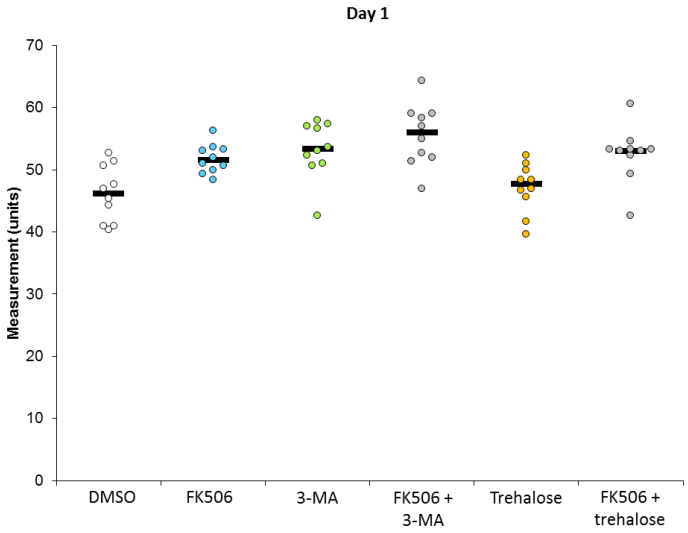

	Day 1	Day 3
DMSO vs. FK506	0.003744	0.010488
DMSO vs. 3-MA	0.00264	0.014182
3-MA vs. FK506 + 3-MA	0.290332	0.03079
DMSO vs. trehalose	0.62918	0.48969
trehalose vs. FK506 + trehalose	0.009469	0.002843

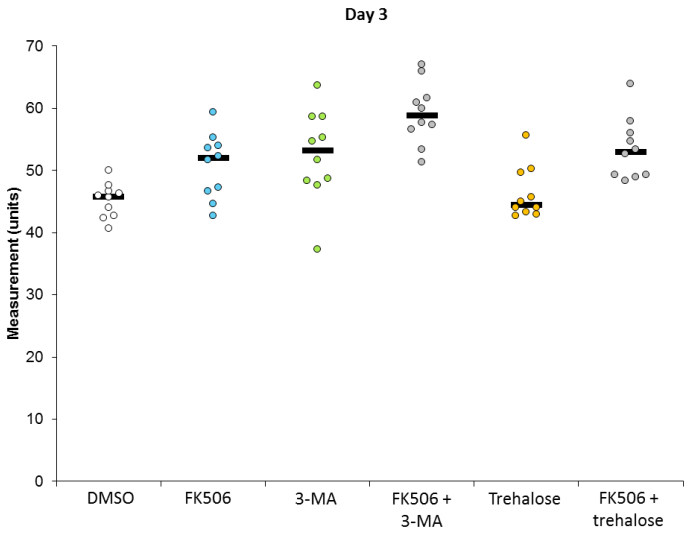

Biological repeat	Day 1	Day 3
DMSO vs. FK506	0.063235	0.000727417
DMSO vs. 3-MA	0.000753	3.39169E-06
3-MA vs. FK506 + 3-MA	0.099215	0.021380155
DMSO vs. trehalose	0.863874	0.001924581
trehalose vs. FK506 + trehalose	0.116977	0.366569856

Biological repeat	Day 1	Day 3
DMSO vs. FK506	3.07E-05	0.015024
DMSO vs. 3-MA	0.000375	0.001806
3-MA vs. FK506 + 3-MA	0.007341	0.105735
DMSO vs. trehalose	0.039593	0.004715
trehalose vs. FK506 + trehalose	0.076076	0.003021

Figure 4.20 FK506 inconsistently increased C. elegans bus-5 thrashing rate in the presence of 3-MA and trehalose, in three biological repeats. 50 µg/ml FK506 significantly increased C. elegans bus-5 thrashing rate at days 1 and 3 of adulthood. 1.5 mg/ml 3-MA significantly increased thrashing rate in all three repeats, but the effect of 5 mM trehalose was inconsistent, sometimes increasing thrashing rate and sometimes having no significant effect. Co-treating with FK506 and 3-MA inconsistently increased thrashing rate or had no effect compared to 3-MA alone, and co-treating with FK506 and trehalose in comparison to trehalose alone was inconsistent, with FK506 either significantly increasing thrashing rate or having no significant effect. Bar = median, n = 10, P values calculated using T Test.

Next, the requirement of the FK506-induced lifespan extension for autophagy was tested. *C. elegans bus*-5 were co-treated with 50 µg/ml FK506 and 1.5 mg/ml 3-MA or 5 mM trehalose from hatching and lifespan with population crowding was assayed (Figure 4.21), in two biological repeats. Treating with FK506 or trehalose alone significantly increased *bus-5* lifespan, but treating with 3-MA alone had no significant effect. Co-treating with both FK506 and 3-MA significantly increased lifespan compared to 3-MA alone, but co-treating with FK506 and trehalose was not significantly different to treating with trehalose alone.

FK506 was able to increase *C. elegans bus*-5 lifespan independently of 3-MA inhibition, but had no additive effect on lifespan with trehalose. Therefore, FK506 and 3-MA have independent targets, whereas FK506 and trehalose have overlapping mechanisms on autophagy regulation. 3-MA influences autophagy via TOR, whereas trehalose and calcineurin act independently of TOR, suggesting the lifespan extension effect of FK506 requires a TOR-independent alteration of autophagy. FK506 inhibits calcineurin, potentially resulting in inhibition of autophagy in a TOR-independent manner. FKBP51 and FKBP38 bind BECN1 and Bcl-2 autophagy proteins respectively and FK506 increases levels of autophagy proteins in cell culture (Nakagaki et al. 2013), so FK506 may induce autophagy. In conclusion, the TOR-independent targeting of autophagy by FK506 is not required to increase thrashing rate, but is required for lifespan extension. However, whether FK506 upregulates or downregulates autophagy is unknown.

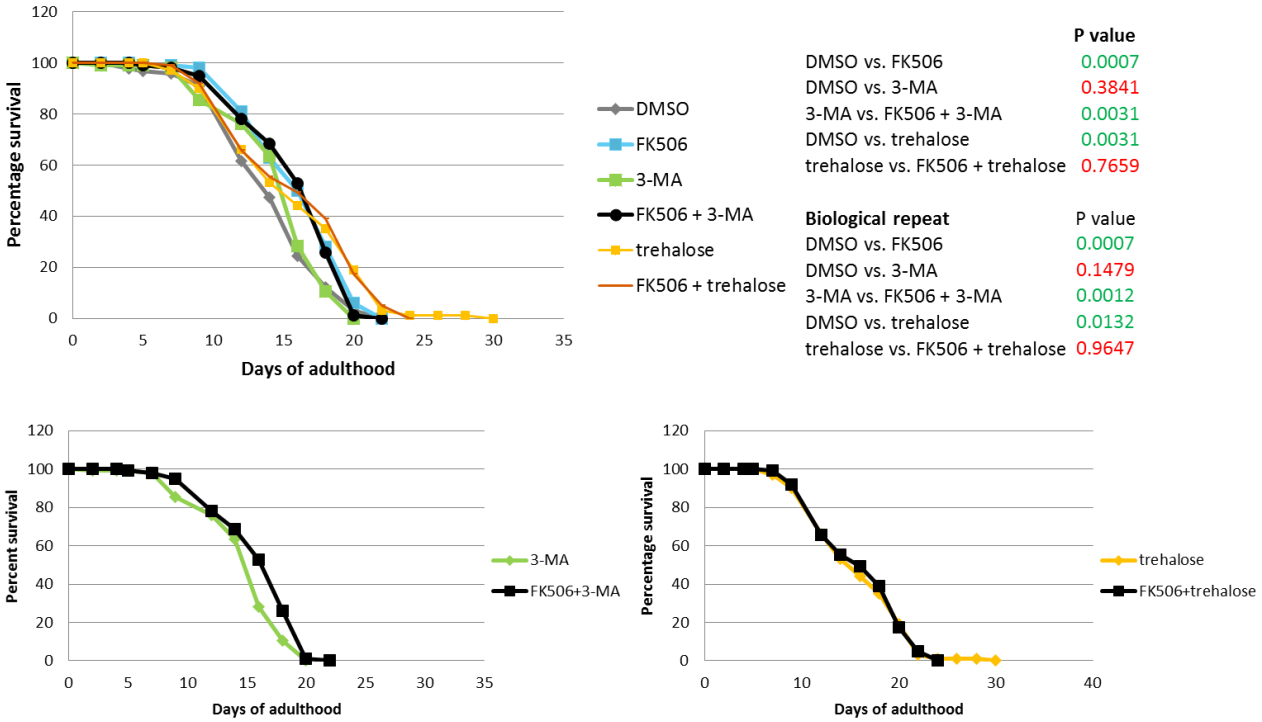

Figure 4.21 FK506 increased C. elegans bus-5 lifespan (with population crowding) in the presence of 3-MA, but not in the presence of trehalose, in two biological repeats. Co-treating with FK506 and 3-MA significantly increased lifespan compared to treating with 3-MA alone, but co-treating with FK506 and trehalose had no effect compared to treating with trehalose alone. 50 µg/ml FK506 alone extended bus-5 lifespan compared to the DMSO vehicle-treated control but 1.5 mg/ml 3-MA alone had no significant effect, whilst 5 mM trehalose increased lifespan. 100 worms/plate, n = 100, P values calculated using OASIS Log-Rank Test.

4.5.5 FK506 action was serotonin signalling independent

Serotonin signalling regulates lipid metabolism, and has also been linked to lifespan. Since FK506 alters both lipid metabolism and lifespan, *C. elegans bus-5* were co-treated with serotonin to investigate whether the mechanism of FK506 requires serotonin signalling.

First, the combination of FK506 and serotonin was tested on thrashing rate. *C. elegans bus*-5 were co-treated with 50 µg/ml FK506 and 5 mM serotonin (Srinivasan et al. 2008) from hatching and thrashing rate was assayed at days 1 and 3 of adulthood (Figure 4.22). When treated with FK506 *C. elegans bus-5* thrashing rate was significantly increased, but

serotonin treatment had no significant effect on thrashing rate in two biological repeats. Co-treating with FK506 and serotonin significantly (or with near-significance at day 1 in one repeat) increased *bus-5* thrashing rate in comparison to serotonin alone at both days of adulthood. This suggests that serotonin signalling is not required for FK506 to increase thrashing rate.

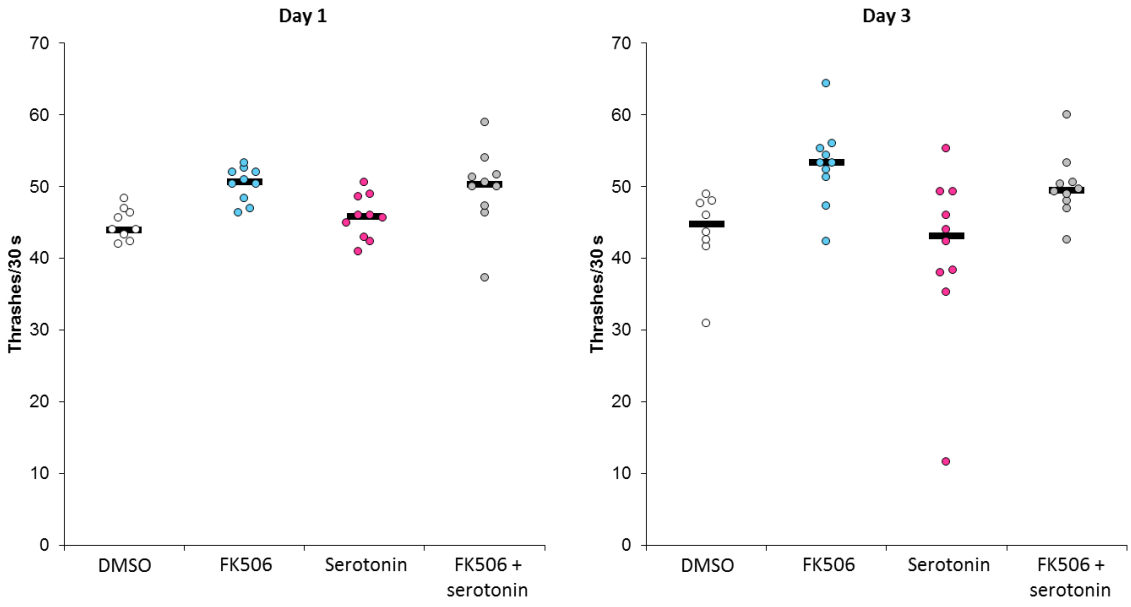

Figure 4.22 FK506 increased C. elegans bus-5 thrashing rate in the presence of serotonin in two biological repeats. 50 µg/ml FK506 significantly increased C. elegans bus-5 thrashing rate at days 1 and 3 of adulthood, but 5 mM serotonin had no significant effect. Co-treating with FK506 and serotonin produced a significant (or near-significant at day 1 in one repeat) increase in thrashing rate over treating with serotonin alone at both days, in two biological repeats. Bar = median, n = 10, P values calculated using T Test. Data collected in repeat by summer student Hannah Street under my supervision.

Next, the combination of FK506 and serotonin was tested on lifespan. *C. elegans bus*-5 were co-treated with 50 µg/ml FK506 and 5 mM serotonin from hatching and lifespan with population crowding was assayed (Figure 4.23), in three biological repeats. Treating

with serotonin alone had no significant effect on *bus-5* lifespan in two repeats, and decreased lifespan in one repeat. Treating with FK506 alone had no effect on *bus-5* lifespan, suggesting FK506 had lost activity. However, co-treating with both FK506 and serotonin significantly increased lifespan compared to serotonin alone in all three repeats. FK506 was able to increase lifespan (as well as thrashing rate) in the presence of serotonin, suggesting the mechanism of action of FK506 is independent of serotonin signalling. However, as FK506 was able to increase lifespan in the presence of serotonin despite having no effect in the absence of serotonin in these experiments, this suggests there is synergy between FK506 and serotonin on lifespan extension.

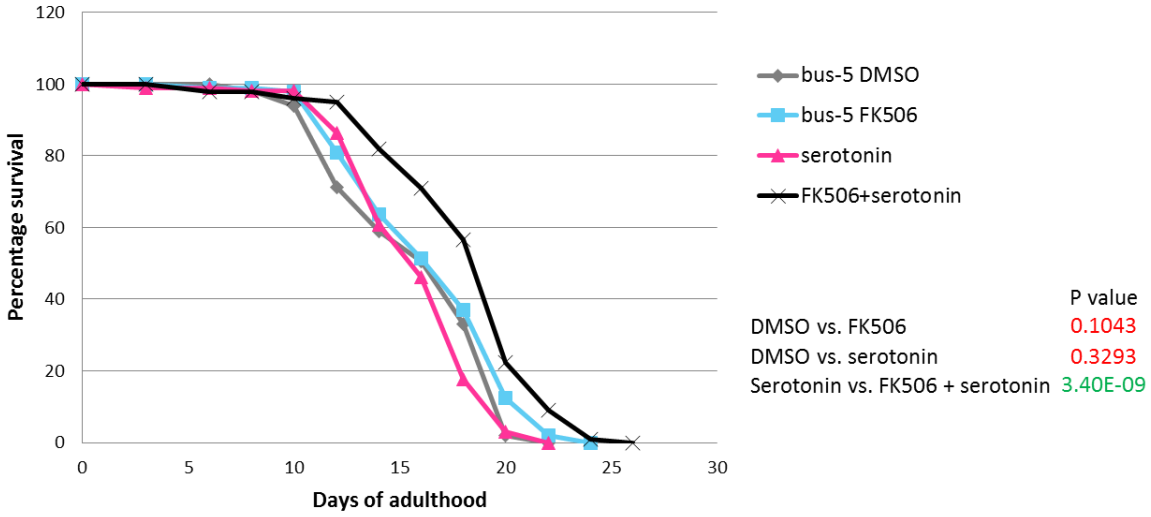

	P value
DMSO vs. FK506	0.1043
DMSO vs. serotonin	0.3293
Serotonin vs. FK506 + serotonin	3.40E-09

Biological repeat	P value
DMSO vs. FK506	0.8132
DMSO vs. serotonin	0.4528
Serotonin vs. FK506 + serotonin	0.0157

Biological repeat	P value
DMSO vs. FK506	0.8693
DMSO vs. serotonin	6.4e-07 (decreased)
Serotonin vs. FK506 + serotonin	1.10E-06

Figure 4.23 FK506 increased C. elegans bus-5 lifespan (with population crowding) in the presence of serotonin. Co-treating with FK506 and serotonin significantly increased lifespan compared to treating with serotonin alone in three biological repeats. However, 50 µg/ml FK506 alone had no effect on bus-5 lifespan compared to the DMSO vehicle-treated control. 5 mM serotonin alone had no effect in two repeats, but significantly decreased lifespan in another repeat. 100 worms/plate, n = 100, P values calculated using OASIS Log-Rank Test.

4.5.6 The effect of FK506 on thrashing rate was sirtuin-independent

The sirtuin family of proteins regulate lifespan and are involved in the mechanism of action of dietary restriction. As FK506 and DR have overlapping mechanisms, FK506 may also target the sirtuins. Nicotinamide, the product of the deacetylation reaction sirtuins catalyse, is an inhibitor of this protein family. *C. elegans bus-5* were co-treated with nicotinamide to investigate whether the mechanism of FK506 on thrashing rate is sirtuin-dependent.

The combined effect of FK506 and nicotinamide was tested on thrashing rate. *C. elegans bus*-5 were co-treated with 50 µg/ml FK506 and 200 µM nicotinamide from hatching and thrashing rate was assayed at days 1 and 3 of adulthood (Figure 4.24). When treated with FK506 *C. elegans bus-5* thrashing rate was significantly increased, whilst nicotinamide treatment had no significant effect on thrashing rate at days 1 and 3 of adulthood. Co-treating with FK506 and nicotinamide significantly increased *bus-5* thrashing rate in comparison to nicotinamide alone at both days of adulthood. This suggests that FK506 acts independently of the sirtuins to increase thrashing rate.

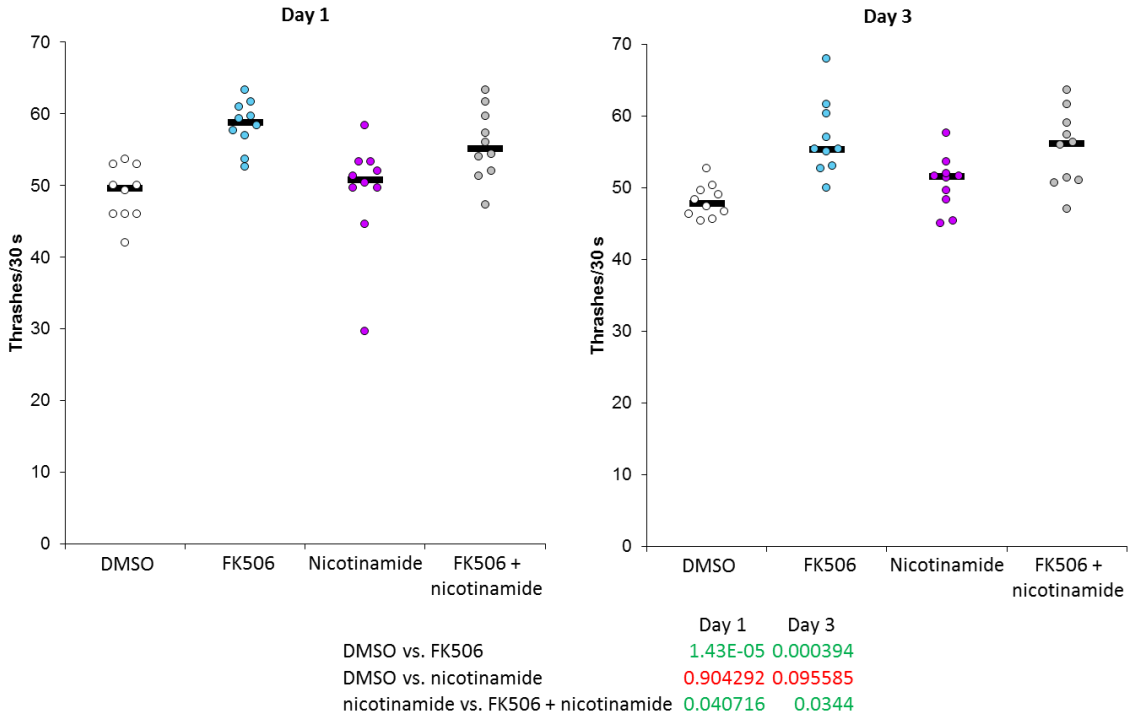

Figure 4.24 FK506 increased C. elegans bus-5 thrashing rate in the presence of nicotinamide. 50 µg/ml FK506 significantly increased C. elegans bus-5 thrashing rate at days 1 and 3 of adulthood, whilst 200 µM nicotinamide had no significant effect at days 1 and 3 of adulthood. Co-treating with FK506 and nicotinamide produced a significant increase in thrashing rate over treating with nicotinamide alone at both days. Bar = median, n = 10, P values calculated using T Test.

4.5.7 FK506 and Li^+ had separate but over lapping mechanisms

Li^+ extends lifespan in *C. elegans* (McColl et al. 2008; Tam et al. 2014) and *Drosophila* (Castillo-Quan et al. 2016), and several mechanisms of action have been suggested: inhibition of glycogen synthase kinase-3 (GSK-3) (Castillo-Quan et al. 2016), regulation of histone methylation (McColl et al. 2008) and upregulation of autophagy (Tam et al. 2014). FK506 also influences metabolism and autophagy, and FKBPs are linked to chromatin regulation (sections 1.2.4, 1.3.11 and 1.3.3 respectively). *C. elegans bus-5* were co-treated with Li^+ to investigate whether the mechanism of FK506 on thrashing rate overlaps with the mechanism of Li^+.

10 mM Li^+ increases *C. elegans* N2 thrashing rate (McColl et al. 2008; Tam et al. 2014), but in the *C. elegans bus-5* strain 10 mM Li^+ decreased thrashing rate at day 3 of adulthood and had no significant effect at day 1 (Figure 4.25 A). A dose response test was performed and suggested 2 mM Li^+ was the optimum dose for *C. elegans bus-5* when added to the surface of NGM plates (Figure 4.25 B), rather than dissolved into liquid NGM (Tam et al. 2014).

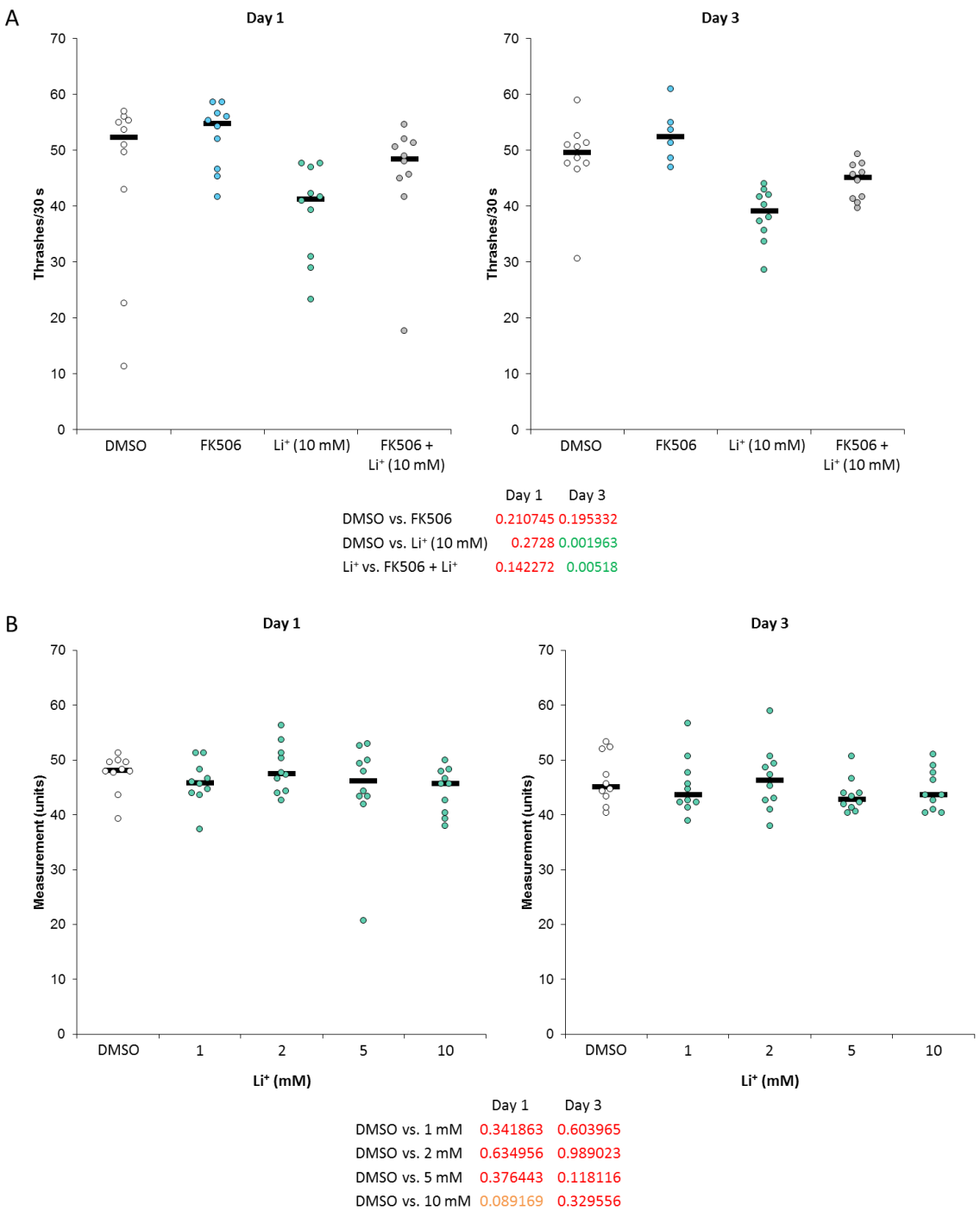

Figure 4.25 Finding the optimal dose of Li^+ on C. elegans bus-5. (A) 10 mM Li^+, the concentration used in the literature, had no significant effect on C. elegans bus-5 thrashing rate at day 1 adulthood and significantly decreased thrashing rate at day 3 of adulthood, and co-treating with 50 µg/ml FK506 and 10 mM Li^+ significantly increased thrashing rate at day 3 but not day 1 in comparison to Li^+ alone. But FK506 alone was unable to increase thrashing rate, possibly due to its unstable nature. (B) Li^+ dose response of C. elegans bus-5 thrashing rate. 1-10 mM Li^+ had no significant effect on thrashing rate, though at 10 mM there was a trend towards decreased thrashing rate. Of the tested doses of Li^+, 2 mM had the highest thrashing rate. Bar = median, n = 10, P values calculated using T Test.

Once the optimal dose of Li^+ was found, the combined effect of Li^+ and FK506 on thrashing rate was tested. *C. elegans bus*-5 were co-treated with 50 µg/ml FK506 and 2 mM Li^+ from hatching and thrashing rate was assayed at days 1 and 3 of adulthood (Figure 4.26). When treated with FK506 *C. elegans bus-5* thrashing rate was significantly increased, whilst 2 mM Li^+ treatment had no significant effect at both days. Co-treating with FK506 and 2 mM Li^+ increased *bus-5* thrashing rate in comparison to 2 mM Li^+ alone with near-significance at days 1 and 3 of adulthood. As FK506 can partially increase *bus-5* thrashing rate in the presence of Li^+, FK506 and Li^+ have separate but slightly overlapping mechanisms of action. The mechanism of action of FK506 on thrashing rate interacts with but does not require autophagy (see section 4.5.4), and autophagy is one of the potential mechanisms of action of Li^+, so this may be the common target.

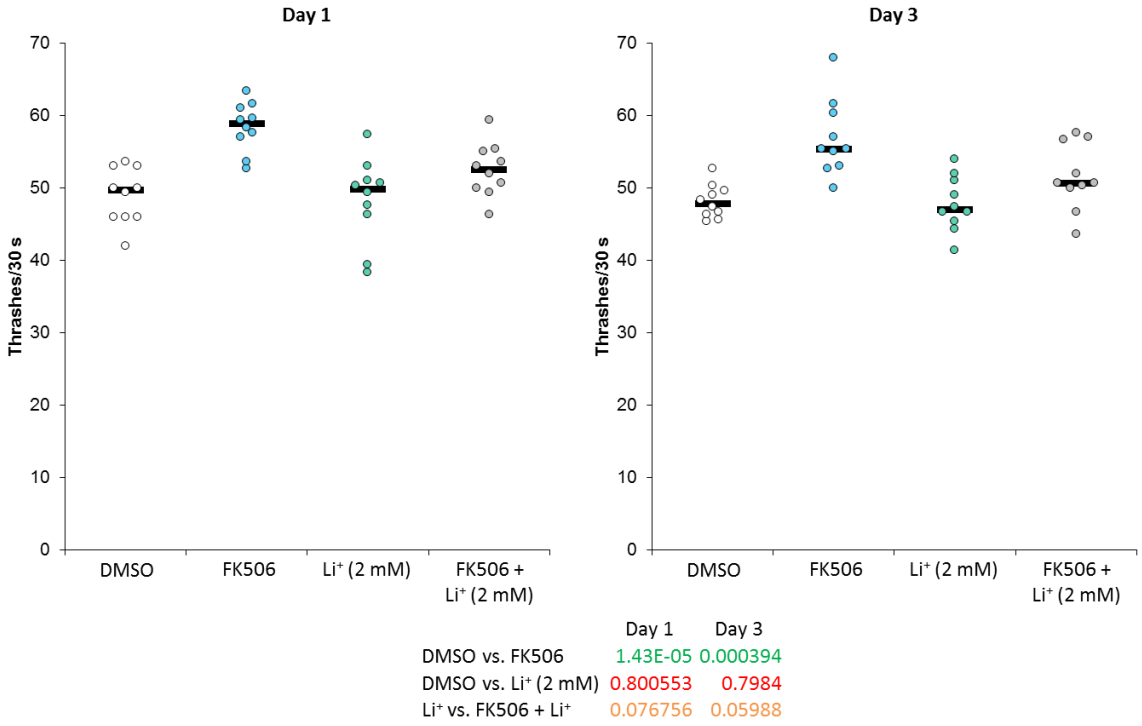

Figure 4.26 FK506 partially increased C. elegans bus-5 thrashing rate in the presence of Li^+. 50 µg/ml FK506 significantly increased C. elegans bus-5 thrashing rate at days 1 and 3 of adulthood, whilst 2 mM Li^+ had no significant effect. Co-treating with FK506 and 2 mM Li^+ produced a near-significant increase in thrashing rate over treating with 2 mM Li^+ alone at days 1 and 3. Bar = median, n = 10, P values calculated using T Test.

4.5.8 FK506 and metformin acted independently on *C. elegans bus-5* thrashing rate

Metformin is an anti-ageing drug, used to treat diabetes in humans. In *C. elegans* the anti-ageing mechanism of metformin is through alteration of folate metabolism in the bacterial food source of the worms, not a direct action on the worms themselves (Cabreiro et al. 2013). As bacterial strain influences FK506 activity (section 4.3), *C. elegans bus-5* were co-treated with metformin to investigate whether FK506 also acts on bacterial folate metabolism.

To test the combined effect of FK506 and metformin on thrashing rate, *C. elegans bus*-5 were co-treated with 50 µg/ml FK506 and 50 mM metformin (Cabreiro et al. 2013) from hatching and thrashing rate was assayed at days 1 and 3 of adulthood (Figure 4.27). When treated with FK506 *C. elegans bus-5* thrashing rate was significantly increased at day 3 and increased with $p = 0.1$ at day 1, whilst metformin treatment had no significant effect. Co-treating with FK506 and metformin significantly increased *bus-5* thrashing rate in comparison to metformin alone at day 3 and increased with $p = 0.1$ at day 1. As the effect of FK506 in the presence of metformin was the same as in the absence of metformin, this suggests that the mechanism of FK506-induced increase in thrashing rate is not via *E. coli* OP50 folate metabolism.

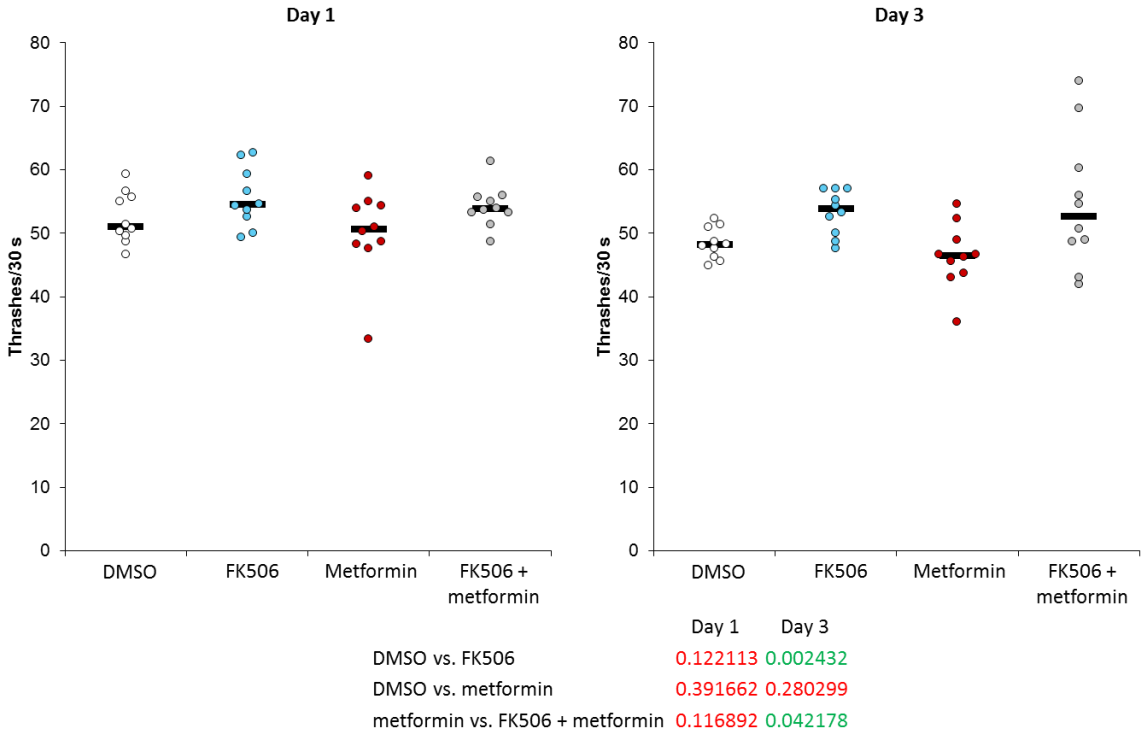

Figure 4.27 FK506 increased C. elegans bus-5 thrashing rate in the presence of metformin. 50 µg/ml FK506 significantly increased C. elegans bus-5 thrashing rate at day 3 of adulthood and with p = 0.1 at day 1, whilst 50 mM metformin had no significant effect. Co-treating with FK506 and metformin produced a significant increase in thrashing rate over treating with metformin alone at day 3 of adulthood and with p = 0.1 at day 1. Bar = median, n = 10, P values calculated using T Test.

4.5.9 FK506 and caffeine had overlapping mechanisms on *C. elegans bus-5* thrashing rate

Caffeine extends lifespan in *C. elegans* (Sutphin et al. 2012; Bridi et al. 2015; Lublin et al. 2011) in a DAF-16 dependent manner (Lublin et al. 2011; Bridi et al. 2015), but the exact mechanism of action is unknown. *C. elegans bus-5* were co-treated with caffeine and FK506 to investigate whether they have an additive effect.

The combined effect of FK506 and caffeine on thrashing rate was tested. *C. elegans bus*-5 were co-treated with 50 µg/ml FK506 and 1 mg/ml caffeine (Lublin et al. 2011) from hatching and thrashing rate was assayed at days 1 and 3 of adulthood (Figure 4.28). When treated with FK506 or caffeine alone *C. elegans bus-5* thrashing rate was increased

at both days 1 and 3 of adulthood. Co-treating with FK506 and caffeine significantly increased *bus-5* thrashing rate in comparison to caffeine alone at day 3, but had no effect at day 1. This suggests that FK506 and caffeine have overlapping, but not identical anti-ageing mechanisms of action, possibly involving the IIS pathway as both are DAF-16 dependent.

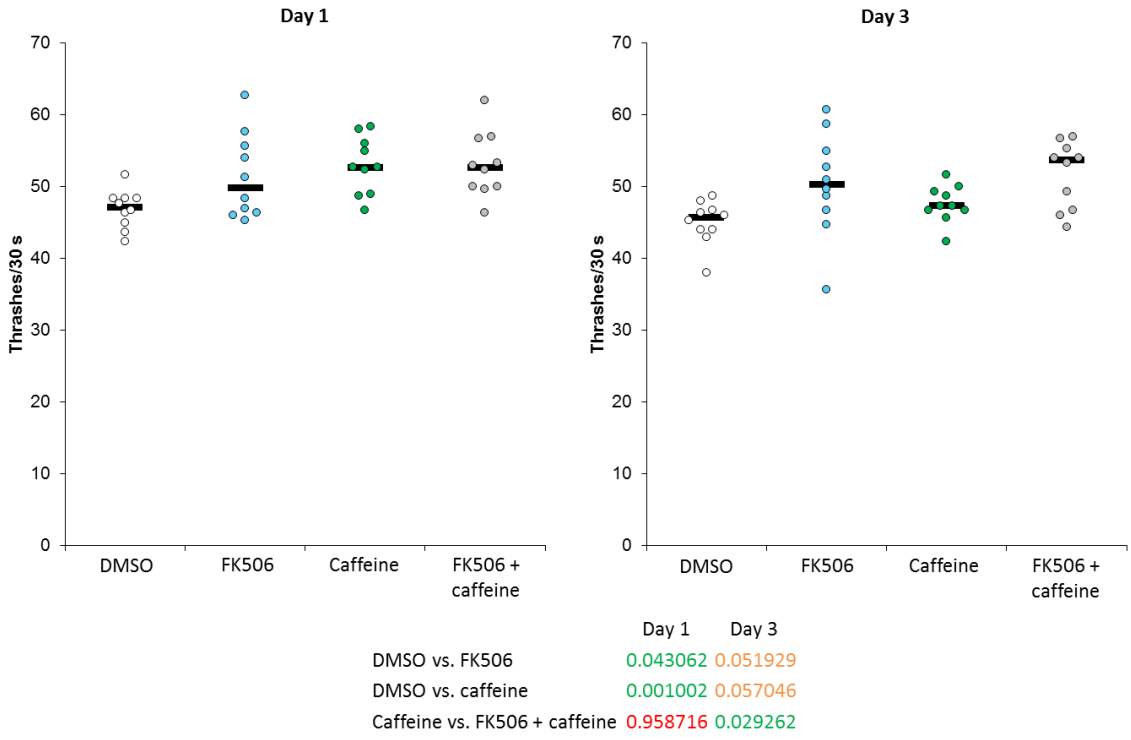

Figure 4.28 FK506 had variable action on C. elegans bus-5 thrashing rate in the presence of caffeine. Both 50 µg/ml FK506 and 1 mg/ml caffeine alone increased C. elegans bus-5 thrashing rate at both days of adulthood. Co-treating with FK506 and caffeine produced a significant increase in thrashing rate over treating with caffeine alone at day 3 of adulthood but had no effect at day 1. Bar = median, n = 10, P values calculated using T Test.

4.5.10 Summary

The results of co-treating *C. elegans bus-5* with FK506 and a range of small molecule drugs is summarised in Table 4.2, showing which cellular functions are required for FK506 to induce an increase in thrashing rate and lifespan (under crowded conditions).

Cellular function/protein	**Compound**	**Blocks the effect of FK506 on…**	
		thrashing	**lifespan**
FKBPs	Rapamycin	Y	Y
Calcineurin	CsA	N	Y
RyR	Dantrolene	partially	N
Autophagy	3-MA	partially	N
	Trehalose	partially	Y
Serotonin signalling	Serotonin	N	N
Sirtuins	Nicotinamide	N	-
Ageing	Li^+	partially	-
Ageing (bacterial metabolism)	Metformin	N	-
Ageing	Caffeine	partially	-

Table 4.2 The dependence of FK506 action on different cellular functions and proteins. Y = interaction, N = independent mechanisms.

4.6 Discussion

RNA-seq of FK506-treated *C. elegans bus-8* found that FK506 altered levels of RNAs associated with lipid and fatty acid metabolism, calcium ion homeostasis, translation and response to stress, suggesting potential mechanisms of action for FK506. These potential targets could not be investigated using RNAi, as the strain *E. coli* HT115 altered the effect of FK506. The IIS pathway dependence of FK506 activity was tested in a *daf-16* null mutant with N2 genetic background. The effect of FK506 on thrashing rate was DAF-16 dependent, but as the control failed in the lifespan experiment, the DAF-16 requirement of FK506-induced lifespan extension cannot be confirmed.

As an alternative to RNAi, the mechanism of action of FK506 was investigated using co-treatment with small molecule inhibitors and inducers. The exact mechanism of action of FK506 on thrashing rate is still unknown. It is DAF-16- and FKBP-dependent, interacts with but does not require autophagy, has overlapping targets with caffeine (potentially DAF-16), and may involve Ca^{2+} flux. It is independent of calcineurin, serotonin signalling, sirtuins and bacterial folate metabolism. Further experiments to investigate the mechanism of FK506-induced increase of thrashing rate could test whether FK506 targets muscle function, as muscle contraction involves Ca^{2+} flux.

The mechanism of action of FK506 on lifespan is FKBP- and calcineurin-dependent, and also dependent on TOR-independent regulation of autophagy. It is independent of RyR, serotonin signalling and TOR-dependent regulation of autophagy. Further experiments are required to determine whether FK506 up or downregulates autophagy. As calcineurin upregulates autophagy in a TOR-independent manner, inhibition of calcineurin by the FK506-FKBP complex could cause inhibition of autophagy. However, FK506 has been reported to induce autophagy by increasing levels of autophagy proteins (Nakagaki et al. 2013). Induction of autophagy increases lifespan (Eisenberg et al. 2009) and has been linked to lifespan extension by TOR inhibition and dietary restriction (Hansen et al. 2008; Madeo et al. 2010), making the promotion of autophagy most likely mechanism of FK506. Autophagy is also linked to lipid metabolism. In germline-less *C. elegans*, autophagy and lipolysis promote lifespan extension in a co-ordinated manner (Lapierre et al. 2011). Autophagy is also one mechanism of lipid breakdown (Glaumann 1982) and is involved in adipocyte differentiation and lipid metabolism (Ro et al. 2013), a potential mechanism of action of FK506 on lipid accumulation.

As FK506-induced lifespan extension is dependent on FKBPs, calcineurin and possibly DAF-16, the interaction of these proteins provides a potential anti-ageing mechanism of action for FK506. Calcineurin dephosphorylates DAF-16, preventing translocation to the nucleus and therefore inactivating DAF-16 and promoting a shortened lifespan (Tao et al. 2013). Inhibition of calcineurin by the FK506-FKBP complex would relieve inhibition of DAF-16, allowing DAF-16 to localise to the nucleus and promote lifespan extension.

5 Results – adipocyte cell culture

5.1 Introduction

In rats, FK506 treatment prevented age-related weight gain and decreased the concentration of TAG in the blood (section 1.2.6). In *C. elegans* FK506 delayed lipid accumulation (Figure 1.9) and RNA-seq showed altered levels of RNA associated with lipid metabolism (section 4.2.1). But it is currently unknown whether FK506 directly targets adipocytes to reduce lipid storage, or whether FK506 influences mechanisms of lipid metabolism regulation in other tissues, such as energy source usage in muscles or nervous system signalling. The aim of these experiments is to assess the effect of FK506 on lipid storage in adipocytes in culture.

The embryonic-derived 3T3-L1 mouse preadipocyte cell line, which can be induced to differentiate into adipocytes (Figure 5.1), is the most commonly used cell culture model of adipocytes. The experiments were conducted using the following protocol, outlined in Figure 5.2. 3T3-L1 were seeded in 6-well plates and two days after reaching confluence were treated with dexamethasone, insulin and IBMX to induce differentiation (days 0-4). During these four days the differentiating cells were also treated with 100 ng/ml FK506 (or vehicle-only control). One plate of pre-adipocytes was harvested at day 0 before treatment, then one plate of FK506-treated and one vehicle-treated plate of adipocytes were harvested every five days up to day 20. 3T3-L1 adipocytes are not cultured past day 20 in the literature as population synchronisation is too low by this point (Yu & Zhu 2004), due to cell death and detachment leaving space for any undifferentiated preadipocytes to

proliferate. When each plate was harvested, three wells on each 6-well plate were formaldehyde fixed and stained with oil-red-O (ORO) and then methylene blue to quantify triacylglycerides (TAG) and cell mass respectively. Cells from the other three wells were detached, cell number counted by Cellometer and RNA was purified from these cells for RNA-seq.

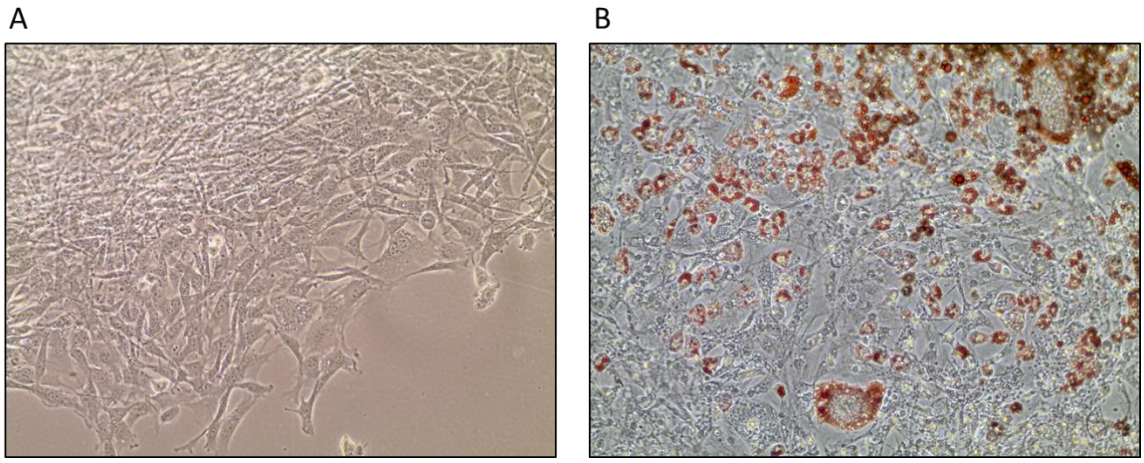

Figure 5.1 Differentiation changed 3T3-L1 cell morphology from long, thin pre-adipocytes (A, day 0 pre-adipocytes) to rounded adipocytes containing lipid droplets (B, ORO stained day 10 adipocytes treated with ethanol).

Experimental timeline:

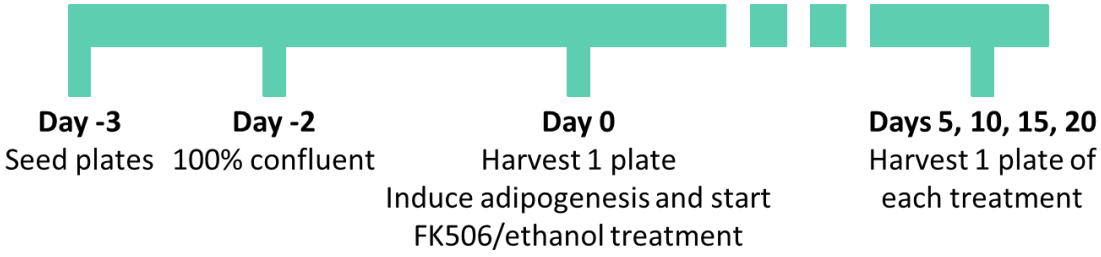

Plate harvesting:

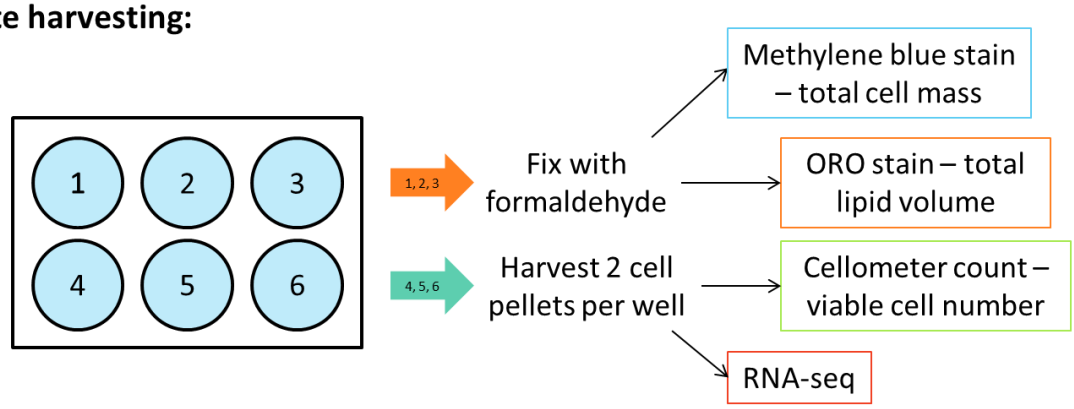

Figure 5.2 The experimental protocol used to differentiate 3T3-L1 into adipocytes and the harvesting of cells. The experimental outputs were methylene blue staining of total cell mass per well, ORO staining of total TAG per well, Cellometer counting of viable cell number per well and also RNA-seq to determine differences in RNA levels caused by FK506 treatment, differentiation and cell ageing.

5.2 Method optimisation

3T3-L1 adipocytes are non-trivial to culture. As adipocytes have a rounded shape, they easily detach from the surface so all medium was pipetted by hand when replaced every second day, instead of aspirating with a vacuum pump. The 3T3-L1 line is not immortalised and their ability to differentiate declines with passage number, so the number of population doublings before differentiation was induced had to be minimised whilst also ensuring there was a sufficient number of cells to become confluent. Other experiment methods also required optimisation, including FK506 vehicle, methylene blue staining of cell mass and RNA purification.

5.2.1 Ethanol instead of DMSO was selected as FK506 vehicle

FK506 is not water-soluble and must be dissolved in a non-polar solvent, such as ethanol or DMSO. DMSO was used as the vehicle for FK506 in the *C. elegans* experiments, so was tested in the 3T3-L1 adipocytes.

DMSO increases cell permeability, so at high concentrations is toxic. Most cell lines can tolerate 1% DMSO without negative effects, but at this concentration DMSO caused the formation of dark inclusions within 3T3-L1 adipocytes (Figure 5.3 A) and high levels of cell death (Figure 5.3 B). The final concentration of DMSO was lowered to 0.1% DMSO (Figure 5.4), and although this had a less severe impact on the 3T3-L1 adipocytes, many inclusions were still present. These inclusions had a different composition to the lipid droplets accumulated within the adipocytes, as they were not stained by ORO (Figure 5.3 A, right).

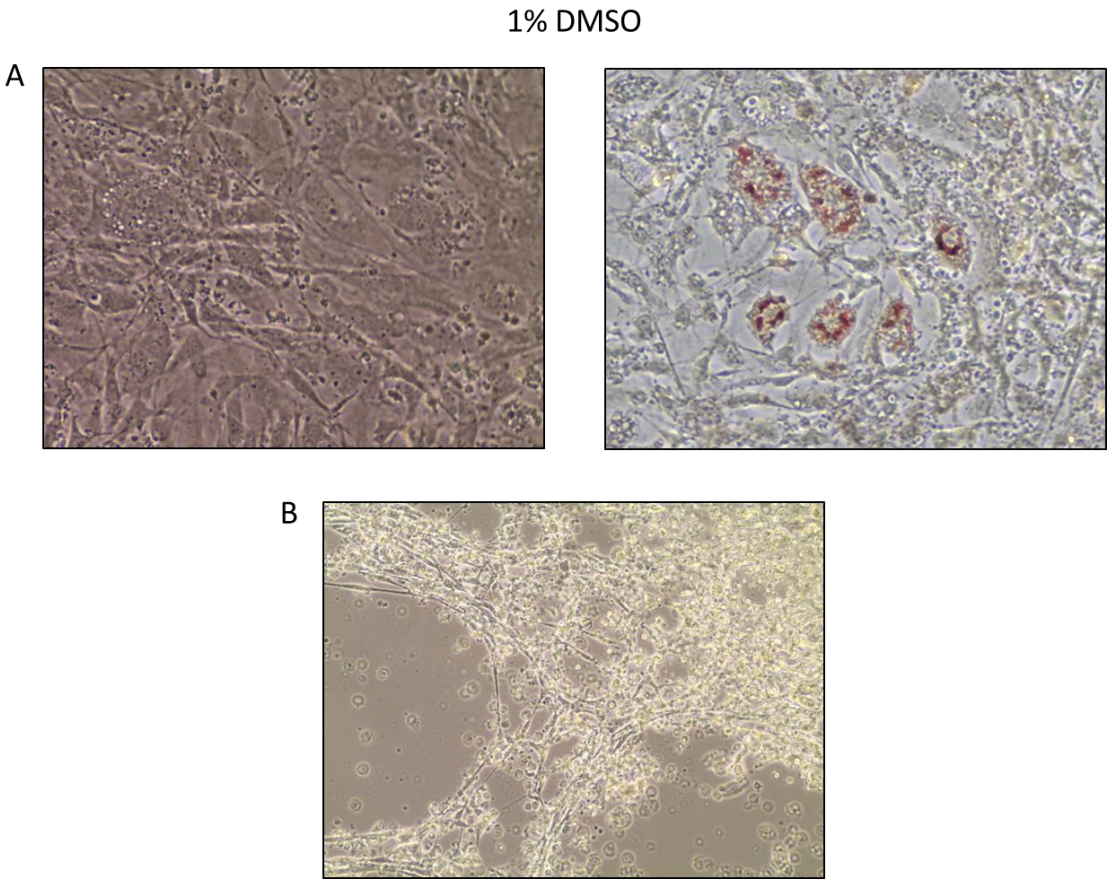

Figure 5.3 3T3-L1 treated with 1% DMSO. (A) At day 5, 3T3-L1 treated with 1% DMSO contained black inclusions (live cells, left) which were different in composition to the ORO-stained lipid droplets (fixed cells, right). (B) At day 2, 1% DMSO treatment killed many cells, causing them to become spherical and detach from the surface of the plate (live cell image).

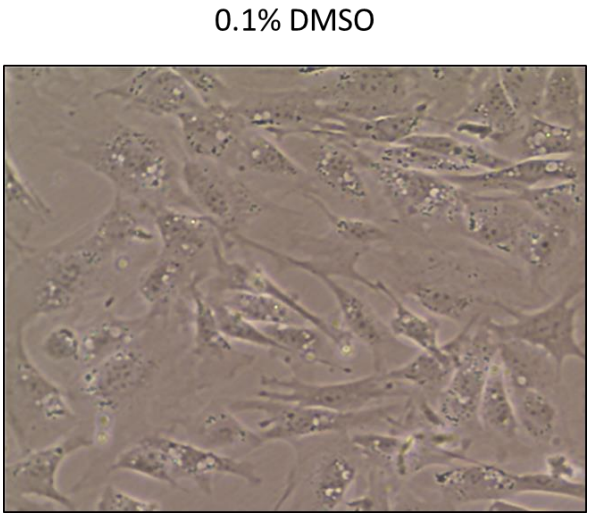

Figure 5.4 3T3-L1 treated with 0.1% DMSO at day 5 contained fewer black inclusions than 1% treated cells (live cell image).

As even 0.1% DMSO was harmful to 3T3-L1 adipocytes, an alternative solvent, ethanol, was tested at a final concentration of 1.25% (Figure 5.5). In comparison to untreated adipocytes (Figure 5.5 A), ethanol did not cause inclusions to form and did not cause cell death (Figure 5.5 B), so was selected as the vehicle to dissolve FK506.

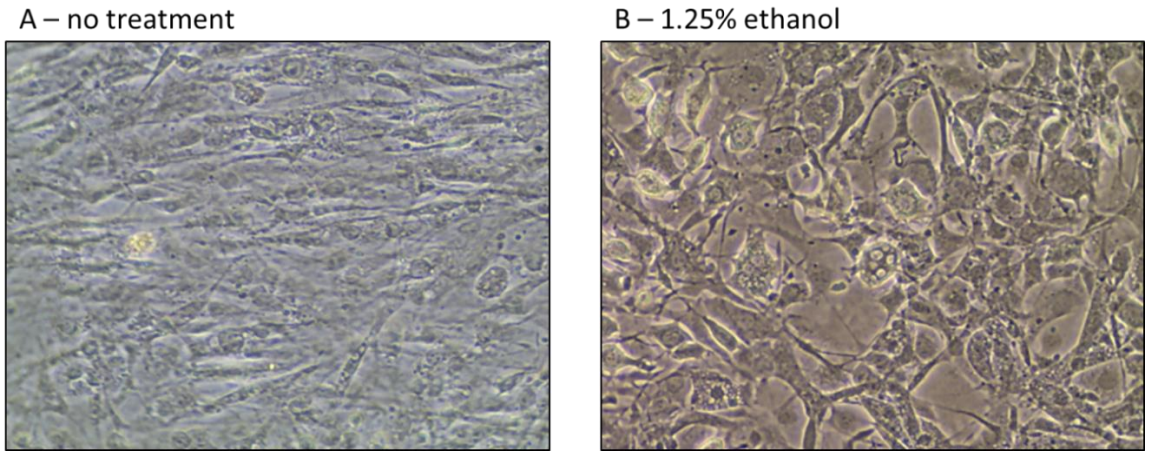

Figure 5.5 Untreated 3T3-L1 (A) and 1.25% ethanol-treated 3T3-L1 (B) at day 5 had similar appearances, containing almost no inclusions (live cell images).

5.2.2 Methylene blue stain concentration was optimised to quantify total cell mass

In order for the amount of lipid to be measured relative to the number of cells, two methods were developed. The total number of viable cells was measured by Cellometer for the three wells of detached and harvested cells. Lipid volume was quantified in the three fixed wells by ORO staining. The mean volume of lipid was divided by the mean number of viable cells to quantify the amount of lipid per viable cell. However, the cell number count in the harvested cells many not accurately reflect the number of fixed cells due to loss of cells during washing steps. To quantify the number of cells in the same fixed wells used for ORO staining, methylene blue was used to stain cell mass, as cell mass is relative to the number of cells. The amount of lipid was divided by the total cell mass in each well, and the mean of the three wells per plate used to quantify lipid

relative to cell mass. However, cell mass is not an exact measure of cell number as the accumulation of lipid within adipocytes increases cell size.

The methylene blue staining protocol was adapted from Oliver *et. al.* (Oliver et al. 1989), but the volume and concentration of methylene blue stain per well had to be optimised. 1%, 0.5% and 0.1% methylene blue (Figure 5.6) gave staining that was too dark, obscuring cell features. The volume used was also critical; a volume of 400 µl per well of stain was too low, as the meniscus of liquid gave uneven coverage of the cell layer. 800 µl of 0.01% methylene blue (Figure 5.6) gave good coverage of the cell layer and a level of staining in which cell features can be observed, so this concentration and volume of stain was selected.

Methylene blue stain		Image
Volume	Concentration	
1ml	1%	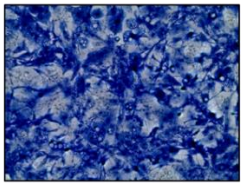
400 µl	0.5%	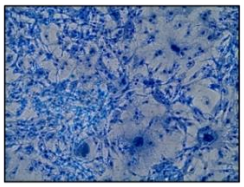
1 ml	0.1%	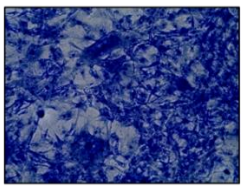
800 µl	0.01%	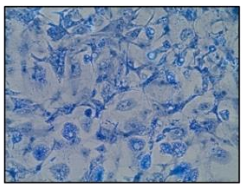

Figure 5.6 Methylene blue stained 3T3-L1 fixed at day 20 (1% DMSO-treated). All images of same well.

5.2.3 RNA purification method was optimised to prevent gDNA contamination

RNA was extracted from the adipocytes in order to produce a transcriptome (by RNA-seq) of FK506-treated and control-treated adipocytes. Lipid can interfere with RNA extraction, so RNA purification methods were tested to ensure a sufficient yield and purity. Three protocols were tried: phenol-chloroform extraction, Qiagen RNeasy kit without DNase and Qiagen RNeasy kit with DNase. All three methods gave a sufficient concentration of RNA to be used in RNA-seq.

To test purity, the RNA was reverse-transcribed (RT) to give cDNA and a 219 bp fragment of β-actin was amplified by PCR. An important control is to test for the level of gDNA contamination in the RNA preparation for all three protocols. To test for gDNA contamination the same RT-PCR reaction was set up, except without the addition of enzyme (no-RT) so no cDNA was synthesised. If the RNA sample contained no gDNA, PCR amplification from the no-RT samples should not produce the 219 bp fragment. However, if gDNA is present in the no-RT sample, the fragment will be amplified.

The phenol chloroform extraction (Figure 5.7) and RNeasy kit without DNase (Figure 5.8) produced RNA contaminated with gDNA, as the 219 bp β-actin fragment was amplified from the no-RT samples. The RNeasy kit with DNase (Figure 5.9) produced RNA without gDNA contamination, as the β-actin fragment was not amplified from the no-RT samples. Therefore, the RNeasy kit with DNase method of RNA purification was selected.

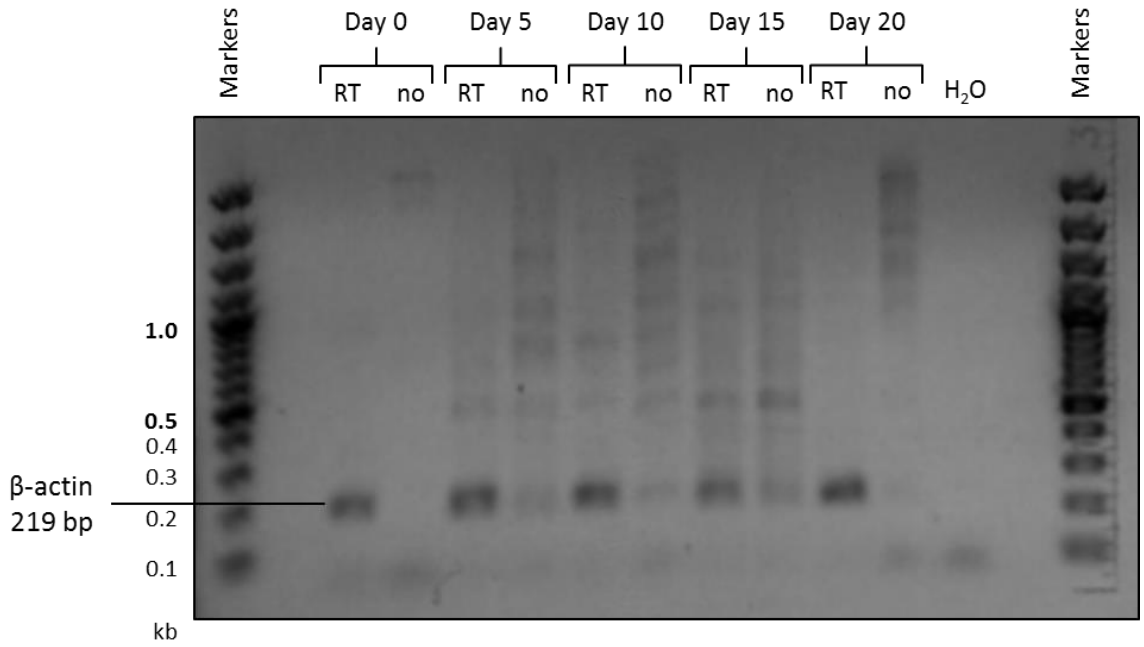

Figure 5.7 PCR amplification of β-actin from cDNA derived from RNA purified from 3T3-L1 adipocytes using the phenol-chloroform protocol. The β-actin fragment was amplified from the reverse-transcribed samples (RT) and the samples incubated without RT enzyme (no). 1% agarose/TBE/EtBr gel, TBE buffer. Run at 110 V for 35 min. 1 µl loading dyes (Thermo) mixed with 3 µl PCR product. Marker 100 bp plus (Thermo). UV image taken with 3 s exposure.

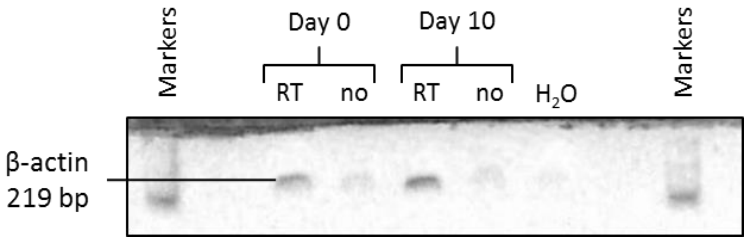

Figure 5.8 PCR amplification of β-actin from cDNA derived from RNA purified using the RNeasy kit without DNase. The β-actin fragment was amplified from the reverse-transcribed samples (RT) and the samples incubated without RT enzyme (no). 1% agarose/TBE/EtBr gel, TBE buffer. Run at 65 V for 15 min. 1 µl loading dyes (Thermo) mixed with 3 µl PCR product. Marker 100 bp plus (Thermo). UV image taken with 5 s exposure.

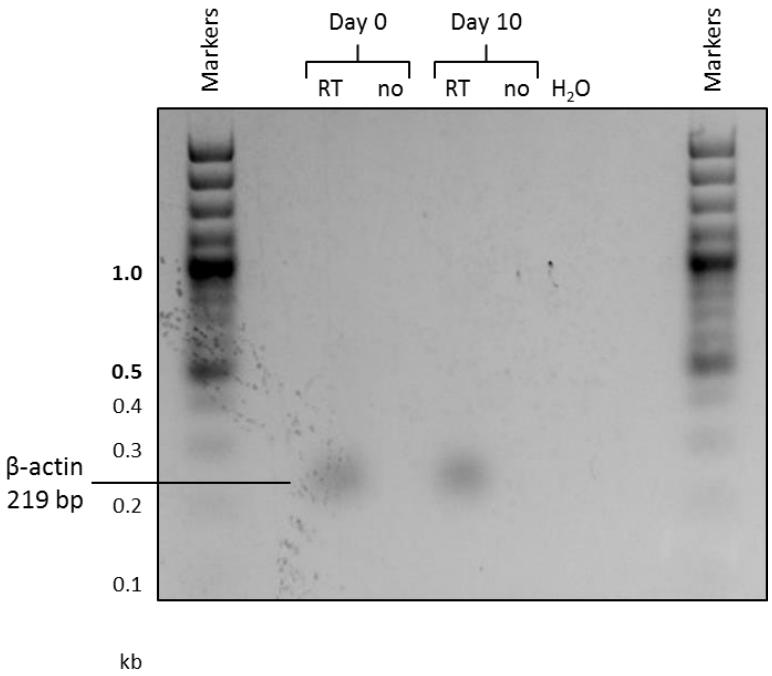

Figure 5.9 PCR amplification of β-actin from cDNA derived from RNA purified using the RNeasy kit with DNase. The β-actin fragment was amplified from the reverse-transcribed samples (RT), but not from the samples incubated without RT enzyme (no). 2% agarose/TBE/EtBr gel, TBE buffer. Run at 110 V for 37 min. 1 µl loading dyes (Thermo) mixed with 3 µl PCR product and 2 µl H_2O. Marker 100 bp plus (Thermo). UV image taken with 0.6 s exposure.

5.3 Mycoplasma testing

Mycoplasma are intracellular bacteria that commonly infect mammalian cell cultures. Mycoplasma infection can alter the results of experiments, so the 3T3-L1 cultures were tested for the presence of mycoplasma using three methods.

Conditioned medium was tested for mycoplasma DNA using the EZ-PCR Mycoplasma Test Kit (Figure 5.10), which amplifies a mycoplasma-specific 270 bp region of 16 S rDNA. The fragment was amplified in the positive control, but not in either sample of conditioned 3T3-L1 medium, suggesting that no mycoplasma were present.

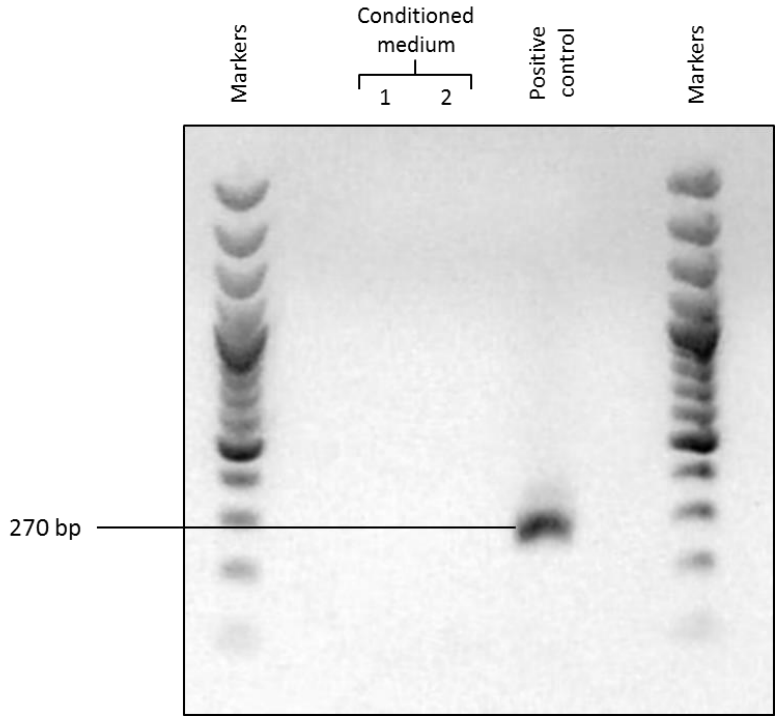

Figure 5.10 Amplification of a 270 bp fragment of mycoplasma 16 S rDNA using EZ-PCR Mycoplasma Test Kit. The fragment was absent in both samples, including the negative control with H_2O instead of conditioned medium, but was present in the positive control. 1% agarose/TBE/EtBr gel, TBE buffer. Run at 110 V for 30 min. 1 µl loading dyes (Thermo) mixed with 3 µl PCR product. Marker 100 bp plus (Thermo). UV image taken with 0.5 s exposure.

To confirm these results, the Mycoplasma Detection Kit – Quick Test (Biotool) was used to detect mycoplasma metabolites in conditioned medium (Figure 5.11). However, in this test two of the three samples of conditioned medium tested positive for mycoplasma.

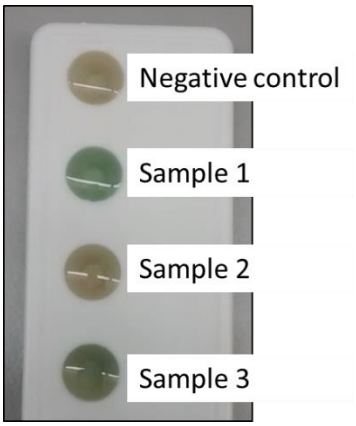

Figure 5.11 Two of the three samples of conditioned 3T3-L1 medium tested positive for the presence of mycoplasma metabolites using the Biotool Mycoplasma Detection Kit. Green = mycoplasma metabolites present, peach = no mycoplasma metabolites.

To resolve this difference, a third test was performed (Figure 5.12). DNA was extracted from the conditioned medium used in the metabolite test and a 425 bp fragment of 16 S rDNA using universal primers which bind DNA from most mycoplasma strains (Molla Kazemiha et al. 2009). However, in all three samples and the negative control, the 425 bp fragment was amplified. This occurred in four experimental repeats, so it could not be determined whether mycoplasma were present or not.

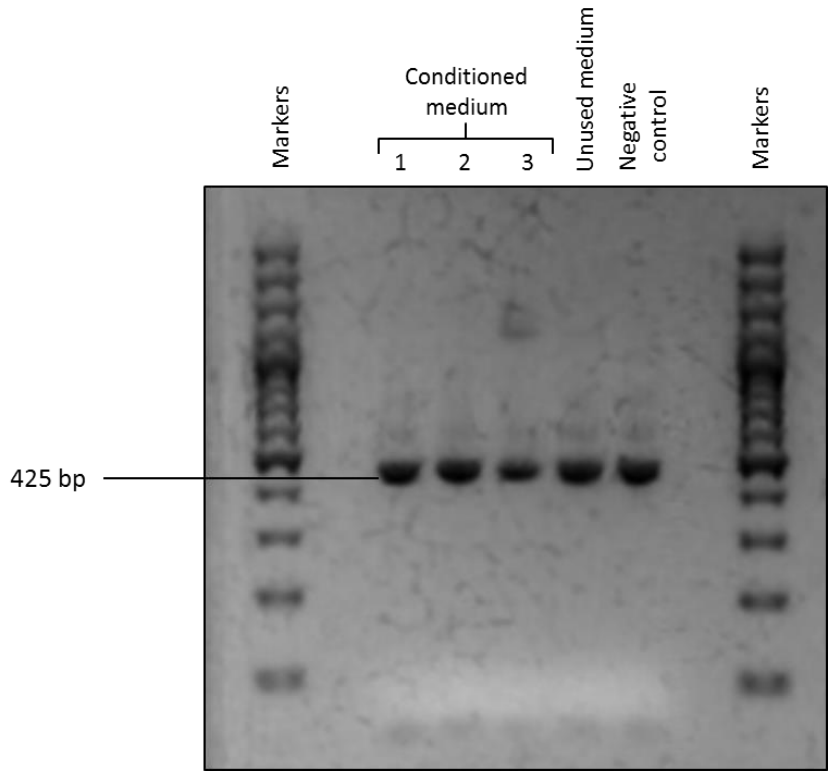

Figure 5.12 Amplification of a 425 bp fragment of mycoplasma 16 S rDNA using universal primers. The fragment was detected in all samples, including the negative control with H_2O instead of DNA extracted from conditioned medium. This occurred in all four repeats. 2% agarose/TBE/EtBr gel, TBE buffer. Run at 100 V for 40 min. 1 µl loading dyes (NEB) mixed with 5 µl PCR product. Marker 100 bp plus (Thermo). UV image taken with 2 s exposure.

As the results of the three tests for mycoplasma were inconclusive, some or all of the adipocyte cultures may or may not be infected with mycoplasma. This could potentially affect the action of FK506.

5.4 FK506 decreased lipid accumulation in 3T3-L1 adipocytes

To investigate whether FK506 acts directly on adipocytes to alter lipid accumulation, and if so what effects FK506 has on these cells, cultured 3T3-L1 adipocytes were differentiated and treated with FK506.

As shown in Figure 5.2, 3T3-L1 pre-adipocytes were seeded in 6-well plates, incubated overnight to reach 100% confluence then incubated for a further two days at 100% confluence until day 0. At day 0, one plate was harvested and stained whilst the others were treated with the differentiation mix (insulin, dexamethasone and IBMX) and either FK506 or ethanol vehicle control until day 4. The medium was replaced every second day and one plate of each treatment condition was harvested and stained every five days.

In both the FK506-treated and ethanol-treated adipocytes, the size of the lipid droplets increased over time, seen in Figure 5.13 stained with ORO. At day 0 the undifferentiated preadipocytes contained effectively no lipid. At day 5 differentiated adipocytes contain small lipid droplets, and by day 20 these have developed into large droplets.

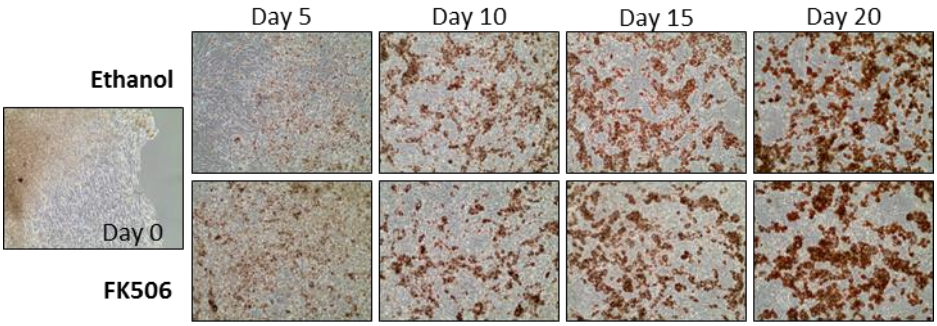

Figure 5.13 ORO staining of TAG in 3T3-L1 adipocytes. At day 0, undifferentiated pre-adipocytes contain almost no TAG. Once the cells have differentiated, they gradually accumulate more TAG as they age (days 5-20) in both FK506-treated and ethanol-treated conditions.

For each 6-well plate harvested, three wells were fixed whilst cells in the other three wells were collected, counted by Cellometer and the cell pellets stored at -80°C. The amount of lipid per well was quantified by ORO staining of the three wells of fixed cells. Two methods were used to quantify the amount of lipid accumulated relative to the number of cells. Firstly, the total number of viable cells was quantified by Cellometer in the three harvested wells of the same plate. For each data point the ratio of the mean amount of lipid and the mean viable cell count was calculated to give an indication of the amount of lipid per cell. Secondly, total cell mass was quantified by methylene blue staining of the same three wells of fixed and ORO-stained cells. For each of the three wells the ratio of lipid to cell mass was calculated, and each data point was the mean of these ratios. There are weaknesses to both methods: Cellometer counting of cells in different wells to those that were ORO-stained may not accurately reflect the number of stained cells. In contrast, methylene blue staining could be done on the same cells as strained with ORO. However, the accumulation of lipid increases cell mass so total cell mass does not have a fixed relationship with cell number.

Using the Cellometer count of viable cell number (Figure 5.14 A), FK506 decreased the accumulation of lipid in 3T3-L1 adipocytes, reaching significance at day 20. Using methylene blue staining, FK506 decreased the accumulation of lipid in 3T3-L1 adipocytes, significantly so at day 10 (Figure 5.14 B). As both measures of lipid per cell number/mass found that FK506 significantly reduced lipid accumulation, albeit reaching significance at different days, it can be concluded that FK506 had a direct effect on adipocytes to reduce lipid storage.

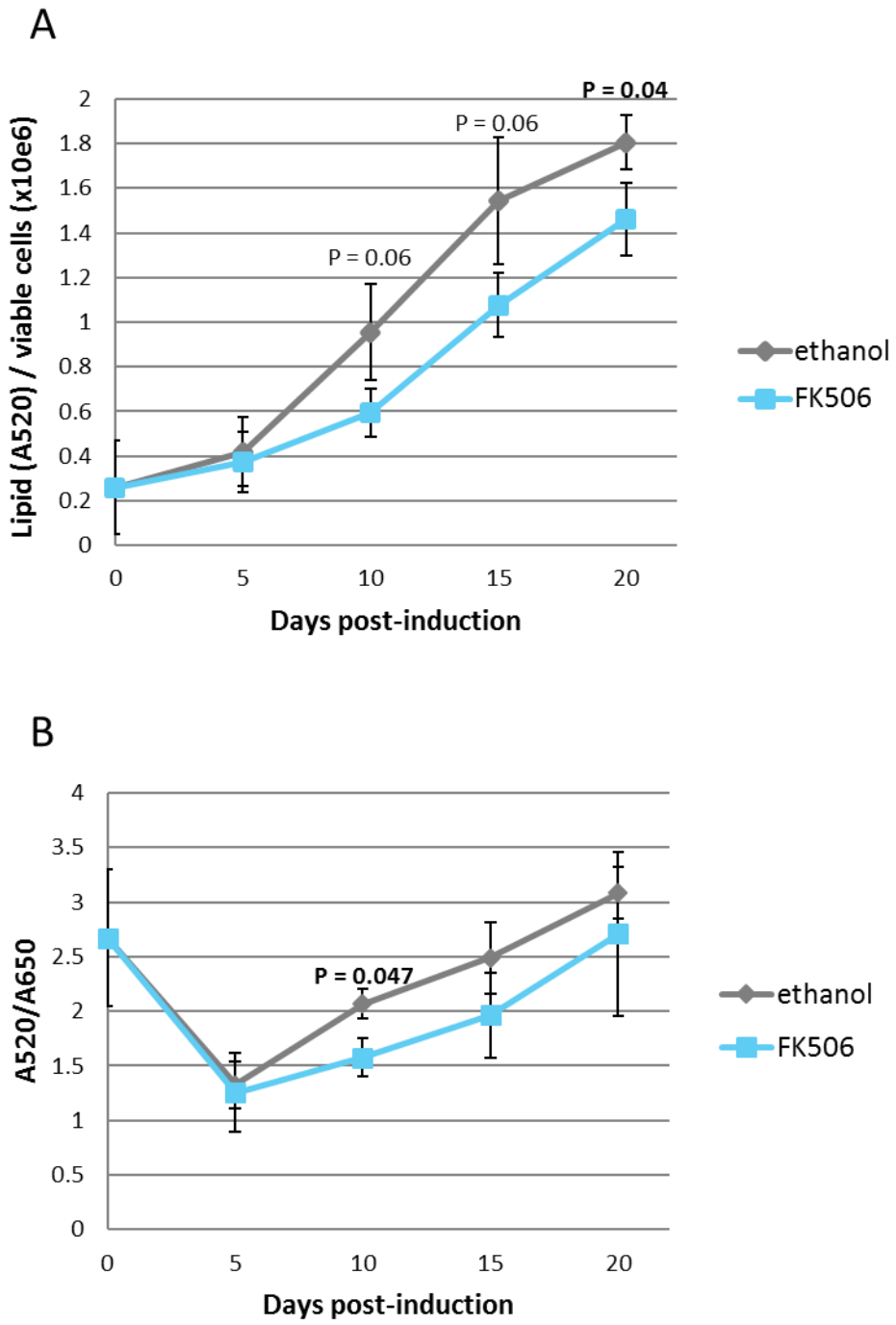

Figure 5.14 FK506 decreased TAG accumulation in 3T3-L1 adipocytes. Different methods of quantifying the amount of lipid relative to cell number resulted in FK506 causing a significant decrease in TAG accumulation at day 20 (A) or day 10 (B). Total volume of TAG per well quantified by ORO staining in both (A) and (B). (A) Cellometer used to count the total number of viable cells in three wells, and TAG quantified in three other wells on the same plate. Means of each used to calculate volume of TAG per viable cell for each data point. (B) After ORO staining, total cell mass was quantified using methylene blue staining in the same three wells per plate. TAG to cell mass ratio was calculated for each well and the mean of the three wells calculated for each data point. N = 3 biological repeats, error bars = SEM, P values calculated using T test.

5.5 FK506 did not measurably affect cell viability

As an anti-ageing treatment, FK506 may affect cell survival and therefore the number of viable cells. When the adipocytes were harvested, cell number was counted using the Cellometer, which also distinguished viable from dead cells and measured the diameter of each cell. Cell diameter increases with age and stress, however the diameter of adipocytes increases as they accumulate lipid, potentially disguising any change due to age.

At each time point for both treatment conditions, cells were harvested from three wells of each plate. Cell counts from these three wells were averaged for each data point, performed for three biological repeats. In comparison to the ethanol-treated control, FK506 treatment did not significantly affect the percentage viability, total number of viable cells or the mean cell diameter (Figure 5.15).

These results may have been influence by the fact cells detach from the surface of the plate when they die. These detached cells are removed each time the medium is replaced, disguising any differences in percentage viability. The detachment of dead cells also leaves space for any undifferentiated pre-adipocytes to proliferate, raising the total number of viable cells and lowering the mean cell diameter. Also, adipocytes increase in size as they accumulate lipid, so an increase in cell diameter does not necessarily indicate an aged cell.

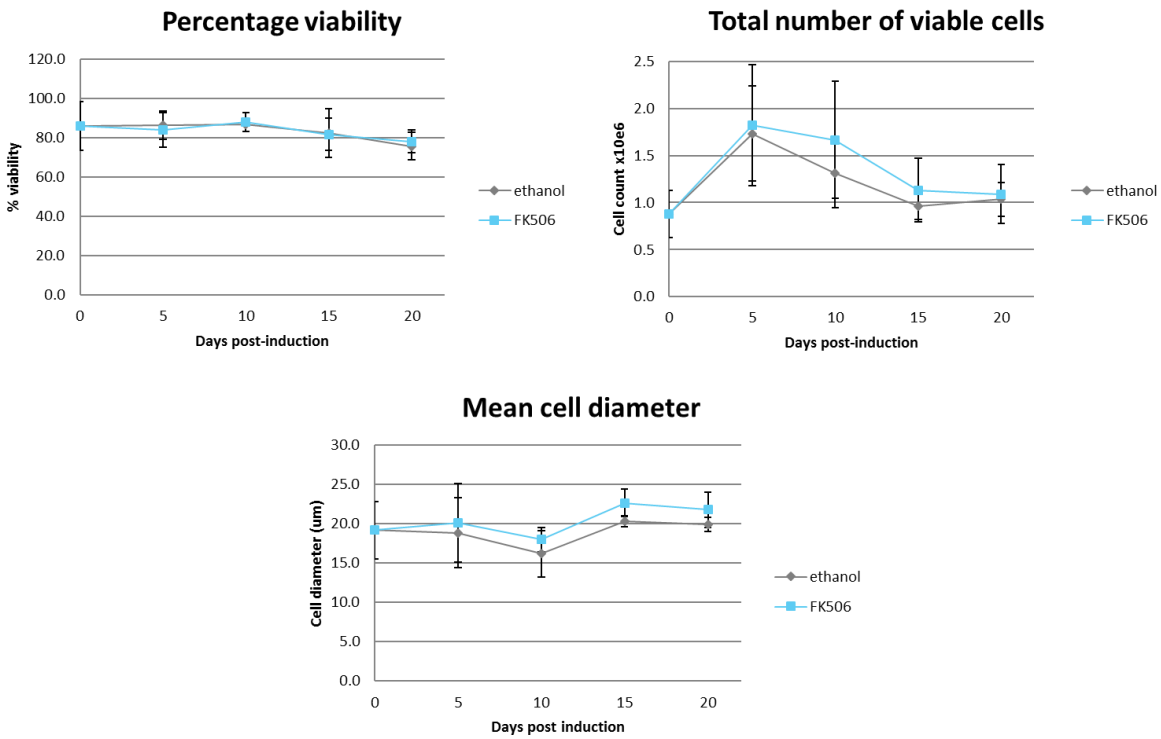

Figure 5.15 FK506 treatment of 3T3-L1 adipocytes did not significantly affect the percentage of viable cells, total number of viable cells or mean cell diameter. Mean of three wells on same plate taken for each data point. N = 3 biological repeats, error bars = SEM, significance calculated using T test.

5.6 FK506 significantly altered RNA levels in 3T3-L1 adipocytes

FK506 acted directly on adipocytes to reduce lipid accumulation, but the mechanism of this effect is unknown. Potentially, FK506 may have the same mechanism of action in adipocytes as in *C. elegans*, and alter lipid metabolism via induction of autophagy. RNA-seq was performed to investigate which cellular processes are altered by FK506, and whether these are similar to the RNA-seq results in *C. elegans* (section 4.2). Significantly altered RNAs were identified by Dr. H. Fischl using the DESeq algorithm (Love et al. 2014).

FK506 treatment significantly altered RNA levels of 179 genes at day 5 post-induction and 264 genes at day 10, suggesting FK506 treatment does alter gene expression. Far fewer genes were altered in the adipocytes than were altered by FK506 in *C. elegans*, which is

to be expected when comparing a single cell type to a whole organism. At day 15, FK506 altered RNA levels of only two genes and had no significant effect at day 20. This decline in the effect of FK506 over time may be because the effect of FK506 is transient (cells were treated at days 0-4). Alternatively, the impact of FK506 may be lost when cells die and the available space is filled by proliferating preadipocytes, a process which increases over time, as these new cells have not been exposed to FK506.

The RNAs upregulated and downregulated by FK506 at days 5 and 10 post-induction were analysed using the PANTHER overrepresentation test.

5.6.1 FK506 increased levels of RNAs associated with translation and the ribosome

Overrepresented at both days 5 (Table 5.1) and 10 (Table 5.2) in the RNAs increased by FK506 treatment, were genes linked to translation and the ribosome. Most of these RNAs encode components of the 60 S ribosomal subunit. This suggests FK506 alters protein synthesis, having an opposite effect to rapamycin. Rapamycin inhibits TOR to inhibit translation of ribosome components (Raught et al. 2001). FK506 also altered levels of translation-associated RNAs in *C. elegans* (section 4.2.4).

Day 5 – genes with expression increased by FK506 treatment

	Fold enrichment	P value
GO-Slim Biological process		
Translation	18	3.77 E-19
Cellular component biogenesis	9.09	1.22 E-9
Biosynthetic process	4.15	3.50 E-7
Organelle organisation	3.77	3.88 E-2
Response to stimulus	<0.2 (underrepresented)	3.91 E-3
GO-Slim Molecular function		
Structural constituent of ribosome	30.69	2.73 E-30
GO-Slim Cellular component		
Ribosome	46.69	2.16 E-31
Cytosol	19.62	1.28 E-24
Organelle	3.03	1.73 E-7
Panther Pathways		
N/A		

Table 5.1 GO-terms associated with genes whose expression is increased in 3T3-L1 adipocytes by FK506 treatment at day 5 post-induction. Analysed using PANTHER overrepresentation test (version 11.0).

Day 10 - genes with expression increased by FK506 treatment

	Fold enrichment	P value
GO-Slim Biological process		
N/A		
GO-Slim Molecular function		
Structural constituent of ribosome	7.92	1.19 E-4
GO-Slim Cellular component		
Ribosome	9.49	6.48 E-4
Cytosol	4.21	4.18 E-2
Panther Pathways		
N/A		

Table 5.2 GO-terms associated with genes whose expression was increased in 3T3-L1 adipocytes by FK506 treatment at day 10 post-induction. Analysed using PANTHER overrepresentation test (version 11.0).

5.6.2 FK506 decreased levels of RNAs associated with lipid transport and metabolism

Amongst RNAs down regulated by FK506 treatment at days 5 (Table 5.3) and 10 (Table 5.4), genes associated with lipid transport and metabolism were overrepresented, similarly to the result in *C. elegans* (section 4.2.1). As the RNA-seq averages RNA levels across a population of adipocytes, it cannot be distinguished whether this reduction is due to a lower number of differentiated adipocytes within the population, or if the same number of cells underwent differentiation but showing a weaker adipocyte phenotype. The transcription factor C/EBPα, significantly downregulated at day 10, is required for maintenance of the adipocyte phenotype. Another marker of adipocyte differentiation is Fabp4, down regulated by FK506 at day 5. FK506 has previously been reported to downregulate expression of GLUT4 (insulin-regulated glucose transporter), and here FK506 was found to significantly decrease GLUT4 RNA at day 10. Glucose uptake is stimulated by adiponectin signalling, and the RNA levels of Adiponectin Receptor 2 was decreased by FK506 treatment at both days 5 and 10.

Day 5 – genes with expression decreased by FK506 treatment

	Fold enrichment	P value
GO-Slim Biological process		
Lipid transport	17.62	2.55 E-3
Lipid metabolic process	5.68	2.35 3-3
GO-Slim Molecular function		
Transferase activity, transferring acyl groups	9.61	3.21 E-2
GO-Slim Cellular component		
N/A		
Panther Pathways		
N/A		

Table 5.3 GO-terms associated with genes whose expression is decreased in 3T3-L1 adipocytes by FK506 treatment at day 5 post-induction. Analysed using PANTHER overrepresentation test (version 11.0).

Day 10 - genes with expression decreased by FK506 treatment		
	Fold enrichment	**P value**
GO-Slim Biological process		
Lipid transport	14.4	1.70 E-4
Lipid metabolic process	5.64	2.31 E-6
GO-Slim Molecular function		
N/A		
GO-Slim Cellular component		
Endoplasmic reticulum	7.55	9.65 E-3
Panther Pathways		
TCA cycle	53.87	4.25 E-3

Table 5.4 GO-terms associated with genes whose expression is decreased in 3T3-L1 adipocytes by FK506 treatment at day 10 post-induction. Analysed using PANTHER overrepresentation test (version 11.0).

5.6.3 FK506 had no effect on the RNA levels of uncoupling proteins

A potential mechanism through which FK506 decreases lipid accumulation is by upregulating the activity of uncoupling proteins (UCP). FK506 had no effect on the RNA levels of UCPs in *C. elegans* (section 4.2.2), so the effect of FK506 in 3T3-L1 was checked. RNA of only one UCP, Ucp2, was detected in the adipocytes. FK506 treatment did not significantly alter expression of Ucp2 at any time point. This suggests that FK506 does not cause decreased lipid accumulation by increasing expression of UCPs, although an effect on the protein activity of UCPs cannot be ruled out.

5.6.4 FK506 upregulated an ER-localised FKBP in both 3T3-L1 adipocytes and *C. elegans*

The endoplasmic reticulum (ER)-localised FKBP *fkb-4* was upregulated in the *C. elegans* RNA-seq data (section 4.2.2). In 3T3-L1 adipocytes, the RNA level of an ER-localised FKBP,

Fkbp2, was increased at day 10. This suggests that FK506 is acting (at least in part) through the same mechanisms in both mouse adipocytes and *C. elegans*.

5.7 Discussion

FK506 treatment decreased lipid accumulation in 3T3-L1 mouse adipocytes, confirming that FK506 has a direct effect on adipocytes. Depending on the method used to calculate lipid per cell number or cell mass, lipid accumulation was significantly decreased at day 20 or day 10 post-induction respectively. There was no detectable effect of FK506 on cell survival or mean cell diameter.

FK506 significantly altered RNA levels at days 5 and 10 post-induction, but this effect was lost by days 15 and 20. This may be because the effect of FK506 is transient, or that as cell death increases with time preadipocytes are able to proliferate, increasing the number of cells not exposed to FK506 and reducing population synchronicity. At days 5 and 10, RNAs associated with translation and the ribosome were up regulated, and RNAs associated with lipid transport and metabolism were down regulated. FK506 could reduce the average levels of lipid metabolism-associated RNAs within each sample either by suppressing the adipocyte phenotype across the population of differentiated cells, or by decreasing the number of cells that underwent differentiation. Anti-ageing interventions associated with downregulation of translation and ribosomal proteins include rapamycin (Raught et al. 2001), reduced IIS and dietary restriction (Depuydt et al. 2013). However, deletion of the ribosomal S6 protein kinase 1 (downstream of TOR) extended mouse lifespan and upregulated translation-associated RNAs in the liver (Selman et al. 2009), and chronic downregulation of translation by the unfolded protein

response pathway may be harmful in neurodegeneration (Ma et al. 2014). Therefore, maintaining translation activity during ageing could be beneficial in some tissues.

There were similarities between the RNA-seq results in adipocytes and *C. elegans*. As well as an effect on RNAs associated with lipid metabolism and translation, there was no effect on UCPs and an ER-localised FKBP was up regulated in both systems. This suggests that FK506 acts at least partially through the same pathways in both *C. elegans* and mammalian cells, so the results regarding the mechanism of action of FK506 in *C. elegans* are relevant to mammals.

6 Discussion

In this study, FK506 has been confirmed as a potential anti-ageing treatment, through its ability to extend lifespan and healthspan in *C. elegans*. In addition, FK506 has also been shown to act directly on mouse adipocytes, resulting in a reduction in lipid accumulation. This action could explain how FK506 caused weight loss in obese aged rats, restoring body mass to a healthy adult weight.

This work has revealed possible mechanisms of action of FK506 on lifespan in *C. elegans*, a hypothesis outlined in Figure 6.1. FK506 binds one or more of the FKBPs and inhibits calcineurin (CN). Inhibition of CN relieves inhibition of DAF-16, as CN phosphorylates DAF-16, blocking its nuclear uptake, which is required to induce the gene expression programme associated with increased viability and lifespan (Kenyon et al. 1993). DAF-16 activity also promotes lipolysis (Wang et al. 2008). CN is thought to promote autophagy via dephosphorylation and activation of TFEB, which activates transcription of autophagy genes (Tong & Song 2015). However, *C. elegans* CN-null mutants have increased autophagy (Dwivedi et al. 2009), suggesting CN activity may reduce autophagy and FK506 inhibition of CN may relieve this inhibition. Upregulation of autophagy promotes increased lifespan (Eisenberg et al. 2009; Morselli et al. 2011). FK506 may also act directly on autophagy by upregulating expression of autophagy genes (Nakagaki et al. 2013).

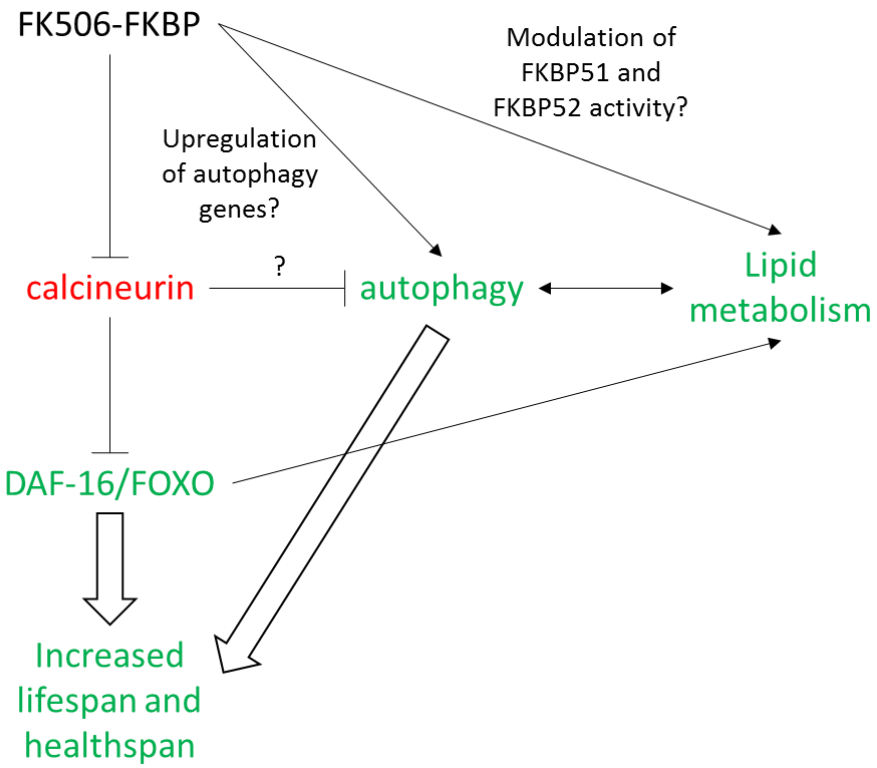

Figure 6.1 A possible mechanism of action of FK506. FK506 binds the FKBPs and inhibits calcineurin (CN). Inhibition of CN relieves inhibition of DAF-16. Increased DAF-16 activity increases lifespan and promotes lipolysis. CN is thought to promote autophagy, but C. elegans CN-null mutants have increased autophagy suggesting CN activity may reduce autophagy and FK506 inhibition of CN may relieve this inhibition. Autophagy promotes increased lifespan. FK506 may also act directly on autophagy by upregulating expression of autophagy genes and may act directly on lipid metabolism by inhibiting or modulating the activity of FKBP51 and FKBP52, both involved in adipogenesis. Red text = inhibited by FK506, green text = upregulated by FK506.

6.1 FK506 extended *C. elegans* lifespan and healthspan

6.1.1 FK506 extended *C. elegans* lifespan

The initial aim of this study was to confirm the results of a phenotypic screen that identified FK506 as able to extend lifespan in yeast and *C. elegans*. This initial observation in *C. elegans* was confirmed, and extended to describe the conditions required for lifespan extension. For example, FK506 was not able to extend the lifespan of *C. elegans* strains N2, *bus-5* and *bus-8* under standard lifespan assay conditions, but showed robust lifespan extension under conditions of population crowding stress of 100 worms per

plate. This suggests that the mechanism of action of FK506 involves the population crowding stress response pathway, or alternatively, that there is synergy between the mild activation of this stress response pathway and FK506 treatment to produce lifespan extension.

Population crowding stress is known to be linked to lifespan. Extreme population crowding stress induces dauer formation (Y. Wang et al. 2009), the alternative *C. elegans* developmental pathway with extended lifespan. Dauer formation is regulated by IIS, also involved in regulation of ageing (Riddle et al. 1981). The complete mechanisms of population crowding stress signalling are unknown and may involve both mechano-sensation and chemical signalling, but secretion and sensing of ascarosides are known to be involved (Kaplan et al. 2012). The *daf-22* gene is required for synthesis of the ascaroside-derivative dauer pheromone, and further work could test whether FK506 requires dauer signalling by treating a *daf-22*-null mutant.

Signalling the presence of population crowding on a plate may occur through other chemicals as well, so an alternative method to investigate whether signalling of a crowded state is through a secreted product that works synergistically with FK506 to extend lifespan would be to assay lifespan in uncrowded conditions, but on plates conditioned with a high density of worms. This would be technically challenging in at least two respects. Firstly, after the conditioning period, all worms and eggs must be removed from the plate before the L4 worms being assayed are added, to ensure a synchronised population during the lifespan assay. Secondly, the timing of the FK506 dose must be optimized. FK506 would need to be applied to the plate before pre-conditioning. In this thesis, the activity of FK506 has been shown to decline over time and

so increasing the length of time between FK506-treating the plates and initiating the lifespan assay may decrease the lifespan-extending effect of FK506 below significance. Furthermore, FK506 is likely to be metabolised while on the plate and therefore fresh treatment is likely to be required. The effect of a fresh dose of FK506 could be tested first using crowded conditions, to ensure that the FK506 is active and at the correct dose, before testing non-crowded conditions. Mass spectrometry could be used to identify novel secreted compounds on plates after growth of worms in crowded conditions compared to uncrowded conditions.

Finally, to test whether there is synergy between FK506 activity and general stress response pathways, the interaction between FK506 and other mild stresses, such as mild (25°C) heat shock or mild oxidative stress, could be assayed on *C. elegans* lifespan.

6.1.2 FK506 did not create dietary restriction conditions

Some interventions that extend *C. elegans* lifespan, such as mutation of *eat-2*, do so by creating dietary restriction (DR) conditions, a mechanism of action unlikely to translate to mammals. Therefore, it was necessary to investigate whether FK506 is creating DR conditions, but no evidence for this was found. FK506 did not limit *C. elegans* food intake by inhibiting *E. coli* OP50 growth or pharyngeal pumping, so did not create DR conditions via these mechanisms. Therefore, FK506 probably does not extend *C. elegans* lifespan by creating DR conditions, although inducing DR by another mechanism cannot be ruled out.

6.1.3 FK506 extended *C. elegans* healthspan

In *C. elegans*, healthspan and lifespan are correlated, but the link between them is not fixed. Although FK506 had been shown to extend lifespan, no work had been done to directly examine an effect on healthspan, the time when the population shows near 100% viability. Potentially, FK506 could extend *C. elegans* lifespan by prolonging the later stages of life spent in ill health. Three measures of healthspan were chosen: a thrashing rate assay to assess muscle function, accumulation of live bacteria in the gut, which can lead to constipation and early death, and pharynx pumping, another muscle function which declines with age. The effect of FK506 on these three measures of *C. elegans* healthspan was assayed in early adulthood, when the percentage of population survival is near 100%. At this time, FK506 showed a small but positive effect on pharynx pumping in *C. elegans bus-5* and *bus-8*, increased thrashing rate in *C. elegans bus-5* and N2, and delayed accumulation of gut bacteria in *C. elegans bus-5* and *bus-8*. Therefore, FK506 extended *C. elegans* healthspan as well as lifespan.

6.2 The mechanism of action of FK506 on C. elegans

6.2.1 FK506 had separate mechanisms of action on *C. elegans* lifespan and healthspan

One of the most interesting findings from this thesis is that FK506 showed different requirements to extend healthspan and lifespan in *C. elegans*, suggesting that FK506 has multiple mechanisms of action. This was observed with both culture conditions and also requirements for different signalling pathways. The thrashing assay was used as the

primary measure of healthspan when investigating the different mechanisms of action of FK506 on healthspan and lifespan.

The first difference reflects the number of worms per plate (population crowding) required for extension of healthspan or lifespan. FK506 had no effect on *C. elegans* lifespan when incubated with 5-10 worms per plate (from L4 stage), but extended lifespan under population crowding conditions of 100 worms per plate. In contrast, all healthspan assays were performed with 20 worms per plate, and FK506 was able to extend *C. elegans* healthspan without population crowding. This suggests FK506 has separate mechanisms of action on lifespan and healthspan. The lifespan-extending effect of FK506 was crowding stress-dependent, whereas the healthspan-extending effect was independent of crowding stress.

Another indication that FK506 had multiple mechanisms of action was the differing requirements for the timing of FK506 treatment. Extension of *C. elegans bus-5* lifespan required constant FK506 treatment from hatching and through adulthood, whereas initiation of FK506 treatment at the L4 stage was sufficient to significantly increase thrashing rate at day 1 of adulthood. Removal of FK506 treatment at the L4 stage caused complete loss of the thrashing rate increase by day 3 of adulthood. This may be because the effect of FK506 on thrashing rate is acute, i.e. the current presence of FK506 is important, or FK506 acts to increase thrashing rate in adults only, so the presence of FK506 during development is not required. In contrast, the ability to extend lifespan required exposure to FK506 during development (as well as during adulthood), perhaps setting up specific patterns of gene expression. Further work could test the effect of FK506 on levels of transcripts encoding products that function in distinct biochemical

pathways in the early adult. Transcriptomics at different lifecycle stages, on FK506- and control-treated *C. elegans* compared with worms treated from the L4 stage onwards, could reveal the different gene expression changes required for healthspan and lifespan extension.

6.2.2 The mechanism of FK506-induced *C. elegans* thrashing rate increase

The mechanism of action of FK506 on *C. elegans* thrashing rate was investigated in three ways. First by testing the effect of FK506 on a *daf-16*-null mutant strain, second by testing the interaction between FK506 and FUdR on thrashing rate, and third by assaying thrashing rate in *C. elegans bus-5* when co-treating with a variety of small molecule inhibitors and inducers to find the cellular functions required for FK506 activity.

The FK506-induced thrashing rate increase required the FKBPs and was DAF-16-dependent. There was a partial interaction between FK506 and caffeine, another DAF-16 dependent anti-ageing intervention (Lublin et al. 2011; Bridi et al. 2015), on thrashing rate. There was also a partial interaction between FK506 and 3-MA and trehalose, inhibitor and inducer of autophagy respectively, suggesting that whilst FK506 interacts with autophagy, it is not required to increase thrashing rate. This interaction with autophagy may explain why there was a partial interaction with Li^+, as upregulation of autophagy is one mechanism of action of Li^+ (Tam et al. 2014). Co-treatment with the RyR inhibitor dantrolene impacted on ability of FK506 to increase thrashing rate, suggesting that whilst RyR activity is not required for FK506 to increase thrashing rate, Ca^{2+} flux may be involved. FK506 also inhibits L-type voltage gated Ca^{2+} channel (L-VGCC) activity (Norris et al. 2002), and as Ca^{2+} flux is involved in muscle contraction, FK506 may alter

thrashing rate by acting on muscle function. This could be further investigated by co-treating with an L-VGCC inhibitor, and assaying the effect of FK506 on *C. elegans* mutants defective in different aspects of muscle function. The effect of FK506 on calcium flux can be imaged *in vivo* using transgenic *C. elegans* expressing GCaMP3, a calcium indicator (Tian et al. 2009).

There is an interaction between FK506 and FUdR on thrashing rate, suggesting FK506 may interact with germline signalling, as FUdR reduces brood size as well as preventing growth of offspring. Preliminary data collected by Chronos Therapeutics suggests that FK506 may cause a small decrease in brood size. The disposable soma theory of ageing proposes that there is a trade-off in resource allocation between damage repair and reproduction. FK506 may shift this balance in favour of repair and therefore promote longevity.

As summarised in Figure 6.2, the mechanism of FK506 action on *C. elegans* thrashing rate was DAF-16 dependent, had partial interactions with FUdR and autophagy, and may involve Ca^{2+} flux.

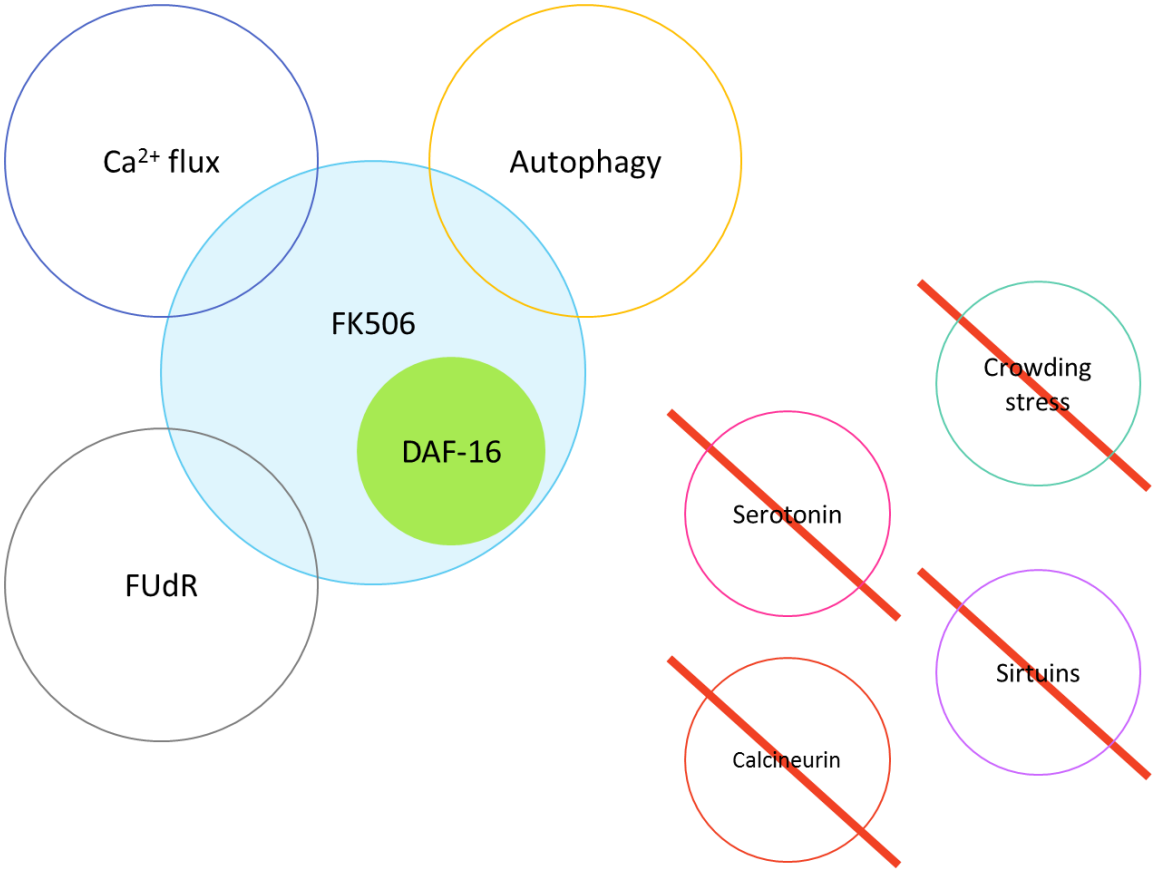

Figure 6.2 Summary of the mechanism of action of FK506 on C. elegans thrashing rate. The FK506-induced increase in thrashing rate was DAF-16 dependent, and had partial interactions with FUdR, autophagy and Ca^{2+} flux. The effect of FK506 on C. elegans thrashing rate was independent of population crowding stress, serotonin signalling, sirtuins and calcineurin.

6.2.3 The mechanism of FK506-induced *C. elegans* lifespan extension

There was no additive effect of FK506 and dietary restriction (DR) on lifespan extension, suggesting FK506 is a DR-mimetic, acting on at least some of the same pathways. FK506 in fact had a slight negative effect on lifespan in combination with DR, possibly because DR that is too severe can become harmful as it approaches starvation. However, this experiment was done only once so further repeats should be performed to confirm the result. In addition, DR influences DAF-16-mediated pathways. However, as the experiments testing the DAF-16 dependence and also the interaction between FK506 and

FUdR on FK506-induced *C. elegans* lifespan extension were not successful, a priority for further work would be to repeat these experiments.

There was no additive effect of FK506 and rapamycin, suggesting that the effect of FK506 on lifespan, as well as thrashing rate (healthspan), requires the FKBPs. An important question remaining is whether FK506 acts on lifespan and healthspan through binding a single FKBP, or whether FK506 has multiple targets. The FK506-induced extension of *C. elegans* lifespan required TOR-independent regulation of autophagy, and also required calcineurin (CN). CN activates autophagy by dephosphorylating and activating TFEB, a transcription factor that promotes expression of autophagy genes (Tong & Song 2015). CN also activates JNK1, part of another signalling pathway that promotes autophagy (Wei et al. 2008; Zhu et al. 2007). This suggests that inhibition of CN and JNK1 by FK506 should inhibit autophagy. However, evidence has been found that JNK1 signalling can decrease autophagy (Palumbo et al. 2016) and *C. elegans* CN-null mutants have increased autophagy (and extended lifespan) (Dwivedi et al. 2009), suggesting that inhibition of CN, and therefore JNK1, by FK506 could promote autophagy and lifespan extension. In cell culture FK506 increases levels of autophagy proteins (Nakagaki et al. 2013), suggesting that FK506 promotes autophagy to extend *C. elegans* lifespan. Autophagy and lipolysis are co-ordinated to extend lifespan in germline-less *C. elegans* (Lapierre et al. 2011), so upregulation of autophagy may be the mechanism through which FK506 decreased lipid accumulation.

Whilst FK506-induced lifespan extension did not require serotonin signalling, there appeared to be synergy between FK506 and serotonin, as FK506 was able to extend *C. elegans* lifespan in the presence of serotonin, despite having no significant effect in the

positive control (i.e. absence of serotonin) in the three repeats performed. Serotonin signalling promotes lipolysis (Watanabe et al. 2010; Srinivasan et al. 2008), and as lipolysis and autophagy are co-ordinated, serotonin may amplify the impact of FK506 on these processes.

As summarised in Figure 6.3, the mechanism of FK506 on *C. elegans* lifespan overlapped with DR and was dependent on calcineurin, TOR-independent regulation of autophagy and the presence of population crowding stress. The interactions with DAF-16 and FUdR are yet to be determined.

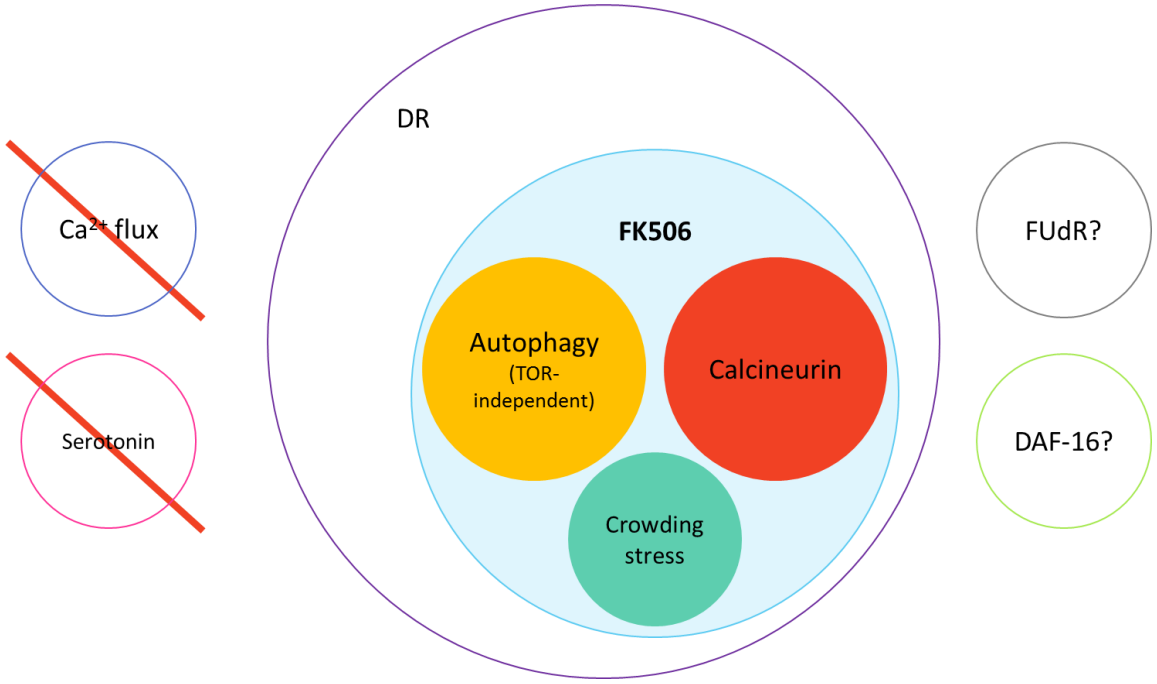

Figure 6.3 Summary of the mechanism of action of FK506 on C. elegans lifespan. The FK506-induced lifespan extension (under conditions of population crowding stress) has no additive effect with DR, and is dependent on calcineurin and TOR-independent regulation of autophagy. The lifespan-extending effect of FK506 is independent of Ca^{2+} flux and serotonin signalling. The interactions of FK506 with DAF-16 and FUdR are not yet determined.

A potential mechanism of action for FK506 is outlined in Figure 6.1. In short, the FK506-FKBP complex inhibits CN, relieving inhibition of DAF-16 to promote longevity. FK506 upregulates autophagy either via CN inhibition or another pathway, possibly upregulation

of autophagy genes. FK506 upregulates lipid metabolism via either DAF-16, the co-ordinated regulation of autophagy and lipolysis, or direct FK506 binding of the *C. elegans* homologue(s) of FKBP51 and FKBP52, both involved in adipogenesis in mammals.

The DAF-16 dependence of FK506-induced lifespan extension must be determined before this hypothesis is tested. If FK506-induced lifespan extension is DAF-16 dependent, the effect of FK506 on DAF-16 activation can be measured using the TJ356 transgenic strain of *C. elegans*, which expresses GFP-tagged DAF-16. FK506-treated and control-treated *C. elegans* can be compared to test whether FK506 increases the proportion of nuclear-localised (i.e. active) DAF-16. To test whether FK506 increases expression of autophagy genes, *C. elegans* strains expressing GFP-tagged autophagy proteins (such as ATG-7) could be treated with FK506 and the intensity of GFP quantified. These experiments using GFP-tagged proteins could also indicate whether the effect of FK506 is cell-type specific, judged by whether FK506 causes changes in all or only some tissues.

6.2.4 FK506 altered *E. coli* HT115 metabolites

In addition to the mechanisms by which FK506 acts directly on *C. elegans*, FK506 could be improving *C. elegans* health and longevity by altering the metabolites produced by its *E. coli* food source. Metabolomic analysis did not find any differences in levels of amino acids and organic acids between FK506-treated and control-treated *E. coli* OP50, although there are many other metabolites not tested that might mediate an effect. The metabolome of FK506-treated *E. coli* HT115 showed increased levels of arginine and alanine. Supplementation with arginine and alanine has positive effects on muscle function (Vallejo et al. 2016; Riddle et al. 2016) and reduces obesity (Araujo et al. 2016;

Hu et al. 2016). Therefore, increasing the arginine and alanine intake of *C. elegans* is another possible mechanism through which FK506 may increase thrashing rate and alter lipid metabolism, although FK506 was unable to extend the lifespan of *C. elegans* grown on this strain of *E. coli*. Nevertheless, a potential role for arginine or alanine in lifespan and healthspan extension could be tested by supplementing the NGM plates used to culture *C. elegans*.

6.3 FK506 decreased lipid accumulation in mouse adipocytes

FK506 significantly decreased lipid accumulation in mouse 3T3-L1 adipocytes when normalised to either cell number or cell mass. Further to this, the accuracy of the processes used to calculate the amount of lipid per cell could be improved by using a colorimeteric test to assay lipid content of the harvested (and Cellometer counted) wells of adipocytes. This FK506-dependent reduction in lipid storage was observed without any measurable effect on the percentage of viable cells, the total number of viable cells or the cell diameter, usually a measure of cell stress and age. This conclusion is complicated by two features of adipocyte cell culture. Firstly, any effect of FK506 on viability may be obscured when dead cells are removed each time the medium is replaced and undifferentiated preadipocytes proliferate to fill the available space. Secondly, adipocytes increase in size as lipid is accumulated, meaning cell diameter is not related to cell stress in adipocytes.

RNA-seq of the harvested cells found that FK506 treatment significantly altered gene expression at days 5 and 10 post-induction. Further analysis of the RNA-seq data could be done using clustering to analyse the differences in RNA levels across all time points,

rather than simple paired analysis at each individual time point. The loss of the FK506 effect in older cells could be caused by FK506 having a transient effect, or by a loss of population synchronisation. Further work could investigate whether the effect of FK506 is transient by continuing treatment beyond day 4 post-induction. The effect of FK506 on preadipocyte capacity for differentiation could also be tested by FK506-treating prior to induction of differentiation.

At days 5 and 10, FK506 treatment increased expression of translation-associated RNAs (mainly ribosomal proteins) and decreased expression of RNAs associated with lipid metabolism and transport. However, it is unknown whether the altered RNA levels reflect altered in protein levels, or whether these effects are transient. Mass spectrometry of the proteome or Western blotting of specific proteins could be used to measure changes in protein levels induced by FK506 treatment. Further work could test whether upregulation of translation is required for the anti-ageing effect of FK506 by co-treating with a translation inhibitor such as cycloheximide, which increases lifespan in *C. elegans* (Takauji et al. 2016).

The effect on lipid metabolism-associated RNAs could be caused either by FK506 reducing the number of cells within the population differentiating into adipocytes, or by FK506 weakening the adipocyte phenotype across the population. In particular, FK506 decreased RNA levels of C/EBPα, Fabp4, GLUT4 and Adiponectin Receptor 2, all important for adipocyte function. Reduced expression of genes required for adipocyte function could be the mechanism through which FK506 reduced lipid storage in 3T3-L1 adipocytes.

The FK506-induced increase in levels of RNAs of ribosomal proteins was also seen in the *C. elegans* RNA-seq. Many anti-ageing interventions have been associated with decreased

expression of translation-associated and ribosomal genes, including rapamycin (Raught et al. 2001), reduced IIS and dietary restriction (Depuydt et al. 2013), although it is not clear whether these reductions are transient or maintained over the long term. However, RNAs associated with translation have been found to be upregulated in the liver of long-lived mice with deletion of ribosomal S6 protein kinase 1 (downstream of TOR) (Selman et al. 2009). In neurodegenerative diseases the long-term activation of the unfolded protein response pathway and subsequent inhibition of translation can be detrimental to neuronal function (Ma et al. 2014). Therefore, maintaining protein synthesis may be important for healthy ageing in some tissues.

6.4 FK506 had similar effects in *C. elegans* and mouse adipocytes

FK506 treatment altered RNA levels of lipid metabolism and translation in both *C. elegans* and 3T3-L1 adipocytes, suggesting that the mechanism of FK506 is conserved between the two different organisms. Many more RNAs were altered by FK506 in *C. elegans* than in the adipocytes, which is to be expected when comparing the number of genes expressed within an entire organism to the number expressed in a single cell type.

Fkbp2 RNA was upregulated by FK506 in adipocytes and *fkb-4* RNA was upregulated in *C. elegans*. Both of these are ER-localised FKBPs, thought to be involved in protein folding or chaperoning. FK506 may act by binding FKB-4, although FK506 inhibits only the PPIase activity and not protein chaperone function of FKBPs (Riggs et al. 2007). The effect of FK506 on thrashing rate, and possibly lifespan, is DAF-16 dependent. Inhibition of the IIS pathway (resulting in activation of DAF-16) extends lifespan, and also down regulates expression of *fkb-4* (Yu & Larsen 2001), so the expression of *fkb-4* would be expected to

decrease if FK506 extended lifespan by inhibiting IIS. However, *fkb-4* is upregulated in response to DR and is required for DR-induced lifespan extension (Ludewig et al. 2014). As FK506 and DR did not have an additive effect on lifespan, *fkb-4* may also be induced by FK506 treatment, and is possibly required for the FK506-induced lifespan extension. Further work could investigate the effect of FK506 on an *fkb-4*-null *C. elegans* strain.

6.5 FK506 and rapamycin have different anti-ageing mechanisms

The interaction between FK506 and autophagy appeared to be TOR-independent, and there is no evidence in the literature that FK506 inhibits TOR despite being structurally similar to rapamycin. Also, rapamycin decreases expression of translation-associated genes (Raught et al. 2001), whereas FK506 upregulated RNAs associated with translation in both *C. elegans* and 3T3-L1 adipocytes. This suggests that FK506 and rapamycin have different mechanisms of action on ageing despite having related structures and both binding the FKBPs.

6.6 Criticisms of methods

6.6.1 The instability of FK506 complicates interpretation of results

The greatest difficulty in studying FK506 was the instability of the compound. Whilst care was taken to preserve FK506 activity, the effect of FK506 was variable in experimental repeats, complicating interpretation of results. This was a particular problem when co-treating *C. elegans* with FK506 and small molecule inhibitors and inducers, as what appeared to be the loss of FK506 activity in the presence of another compound could

indicate an interaction between the compounds, or could be due to FK506 degradation. Controls were performed for every experiment to ensure FK506 was active in the absence of the tested compound, but this doesn't account for stochastic events that could cause FK506 to degrade faster on one plate than another. To maximise FK506 activity, FK506 was stored in powder form and freshly diluted in DMSO or ethanol for most experiments. On the few occasions a stock of FK506 solution was used, following the manufacturer's guidelines this was never more than one month old and repeated freeze/thaw cycles were avoided. FK506-treated NGM plates for *C. elegans* experiments were stored in darkness to minimise light-induced degradation.

6.6.2 The suitability of *C. elegans* as a model organism

C. elegans is a well-established model of ageing, but does have disadvantages. The *C. elegans* adult is effectively post-mitotic, so cannot model the effects of cell senescence seen in mammals, showing constant turnover of cells throughout life. *C. elegans* also has far fewer genes than mammals, having only eight FKBPs whereas mammals have many more. Whilst this simplicity can be useful, for example it is easier to genetically knock-down function of a cellular process when there are fewer, if any, redundant genes, finding the functional homologues of genes in different organisms is not trivial.

The differences in physiology also impact on the usefulness of *C. elegans* as a model organism. Whilst there are many similarities in lipid metabolism regulation between *C. elegans* and mammals, a major difference is the absence of a specialised adipocyte cell type in *C. elegans*. In *C. elegans*, the cells of the gut are multifunctional, taking on the roles of the intestine, liver and adipose tissues. Lipid metabolism regulation differs

between tissues such as the liver and adipose within mammals, and this must be taken into account when comparing mammalian adipocytes to the multifunctional cells of *C. elegans*.

Lastly, there is overlap between longevity-regulating pathways in *C. elegans*, and the pathways that regulate dauer formation, including IIS. There is no direct mammalian equivalent to the dauer life stage in mammals, so an intervention that altered *C. elegans* lifespan by acting on dauer formation pathways would not necessarily have an anti-ageing effect in mammalian systems.

6.6.3 The suitability of 3T3-L1 adipocytes as a model of adipose tissue

The major issue with the use of the 3T3-L1 cell line is the low differentiation efficiency, resulting in a mixed population of post-mitotic, ageing adipocytes and proliferating preadipocytes. However, there were no other readily available adipocyte cell lines.

3T3-L1 pre-adipocytes are an embryonically-derived cell line, so will differ in gene expression from adult adipocytes. Adult adipocytes derived from adipose tissue from different locations within the body have differences in gene expression, and function differently with age (Cartwright et al. 2007), which cannot be modelled in 3T3-L1 cell culture. Also, only 15-50% of cells in adipose tissue are adipocytes (Cartwright et al. 2007), and the interactions between adipocytes and the other cell types within adipose tissue are important to cell function, an aspect which is lost in culture of a single cell type. Cell culture cannot model the interactions between different tissues within an organism. Adipose tissue *in vivo* receives signals from the endocrine and nervous systems (Lafontan

2012), and also secretes hormones to regulate whole organism metabolism (Yu & Zhu 2004).

As well as being unable to model interactions between different cell types and tissues, cell culture can also introduce artefacts due to the non-physiological conditions. There is debate within the literature whether the clonal expansion phase (period of high proliferation) triggered by induction of adipogenesis in 3T3-L1 occurs *in vivo*, or whether it is specific to the method of inducing adipogenesis in cultured 3T3-L1 (Qiu et al. 2001). This could be relevant to the action of FK506, as FKBP51 RNA accumulates during clonal expansion in 3T3-L1 (Yeh, Li, et al. 1995).

6.7 Further work

Further experiments have been suggested throughout this discussion, but some of the key experiments are summarised below.

Firstly, the DAF-16-dependence of FK506-induced lifespan extension should be established, then the hypothesis outlined in Figure 6.1 can be tested. The hypothesis can be tested by assaying DAF-16 localisation and levels of autophagy proteins. The dependence of FK506 activity on other IIS pathway components (e.g. DAF-2 and AGE-1) should also be tested. If FK506 extends lifespan solely by relieving CN inhibition of DAF-16, this activity should be independent of upstream IIS components.

Secondly, further work is needed to establish the mechanism of the FK506-induced thrashing rate increase, and whether this is via Ca^{2+} flux. Thirdly, lipid metabolism

regulation pathways other than serotonin signalling could be inhibited to determine how FK506 acts to alter levels of lipid metabolism RNAs.

Finally, following on from the finding that FK506 upregulated RNA of an ER-localised FKBP in both *C. elegans* and 3T3-L1 adipocytes, Western blotting should be performed in both systems to test whether the altered RNA levels result in altered protein levels. Also, the effect of FK506 in a *fkb-4*-null *C. elegans* strain could be assayed to determine whether FKB-4 is required for FK506 activity. Theoretically, Fkbp2 could be knocked down in 3T3-L1 adipocytes, but this would be much more technically challenging.

7 Appendix

7.1 RNA-seq: *C. elegans bus-8* RNAs upregulated by FK506 treatment

Y5H2B.6	M02G9.4	F21F3.3	F44C8.1	F27C1.8	F36D3.5
C45H4.17	T25D10.5	ZK622.1	ZK783.6	W01B6.6	H12D21.1
Y5H2B.8	C47E8.1	ZK512.10	Y48G8AL.12	F57A8.6	F53G12.6
C28F5.4	C10H11.7	Y116A8C.23	K07E12.2	ZK1025.8	F40H6.1
F35E2.3	C50D2.3	F30A10.12	H12D21.15	T01B7.7	F58F12.3
F16G10.5	W09C3.8	C43F9.6	ZK265.2	C47A4.5	T11G6.7
F41B5.3	C50E10.1	F46F5.9	B0496.6	Y54E2A.9	T06C10.6
C45H4.2	K01A6.7	F11G11.14	F10C1.3	C04E6.5	R102.15
T06E4.12	Y116F11B.7	F44G3.7	Y69E1A.4	C47A4.4	Y38H8A.3
K08E7.4	BE10.5	Y71F9B.14	C18H7.7	C33F10.11	H04M03.1
Y62E10A.3	Y41E3.18	F02C9.4	Y57A10A.11	R07C3.4	H27M09.5
R05D8.9	F49D11.7	Y39G10AR.25	ZK354.6	R08C7.8	M28.9
F47F6.3	Y69A2AR.23	F37A8.1	F39E9.4	Y59H11AM.1	F07A5.2
D2062.4	C18G1.3	ZK1248.20	Y54G2A.24	C36E6.8	Y47D7A.15
ZK1025.2	F10G8.2	H08M01.1	F09C12.8	K06A4.8	B0496.1
C01G10.4	F36F12.7	C47E12.11	ZK1225.4	F12A10.4	B0524.4
ZC373.6	D1081.5	C06A8.16	Y119C1B.1	Y51A2B.4	K05F1.7
T20B6.1	C50E10.2	Y38H6C.15	C09G9.4	C54F6.9	Y38H8A.2
Y70C5C.5	F28E10.4	Y46G5A.25	C15H7.4	C01G10.5	T27A3.5
F36H12.4	F56H1.3	F11G11.12	C01B12.1	F30B5.1	T10E9.4
Y50E8A.2	C01G10.14	C09H10.1	Y57G11C.23	F36H12.5	ZC581.2
F38E1.3	W03G9.6	C52D10.13	C30B5.3	B0511.4	B0261.6
Y39E4A.1	Y57G7A.3	Y71G12B.22	ZK1290.6	Y2H9A.3	M7.7
F15H10.7	F43A11.8	R05D7.2	C17F3.3	E03H12.7	T23B3.5
F41B5.2	Y53F4A.2	T06G6.6	C08F11.10	F36H12.11	Y71F9B.15
Y57G11C.970	C02G6.2	C47A4.3	C28D4.7	Y41E3.2	C05C12.5
F56G4.7	K08C9.1	W08D2.8	Y37E3.19	T28B8.4	C32E8.4
Y32G9A.11	T25B9.2	F36G9.13	B0491.2	R102.8	Y116A8C.38
F58D5.8	AC7.3	ZK180.6	ZK1290.3	C54D10.4	F41G3.4
Y37E11AL.12	K08F4.5	H12D21.13	E02C12.6	Y25C1A.1	R08A2.1
D1081.12	F46B3.5	C55B7.10	F10D11.4	C09F9.1	F55D12.6
R02D5.10	E02C12.10	R102.10	C38C10.3	F58G1.3	H05L14.1
F46A8.9	F35H8.1	C01G12.9	ZK546.7	Y67A6A.1	K03H1.12
F58A4.12	C35B8.1	W05G11.3	F20D6.6	C17G10.3	Y106G6E.3
W08D2.9	F28A10.1	T07G12.3	Y69A2AR.9	C04G2.5	C49A1.3
Y116A8A.4	C01G10.17	W09C3.2	F13A7.7	F11G11.8	C18E9.8
B0524.5	T01C3.5	Y106G6G.3	F36H12.10	ZC250.5	T13F2.12
D2089.2	ZK1251.3	K09C6.2	C45B11.9	C03C11.1	F41H10.2
ZC21.8	D1081.3	F36A4.2	F36D1.4	F11G11.9	K09H9.3
ZC513.10	F56D5.2	C06G4.6	R102.1	F44D12.8	C25D7.2
F59E12.12	F47B8.11	F57B7.3	H32C10.3	R148.7	Y4C6A.1
ZC376.8	E03H12.5	Y11D7A.11	R155.2	T08G3.7	F27C1.1

F40G12.10	F27C8.5	Y39F10A.3	Y57G11C.48	F36A4.4	K05F1.3
F54C1.9	F26G1.8	R13H9.5	F46B3.4	C34F11.2	T27A3.4
ZK616.7	C24D10.7	F36H12.14	H06I04.5	T28H11.1	C24D10.1
C02F5.5	T27C10.7	F37E3.3	ZC477.7	M176.9	Y67D8B.5
ZC116.2	F43G6.6	C28D4.5	W01C9.4	F52F12.9	C04G2.9
T10E9.12	F44D12.5	C36H8.1	T03F6.6	F36A4.3	F56D6.14
C04F12.12	F13G11.2	C14C10.1	C35D10.11	R13H9.2	T13F2.10
ZK1248.6	R08C7.5	D2062.6	ZK637.12	C35D10.2	C18H2.5
F01G10.5	ZC513.3	F52H3.6	F59A6.4	W09C3.6	E01G4.6
Y47D3A.13	T13F2.9	W04E12.4	F21F3.2	C10G11.8	Y6E2A.9
Y57G11C.52	T02E1.7	C16C8.18	F47B3.4	B0041.1	F13H8.12
F46F5.6	ZK1025.4	Y47G6A.26	W03F11.3	B0379.7	F14E5.3
C04G2.3	ZC412.6	F52F12.8	F59A3.8	F44D12.7	T04B2.2
F58A6.5	R13H9.4	C54F6.3	R08C7.6	H12D21.14	ZC477.1
C04F12.6	Y46G5A.30	ZK484.5	ZK930.4	Y54G2A.13	K08F4.8
ZK617.3	AH6.3	Y57G7A.5	F20D6.1	Y54E2A.7	T23B7.1
F59A6.2	F36H12.8	F44G4.5	K07A1.4	M05B5.7	C27D6.11
F19C7.7	Y43C5A.1	F19B6.4	C50B6.4	Y43F8A.2	C18A3.7
C41G7.6	ZC168.6	E03H12.10	F44D12.3	ZK1225.5	T09F5.10
K02E11.10	R13H9.6	F17C8.7	Y47D3A.11	C09B9.6	T05F1.5
F35E2.6	C25G4.7	F55H12.5	F43G9.15	C32H11.5	W04H10.1
W03D8.9	Y39B6A.25	ZK512.13	ZK1251.6	K01H12.4	F02E11.1
F36H12.6	C05C12.1	F47C12.4	C18G1.9	D2062.7	B0207.11
C06C6.7	T25B9.4	Y57G11A.2	M195.1	ZK938.1	ZK354.10
C33A12.15	F22B3.8	C25D7.1	T22H9.3	C33F10.1	C02B10.6
F26G1.7	Y51B9A.3	B0025.5	T28C12.3	Y53C10A.10	C39H7.1
ZK596.2	Y47D3A.10	Y69E1A.1	K07F5.3	ZK354.11	ZK970.8
F46A9.2	C48B6.4	C33H5.16	T22B3.2	Y73F8A.20	Y59E9AR.7
F10F2.6	C47A10.1	F40F12.3	Y59E9AL.6	C04F12.7	T15H9.4
C34D4.2	T28H11.6	F10G7.6	C34D4.3	ZK1010.5	Y113G7C.1
ZK688.10	M70.3	T28H11.5	F38A5.6	T08H10.3	K07F5.4
T23B7.2	R09E10.2	C34F11.6	Y59H11AM.3	K02E11.1	F47B3.6
ZC412.7	C24D10.8	F44D12.4	F36H12.9	Y116A8C.24	F36H12.3
C10G11.9	K07F5.5	K08D10.7	T13F2.11	C15H11.1	C24H11.1
R08A2.3	T27E7.1	C24H11.2	C24D10.2	C34F11.4	F32B6.5
AH10.1	C04G2.8	C27D6.3	T28H11.7	F11G11.10	ZK265.3
C09H5.7	F58A6.9	B0205.10	Y39B6A.30	C14A6.13	C43G2.3
R08A2.2	W02B12.12	K09E4.1	B0524.2	F08H9.2	C05D2.3
ZK1025.3	Y38C1AA.7	T22B3.3	F13A7.1	ZC477.2	F32H2.7
R07C3.13	C01G10.1	C05B5.2	F46A8.10	W09D6.4	T16H12.6
T25C8.3	C27D8.1	Y46H3D.1	W03C9.8	F46A8.6	T01E8.9
F32G8.5	W03D8.5	D1086.17	F36H12.7	K07F5.1	M70.1
F22D6.10	C25A8.5	ZC581.7	W01B11.1	C14A4.8	F32A11.3
Y6E2A.10	ZK945.7	ZK484.8	F26A1.4	F11G11.4	Y106G6H.13
B0393.4	ZK418.2	F15H9.7	T08G3.4	B0432.12	F18A12.4
W03F11.4	C48E7.7	T08B6.9	K05F1.2	F58F6.1	ZK1053.6

ZC477.10	K07F5.11	E02C12.11	F09C12.7	C31H1.1	T05C12.3
ZK354.1	K05F1.9	W06D4.2	C01G5.4	C27D8.2	Y48B6A.5
H20J04.1	ZK354.5	C09B9.4	F01D5.7	F26A1.3	T02E1.1
F58A6.8	F47B3.7	ZK1053.2	Y43F8C.5	F41B5.7	F35C11.3
M162.7	F12F6.9	ZK354.4	F47G6.3	K07F5.9	C17H12.3
T08B2.12	F44F1.3	H38K22.6	T28D9.9	Y37E11B.10	C26E6.1
F54C1.8	F42C5.5	Y59E9AR.1	ZK945.6	W01B6.5	R03D7.8
C55C3.4	B0207.1	C32D5.4	F56D6.13	K10C9.7	R05H5.2
T14D7.3	F36A2.10	Y73F8A.15	C33F10.9	Y106G6E.2	Y106G6D.3
K07F5.2	ZK354.8	C54G4.3	F26D2.10	F14H3.2	Y45F10C.1
Y49F6B.10	ZK1307.4	C50F2.5	Y69A2AR.19	C36F7.5	M110.7
T21G5.1	C08F8.6	C34F11.5	F59A1.15	F58B4.7	C25D7.14
Y51A2B.5	K03H1.1	F10F2.8	F21H7.5	K06A5.2	ZK1248.5
H38K22.7	K08C9.2	Y76A2A.1	T16A9.5	T15B12.2	F56H11.3
F47D12.7	Y18H1A.10	R09E10.6	W03D8.10	Y69A2AR.14	Y38H8A.4
Y116A8C.4	F23B12.1	R07E5.15	C31H1.5	Y73B6BL.34	T16A9.6
T08B6.4	F36D3.4	F17E9.5	F58D2.2	Y106G6G.4	C55C3.6
T27A3.3	Y105C5B.18	C15C6.2	C09B9.7	C17H12.5	F41F3.1
Y73F8A.12	F10F2.7	C17F3.1	C25G4.6	F26B1.5	ZK892.5
Y46C8AL.1	Y39A1A.2	Y51H7C.9	F32B6.4	K07F5.6	ZK757.3
F47B3.1	C28D4.4	F38H4.4	Y46G5A.22	K05D4.4	C03A7.7
H34I24.1	Y39B6A.31	K07A3.3	D2062.1	F07D3.3	F48C1.7
F32B4.2	T23F11.2	ZK1225.6	F37C4.3	C56C10.6	R01H2.4
C55C2.2	T04F3.3	R07E5.6	R10D12.10	ZK1010.7	C43E11.5
R05F9.13	Y6E2A.8	F58D5.7	T02B11.9	B0207.9	Y38F2AR.10
T22C1.8	ZK546.6	ZK550.5	F26B1.8	F46F5.7	C02E7.7
T04A8.13	C38C6.5	F54C9.4	C50F4.10	K08H2.5	C03C10.2
F32B6.6	Y51A2B.6	ZK783.5	F42A9.7	Y59E9AL.3	Y73F8A.14
T03D3.1	C04G2.4	F32B5.4	K08D10.8	Y38E10A.17	Y39F10C.1
Y47G6A.15	C54G4.2	F36A2.12	Y57G7A.6	T25B9.6	F37H8.4
F40F9.3	R10E9.2	Y71G12B.3	F58E6.5	D2062.5	ZK856.18
K03H9.3	F36A2.14	T22C1.9	C53D6.10	ZK354.2	Y71G12B.27
C18H7.4	T04F3.7	T06C10.3	F49E11.7	Y37D8A.5	F36H1.3
B0491.3	R05F9.8	F37A4.5	F10D11.3	C33F10.12	T20D4.10
M05B5.1	F55F8.7	C32E12.1	Y59E9AL.2	C27B7.6	F21D9.2
C37A2.3	K09B11.5	K04H4.5	T03F1.5	R02F2.5	T23G11.1
Y69E1A.2	Y49F6B.15	C50F4.2	C35E7.10	F55C5.2	ZK84.5
T09A12.1	T02H6.7	Y41C4A.18	F46F5.11	H32C10.1	F55C5.1
R13H9.1	F59C6.3	Y45F10B.3	ZK484.7	ZK1307.3	F36A2.11
ZK354.7	C45G9.4	C45G9.9	K11C4.1	M05D6.1	C50F7.3
T21G5.4	ZC581.10	C08F11.14	K07A1.5	AC3.10	C14C6.12
F57F4.1	C15H7.3	ZK858.8	ZK849.6	W03G9.5	C50C3.2
T04A6.3	F01D4.3	C47E12.10	T20D4.12	ZK1098.12	B0361.11
F46A9.1	F47B3.2	F53G12.8	H23N18.5	C07G1.6	T19C3.2
C45G9.15	Y113G7A.10	F59G1.2	Y69E1A.8	F58F12.2	ZK930.6
ZK666.2	F07E5.8	R01H2.2	F42H11.1	F37A8.2	F34D10.8

C09D4.3	C17C3.11	C38C6.6	F14E5.8	T05H4.2	K06B4.15
Y40B10A.4	Y47D3A.31	K03H1.9	D2092.8	Y47D7A.6	F59H6.4
F37A4.4	ZK616.61	F35E2.9	F54F12.1	C44C10.1	R155.3
Y39G10AR.16	Y18H1A.1	B0280.11	F58E6.12	C46E10.1	C50H2.10
C18B10.6	F27E5.3	Y66A7A.9	Y54G2A.15	M28.4	F26F4.2
R105.1	Y47D7A.7	W03G1.2	ZC581.6	F14F7.4	Y41C4A.7
C38C3.3	C34B2.3	C52E4.7	W06D11.4	Y53H1C.3	T05D4.5
T04A8.3	F44F4.10	F13E9.14	T28A11.19	R01E6.5	F42A9.3
F55H12.1	F29B9.7	F26A1.10	F02E9.3	ZK795.2	Y8G1A.1
C01G12.8	T18H9.1	Y59H11AM.2	Y69A2AR.8	F33D11.7	ZK849.4
C06A1.3	K10H10.7	Y65B4A.9	ZK353.3	F38H4.6	Y69E1A.3
C35E7.9	Y39B6A.18	B0379.2	Y40B10A.10	F54D1.3	R07B1.13
R09E10.4	C48E7.8	Y55B1AR.4	ZK1025.7	F52B11.4	C07E3.4
C29E6.3	C09B9.3	F49C12.15	F44F1.1	C49C8.1	M04G7.2
T13A10.11	F40F12.8	R06B10.1	M117.4	T06A4.2	F28H6.3
F13E9.16	K09C6.7	C46A5.3	E03A3.4	F08G5.4	F53C3.1
C04E6.4	F18C5.4	F13E9.5	C49G7.1	C55C3.8	K09F6.3
F53B6.4	F56A11.6	R05F9.3	F44D12.6	Y51H7C.13	F58H1.6
C33C12.7	C17H12.12	T05C12.1	C49C3.20	Y59H11AM.4	M02B1.4
F52F12.5	F35E2.10	Y105E8A.27	F56B3.6	Y51H4A.935	C04G2.2
C25G4.8	T20B6.2	ZK892.3	C24A11.1	F59C6.2	C30H6.5
Y1A5A.1	C10C6.3	C35A11.2	T21C9.9	C14A4.13	C12D8.16
R09E10.3	F09G8.6	Y51B9A.5	W06F12.3	ZK520.5	R09B5.12
Y44A6D.5	H23L24.2	Y53F4B.36	K01D12.8	F14F9.6	Y4C6A.4
ZK1251.1	F12A10.3	C01G5.3	C44F1.2	F59A6.8	C34G6.3
T28B8.6	F56F4.3	B0218.7	Y53F4B.19	ZK593.9	C01F1.5
C30G7.3	F58D5.6	ZK512.8	F32B6.7	T06D4.4	T28F4.3
F41C6.5	F31E8.5	B0244.9	Y38C1BA.3	B0240.2	F19B6.3
Y47D9A.5	H06H21.9	ZK892.4	F35C11.2	T05F1.8	F26E4.5
B0207.7	BE10.1	Y50E8A.10	F35B3.4	T04B2.7	ZK836.1
T16A1.2	K01D12.15	B0545.3	ZK616.8	F26B1.4	H04J21.1
C34F11.1	Y57G11C.6	F18A12.1	F19G12.8	F54B3.2	W03B1.5
T08G11.2	ZK353.4	W01B6.2	ZC155.2	Y43F8C.9	F47B3.5
C14A6.6	Y46G5A.36	Y65B4BR.6	C36B1.10	C05B5.6	F47F6.5
T05A7.6	F58G1.5	F54D1.2	K06H7.8	Y47D3A.30	F58E6.13
AH6.2	K09C6.8	Y47D7A.5	W03F9.3	C33F10.8	C12D8.9
F43G9.8	F09E8.1	Y57A10B.7	Y40H4A.2	K09H11.4	F25F2.1
C09B9.2	F21H7.2	F21A3.4	T05B4.14	Y48G8AL.16	F33D11.2
T10E9.6	Y18H1A.15	F22B5.5	F33D4.6	C28D4.8	Y46G5A.14
F54H12.7	Y40B10A.6	F48G7.10	M05B5.3	Y39G8C.2	C50H2.12
F42G4.2	C26C6.6	R12E2.7	R02E4.3	F55B11.7	R09E10.1
F59B2.15	ZK1128.3	C48D1.9	W02A2.8	F13H8.5	F53F4.18
ZK688.12	F08G5.2	K09C6.1	F16H6.7	K07F5.8	Y106G6A.4
ZK809.1	F15B9.2	ZK1290.9	B0399.2	C34E10.9	B0457.3
F56C9.5	Y47D9A.3	T16G12.7	W02F12.8	Y52D5A.2	Y11D7A.5
R09A8.4	Y50E8A.9	F18A12.6	F46C8.8	Y66A7A.4	F25H5.7

T13H10.1	C16A11.7	Y38F1A.1	F08B4.2	C08F8.4	T19D12.5
R10H10.2	C32C4.3	ZK546.3	C10G11.10	T21D12.2	Y37E11AL.2
F48G7.5	Y42H9B.1	F36D3.8	Y22D7AL.14	C29F4.1	T10B5.2
F41G3.5	ZC373.3	F43G9.6	C26B2.2	C02A12.1	F52D1.3
F59A7.9	C46A5.1	C06E7.6	C53A5.4	R10H1.4	Y54E10BL.2
F21C3.6	R12B2.3	Y116A8A.6	B0261.5	C28C12.11	H03E18.2
F23B2.7	AC3.3	C01G6.2	Y87G2A.20	Y43C5B.3	ZK84.1
F29D10.1	F53B6.7	R11E3.1	C15A11.5	T05A10.5	Y23H5A.4
T28C6.5	W03B1.9	F54H5.3	Y37D8A.8	Y43C5B.2	F56F4.2
F15H10.4	C17D12.5	F08G2.6	F42G8.9	R13G10.4	F41F3.4
T13F3.8	Y106G6G.1	F57A10.2	H12D21.5	R102.3	Y80D3A.8
ZK678.5	F53B2.5	Y75B7B.1	Y53C10A.9	H42K12.3	F38A3.1
Y71F9AL.2	F42G8.8	B0222.7	ZK84.2	R02D5.7	F35H10.2
Y57G11B.7	F10G7.12	D1022.9	T11F9.9	C15A11.6	M18.1
B0213.12	F10G8.1	C25A8.2	C17D12.6	T20D4.11	C38D9.5
C15A11.2	F59C6.6	ZK377.1	Y53F4B.24	F15H10.1	C33C12.4
Y73B6A.1	T28A11.3	D2045.5	F54H12.8	R05H10.6	W08E3.4
F54D1.1	ZC190.8	C09H10.9	C09G5.6	H12I13.5	Y69F12A.1
F21C3.7	B0252.5	B0024.1	ZC317.6	C45B2.2	T06E4.6
W06A7.5	Y43D4A.5	K09G1.2	F56F4.9	T01B11.4	R13F6.5
F07F6.10	F28H1.5	C35D10.3	C29E4.14	C02E7.6	F15B9.1
K06A1.2	C07A9.13	F56F3.4	Y67A10A.3	Y65B4BL.6	F43E2.6
K08A2.2	W04E12.5	F20H11.4	W03D8.2	K01D12.7	C39B5.5
M02G9.3	Y49E10.10	T27E4.6	Y116F11B.8	C29F5.3	B0511.11
Y22D7AR.12	ZK524.1	Y53F4B.11	F26H9.8	Y71G12B.30	D1037.5
Y38F1A.7	T11F8.4	Y51H7C.8	Y41E3.6	T22A3.6	ZK1127.2
ZC412.5	Y65B4A.7	F55G11.9	B0513.6	F18A12.5	F17E9.11
C09G5.3	C11H1.5	F45E4.6	Y53F4B.27	Y18D10A.21	C06A8.6
B0273.1	AC3.4	C34B2.4	F54A3.4	C02F5.2	K07B1.1
F07F6.1	Y75B8A.23	W02B12.7	Y66D12A.11	C14C11.1	C42D4.3
Y105C5B.17	C06C6.8	Y51H4A.9	F26A3.5	H12I13.6	ZK180.5
F40E12.2	B0218.5	Y37E11AR.7	B0523.1	W03D8.1	ZK1251.5
H10E21.4	ZK829.2	ZC190.7	T24F1.4	K06A5.3	F57B9.9
ZK666.8	T28A11.20	F54H5.2	H12I13.1	B0024.15	Y77E11A.10
T05C12.10	T23F6.3	C03B8.3	K07H8.5	M05D6.3	C33G3.3
Y37F4.5	F54B11.8	Y54E2A.5	K01D12.18	ZC434.3	ZK354.3
ZK507.3	K10D2.8	C16C10.12	Y47D3A.5	F35E2.5	K08F8.5
F45G2.5	K11H3.2	W03B1.3	F38B6.5	K04C2.8	Y18H1A.13
F37C12.18	R13A5.11	C55C3.3	C17B7.10	F35F10.13	ZK105.3
K04A8.10	F26C11.1	Y32F6B.1	Y59E9AR.8	R10E4.7	K09C8.3
F15H10.2	D2092.7	Y42H9AR.2	F19G12.4	K10C9.9	ZC8.1
C47E12.12	T08H10.4	K12B6.2	R12E2.15	F22E10.3	C06A5.2
C09E8.2	T02E9.2	Y54G2A.37	F57H12.5	Y48G1C.5	W01B11.2
C39E9.3	Y71G12B.17	Y57G11C.5	Y105C5B.11	E03A3.1	Y95B8A.4
K08C9.4	R90.4	Y102A11A.5	R90.3	Y75B8A.20	F28H7.6
C31H2.2	F08F1.6	Y46H3A.4	F26F12.5	T27C10.8	F25B3.4

ZK673.6	Y39E4B.11	F32B6.10	F09B9.1	C06A6.7	T09B4.3
B0024.2	F44D12.11	C12D5.3	T02E1.6	Y54F10BM.3	C24F3.5
C28A5.6	F35F11.2	F08F8.1	F46F3.3	T06E4.4	
C46H11.6	T15B7.5	B0280.17	F56D6.12	B0563.5	
R11A8.8	R07B7.4	F32E10.3	Y48A6B.1	F26G1.5	
Y47D7A.13	F33A8.7	T10C6.18	T06D8.10	F15B9.3	

7.2 RNA-seq: *C. elegans bus-8* RNAs downregulated by FK506 treatment

F14H12.1
F38A1.14
F22B5.3
ZK1248.2
C18H7.1
C01B10.5
T05B4.11
R09E10.5
T05H10.3
C08B6.4
R05A10.1
C32H11.1
T23F1.6
T25E4.1
T23F1.5
ZC84.1
R09B5.2
T06E4.10

7.3 RNA-seq: 3T3-L1 adipocyte RNAs altered by FK506

7.3.1 Day 5 – increased by FK506

Gm13611	Mecom	Rpl28
Gm8355	Anxa5	Rps27l
Rps19	Amot	Rpl36al
Rpl36	Thy1	Rps16
Sulf2	Ly6a	Eef1d
Rpl18a	Rpl3	Ngfrap1
Rpl36-ps2	Aldh2	Rps10-ps1
Tpi1	Tmsb10	Rab1
WI1-1003N17.1	Anxa3	Rpn1
Gm8129	Trmt1	Dazap2
Rpl10	1110038B12Rik	Gm10275
Krtcap2	Rplp1	Rps12
Hspa8	Cfl1	Gm2000
Rpl38	Gm10036	Nme1
Pls3	Sdc1	Asap1
Fbxo25	Rpl13	Rps13
Psmg4	Rpl26	Rpl3-ps1
Eif3i	Pdap1	Mmp14
Ptrh1	Nnt	Pdlim2
Sdhd	Prmt3	Rps12-ps10
Rpl38-ps2	Gm11518	Eef1b2
Il11ra1	Smarce1	Rpl27a
Rab26os	Malsu1	Rpl23a-ps3
Gm15772	Zyx	Emp3
Gm15501	Rps23	Rpl5
Emp2	Actg1	Rps28
Rps20	Rpl23a	Rps8
Rps19-ps6	Ola1	Gm10073
Mrpl52	Gm12918	
Bola2	Gm7536	
Pcdh19	Gm15459	
Rps12-ps9	Rps29	
Dpm2	Gm3362	
Gm8624	Gm17511	
Rps10	Ppia	
Gm15427	Rpl12	
Cdr2l	Capn6	
Flnb	Rpl10-ps3	
Basp1	Gm14303	
Gm9844	Rpl22	
Gm6169	Arhgdia	
Mitd1	Arhgef10	

7.3.2 Day 5 – decreased by FK506

Mmadhc	Ccdc80
Rab14	Dgat1
Rab34	Rhou
Ppp2r4	Suz12
Slc25a51	Tapt1
Ece1	mt-Rnr1
Atp5b	Btg1
Exoc3	Dbt
Dlat	Cat
Lias	Mknk2
Blcap	Chrdl1
Mrpl15	Pex11a
Sh3pxd2a	Aoc3
Eif4g1	Abca1
Ak2	Gm6166
Gpbp1l1	Tmem167b
Cept1	Nrip1
Ermp1	Sort1
Hibadh	Pla2g16
Ndufs1	C3
Phldb1	Zbtb5
Hdac5	Fam73b
Dnmt3a	Pick1
Gnpat	Pdpr
Dbi	Lipe
Pex19	Pnpla2
Ept1	Slc1a3
Sod1	Fabp4
Fgfrl1	Thrsp
Lpl	Rgs16
Adipor2	Acsl1
Pkdcc	Yam1
Ivd	Adrb3
Pdk2	

7.3.3 Day 10 – increased by FK506

Txn-ps1	Ddx50	Rpl10	Arpc1a
Gm8292	Pim1	Cog3	Arcn1
Gm12739	Osbp	Abhd2	Rps23
Gm10260	Unk	Frmd6	Cstf2t
Gm2830	Crtc2	Sgms1	Pqbp1
Gm7618	Rpl38-ps2	Lta4h	Hsp90b1
Gm7079	Senp3	Glyr1	Tmem256
RP23-389J8.3	Fzd2	Tollip	Pbx1
Trim68	Gm8430	Rspry1	Limd1
Gm6977	Hic1	D10Jhu81e	Kdelr1
Slc20a2	Nid2	Supt16	Smim14
Fkbp2	Cdh11	Cldn25	Ndfip2
Llgl1	Cystm1	Edc4	Hnrnpab
Eno1b	Plcb4	Rplp1	Chmp5
Lrp4	Slc7a5	Ssbp1	Calm2
Gm10059	Sptssa	Uckl1	Gnb2
Fzd1	Rps19	Sep-15	
Gm13436	Ice1	Rpl38	
Psap	RP23-459L15.7	Polr2m	
Gm9840	Olfml2b	Krcc1	
Eno1	Usmg5	Rce1	
Gm10320	Zkscan17	Capzb	
Rpl17	Src	Sgol2	
Brat1	Cdc5l	Calu	
Atxn2l	Cep44	Rps16	
Plac8	Dse	Gm28438	
Gdi1	Wdr11	Ppp1r2	
Bcl7c	Cmtm3	Man2a1	
Rps27a	Itm2c	Sh3bp2	
2510039O18Rik	Rps29	Smad3	
Gm16061	Ppp1r14b	Cd63	
Rps19-ps1	Rap2a	Apaf1	
Gm14633	Lmtk2	Dock1	
Gm14539	Ccdc115	Tmem43	
Snrnp70	Hnrnpf	Gm14303	
Tmem181b-ps	Abhd4	Tmsb10	
Gm10653	Rps15a-ps7	Adam10	
Gm6433	Pdk4	Col1a2	
Lhfp	Rpl34	Arsa	
Fst	Islr	Fermt2	
Zfp384	Aldh18a1	Syvn1	
Cntrob	Mylip	Eif4g1	
Adam9	Ctnnd1	Akirin2	

7.3.4 Day 10 – decreased by FK506

Tspan4	Zfp330	Uqcrq	Acads	Slc22a23	Abcd2
Gm28661	Suclg1	BC003965	BC023829	Pla2g16	Acsl1
Atp5b	Fgfrl1	Esyt1	Lnpep	Ppa1	Fam73b
Ergic1	Ipo9	Cav2	Apmap	Cebpa	Aqp7
H2-D1	Por	Tenm4	Gm6166	Agpat9	Cachd1
Skp1a	Tspo	Mdh1	Dgat1	Tmcc3	Aoc3
Tnpo2	Hsd17b10	Ppan	Mavs	Prps1	Adrb3
Ndufs6	Bcap31	Idh3g	Gstz1	Gnpat	mt-Atp8
Psmd4	Atp5l2-ps	mt-Rnr1	Ptcd3	Sdpr	Itga7
Dnajc5	Poldip2	Srprb	Scp2	Pnpla2	Lipe
Map1lc3a	Afap1	Mapk6	Slc25a10	Agpat2	Rnf125
Actr1a	Pank3	Eef1a1	Crat	Cldn15	Ffar2
Mpdu1	Arhgap29	Lpl	Akr7a5	Kank1	Sort1
Aldh2	Itga6	Gcsh	Stom	Tspan12	Orm1
Ubac2	Taldo1	Sc5d	Pdk2	Anxa8	Atp1a2
Sspn	Fam49b	Mknk2	Dbi	Rgs16	Smim5
Lap3	Sidt2	Adipor2	Ganc	Gm22710	Gm22748
Atp5k	Cd151	Slc1a3	Mvd	Apol6	Wfdc21
Ccdc80	Coasy	mt-Nd2	Ivd	Arxes2	Slc2a4
Fabp5	Ndufa9	Hmgcs1	Nrip1	Car5b	Csrnp1

7.3.5 Day 15 – decreased by FK506 (none increased)

Fxr1

Dcun1d3

Bibliography

Aitlhadj, L. & Stürzenbaum, S.R., 2010. The use of FUdR can cause prolonged longevity in mutant nematodes. *Mechanisms of ageing and development*, 131(5), pp.364–5. Available at: http://www.ncbi.nlm.nih.gov/pubmed/20236608 [Accessed September 27, 2016].

Akashi, T. et al., 1996. Quantitative determination of tautomeric FK506 by reversed-phase liquid chromatography. *Journal of Pharmaceutical and Biomedical Analysis*, 14, pp.339–346. Available at: https://www.ncbi.nlm.nih.gov/pubmed/8851758 [Accessed September 23, 2016].

Alper, S. et al., 2010. The Caenorhabditis elegans germ line regulates distinct signaling pathways to control lifespan and innate immunity. *The Journal of biological chemistry*, 285(3), pp.1822–8. Available at: http://www.ncbi.nlm.nih.gov/pubmed/19923212 [Accessed October 2, 2016].

Antebi, A., 2007. Genetics of aging in Caenorhabditis elegans. S. K. Kim, ed. *PLoS genetics*, 3(9), pp.1565–71. Available at: http://dx.plos.org/10.1371/journal.pgen.0030129 [Accessed August 7, 2013].

Araujo, T.R. et al., 2016. Benefits of L-alanine or L-arginine supplementation against adiposity and glucose intolerance in monosodium glutamate-induced obesity. *European journal of nutrition*. Available at: http://www.ncbi.nlm.nih.gov/pubmed/27317126 [Accessed September 28, 2016].

Argüelles, J.C., 2000. Physiological roles of trehalose in bacteria and yeasts: a comparative analysis. *Archives of microbiology*, 174(4), pp.217–24. Available at: http://www.ncbi.nlm.nih.gov/pubmed/11081789 [Accessed September 8, 2016].

Atkison, P. et al., 1995. Hypertrophic cardiomyopathy associated with tacrolimus in paediatric transplant patients. *Lancet*, 345(8954), pp.894–6. Available at: http://www.ncbi.nlm.nih.gov/pubmed/7535875 [Accessed July 31, 2013].

Augustin, H. & Partridge, L., 2009. Invertebrate models of age-related muscle degeneration. *Biochimica et Biophysica Acta (BBA) - General Subjects*, 1790(10), pp.1084–1094. Available at: http://www.ncbi.nlm.nih.gov/pubmed/19563864 [Accessed September 30, 2015].

Bai, L. et al., 2010. Low- but not high-dose FK506 treatment confers atheroprotection due to alternative macrophage activation and unaffected cholesterol levels. *Thrombosis and haemostasis*, 104(1), pp.143–50. Available at: http://www.ncbi.nlm.nih.gov/pubmed/20458432 [Accessed October 5, 2015].

Baker, D.J. et al., 2011. Clearance of p16Ink4a-positive senescent cells delays ageing-associated disorders. *Nature*, 479(7372), pp.232–6. Available at: http://www.ncbi.nlm.nih.gov/pubmed/22048312 [Accessed September 21, 2016].

Baker, D.J. et al., 2016. Naturally occurring p16(Ink4a)-positive cells shorten healthy lifespan. *Nature*, 530(7589), pp.184–9. Available at: http://www.ncbi.nlm.nih.gov/pubmed/26840489 [Accessed September 21, 2016].

Baker, D.J. et al., 2008. Opposing roles for p16Ink4a and p19Arf in senescence and ageing caused by BubR1 insufficiency. *Nature cell biology*, 10(7), pp.825–36. Available at: http://www.ncbi.nlm.nih.gov/pubmed/18516091 [Accessed September 21, 2016].

Balaban, R.S. et al., 2005. Mitochondria, oxidants, and aging. *Cell*, 120(4), pp.483–95. Available at: http://www.ncbi.nlm.nih.gov/pubmed/15734681 [Accessed September 20, 2016].

Balsevich, G. et al., 2014. Interplay between diet-induced obesity and chronic stress in mice: potential role of FKBP51. *The Journal of endocrinology*, 222(1), pp.15–26. Available at: http://www.ncbi.nlm.nih.gov/pubmed/24781256 [Accessed September 10, 2014].

Barna, J. et al., 2012. Heat shock factor-1 intertwines insulin/IGF-1, TGF-β and cGMP signaling to control

development and aging. *BMC developmental biology*, 12, p.32. Available at: http://www.pubmedcentral.nih.gov/articlerender.fcgi?artid=3558376&tool=pmcentrez&rendertype=abstract [Accessed November 25, 2015].

Bell, A., Monaghan, P. & Page, A.P., 2006. Peptidyl-prolyl cis-trans isomerases (immunophilins) and their roles in parasite biochemistry, host-parasite interaction and antiparasitic drug action. *International journal for parasitology*, 36(3), pp.261–76. Available at: http://www.sciencedirect.com/science/article/pii/S0020751905003905 [Accessed June 12, 2015].

Benedetti, G. et al., 2013. A screen for apoptotic synergism between clinical relevant nephrotoxicant and the cytokine TNF-α. *Toxicology in vitro : an international journal published in association with BIBRA*, 27(8), pp.2264–2272. Available at: http://www.ncbi.nlm.nih.gov/pubmed/24041534 [Accessed November 21, 2013].

Bianchin, A. et al., 2015. Two crystal structures of the FK506-binding domain of Plasmodium falciparum FKBP35 in complex with rapamycin at high resolution. *Acta crystallographica. Section D, Biological crystallography*, 71(Pt 6), pp.1319–27. Available at: http://www.ncbi.nlm.nih.gov/pubmed/26057671 [Accessed July 22, 2015].

Bierer, B.E. et al., 1990. Probing immunosuppressant action with a nonnatural immunophilin ligand. *Science (New York, N.Y.)*, 250(4980), pp.556–9. Available at: http://www.ncbi.nlm.nih.gov/pubmed/1700475 [Accessed February 19, 2014].

Binder, E.B. et al., 2004. Polymorphisms in FKBP5 are associated with increased recurrence of depressive episodes and rapid response to antidepressant treatment. *Nature genetics*, 36(12), pp.1319–25. Available at: http://www.ncbi.nlm.nih.gov/pubmed/15565110 [Accessed November 25, 2013].

Birzele, F. et al., 2012. Analysis of the transcriptome of differentiating and non-differentiating preadipocytes from rats and humans by next generation sequencing. *Molecular and cellular biochemistry*, 369(1–2), pp.175–81. Available at: http://www.ncbi.nlm.nih.gov/pubmed/22773307 [Accessed October 9, 2013].

Blair, L.J. et al., 2013. Accelerated neurodegeneration through chaperone-mediated oligomerization of tau. *The Journal of clinical investigation*, 123(10), pp.4158–69. Available at: http://www.pubmedcentral.nih.gov/articlerender.fcgi?artid=3784538&tool=pmcentrez&rendertype=abstract [Accessed November 21, 2013].

Blair, L.J. et al., 2015. The emerging role of peptidyl-prolyl isomerase chaperones in tau oligomerization, amyloid processing and Alzheimer's disease. *Journal of neurochemistry*, 133(1), pp.1–13. Available at: http://www.ncbi.nlm.nih.gov/pubmed/25628064 [Accessed February 3, 2015].

Bonthuis, M. et al., 2013. Dyslipidaemia in children on renal replacement therapy. *Nephrology, dialysis, transplantation : official publication of the European Dialysis and Transplant Association - European Renal Association*, 29(3), pp.594–603. Available at: http://www.ncbi.nlm.nih.gov/pubmed/24170813 [Accessed November 21, 2013].

Borda, B. et al., 2014. Side effects of the calcineurin inhibitor, such as new-onset diabetes after kidney transplantation. *Acta physiologica Hungarica*, 101(3), pp.388–94. Available at: http://www.ncbi.nlm.nih.gov/pubmed/25183511 [Accessed September 5, 2014].

Breckner, A. et al., 2013. Effect of Calstabin1 depletion on calcium transients and energy utilization in muscle fibers and treatment opportunities with RyR1 stabilizers. *PloS one*, 8(11), p.e81277. Available at: http://www.pubmedcentral.nih.gov/articlerender.fcgi?artid=3841141&tool=pmcentrez&rendertype=abstract [Accessed October 28, 2015].

Bridi, J.C. et al., 2015. Lifespan Extension Induced by Caffeine in Caenorhabditis elegans is Partially Dependent on Adenosine Signaling. *Frontiers in aging neuroscience*, 7, p.220. Available at: http://www.pubmedcentral.nih.gov/articlerender.fcgi?artid=4672644&tool=pmcentrez&rendertype=abstract [Accessed December 29, 2015].

Brooks, K.K., Liang, B. & Watts, J.L., 2009. The influence of bacterial diet on fat storage in C. elegans. *PLoS ONE*, 4(10). Available at: http://journals.plos.org/plosone/article?id=10.1371/journal.pone.0007545.

Bround, M.J. et al., 2013. Cardiomyocyte ATP production, metabolic flexibility, and survival require calcium flux through cardiac ryanodine receptors in vivo. *The Journal of biological chemistry*, 288(26), pp.18975–86. Available at: http://www.jbc.org/content/288/26/18975.long [Accessed February 27, 2015].

Cabreiro, F. et al., 2013. Metformin Retards Aging in C. elegans by Altering Microbial Folate and Methionine Metabolism. *Cell*, 153(1), pp.228–239. Available at: http://www.sciencedirect.com/science/article/pii/S0092867413002675 [Accessed January 7, 2014].

Cabreiro, F. & Gems, D., 2013. Worms need microbes too: microbiota, health and aging in Caenorhabditis elegans. *EMBO molecular medicine*, 5(9), pp.1300–10. Available at: http://www.pubmedcentral.nih.gov/articlerender.fcgi?artid=3799487&tool=pmcentrez&rendertype=abstract [Accessed February 19, 2014].

Caraveo, G. et al., 2014. Calcineurin determines toxic versus beneficial responses to α-synuclein. *Proceedings of the National Academy of Sciences of the United States of America*, 111(34), pp.E3544-52. Available at: http://www.pubmedcentral.nih.gov/articlerender.fcgi?artid=4151770&tool=pmcentrez&rendertype=abstract [Accessed February 27, 2015].

Carmona-Gutierrez, D. et al., 2016. The crucial impact of lysosomes in aging and longevity. *Ageing Research Reviews*, 32, pp.2–12. Available at: http://www.sciencedirect.com/science/article/pii/S1568163716300666 [Accessed October 6, 2016].

Cartwright, M.J., Tchkonia, T. & Kirkland, J.L., 2007. Aging in adipocytes: potential impact of inherent, depot-specific mechanisms. *Experimental gerontology*, 42(6), pp.463–71. Available at: http://www.pubmedcentral.nih.gov/articlerender.fcgi?artid=1961638&tool=pmcentrez&rendertype=abstract [Accessed October 16, 2013].

Castillo-Quan, J.I. et al., 2016. Lithium promotes longevity through GSK3/NRF2-dependent hormesis. *Cell Reports*, 15(3), pp.638–50. Available at: http://www.cell.com/cell-reports/abstract/S2211-1247(16)30297-2?_returnURL=http%3A%2F%2Flinkinghub.elsevier.com%2Fretrieve%2Fpii%2FS2211124716302972%3Fshowall%3Dtrue.

Castro, G. et al., 2013. Diet-induced obesity induces endoplasmic reticulum stress and insulin resistance in the amygdala of rats. *FEBS Open Bio*, 3, pp.443–449. Available at: http://www.sciencedirect.com/science/article/pii/S221154631300051X [Accessed November 21, 2013].

Cavallucci, V. et al., 2013. Calcineurin inhibition rescues early synaptic plasticity deficits in a mouse model of Alzheimer's disease. *Neuromolecular medicine*, 15(3), pp.541–8. Available at: http://www.ncbi.nlm.nih.gov/pubmed/23821337 [Accessed November 21, 2013].

Chambraud, B. et al., 2010. A role for FKBP52 in Tau protein function. *Proceedings of the National Academy of Sciences of the United States of America*, 107(6), pp.2658–63. Available at: http://www.pnas.org/content/107/6/2658.long [Accessed July 23, 2015].

Chang, R.K. et al., 2001. Echocardiographic findings of hypertrophic cardiomyopathy in children after orthotopic liver transplantation. *Pediatric transplantation*, 5(3), pp.187–91. Available at: http://www.ncbi.nlm.nih.gov/pubmed/11422821 [Accessed July 31, 2013].

Chen, Z. et al., 2010. FKBP12.6-knockout mice display hyperinsulinemia and resistance to high-fat diet-induced hyperglycemia. *FASEB journal : official publication of the Federation of American Societies for Experimental Biology*, 24(2), pp.357–63. Available at: http://www.pubmedcentral.nih.gov/articlerender.fcgi?artid=2812035&tool=pmcentrez&rendertype=abstract [Accessed May 6, 2015].

Christensen, K., Johnson, T.E. & Vaupel, J.W., 2006. The quest for genetic determinants of human longevity: challenges and insights. *Nature reviews. Genetics*, 7(6), pp.436–48. Available at: http://www.ncbi.nlm.nih.gov/pubmed/16708071 [Accessed October 1, 2016].

Christodoulides, C. et al., 2009. Adipogenesis and WNT signalling. *Trends in endocrinology and metabolism: TEM*, 20(1), pp.16–24. Available at: http://www.ncbi.nlm.nih.gov/pubmed/19008118 [Accessed October 6, 2016].

Clancy, D.J. et al., 2001. Extension of life-span by loss of CHICO, a Drosophila insulin receptor substrate protein. *Science (New York, N.Y.)*, 292(5514), pp.104–6. Available at: http://www.ncbi.nlm.nih.gov/pubmed/11292874 [Accessed December 3, 2014].

Colman, R.J. et al., 2009. Caloric restriction delays disease onset and mortality in rhesus monkeys. *Science (New York, N.Y.)*, 325(5937), pp.201–4. Available at: http://www.pubmedcentral.nih.gov/articlerender.fcgi?artid=2812811&tool=pmcentrez&rendertype=abstract [Accessed January 21, 2014].

Colman, R.J. et al., 2014. Caloric restriction reduces age-related and all-cause mortality in rhesus monkeys. *Nature communications*, 5, p.3557. Available at: http://www.pubmedcentral.nih.gov/articlerender.fcgi?artid=3988801&tool=pmcentrez&rendertype=abstract [Accessed May 25, 2014].

Cox, K.L. & Freese, D.K., 1996. Tacrolimus (FK506): the pros and cons of its use as an immunosuppressant in pediatric liver transplantation. *Clinical and investigative medicine. Médecine clinique et experimentale*, 19(5), pp.389–92. Available at: http://www.ncbi.nlm.nih.gov/pubmed/8889279 [Accessed July 31, 2013].

D'Angelillo, A. et al., 2015. Molecular Aspects of FKBP51 that Enable Melanoma Dissemination. *Current molecular pharmacology*, 9(2), pp.141–7. Available at: http://www.ncbi.nlm.nih.gov/pubmed/25986563 [Accessed July 22, 2015].

Davis, J.R., Li, Y. & Rankin, C.H., 2008. Effects of developmental exposure to ethanol on Caenorhabditis elegans. *Alcoholism, clinical and experimental research*, 32(5), pp.853–67. Available at: http://www.ncbi.nlm.nih.gov/pubmed/18336629 [Accessed August 29, 2016].

Depuydt, G. et al., 2016. Increased Protein Stability and Decreased Protein Turnover in the Caenorhabditis elegans Ins/IGF-1 daf-2 Mutant. *The journals of gerontology. Series A, Biological sciences and medical sciences*, 71(12), pp.1553–1559. Available at: http://biomedgerontology.oxfordjournals.org/content/early/2016/02/10/gerona.glv221.long [Accessed March 17, 2016].

Depuydt, G. et al., 2013. Reduced insulin/insulin-like growth factor-1 signaling and dietary restriction inhibit translation but preserve muscle mass in Caenorhabditis elegans. *Molecular & cellular proteomics : MCP*, 12(12), pp.3624–39. Available at: http://www.ncbi.nlm.nih.gov/pubmed/24002365 [Accessed October 5, 2016].

Diémé, B. et al., 2014. Assessing the metabolic effects of calcineurin inhibitors in renal transplant recipients by urine metabolic profiling. *Transplantation*, 98(2), pp.195–201. Available at: http://www.ncbi.nlm.nih.gov/pubmed/24598938 [Accessed September 5, 2014].

DiMartini, A.F., Trzepacz, P.T. & Daviss, S.R., 1996. Prospective study of FK506 side effects: anxiety or akathisia? *Biological psychiatry*, 40(5), pp.407–11. Available at: http://www.sciencedirect.com/science/article/pii/0006322395003959 [Accessed September 5, 2014].

Dineley, K.T. et al., 2007. Acute inhibition of calcineurin restores associative learning and memory in Tg2576 APP transgenic mice. *Neurobiology of learning and memory*, 88(2), pp.217–24. Available at: http://www.pubmedcentral.nih.gov/articlerender.fcgi?artid=2031869&tool=pmcentrez&rendertype=abstract [Accessed September 24, 2015].

Dollinger, M.M. et al., 1995. Tacrolimus and cardiotoxicity in adult liver transplant recipients. *Lancet*,

346(8973), p.507. Available at: http://www.ncbi.nlm.nih.gov/pubmed/7543645 [Accessed July 31, 2013].

Donohoe, D.R. et al., 2009. Behavioral adaptation in C. elegans produced by antipsychotic drugs requires serotonin and is associated with calcium signaling and calcineurin inhibition. *Neuroscience research*, 64(3), pp.280–9. Available at: http://www.sciencedirect.com/science/article/pii/S0168010209000923 [Accessed December 29, 2015].

Dwivedi, M., Song, H.-O. & Ahnn, J., 2009. Autophagy genes mediate the effect of calcineurin on life span in C. elegans. *Autophagy*, 5(5), pp.604–7. Available at: http://www.ncbi.nlm.nih.gov/pubmed/19279398 [Accessed September 29, 2015].

Dzitoyeva, S. & Manev, H., 2013. Reduction of Cellular Lipid Content by a Knockdown of Drosophila PDP1 γ and Mammalian Hepatic Leukemia Factor. *Journal of lipids*, 2013, p.297932. Available at: http://www.pubmedcentral.nih.gov/articlerender.fcgi?artid=3766575&tool=pmcentrez&rendertype=abstract [Accessed November 5, 2013].

Eguchi, J. et al., 2008. Interferon Regulatory Factors Are Transcriptional Regulators of Adipogenesis. *Cell Metabolism*, 7(1), pp.86–94. Available at: http://www.sciencedirect.com/science/article/pii/S1550413107003373 [Accessed October 23, 2013].

Eisenberg, T. et al., 2009. Induction of autophagy by spermidine promotes longevity. *Nature cell biology*, 11(11), pp.1305–14. Available at: http://dx.doi.org/10.1038/ncb1975 [Accessed July 10, 2014].

Eltit, J.M. et al., 2010. Ablation of skeletal muscle triadin impairs FKBP12/RyR1 channel interactions essential for maintaining resting cytoplasmic Ca2+. *The Journal of biological chemistry*, 285(49), pp.38453–62. Available at: http://www.pubmedcentral.nih.gov/articlerender.fcgi?artid=2992278&tool=pmcentrez&rendertype=abstract [Accessed May 6, 2015].

Fan, J.-Y. et al., 2013. Noncanonical FK506-Binding Protein BDBT Binds DBT to Enhance Its Circadian Function and Forms Foci at Night. *Neuron*, 80(4), pp.984–96. Available at: http://www.ncbi.nlm.nih.gov/pubmed/24210908 [Accessed November 21, 2013].

Fasseas, M.K., Dimou, M. & Katinakis, P., 2012. The Caenorhabditis elegans parvulin gene subfamily and their expression under cold or heat stress along with the fkb subfamily. *Biochemical and biophysical research communications*, 423(3), pp.520–5. Available at: http://www.ncbi.nlm.nih.gov/pubmed/22683625 [Accessed September 10, 2014].

Földes, G. et al., 2014. Immunosuppressive agents modulate function, growth, and survival of cardiomyocytes and endothelial cells derived from human embryonic stem cells. *Stem cells and development*, 23(5), pp.467–76. Available at: http://www.ncbi.nlm.nih.gov/pubmed/24192059 [Accessed February 21, 2014].

Fontana, L., Partridge, L. & Longo, V.D., 2010. Extending healthy life span--from yeast to humans. *Science (New York, N.Y.)*, 328(5976), pp.321–6. Available at: http://www.sciencemag.org/content/328/5976/321.abstract [Accessed August 6, 2013].

Frankowski, H. et al., 2013. Dimethyl sulfoxide and dimethyl formamide increase lifespan of C. elegans in liquid. *Mechanisms of ageing and development*, 134(3–4), pp.69–78. Available at: http://www.sciencedirect.com/science/article/pii/S004763741300002X [Accessed March 9, 2016].

Fraser, A.G. et al., 2000. Functional genomic analysis of C. elegans chromosome I by systematic RNA interference. *Nature*, 408(6810), pp.325–30. Available at: http://dx.doi.org/10.1038/35042517 [Accessed March 28, 2015].

Fries, G.R. et al., 2015. The FKBP51-Glucocorticoid Receptor Balance in Stress-Related Mental Disorders. *Current molecular pharmacology*, 9(2), pp.126–40. Available at: http://www.ncbi.nlm.nih.gov/pubmed/25986564 [Accessed July 22, 2015].

Fu, Y.T. et al., 2015. Silencing FKBP38 gene by siRNA induces activation of mTOR signaling in goat fetal

fibroblasts. *Genetics and molecular research : GMR*, 14(3), pp.9675–82. Available at: http://www.ncbi.nlm.nih.gov/pubmed/26345900 [Accessed September 29, 2015].

Fujii, T., Ota, M., Hori, H., Hattori, K., Teraishi, T., Sasayama, D., et al., 2014. Association between the common functional FKBP5 variant (rs1360780) and brain structure in a non-clinical population. *Journal of psychiatric research*, 58, pp.96–101. Available at: http://www.ncbi.nlm.nih.gov/pubmed/25088286 [Accessed September 10, 2014].

Fujii, T., Ota, M., Hori, H., Hattori, K., Teraishi, T., Matsuo, J., et al., 2014. The common functional FKBP5 variant rs1360780 is associated with altered cognitive function in aged individuals. *Scientific reports*, 4, p.6696. Available at: http://www.pubmedcentral.nih.gov/articlerender.fcgi?artid=4204028&tool=pmcentrez&rendertype=abstract [Accessed January 14, 2015].

Galat, A., 2003. Peptidylprolyl cis/trans isomerases (immunophilins): biological diversity--targets--functions. *Current topics in medicinal chemistry*, 3(12), pp.1315–47. Available at: http://www.ncbi.nlm.nih.gov/pubmed/12871165 [Accessed March 10, 2014].

Galfré, E. et al., 2012. FKBP12 Activates the Cardiac Ryanodine Receptor Ca2+-Release Channel and Is Antagonised by FKBP12.6 B. S. Launikonis, ed. *PLoS ONE*, 7(2), p.e31956. Available at: http://journals.plos.org/plosone/article?id=10.1371/journal.pone.0031956#s4 [Accessed March 25, 2015].

Gallo, L.I. et al., 2011. The 90-kDa heat-shock protein (Hsp90)-binding immunophilin FKBP51 is a mitochondrial protein that translocates to the nucleus to protect cells against oxidative stress. *The Journal of biological chemistry*, 286(34), pp.30152–60. Available at: http://www.pubmedcentral.nih.gov/articlerender.fcgi?artid=3191054&tool=pmcentrez&rendertype=abstract [Accessed November 27, 2013].

Gandhi, S. et al., 1980. A simple method for maintaining large, aging populations of Caenorhabditis elegans. *Mechanisms of ageing and development*, 12(2), pp.137–50. Available at: http://www.ncbi.nlm.nih.gov/pubmed/6445025 [Accessed September 27, 2016].

Gant, J.C. et al., 2011. Disrupting function of FK506-binding protein 1b/12.6 induces the Ca^{2}+-dysregulation aging phenotype in hippocampal neurons. *The Journal of neuroscience : the official journal of the Society for Neuroscience*, 31(5), pp.1693–703. Available at: http://www.pubmedcentral.nih.gov/articlerender.fcgi?artid=3092371&tool=pmcentrez&rendertype=abstract [Accessed August 4, 2015].

Gant, J.C. et al., 2014. FK506-binding protein 1b/12.6: a key to aging-related hippocampal Ca2+ dysregulation? *European journal of pharmacology*, 739, pp.74–82. Available at: http://www.sciencedirect.com/science/article/pii/S0014299913008819 [Accessed January 16, 2015].

Gant, J.C. et al., 2015. Reversal of Aging-Related Neuronal Ca2+ Dysregulation and Cognitive Impairment by Delivery of a Transgene Encoding FK506-Binding Protein 12.6/1b to the Hippocampus. *Journal of Neuroscience*, 35(30), pp.10878–10887. Available at: http://www.jneurosci.org/cgi/doi/10.1523/JNEUROSCI.1248-15.2015.

Gassen, N.C. et al., 2014. Association of FKBP51 with priming of autophagy pathways and mediation of antidepressant treatment response: evidence in cells, mice, and humans. *PLoS medicine*, 11(11), p.e1001755. Available at: http://journals.plos.org/plosmedicine/article?id=10.1371/journal.pmed.1001755 [Accessed January 14, 2015].

Gassen, N.C. et al., 2015. FKBP5/FKBP51 enhances autophagy to synergize with antidepressant action. *Autophagy*, 11(3), pp.578–80. Available at: http://www.pubmedcentral.nih.gov/articlerender.fcgi?artid=4502647&tool=pmcentrez&rendertype=abstract [Accessed March 24, 2016].

Ge, D. et al., 2014. Identification of a novel MTOR activator and discovery of a competing endogenous RNA regulating autophagy in vascular endothelial cells. *Autophagy*, 10(6), pp.957–71. Available at:

http://www.ncbi.nlm.nih.gov/pubmed/24879147 [Accessed January 14, 2015].

Gems, D. & Partridge, L., 2013. Genetics of longevity in model organisms: debates and paradigm shifts. *Annual review of physiology*, 75, pp.621–44. Available at: http://www.ncbi.nlm.nih.gov/pubmed/23190075 [Accessed September 21, 2013].

Glaumann, H., 1982. Degradation of proteins and lipids in autophagic vacuoles and secretory vesicles. *Acta biologica et medica Germanica*, 41(1), pp.103–111. Available at: http://www.ncbi.nlm.nih.gov/pubmed/7113542 [Accessed October 5, 2016].

Gold, B.G., Storm-Dickerson, T. & Austin, D.R., 1994. The immunosuppressant FK506 increases functional recovery and nerve regeneration following peripheral nerve injury. *Restorative neurology and neuroscience*, 6(4), pp.287–96. Available at: http://www.ncbi.nlm.nih.gov/pubmed/21551759 [Accessed July 23, 2015].

Gragnoli, C., 2014. Hypothesis of the neuroendocrine cortisol pathway gene role in the comorbidity of depression, type 2 diabetes, and metabolic syndrome. *The application of clinical genetics*, 7, pp.43–53. Available at: http://www.pubmedcentral.nih.gov/articlerender.fcgi?artid=4012344&tool=pmcentrez&rendertype=abstract [Accessed September 10, 2014].

Gravato-Nobre, M.J. et al., 2005. Multiple Genes Affect Sensitivity of Caenorhabditis elegans to the Bacterial Pathogen Microbacterium nematophilum. *Genetics*, 171(3), pp.1033–45. Available at: http://www.genetics.org/content/171/3/1033.long [Accessed October 2, 2016].

Greer, E.L. et al., 2007. An AMPK-FOXO pathway mediates longevity induced by a novel method of dietary restriction in C. elegans. *Current biology : CB*, 17(19), pp.1646–56. Available at: http://www.ncbi.nlm.nih.gov/pubmed/17900900 [Accessed September 21, 2016].

Greer, E.L. & Brunet, A., 2009. Different dietary restriction regimens extend lifespan by both independent and overlapping genetic pathways in C. elegans. *Aging cell*, 8(2), pp.113–27. Available at: http://www.pubmedcentral.nih.gov/articlerender.fcgi?artid=2680339&tool=pmcentrez&rendertype=abstract [Accessed April 1, 2014].

Guasch, A. et al., 2015. Calcineurin Undergoes a Conformational Switch Evoked via Peptidyl-Prolyl Isomerization A. Wlodawer, ed. *PLOS ONE*, 10(8), p.e0134569. Available at: http://www.pubmedcentral.nih.gov/articlerender.fcgi?artid=4527731&tool=pmcentrez&rendertype=abstract [Accessed October 5, 2015].

Gudavicius, G. et al., 2013. Resolving the functions of peptidylprolyl isomerases: insights from the mutagenesis of the nuclear FKBP25 enzyme. *Biochemical Society transactions*, 41(3), pp.761–8. Available at: http://www.ncbi.nlm.nih.gov/pubmed/23697935 [Accessed November 21, 2013].

Gurnell, M. et al., 2000. A dominant-negative peroxisome proliferator-activated receptor gamma (PPARgamma) mutant is a constitutive repressor and inhibits PPARgamma-mediated adipogenesis. *The Journal of biological chemistry*, 275(8), pp.5754–9. Available at: http://www.ncbi.nlm.nih.gov/pubmed/10681562 [Accessed November 6, 2013].

Guy, N.C., Garcia, Y.A. & Cox, M.B., 2015. Therapeutic Targeting of the FKBP52 Co-Chaperone in Steroid Hormone Receptor-Regulated Physiology and Disease. *Current molecular pharmacology*, 9(2), pp.109–25. Available at: http://www.ncbi.nlm.nih.gov/pubmed/25986565 [Accessed July 22, 2015].

Hansen, M. et al., 2008. A role for autophagy in the extension of lifespan by dietary restriction in C. elegans. *PLoS genetics*, 4(2), p.e24. Available at: http://www.pubmedcentral.nih.gov/articlerender.fcgi?artid=2242811&tool=pmcentrez&rendertype=abstract [Accessed May 26, 2014].

Harbour, M.E., Breusegem, S.Y. & Seaman, M.N.J., 2012. Recruitment of the endosomal WASH complex is mediated by the extended “tail” of Fam21 binding to the retromer protein Vps35. *The Biochemical journal*, 442(1), pp.209–20. Available at: http://www.ncbi.nlm.nih.gov/pubmed/22070227 [Accessed February 27, 2014].

Harikishore, A. et al., 2013. Small molecule Plasmodium FKBP35 inhibitor as a potential antimalaria agent. *Scientific reports*, 3, p.2501. Available at: http://www.pubmedcentral.nih.gov/articlerender.fcgi?artid=3752609&tool=pmcentrez&rendertype=abstract [Accessed November 21, 2013].

Harraz, O.F. & Altier, C., 2014. STIM1-mediated bidirectional regulation of Ca2+ entry through voltage-gated calcium channels (VGCC) and calcium-release activated channels (CRAC). *Frontiers in Cellular Neuroscience*, 8, p.43. Available at: http://journal.frontiersin.org/article/10.3389/fncel.2014.00043/abstract [Accessed October 6, 2016].

Hartl, F.U., Bracher, A. & Hayer-Hartl, M., 2011. Molecular chaperones in protein folding and proteostasis. *Nature*, 475(7356), pp.324–332. Available at: http://www.nature.com/doifinder/10.1038/nature10317 [Accessed October 6, 2016].

Hartmann, J. et al., 2015. Pharmacological Inhibition of the Psychiatric Risk Factor FKBP51 Has Anxiolytic Properties. *The Journal of neuroscience : the official journal of the Society for Neuroscience*, 35(24), pp.9007–16. Available at: http://www.ncbi.nlm.nih.gov/pubmed/26085626 [Accessed July 22, 2015].

Hartmann, J. et al., 2012. The involvement of FK506-binding protein 51 (FKBP5) in the behavioral and neuroendocrine effects of chronic social defeat stress. *Neuropharmacology*, 62(1), pp.332–9. Available at: http://www.sciencedirect.com/science/article/pii/S0028390811003297 [Accessed October 23, 2014].

Hausch, F., 2015. FKBPs and their role in neuronal signaling. *Biochimica et biophysica acta*, 1850(10), pp.2035–40. Available at: http://www.ncbi.nlm.nih.gov/pubmed/25615537 [Accessed January 30, 2015].

Hayflick, L., 1965. The limited in vitro lifetime of human diploid cell strains. *Experimental cell research*, 37, pp.614–36. Available at: http://www.ncbi.nlm.nih.gov/pubmed/14315085 [Accessed September 21, 2016].

Helledie, T. et al., 2002. The gene encoding the Acyl-CoA-binding protein is activated by peroxisome proliferator-activated receptor gamma through an intronic response element functionally conserved between humans and rodents. *The Journal of biological chemistry*, 277(30), pp.26821–30. Available at: http://www.ncbi.nlm.nih.gov/pubmed/12015306 [Accessed October 24, 2013].

Hesselink, D.A. et al., 2014. The Role of Pharmacogenetics in the Disposition of and Response to Tacrolimus in Solid Organ Transplantation. *Clinical pharmacokinetics*, 53(2), pp.123–39. Available at: http://www.ncbi.nlm.nih.gov/pubmed/24249597 [Accessed November 21, 2013].

Ho, S. et al., 1996. The mechanism of action of cyclosporin A and FK506. *Clinical immunology and immunopathology*, 80(3 Pt 2), pp.S40-5. Available at: http://www.ncbi.nlm.nih.gov/pubmed/8811062 [Accessed November 21, 2013].

Honda, Y. et al., 2011. Lifespan-extending effects of royal jelly and its related substances on the nematode Caenorhabditis elegans. *PloS one*, 6(8), p.e23527. Available at: http://www.pubmedcentral.nih.gov/articlerender.fcgi?artid=3153499&tool=pmcentrez&rendertype=abstract [Accessed August 27, 2014].

Honjoh, S. et al., 2009. Signalling through RHEB-1 mediates intermittent fasting-induced longevity in C. elegans. *Nature*, 457(7230), pp.726–30. Available at: http://www.ncbi.nlm.nih.gov/pubmed/19079239 [Accessed September 21, 2016].

Horii, T. et al., 2009. Epigenetic regulation of adipocyte differentiation by a Rho guanine nucleotide exchange factor, WGEF. *PloS one*, 4(6), p.e5809. Available at: http://www.pubmedcentral.nih.gov/articlerender.fcgi?artid=2686168&tool=pmcentrez&rendertype=abstract [Accessed October 8, 2013].

Hosono, R., 1978. Sterilization and growth inhibition of Caenorhabditis elegans by 5-fluorodeoxyuridine. *Experimental gerontology*, 13(5), pp.369–74. Available at: http://www.ncbi.nlm.nih.gov/pubmed/153845 [Accessed September 27, 2016].

Hosono, T. et al., 2005. RNA interference of PPARγ using fiber-modified adenovirus vector efficiently suppresses preadipocyte-to-adipocyte differentiation in 3T3-L1 cells. *Gene*, 348, pp.157–165. Available at: http://www.sciencedirect.com/science/article/pii/S0378111905000211 [Accessed October 25, 2013].

House of Lords Select Committee on Public Service and Demographic Change, 2013. *Ready for Ageing?*,

Howes, R.M., 2006. The free radical fantasy: a panoply of paradoxes. *Annals of the New York Academy of Sciences*, 1067, pp.22–6. Available at: http://www.ncbi.nlm.nih.gov/pubmed/16803966 [Accessed September 20, 2016].

Hsin, H. & Kenyon, C., 1999. Signals from the reproductive system regulate the lifespan of C. elegans. *Nature*, 399(6734), pp.362–6. Available at: http://www.ncbi.nlm.nih.gov/pubmed/10360574 [Accessed October 2, 2016].

Hu, E., Tontonoz, P. & Spiegelman, B.M., 1995. Transdifferentiation of myoblasts by the adipogenic transcription factors PPAR gamma and C/EBP alpha. *Proceedings of the National Academy of Sciences of the United States of America*, 92(21), pp.9856–60. Available at: http://www.pubmedcentral.nih.gov/articlerender.fcgi?artid=40901&tool=pmcentrez&rendertype=abstract [Accessed November 6, 2013].

Hu, S. et al., 2016. The Mechanism of L-Arginine Modulates Signal Proteins Involved in Glucose and Lipid Metabolic Imbalance. *Curr Protein Pept Sci*. Available at: http://www.ncbi.nlm.nih.gov/pubmed/27356939 [Accessed September 28, 2016].

Huang, Y.J. et al., 2015. The airway microbiome in patients with severe asthma: Associations with disease features and severity. *The Journal of allergy and clinical immunology*, 136(4), pp.874–84. Available at: http://www.ncbi.nlm.nih.gov/pubmed/26220531 [Accessed August 3, 2015].

Ikeda, H. & Fujiwara, K., 1995. Cyclosporin A and FK-506 in inhibition of rat Ito cell activation in vitro. *Hepatology (Baltimore, Md.)*, 21(4), pp.1161–6. Available at: http://www.ncbi.nlm.nih.gov/pubmed/7535735 [Accessed March 12, 2015].

Isaksson, J. et al., 2015. Polymorphisms in the FK506 binding protein 5 gene are associated with attention deficit hyperactivity disorder and diurnal cortisol levels. *Acta paediatrica*, 104(9), pp.910–5. Available at: http://www.ncbi.nlm.nih.gov/pubmed/26032970 [Accessed June 7, 2015].

Jenkins, S. et al., 2013. Global LC/MS Metabolomics Profiling of Calcium Stressed and Immunosuppressant Drug Treated Saccharomyces cerevisiae. *Metabolites*, 3(4), pp.1102–17. Available at: http://www.pubmedcentral.nih.gov/articlerender.fcgi?artid=3937837&tool=pmcentrez&rendertype=abstract [Accessed September 5, 2014].

Jeyapalan, J.C. et al., 2007. Accumulation of senescent cells in mitotic tissue of aging primates. *Mechanisms of ageing and development*, 128(1), pp.36–44. Available at: http://www.ncbi.nlm.nih.gov/pubmed/17116315 [Accessed September 21, 2016].

Jin, L. et al., 2014. Dipeptidyl peptidase IV inhibitor MK-0626 attenuates pancreatic islet injury in tacrolimus-induced diabetic rats. *PloS one*, 9(6), p.e100798. Available at: http://www.pubmedcentral.nih.gov/articlerender.fcgi?artid=4069160&tool=pmcentrez&rendertype=abstract [Accessed September 10, 2014].

Jochems, J. et al., 2015. Enhancement of Stress Resilience Through Histone Deacetylase 6-Mediated Regulation of Glucocorticoid Receptor Chaperone Dynamics. *Biological psychiatry*, 77(4), pp.345–55. Available at: http://www.ncbi.nlm.nih.gov/pubmed/25442004 [Accessed December 8, 2014].

Jung, S.H. et al., 2015. Molecular mechanisms of repeated social defeat-induced glucocorticoid resistance: Role of microRNA. *Brain, behavior, and immunity*, 44, pp.195–206. Available at: http://www.ncbi.nlm.nih.gov/pubmed/25317829 [Accessed January 12, 2015].

Kaeberlein, T.L. et al., 2006. Lifespan extension in Caenorhabditis elegans by complete removal of food. *Aging cell*, 5(6), pp.487–94. Available at: http://www.ncbi.nlm.nih.gov/pubmed/17081160 [Accessed

January 15, 2016].

Kaiser, E. et al., 2012. FK506-binding protein 51 interacts with Clostridium botulinum C2 toxin and FK506 inhibits membrane translocation of the toxin in mammalian cells. *Cellular microbiology*, 14(8), pp.1193–205. Available at: http://www.ncbi.nlm.nih.gov/pubmed/22420783 [Accessed March 10, 2014].

Kang, C.B. et al., 2008. FKBP family proteins: immunophilins with versatile biological functions. *Neuro-Signals*, 16(4), pp.318–25. Available at: http://www.ncbi.nlm.nih.gov/pubmed/18635947 [Accessed July 24, 2015].

Kapahi, P. et al., 2004. Regulation of lifespan in Drosophila by modulation of genes in the TOR signaling pathway. *Current biology : CB*, 14(10), pp.885–90. Available at: http://www.ncbi.nlm.nih.gov/pubmed/15186745 [Accessed September 21, 2016].

Kaplan, F. et al., 2011. Ascaroside expression in Caenorhabditis elegans is strongly dependent on diet and developmental stage. *PloS one*, 6(3), p.e17804. Available at: http://www.ncbi.nlm.nih.gov/pubmed/21423575 [Accessed October 2, 2016].

Kaplan, F. et al., 2012. Interspecific nematode signals regulate dispersal behavior. *PloS one*, 7(6), p.e38735. Available at: http://www.ncbi.nlm.nih.gov/pubmed/22701701 [Accessed October 4, 2016].

Karagiannides, I. et al., 2001. Altered expression of C/EBP family members results in decreased adipogenesis with aging. *American journal of physiology. Regulatory, integrative and comparative physiology*, 280(6), pp.R1772-80. Available at: http://www.ncbi.nlm.nih.gov/pubmed/11353682 [Accessed November 6, 2013].

Karagiannides, I. et al., 2006. Increased CUG triplet repeat-binding protein-1 predisposes to impaired adipogenesis with aging. *The Journal of biological chemistry*, 281(32), pp.23025–33. Available at: http://www.ncbi.nlm.nih.gov/pubmed/16754681 [Accessed November 6, 2013].

Kawahara, T., Kashiwagi, E., Ide, H., Li, Y., Zheng, Y., Miyamoto, Y., et al., 2015. Cyclosporine A and tacrolimus inhibit bladder cancer growth through down-regulation of NFATc1. *Oncotarget*, 6(3), pp.1582–93. Available at: http://www.ncbi.nlm.nih.gov/pubmed/25638160 [Accessed February 3, 2015].

Kawahara, T. et al., 2016. Cyclosporine A and tacrolimus inhibit urothelial tumorigenesis. *Molecular carcinogenesis*, 55(2), pp.161–9. Available at: http://www.ncbi.nlm.nih.gov/pubmed/25594762 [Accessed February 3, 2015].

Kawahara, T., Kashiwagi, E., Ide, H., Li, Y., Zheng, Y., Ishiguro, H., et al., 2015. The role of NFATc1 in prostate cancer progression: Cyclosporine A and tacrolimus inhibit cell proliferation, migration, and invasion. *The Prostate*, 75(6), pp.573–84. Available at: http://www.ncbi.nlm.nih.gov/pubmed/25631176 [Accessed February 3, 2015].

Kędzierska, K. et al., 2014. Effects of immunosuppressive treatment on protein expression in rat kidney. *Drug design, development and therapy*, 8, pp.1695–708. Available at: http://www.pubmedcentral.nih.gov/articlerender.fcgi?artid=4196885&tool=pmcentrez&rendertype=abstract [Accessed April 2, 2015].

Kenyon, C. et al., 1993. A C. elegans mutant that lives twice as long as wild type. *Nature*, 366(6454), pp.461–4. Available at: http://www.ncbi.nlm.nih.gov/pubmed/8247153 [Accessed October 1, 2016].

Kenyon, C.J., 2010. The genetics of ageing. *Nature*, 464(7288), pp.504–12. Available at: http://www.ncbi.nlm.nih.gov/pubmed/20336132 [Accessed September 20, 2016].

Kim, C.-D. et al., 2010. Metabonomic analysis of serum metabolites in kidney transplant recipients with cyclosporine A- or tacrolimus-based immunosuppression. *Transplantation*, 90(7), pp.748–56. Available at: http://www.ncbi.nlm.nih.gov/pubmed/20842074 [Accessed September 5, 2014].

Kino, T. et al., 1987. FK-506, a novel immunosuppressant isolated from a Streptomyces. I. Fermentation, isolation, and physico-chemical and biological characteristics. *The Journal of antibiotics*, 40(9),

pp.1249–55. Available at: http://www.ncbi.nlm.nih.gov/pubmed/2445721 [Accessed April 1, 2014].

Kirkwood, T.B.L., 1977. Evolution of ageing. *Nature*, 270(5635), pp.301–304. Available at: http://www.nature.com/doifinder/10.1038/270301a0 [Accessed September 20, 2016].

Kitagawa, N. et al., 2003. The role of the presenilin-1 homologue gene sel-12 of Caenorhabditis elegans in apoptotic activities. *The Journal of biological chemistry*, 278(14), pp.12130–4. Available at: http://www.jbc.org/content/278/14/12130.full [Accessed October 28, 2015].

Klass, M.R., 1977. Aging in the nematode Caenorhabditis elegans: major biological and environmental factors influencing life span. *Mechanisms of ageing and development*, 6(6), pp.413–29. Available at: http://www.ncbi.nlm.nih.gov/pubmed/926867 [Accessed October 6, 2016].

Klein, J. et al., 2002. Novel adipocyte lines from brown fat: a model system for the study of differentiation, energy metabolism, and insulin action. *BioEssays : news and reviews in molecular, cellular and developmental biology*, 24(4), pp.382–8. Available at: http://www.ncbi.nlm.nih.gov/pubmed/11948624 [Accessed October 8, 2013].

Klengel, T. et al., 2013. Allele-specific FKBP5 DNA demethylation mediates gene-childhood trauma interactions. *Nature neuroscience*, 16(1), pp.33–41. Available at: http://www.ncbi.nlm.nih.gov/pubmed/23201972 [Accessed November 22, 2013].

Klettner, A. et al., 2001. The neuroprotective actions of FK506 binding protein ligands: neuronal survival is triggered by de novo RNA synthesis, but is independent of inhibition of JNK and calcineurin. *Molecular Brain Research*, 97(1), pp.21–31. Available at: http://www.sciencedirect.com/science/article/pii/S0169328X01002868 [Accessed August 8, 2016].

Kojima, T. et al., 2004. Association analysis between longevity in the Japanese population and polymorphic variants of genes involved in insulin and insulin-like growth factor 1 signaling pathways. *Experimental gerontology*, 39(11–12), pp.1595–8. Available at: http://www.ncbi.nlm.nih.gov/pubmed/15582274 [Accessed September 21, 2016].

Kourtis, N. & Tavernarakis, N., 2011. Cellular stress response pathways and ageing: intricate molecular relationships. *The EMBO journal*, 30(13), pp.2520–31. Available at: http://www.ncbi.nlm.nih.gov/pubmed/21587205 [Accessed October 6, 2016].

Kraemer, B.C. et al., 2006. Molecular pathways that influence human tau-induced pathology in Caenorhabditis elegans. *Human molecular genetics*, 15(9), pp.1483–96. Available at: http://hmg.oxfordjournals.org/content/15/9/1483.full [Accessed February 23, 2015].

Lafontan, M., 2012. Historical perspectives in fat cell biology: the fat cell as a model for the investigation of hormonal and metabolic pathways. *American journal of physiology. Cell physiology*, 302(2), pp.C327-59. Available at: http://www.ncbi.nlm.nih.gov/pubmed/21900692 [Accessed October 8, 2013].

Lakowski, B. & Hekimi, S., 1998. The genetics of caloric restriction in Caenorhabditis elegans. *Proceedings of the National Academy of Sciences of the United States of America*, 95(22), pp.13091–6. Available at: http://www.pubmedcentral.nih.gov/articlerender.fcgi?artid=23719&tool=pmcentrez&rendertype=abstract [Accessed June 11, 2014].

Lamoth, F. et al., 2015. Antifungal activity of compounds targeting the Hsp90-calcineurin pathway against various mould species. *The Journal of antimicrobial chemotherapy*, 70(5), pp.1408–11. Available at: http://www.ncbi.nlm.nih.gov/pubmed/25558076 [Accessed January 7, 2015].

Lapierre, L.R. et al., 2011. Autophagy and lipid metabolism coordinately modulate life span in germline-less C. elegans. *Current biology : CB*, 21(18), pp.1507–14. Available at: http://www.ncbi.nlm.nih.gov/pubmed/21906946 [Accessed January 15, 2014].

Lapointe, J. et al., 2009. Reversal of the mitochondrial phenotype and slow development of oxidative biomarkers of aging in long-lived Mclk1+/- mice. *The Journal of biological chemistry*, 284(30), pp.20364–74. Available at: http://www.ncbi.nlm.nih.gov/pubmed/19478076 [Accessed September 20, 2016].

Laukova, M. et al., 2014. Early intervention with intranasal NPY prevents single prolonged stress-triggered impairments in hypothalamus and ventral hippocampus in male rats. *Endocrinology*, 155(10), pp.3920–33. Available at: http://www.ncbi.nlm.nih.gov/pubmed/25057792 [Accessed December 9, 2014].

Lee, K.Y. et al., 2007. Bmp2 is critical for the murine uterine decidual response. *Molecular and cellular biology*, 27(15), pp.5468–78. Available at: http://mcb.asm.org/content/27/15/5468.long [Accessed July 21, 2015].

Lee, S.-I. et al., 2015. Expression of thymosin beta-4 in human periodontal ligament cells and mouse periodontal tissue and its role in osteoblastic/cementoblastic differentiation. *Differentiation; research in biological diversity*, 90(1–3), pp.16–26. Available at: http://www.sciencedirect.com/science/article/pii/S0301468115000560 [Accessed October 28, 2015].

Lees, H., Walters, H. & Cox, L.S., 2016. Animal and human models to understand ageing. *Maturitas*, 93, pp.18–27. Available at: http://www.ncbi.nlm.nih.gov/pubmed/27372369 [Accessed October 2, 2016].

LeMaster, D.M. et al., 2015. Coupling of Conformational Transitions in the N-terminal Domain of the 51-kDa FK506-binding Protein (FKBP51) Near Its Site of Interaction with the Steroid Receptor Proteins. *The Journal of biological chemistry*, 290(25), pp.15746–57. Available at: http://www.ncbi.nlm.nih.gov/pubmed/25953903 [Accessed July 9, 2015].

Leng, X. et al., 2013. Genome-wide identification and analysis of FK506-binding protein gene family in strawberry (Fragaria×ananassa). *Gene*, 534(2), pp.390–399. Available at: http://www.sciencedirect.com/science/article/pii/S0378111913010998 [Accessed November 21, 2013].

Lessard, J. & Holman, E.A., 2014. FKBP5 and CRHR1 polymorphisms moderate the stress-physical health association in a national sample. *Health psychology : official journal of the Division of Health Psychology, American Psychological Association*, 33(9), pp.1046–56. Available at: http://www.ncbi.nlm.nih.gov/pubmed/24099078 [Accessed January 16, 2015].

Lhoest, G. et al., 1995. The in vitro immunosuppressive activity of the C15-demethylated metabolite of FK-506 is governed by ring- and open-chain tautomerism effects. *The Journal of pharmacology and experimental therapeutics*, 274(2), pp.622–626. Available at: http://jpet.aspetjournals.org/content/274/2/622.long [Accessed September 23, 2016].

Liu, J. et al., 1991. Calcineurin is a common target of cyclophilin-cyclosporin A and FKBP-FK506 complexes. *Cell*, 66(4), pp.807–15. Available at: http://www.ncbi.nlm.nih.gov/pubmed/1715244 [Accessed May 27, 2014].

Liu, Z. et al., 2014. Protein kinase RNA- like endoplasmic reticulum kinase (PERK)/calcineurin signaling is a novel pathway regulating intracellular calcium accumulation which might be involved in ventricular arrhythmias in diabetic cardiomyopathy. *Cellular signalling*, 26(12), pp.2591–2600. Available at: http://www.ncbi.nlm.nih.gov/pubmed/25152364 [Accessed August 26, 2014].

Lopez, E. et al., 2015. FKBP25 and FKBP38 regulate non-capacitative calcium entry through TRPC6. *Biochimica et biophysica acta*, 1853(10 Pt A), pp.2684–96. Available at: http://www.ncbi.nlm.nih.gov/pubmed/26239116 [Accessed October 26, 2015].

Love, M.I., Huber, W. & Anders, S., 2014. Moderated estimation of fold change and dispersion for RNA-seq data with DESeq2. *Genome biology*, 15(12), p.550. Available at: http://www.ncbi.nlm.nih.gov/pubmed/25516281 [Accessed October 5, 2016].

Lublin, A. et al., 2011. FDA-approved drugs that protect mammalian neurons from glucose toxicity slow aging dependent on cbp and protect against proteotoxicity. *PloS one*, 6(11), p.e27762. Available at: http://www.pubmedcentral.nih.gov/articlerender.fcgi?artid=3218048&tool=pmcentrez&rendertype=abstract [Accessed January 15, 2016].

Lucanic, M., Lithgow, G.J. & Alavez, S., 2013. Pharmacological lifespan extension of invertebrates. *Ageing research reviews*, 12(1), pp.445–58. Available at:

http://www.pubmedcentral.nih.gov/articlerender.fcgi?artid=3552093&tool=pmcentrez&rendertype=abstract [Accessed January 15, 2014].

Ludewig, A.H., Klapper, M. & Döring, F., 2014. Identifying evolutionarily conserved genes in the dietary restriction response using bioinformatics and subsequent testing in Caenorhabditis elegans. *Genes & nutrition*, 9(1), p.363. Available at: http://www.pubmedcentral.nih.gov/articlerender.fcgi?artid=3896620&tool=pmcentrez&rendertype=abstract [Accessed September 10, 2014].

Lukic, I. et al., 2014. Accumulation of Cytoplasmic Glucocorticoid Receptor Is Related to Elevation of FKBP5 in Lymphocytes of Depressed Patients. *Journal of molecular neuroscience : MN*, 55(4), pp.951–8. Available at: http://www.ncbi.nlm.nih.gov/pubmed/25355489 [Accessed January 16, 2015].

Ma, T. et al., 2014. PERK: a novel therapeutic target for neurodegenerative diseases? *Alzheimer's Research & Therapy*, 6(3), p.30. Available at: http://alzres.biomedcentral.com/articles/10.1186/alzrt260 [Accessed October 5, 2016].

MacDonald, C.A. & Boyd, R.J., 2015. Computational insights into the suicide inhibition of Plasmodium falciparum Fk506-binding protein 35. *Bioorganic & Medicinal Chemistry Letters*, 25(16), pp.3221–5. Available at: http://www.ncbi.nlm.nih.gov/pubmed/26091727 [Accessed June 20, 2015].

Madeo, F., Tavernarakis, N. & Kroemer, G., 2010. Can autophagy promote longevity? *Nature cell biology*, 12(9), pp.842–6. Available at: http://dx.doi.org/10.1038/ncb0910-842 [Accessed October 9, 2014].

Malat, G.E. et al., 2002. Tacrolimus-induced pain syndrome in a pediatric orthotopic liver transplant patient. *Pediatric transplantation*, 6(5), pp.435–8. Available at: http://www.ncbi.nlm.nih.gov/pubmed/12390434 [Accessed July 31, 2013].

Martinez, N.J. et al., 2013. The co-chaperones Fkbp4/5 control Argonaute2 expression and facilitate RISC assembly. *RNA (New York, N.Y.)*, 19(11), pp.1583–93. Available at: http://www.ncbi.nlm.nih.gov/pubmed/24049110 [Accessed November 11, 2013].

Matsuda, S. et al., 2000. Two distinct action mechanisms of immunophilin-ligand complexes for the blockade of T-cell activation. *EMBO reports*, 1(5), pp.428–34. Available at: http://www.pubmedcentral.nih.gov/articlerender.fcgi?artid=1083763&tool=pmcentrez&rendertype=abstract.

McColl, G. et al., 2008. Pharmacogenetic analysis of lithium-induced delayed aging in Caenorhabditis elegans. *Journal of Biological Chemistry*, 283(1), pp.350–357. Available at: http://www.jbc.org/content/283/1/350.long.

Medawar, P.B., 1952. An unsolved problem of biology. *Evolution in Health and Disease*, p.24.

Mi, H. et al., 2016. PANTHER version 10: expanded protein families and functions, and analysis tools. *Nucleic acids research*, 44(D1), pp.D336-42. Available at: http://www.ncbi.nlm.nih.gov/pubmed/26578592 [Accessed September 11, 2016].

Mi, H. & Thomas, P., 2009. *Protein Networks and Pathway Analysis* Y. Nikolsky & J. Bryant, eds., Totowa, NJ: Humana Press. Available at: http://link.springer.com/10.1007/978-1-60761-175-2 [Accessed September 11, 2016].

Mikkelsen, T.S. et al., 2010. Comparative epigenomic analysis of murine and human adipogenesis. *Cell*, 143(1), pp.156–69. Available at: http://www.pubmedcentral.nih.gov/articlerender.fcgi?artid=2950833&tool=pmcentrez&rendertype=abstract [Accessed September 20, 2013].

Mitchell, D.H. et al., 1979. Synchronous growth and aging of Caenorhabditis elegans in the presence of fluorodeoxyuridine. *Journal of gerontology*, 34(1), pp.28–36. Available at: http://www.ncbi.nlm.nih.gov/pubmed/153363 [Accessed September 27, 2016].

Miyata, S., Ohkubo, Y. & Mutoh, S., 2005. A review of the action of tacrolimus (FK506) on experimental models of rheumatoid arthritis. *Inflammation research : official journal of the European Histamine*

Research Society ... [et al.], 54(1), pp.1–9. Available at: http://www.ncbi.nlm.nih.gov/pubmed/15723198 [Accessed August 14, 2016].

Molla Kazemiha, V. et al., 2009. PCR-based detection and eradication of mycoplasmal infections from various mammalian cell lines: a local experience. *Cytotechnology*, 61(3), pp.117–24. Available at: http://www.pubmedcentral.nih.gov/articlerender.fcgi?artid=2825298&tool=pmcentrez&rendertype=abstract [Accessed May 5, 2015].

Monneau, Y.R. et al., 2013. Structure and activity of the peptidyl-prolyl isomerase domain from the histone chaperone Fpr4 toward histone H3 proline isomerization. *The Journal of biological chemistry*, 288(36), pp.25826–37. Available at: http://www.ncbi.nlm.nih.gov/pubmed/23888048 [Accessed November 21, 2013].

Morselli, E. et al., 2011. Spermidine and resveratrol induce autophagy by distinct pathways converging on the acetylproteome. *Journal of Cell Biology*, 192(4), pp.615–629. Available at: http://jcb.rupress.org/content/192/4/615.long.

Mustafi, S.M. et al., 2013. Analysing the visible conformational substates of the FK506-binding protein FKBP12. *The Biochemical journal*, 453(3), pp.371–80. Available at: http://www.pubmedcentral.nih.gov/articlerender.fcgi?artid=3727217&tool=pmcentrez&rendertype=abstract [Accessed November 21, 2013].

Nakagaki, T. et al., 2013. FK506 reduces abnormal prion protein through the activation of autolysosomal degradation and prolongs survival in prion-infected mice. *Autophagy*, 9(9), pp.1386–94. Available at: http://www.ncbi.nlm.nih.gov/pubmed/23800841.

Nakata, Y. et al., 2000. Tacrolimus and myocardial hypertrophy. *Transplantation*, 69(9), pp.1960–2. Available at: http://www.ncbi.nlm.nih.gov/pubmed/10830241 [Accessed August 1, 2013].

Nath, P.R. & Isakov, N., 2015. Insights into peptidyl-prolyl cis – trans isomerase structure and function in immunocytes. *Immunology Letters*, 163(1), pp.120–131. Available at: http://dx.doi.org/10.1016/j.imlet.2014.11.002.

Neal, J.W. & Clipstone, N. a, 2002. Calcineurin mediates the calcium-dependent inhibition of adipocyte differentiation in 3T3-L1 cells. *The Journal of biological chemistry*, 277(51), pp.49776–81. Available at: http://www.ncbi.nlm.nih.gov/pubmed/12351639 [Accessed February 14, 2014].

Nedelcovych, M.T. et al., 2015. A Rodent Model of Traumatic Stress Induces Lasting Sleep and Quantitative Electroencephalographic Disturbances. *ACS chemical neuroscience*, 6(3), pp.485–93. Available at: http://www.ncbi.nlm.nih.gov/pubmed/25581551 [Accessed February 3, 2015].

Nishimura, M. et al., 2002. Tacrolimus-induced life-threatening arrhythmia in a pediatric liver-transplant patient. *Intensive care medicine*, 28(11), pp.1683–4. Available at: http://www.ncbi.nlm.nih.gov/pubmed/12583382 [Accessed July 31, 2013].

Niu, X.-W. et al., 2013. The Fusarium Graminearum virulence factor FGL targets an FKBP12 immunophilin of wheat. *Gene*, 525(1), pp.77–83. Available at: http://www.ncbi.nlm.nih.gov/pubmed/23648486 [Accessed November 19, 2013].

Nomoto, S. et al., 1994. Cardiotoxicity of long-term intravenous administration of FK506 in rabbits: dose relationship and recovery after discontinuance. *Transplantation proceedings*, 26(2), pp.855–7. Available at: http://www.ncbi.nlm.nih.gov/pubmed/7513477 [Accessed August 1, 2013].

Norris, C.. et al., 2002. Calcineurin enhances L-type Ca2+ channel activity in hippocampal neurons: increased effect with age in culture. *Neuroscience*, 110(2), pp.213–225. Available at: http://www.sciencedirect.com/science/article/pii/S0306452201005747 [Accessed September 23, 2015].

Norris, C.M. et al., 2010. Hippocampal “zipper” slice studies reveal a necessary role for calcineurin in the increased activity of L-type Ca(2+) channels with aging. *Neurobiology of aging*, 31(2), pp.328–38. Available at: http://www.sciencedirect.com/science/article/pii/S0197458008001073 [Accessed

September 23, 2015].

Ogg, S. et al., 1997. The Fork head transcription factor DAF-16 transduces insulin-like metabolic and longevity signals in C. elegans. *Nature*, 389(6654), pp.994–9. Available at: http://www.ncbi.nlm.nih.gov/pubmed/9353126 [Accessed September 28, 2016].

Oliver, M.H. et al., 1989. A rapid and convenient assay for counting cells cultured in microwell plates: application for assessment of growth factors. *Journal of cell science*, (92), pp.513–518. Available at: http://citeseerx.ist.psu.edu/viewdoc/download?doi=10.1.1.326.2853&rep=rep1&type=pdf [Accessed March 23, 2015].

Ostrow, K.L. et al., 2009. Pharmacologic unmasking of epigenetically silenced genes in breast cancer. *Clinical cancer research : an official journal of the American Association for Cancer Research*, 15(4), pp.1184–91. Available at: http://www.pubmedcentral.nih.gov/articlerender.fcgi?artid=3082476&tool=pmcentrez&rendertype=abstract [Accessed April 26, 2015].

Owens, M. et al., 2015. Eye tracking indices of attentional bias in children of depressed mothers: Polygenic influences help to clarify previous mixed findings. *Development and psychopathology*, pp.1–13. Available at: http://www.ncbi.nlm.nih.gov/pubmed/26030911 [Accessed July 22, 2015].

Palumbo, C. et al., 2016. c-Jun N-terminal kinase activation by nitrobenzoxadiazoles leads to late-stage autophagy inhibition. *Journal of translational medicine*, 14, p.37. Available at: http://www.ncbi.nlm.nih.gov/pubmed/26847645 [Accessed October 4, 2016].

Pare, J.M., LaPointe, P. & Hobman, T.C., 2013. Hsp90 cochaperones p23 and FKBP4 physically interact with hAgo2 and activate RNA interference-mediated silencing in mammalian cells. *Molecular biology of the cell*, 24(15), pp.2303–10. Available at: http://www.pubmedcentral.nih.gov/articlerender.fcgi?artid=3727923&tool=pmcentrez&rendertype=abstract [Accessed March 10, 2014].

Park, H.-J. et al., 2015. The Cooperation of CREB and NFAT Is Required for PTHrP-Induced RANKL Expression in Mouse Osteoblastic Cells. *Journal of cellular physiology*, 230(3), pp.667–79. Available at: http://www.ncbi.nlm.nih.gov/pubmed/25187507 [Accessed January 7, 2015].

Pawlikowska, L. et al., 2009. Association of common genetic variation in the insulin/IGF1 signaling pathway with human longevity. *Aging cell*, 8(4), pp.460–72. Available at: http://www.ncbi.nlm.nih.gov/pubmed/19489743 [Accessed September 21, 2016].

Peng, L. et al., 2014. The calcineurin inhibitor tacrolimus reduces proteinuria in membranous nephropathy accompanied by a decrease in angiopoietin-like-4. *PloS one*, 9(8), p.e106164. Available at: http://www.pubmedcentral.nih.gov/articlerender.fcgi?artid=4148427&tool=pmcentrez&rendertype=abstract [Accessed September 5, 2014].

Pereira, M.J. et al., 2014. FKBP5 expression in human adipose tissue increases following dexamethasone exposure and is associated with insulin resistance. *Metabolism*, 63(9), pp.1198–1208. Available at: http://www.ncbi.nlm.nih.gov/pubmed/24997500 [Accessed March 12, 2015].

Pereira, M.J. et al., 2013. The immunosuppressive agents rapamycin, cyclosporin A and tacrolimus increase lipolysis, inhibit lipid storage and alter expression of genes involved in lipid metabolism in human adipose tissue. *Molecular and cellular endocrinology*, 365(2), pp.260–9. Available at: http://www.ncbi.nlm.nih.gov/pubmed/23160140 [Accessed March 12, 2015].

Perrea, D.N. et al., 2008. Correlation between lipid abnormalities and immunosuppressive therapy in renal transplant recipients with stable renal function. *International urology and nephrology*, 40(2), pp.521–7. Available at: http://www.ncbi.nlm.nih.gov/pubmed/17978855 [Accessed January 4, 2016].

Pfluger, P.T. et al., 2015. Calcineurin Links Mitochondrial Elongation with Energy Metabolism. *Cell metabolism*, 22(5), pp.838–50. Available at: http://www.cell.com/article/S1550413115004556/fulltext [Accessed March 15, 2016].

Pinton, P. et al., 2007. Protein kinase C beta and prolyl isomerase 1 regulate mitochondrial effects of the life-span determinant p66Shc. *Science (New York, N.Y.)*, 315(5812), pp.659–63. Available at: http://www.ncbi.nlm.nih.gov/pubmed/17272725 [Accessed September 20, 2016].

Qiu, Z. et al., 2001. DNA synthesis and mitotic clonal expansion is not a required step for 3T3-L1 preadipocyte differentiation into adipocytes. *The Journal of biological chemistry*, 276(15), pp.11988–95. Available at: http://www.ncbi.nlm.nih.gov/pubmed/11278974 [Accessed October 5, 2016].

Rajan, S., Baek, K. & Yoon, H.S., 2013. C-H…O hydrogen bonds in FK506-binding protein-ligand interactions. *Journal of molecular recognition : JMR*, 26(11), pp.550–5. Available at: http://www.ncbi.nlm.nih.gov/pubmed/24089362 [Accessed November 21, 2013].

Rangaraju, S. et al., 2015. Suppression of transcriptional drift extends C. elegans lifespan by postponing the onset of mortality. *eLife*, 4, p.e08833. Available at: http://elifesciences.org/content/4/e08833.abstract [Accessed December 2, 2015].

Raught, B., Gingras, A.C. & Sonenberg, N., 2001. The target of rapamycin (TOR) proteins. *Proceedings of the National Academy of Sciences of the United States of America*, 98(13), pp.7037–44. Available at: http://www.ncbi.nlm.nih.gov/pubmed/11416184 [Accessed October 1, 2016].

Richardson, J.M. et al., 2007. Cloning, expression and characterisation of FKB-6, the sole large TPR-containing immunophilin from C. elegans. *Biochemical and biophysical research communications*, 360(3), pp.566–72. Available at: http://www.sciencedirect.com/science/article/pii/S0006291X07012946 [Accessed March 23, 2016].

Riddle, D.L., Swanson, M.M. & Albert, P.S., 1981. Interacting genes in nematode dauer larva formation. *Nature*, 290(5808), pp.668–71. Available at: http://www.ncbi.nlm.nih.gov/pubmed/7219552 [Accessed October 4, 2016].

Riddle, E.S., Stipanuk, M.H. & Thalacker-Mercer, A.E., 2016. Amino acids in healthy aging skeletal muscle. *Frontiers in bioscience (Elite edition)*, 8, pp.326–50. Available at: http://www.ncbi.nlm.nih.gov/pubmed/26709665 [Accessed September 28, 2016].

Rider, M.A. et al., 2013. Quantitative proteomic analysis of the Anopheles gambiae (Diptera: Culicidae) midgut infected with o'nyong-nyong virus. *Journal of medical entomology*, 50(5), pp.1077–88. Available at: http://www.ncbi.nlm.nih.gov/pubmed/24180113 [Accessed November 21, 2013].

Riggs, D.L. et al., 2007. Noncatalytic role of the FKBP52 peptidyl-prolyl isomerase domain in the regulation of steroid hormone signaling. *Molecular and cellular biology*, 27(24), pp.8658–69. Available at: http://www.ncbi.nlm.nih.gov/pubmed/17938211 [Accessed October 4, 2016].

Ro, S.-H. et al., 2013. Distinct functions of Ulk1 and Ulk2 in the regulation of lipid metabolism in adipocytes. *Autophagy*, 9(12). Available at: http://www.ncbi.nlm.nih.gov/pubmed/24135897 [Accessed October 30, 2013].

Rogina, B. & Helfand, S.L., 2004. Sir2 mediates longevity in the fly through a pathway related to calorie restriction. *Proceedings of the National Academy of Sciences of the United States of America*, 101(45), pp.15998–6003. Available at: http://www.ncbi.nlm.nih.gov/pubmed/15520384 [Accessed September 21, 2016].

Romano, S., D'Angelillo, A. & Romano, M.F., 2015. Pleiotropic roles in cancer biology for multifaceted proteins FKBPs. *Biochimica et Biophysica Acta (BBA) - General Subjects*, 1850(10), pp.2061–8. Available at: http://linkinghub.elsevier.com/retrieve/pii/S0304416515000239.

Rosen, E.D. et al., 1999. PPARγ Is Required for the Differentiation of Adipose Tissue In Vivo and In Vitro. *Molecular Cell*, 4(4), pp.611–617. Available at: http://www.sciencedirect.com/science/article/pii/S1097276500802117 [Accessed November 6, 2013].

Rosen, E.D. et al., 2000. Transcriptional regulation of adipogenesis. *Genes & development*, 14(11), pp.1293–307. Available at: http://www.ncbi.nlm.nih.gov/pubmed/10837022 [Accessed October 29, 2013].

Rosen, E.D. & MacDougald, O.A., 2006. Adipocyte differentiation from the inside out. *Nature reviews. Molecular cell biology*, 7(12), pp.885–96. Available at: http://www.ncbi.nlm.nih.gov/pubmed/17139329 [Accessed September 25, 2013].

Rossetto, A.M. et al., 2015. The full electron structure of the FKBP12/FK506 complex. *Journal of biomolecular structure & dynamics*, 33(2), pp.388–94. Available at: http://www.ncbi.nlm.nih.gov/pubmed/24471694 [Accessed January 7, 2015].

Sabbagh, J.J. et al., 2014. Age-Associated Epigenetic Upregulation of the FKBP5 Gene Selectively Impairs Stress Resiliency. T. Yoshikawa, ed. *PloS one*, 9(9), p.e107241. Available at: http://dx.plos.org/10.1371/journal.pone.0107241 [Accessed September 10, 2014].

Saita, S. et al., 2014. Role of the ANKMY2-FKBP38 axis in regulation of the Sonic hedgehog (Shh) signaling pathway. *The Journal of biological chemistry*, 289(37), pp.25639–54. Available at: http://www.ncbi.nlm.nih.gov/pubmed/25077969 [Accessed January 7, 2015].

Salminen, A. et al., 2013. Impaired autophagy and APP processing in Alzheimer's disease: The potential role of Beclin 1 interactome. *Progress in Neurobiology*, 106, pp.33–54. Available at: http://www.sciencedirect.com/science/article/pii/S0301008213000518 [Accessed November 21, 2013].

Samokhvalov, V., Scott, B.A. & Crowder, C.M., 2008. Autophagy protects against hypoxic injury in C. elegans. *Autophagy*, 4(8), pp.1034–41. Available at: http://www.pubmedcentral.nih.gov/articlerender.fcgi?artid=3670992&tool=pmcentrez&rendertype=abstract [Accessed March 17, 2016].

Sanchez, E.R., 2012. Chaperoning steroidal physiology: lessons from mouse genetic models of Hsp90 and its cochaperones. *Biochimica et biophysica acta*, 1823(3), pp.722–9. Available at: http://www.sciencedirect.com/science/article/pii/S0167488911003089 [Accessed October 23, 2014].

Selman, C. et al., 2008. Evidence for lifespan extension and delayed age-related biomarkers in insulin receptor substrate 1 null mice. *FASEB journal : official publication of the Federation of American Societies for Experimental Biology*, 22(3), pp.807–18. Available at: http://www.ncbi.nlm.nih.gov/pubmed/17928362 [Accessed December 3, 2014].

Selman, C. et al., 2009. Ribosomal protein S6 kinase 1 signaling regulates mammalian life span. *Science (New York, N.Y.)*, 326(5949), pp.140–4. Available at: http://www.ncbi.nlm.nih.gov/pubmed/19797661 [Accessed September 22, 2013].

Seo, K. et al., 2013. Heat shock factor 1 mediates the longevity conferred by inhibition of TOR and insulin/IGF-1 signaling pathways in C. elegans. *Aging cell*, 12(6), pp.1073–81. Available at: http://www.ncbi.nlm.nih.gov/pubmed/23879233 [Accessed November 24, 2015].

Spiekerkoetter, E. et al., 2013. FK506 activates BMPR2, rescues endothelial dysfunction, and reverses pulmonary hypertension. *The Journal of clinical investigation*, 123(8), pp.3600–13. Available at: http://www.pubmedcentral.nih.gov/articlerender.fcgi?artid=3726153&tool=pmcentrez&rendertype=abstract [Accessed November 21, 2013].

Srinivasan, J. et al., 2012. A modular library of small molecule signals regulates social behaviors in Caenorhabditis elegans. *PLoS biology*, 10(1), p.e1001237. Available at: http://journals.plos.org/plosbiology/article?id=10.1371/journal.pbio.1001237#s4 [Accessed January 7, 2015].

Srinivasan, S. et al., 2008. Serotonin regulates C. elegans fat and feeding through independent molecular mechanisms. *Cell metabolism*, 7(6), pp.533–44. Available at: http://www.ncbi.nlm.nih.gov/pubmed/18522834 [Accessed September 30, 2016].

Stechschulte, L.A. et al., 2014. FKBP51 controls cellular adipogenesis through p38 kinase-mediated phosphorylation of GRα and PPARγ. *Molecular endocrinology (Baltimore, Md.)*, 28(8), pp.1265–75. Available at: http://www.pubmedcentral.nih.gov/articlerender.fcgi?artid=4116587&tool=pmcentrez&rendertype=

abstract [Accessed August 24, 2015].

Stechschulte, L. a et al., 2014. FKBP51 controls cellular adipogenesis through p38 kinase-mediated phosphorylation of GRα and PPARγ. *Molecular endocrinology (Baltimore, Md.)*, 28(8), pp.1265–75. Available at: http://www.ncbi.nlm.nih.gov/pubmed/24933247 [Accessed January 14, 2015].

Subasranjan, A., Srinivasulu, C. & Hemant, R., 2010. An improved validated ultra high pressure liquid chromatography method for separation of tacrolimus impurities and its tautomers Acharya Subasranjan , a , b ∗ Srinivasulu C a and Raoutray Hemant b. *Drug Test. Analysis*, 2(3), pp.107–112. Available at: http://onlinelibrary.wiley.com/doi/10.1002/dta.112/abstract [Accessed September 23, 2016].

Suh, Y. et al., 2008. Functionally significant insulin-like growth factor I receptor mutations in centenarians. *Proceedings of the National Academy of Sciences of the United States of America*, 105(9), pp.3438–42. Available at: http://www.ncbi.nlm.nih.gov/pubmed/18316725 [Accessed September 21, 2016].

Sulistio, Y.A. & Heese, K., 2015. The Ubiquitin-Proteasome System and Molecular Chaperone Deregulation in Alzheimer's Disease. *Molecular neurobiology*, 53(2), pp.905–31. Available at: http://www.ncbi.nlm.nih.gov/pubmed/25561438 [Accessed January 8, 2015].

Sutphin, G.L. et al., 2012. Caffeine extends life span, improves healthspan, and delays age-associated pathology in Caenorhabditis elegans. *Longevity & Healthspan*, 1(1), p.9. Available at: http://www.longevityandhealthspan.com/content/1/1/9 [Accessed January 6, 2016].

Suzuki, A. et al., 2014. Relationship of the FKBP5 C/T polymorphism with dysfunctional attitudes predisposing to depression. *Comprehensive psychiatry*, 55(6), pp.1422–5. Available at: http://www.ncbi.nlm.nih.gov/pubmed/24889341 [Accessed January 16, 2015].

Sze, J.Y. et al., 2000. Food and metabolic signalling defects in a Caenorhabditis elegans serotonin-synthesis mutant. *Nature*, 403(6769), pp.560–564. Available at: http://www.ncbi.nlm.nih.gov/pubmed/10676966.

Takahashi, K. et al., 2009. Regulation of IL-2 production in Jurkat cells by Dictyostelium-derived factors. *Life sciences*, 85(11–12), pp.438–43. Available at: http://www.ncbi.nlm.nih.gov/pubmed/19632244 [Accessed February 19, 2014].

Takauji, Y. et al., 2016. Restriction of protein synthesis abolishes senescence features at cellular and organismal levels. *Scientific reports*, 6(January), p.18722. Available at: https://www.ncbi.nlm.nih.gov/pubmed/26729469.

Tam, Z.Y. et al., 2014. Effects of lithium on age-related decline in mitochondrial turnover and function in caenorhabditis elegans. *Journals of Gerontology - Series A Biological Sciences and Medical Sciences*, 69(7), pp.810–820. Available at: http://biomedgerontology.oxfordjournals.org/content/69/7/810.long.

Tamori, Y. et al., 2002. Role of peroxisome proliferator-activated receptor-gamma in maintenance of the characteristics of mature 3T3-L1 adipocytes. *Diabetes*, 51(7), pp.2045–55. Available at: http://www.ncbi.nlm.nih.gov/pubmed/12086932 [Accessed November 6, 2013].

Tao, L. et al., 2013. CAMKII and calcineurin regulate the lifespan of Caenorhabditis elegans through the FOXO transcription factor DAF-16. *eLife*, 2, p.e00518. Available at: http://www.pubmedcentral.nih.gov/articlerender.fcgi?artid=3691573&tool=pmcentrez&rendertype=abstract [Accessed July 1, 2015].

Thomson, A.W., Bonham, C.A. & Zeevi, A., 1995. Mode of action of tacrolimus (FK506): molecular and cellular mechanisms. *Therapeutic drug monitoring*, 17(6), pp.584–91. Available at: http://www.ncbi.nlm.nih.gov/pubmed/8588225 [Accessed November 21, 2013].

Tian, L. et al., 2009. Imaging neural activity in worms, flies and mice with improved GCaMP calcium indicators. *Nature methods*, 6(12), pp.875–81. Available at: http://www.ncbi.nlm.nih.gov/pubmed/19898485 [Accessed October 5, 2016].

Timischl, B. et al., 2008. Development of a quantitative, validated Capillary electrophoresis-time of flight-mass spectrometry method with integrated high-confidence analyte identification for metabolomics. *Electrophoresis*, 29(10), pp.2203–2214. Available at: http://onlinelibrary.wiley.com/doi/10.1002/elps.200700517/abstract.

Tokunaga, M. et al., 2013. Hereditary spastic paraplegia protein spartin is an FK506-binding protein identified by mRNA display. *Chemistry and Biology*, 20(7), pp.935–942. Available at: http://dx.doi.org/10.1016/j.chembiol.2013.05.011.

Toneatto, J. et al., 2013. Dynamic mitochondrial-nuclear redistribution of the immunophilin FKBP51 is regulated by PKA signaling pathway to control gene expression in the process of adipocyte differentiation. *Journal of cell science*, 126(Pt 23), pp.5357–68. Available at: http://www.ncbi.nlm.nih.gov/pubmed/24101724 [Accessed October 30, 2013].

Tong, Y. & Song, F., 2015. Intracellular calcium signaling regulates autophagy via calcineurin-mediated TFEB dephosphorylation. *Autophagy*, 11(7), pp.1192–5. Available at: http://www.ncbi.nlm.nih.gov/pubmed/26043755 [Accessed October 4, 2016].

Tozzi, L. et al., 2015. Single-Nucleotide Polymorphism of the FKBP5 Gene and Childhood Maltreatment as Predictors of Structural Changes in Brain Areas Involved in Emotional Processing in Depression. *Neuropsychopharmacology : official publication of the American College of Neuropsychopharmacology*, 41(2), pp.487–97. Available at: http://www.ncbi.nlm.nih.gov/pubmed/26076833 [Accessed July 22, 2015].

Turska-Kmieć, A. et al., 2007. Reversal of tacrolimus-related hypertrophic cardiomyopathy after conversion to rapamycin in a pediatric liver transplant recipient. *Pediatric transplantation*, 11(3), pp.319–23. Available at: http://www.ncbi.nlm.nih.gov/pubmed/17430490 [Accessed July 31, 2013].

Ünal, C.M. & Steinert, M., 2015. FKBPs in bacterial infections. *Biochimica et Biophysica Acta (BBA) - General Subjects*, 1850(10), pp.2096–2102. Available at: http://www.sciencedirect.com/science/article/pii/S0304416514004267 [Accessed August 23, 2016].

Vafadari, R. et al., 2012. Inhibitory effect of tacrolimus on p38 mitogen-activated protein kinase signaling in kidney transplant recipients measured by whole-blood phosphospecific flow cytometry. *Transplantation*, 93(12), pp.1245–51. Available at: http://www.ncbi.nlm.nih.gov/pubmed/22643331 [Accessed November 21, 2013].

Vallejo, J. et al., 2016. Cellular and Physiological Effects of Dietary Supplementation with β-Hydroxy-β-Methylbutyrate (HMB) and β-Alanine in Late Middle-Aged Mice. *PloS one*, 11(3), p.e0150066. Available at: http://www.ncbi.nlm.nih.gov/pubmed/26953693 [Accessed September 28, 2016].

Wallemacq, P.E. & Reding, R., 1993. FK506 (tacrolimus), a novel immunosuppressant in organ transplantation: clinical, biomedical, and analytical aspects. *Clinical chemistry*, 39(11 Pt 1), pp.2219–28. Available at: http://www.pubmedcentral.nih.gov/articlerender.fcgi?artid=2978067&tool=pmcentrez&rendertype=abstract [Accessed April 4, 2014].

Wang, C. et al., 2009. DNA damage response and cellular senescence in tissues of aging mice. *Aging cell*, 8(3), pp.311–23. Available at: http://www.ncbi.nlm.nih.gov/pubmed/19627270 [Accessed September 21, 2016].

Wang, M.C., O'Rourke, E.J. & Ruvkun, G., 2008. Fat metabolism links germline stem cells and longevity in C. elegans. *Science (New York, N.Y.)*, 322(5903), pp.957–60. Available at: http://www.ncbi.nlm.nih.gov/pubmed/18988854 [Accessed October 4, 2016].

Wang, Y. et al., 2013. Increasing the efficiency of ligands for FK506-binding protein 51 by conformational control. *Journal of medicinal chemistry*, 56(10), pp.3922–35. Available at: http://www.ncbi.nlm.nih.gov/pubmed/23647266 [Accessed November 21, 2013].

Wang, Y. et al., 2009. Understanding the mechanism of the dormant dauer formation of C. elegans: from genetics to biochemistry. *IUBMB life*, 61(6), pp.607–12. Available at:

http://www.ncbi.nlm.nih.gov/pubmed/19472183 [Accessed October 4, 2016].

Warrier, M. et al., 2010. Susceptibility to diet-induced hepatic steatosis and glucocorticoid resistance in FK506-binding protein 52-deficient mice. *Endocrinology*, 151(7), pp.3225–36. Available at: http://www.pubmedcentral.nih.gov/articlerender.fcgi?artid=2903936&tool=pmcentrez&rendertype=abstract [Accessed May 6, 2015].

Watanabe, H. et al., 2010. Peripheral serotonin enhances lipid metabolism by accelerating bile acid turnover. *Endocrinology*, 151(10), pp.4776–86. Available at: http://www.ncbi.nlm.nih.gov/pubmed/20685881 [Accessed September 28, 2016].

Wei, Y. et al., 2008. JNK1-mediated phosphorylation of Bcl-2 regulates starvation-induced autophagy. *Molecular cell*, 30(6), pp.678–88. Available at: http://www.ncbi.nlm.nih.gov/pubmed/18570871 [Accessed October 4, 2016].

Weismann, A. et al., 1891. *Essays upon heredity and kindred biological problems* 2d ed., Oxford,: Clarendon Press,. Available at: http://www.biodiversitylibrary.org/bibliography/28066 [Accessed September 20, 2016].

Wilker, S. et al., 2014. The role of FKBP5 genotype in moderating long-term effectiveness of exposure-based psychotherapy for posttraumatic stress disorder. *Translational psychiatry*, 4, p.e403. Available at: http://www.pubmedcentral.nih.gov/articlerender.fcgi?artid=4080328&tool=pmcentrez&rendertype=abstract [Accessed January 14, 2015].

Williams, G.C., 1957. Pleiotropy, Natural Selection, and the Evolution of Senescence. *Evolution*, 11(4), pp.398–411. Available at: http://www.jstor.org/stable/2406060?__redirected [Accessed June 12, 2014].

Winter, A.D. et al., 2007. Loss of secretory pathway FK506-binding proteins results in cold-sensitive lethality and associate extracellular matrix defects in the nematode Caenorhabditis elegans. *The Journal of biological chemistry*, 282(17), pp.12813–21. Available at: http://www.jbc.org/content/282/17/12813.long [Accessed June 12, 2015].

WormBook, WormBook. Available at: http://www.wormbook.org/.

Xiao, J. et al., 2007. Removal of FKBP12.6 does not alter the conductance and activation of the cardiac ryanodine receptor or the susceptibility to stress-induced ventricular arrhythmias. *The Journal of biological chemistry*, 282(48), pp.34828–38. Available at: http://www.pubmedcentral.nih.gov/articlerender.fcgi?artid=2760432&tool=pmcentrez&rendertype=abstract [Accessed May 6, 2015].

Xu, K., Tavernarakis, N. & Driscoll, M., 2001. Necrotic Cell Death in C. elegans Requires the Function of Calreticulin and Regulators of Ca2+ Release from the Endoplasmic Reticulum. *Neuron*, 31(6), pp.957–971. Available at: http://www.sciencedirect.com/science/article/pii/S0896627301004329 [Accessed March 10, 2016].

Yang, J.S. et al., 2011. OASIS: Online application for the survival analysis of lifespan assays performed in aging research. *PLoS ONE*, 6(8), p.e23525. Available at: http://journals.plos.org/plosone/article?id=10.1371/journal.pone.0023525.

Yang, R.K. et al., 2003. Dose-dependent effects of FK506 on neuroregeneration in a rat model. *Plastic and reconstructive surgery*, 112(7), pp.1832–40. Available at: http://www.ncbi.nlm.nih.gov/pubmed/14663227 [Accessed December 2, 2013].

Yang, Y. et al., 2015. Inhibition of the mevalonate pathway ameliorates anoxia-induced down-regulation of FKBP12.6 and intracellular calcium handling dysfunction in H9c2 cells. *Journal of molecular and cellular cardiology*, 80, pp.166–74. Available at: http://www.ncbi.nlm.nih.gov/pubmed/25636197 [Accessed February 3, 2015].

Yeh, W.C., Li, T.K., et al., 1995. Identification and characterization of an immunophilin expressed during the

clonal expansion phase of adipocyte differentiation. *Proceedings of the National Academy of Sciences of the United States of America*, 92(24), pp.11081–5. Available at: http://www.pubmedcentral.nih.gov/articlerender.fcgi?artid=40575&tool=pmcentrez&rendertype=abstract [Accessed February 19, 2014].

Yeh, W.C., Bierer, B.E. & McKnight, S.L., 1995. Rapamycin inhibits clonal expansion and adipogenic differentiation of 3T3-L1 cells. *Proceedings of the National Academy of Sciences of the United States of America*, 92(24), pp.11086–90. Available at: http://www.pubmedcentral.nih.gov/articlerender.fcgi?artid=40576&tool=pmcentrez&rendertype=abstract.

Yehuda, R. et al., 2015. Holocaust exposure induced intergenerational effects on FKBP5 methylation. *Biological Psychiatry*, 80(5), pp.372–80. Available at: http://www.ncbi.nlm.nih.gov/pubmed/26410355 [Accessed August 17, 2015].

Yoon, M.-S. et al., 2011. Phosphatidic acid activates mammalian target of rapamycin complex 1 (mTORC1) kinase by displacing FK506 binding protein 38 (FKBP38) and exerting an allosteric effect. *The Journal of biological chemistry*, 286(34), pp.29568–74. Available at: http://www.pubmedcentral.nih.gov/articlerender.fcgi?artid=3190997&tool=pmcentrez&rendertype=abstract [Accessed March 4, 2015].

Yoshiyama, Y. et al., 2007. Synapse Loss and Microglial Activation Precede Tangles in a P301S Tauopathy Mouse Model. *Neuron*, 53(3), pp.337–351. Available at: http://www.cell.com/neuron/abstract/S0896-6273(07)00030-X?_returnURL=http%3A%2F%2Flinkinghub.elsevier.com%2Fretrieve%2Fpii%2FS089662730700030X%3Fshowall%3Dtrue.

Yu, H. & Larsen, P.L., 2001. DAF-16-dependent and independent expression targets of DAF-2 insulin receptor-like pathway in Caenorhabditis elegans include FKBPs. *Journal of molecular biology*, 314(5), pp.1017–28. Available at: http://www.ncbi.nlm.nih.gov/pubmed/11743719 [Accessed June 12, 2015].

Yu, S.J., Chang, Y.L. & Chen, Y.L., 2015. Calcineurin signaling: Lessons from Candida species. *FEMS Yeast Research*, 15(4), p.fov016. Available at: http://femsyr.oxfordjournals.org/content/15/4/fov016.long [Accessed October 1, 2016].

Yu, Y.-H. & Zhu, H., 2004. Chronological changes in metabolism and functions of cultured adipocytes: a hypothesis for cell aging in mature adipocytes. *American journal of physiology. Endocrinology and metabolism*, 286(3), pp.E402-10. Available at: http://ajpendo.physiology.org/content/286/3/E402 [Accessed October 16, 2013].

Zalk, R., Lehnart, S.E. & Marks, A.R., 2007. Modulation of the Ryanodine Receptor and Intracellular Calcium. *Annual review of biochemistry*, 76, pp.367–385. Available at: http://www.annualreviews.org/doi/full/10.1146/annurev.biochem.76.053105.094237 [Accessed September 23, 2015].

Zannas, A.S. et al., 2015. Gene-Stress-Epigenetic Regulation of FKBP5: Clinical and Translational Implications. *Neuropsychopharmacology : official publication of the American College of Neuropsychopharmacology*, 41(1), pp.261–74. Available at: http://www.ncbi.nlm.nih.gov/pubmed/26250598 [Accessed September 29, 2015].

Zannas, A.S. & Binder, E.B., 2013. Gene-environment interactions at the FKBP5 locus: sensitive periods, mechanisms and pleiotropism. *Genes, brain, and behavior*, 13(1), pp.25–37. Available at: http://www.ncbi.nlm.nih.gov/pubmed/24219237 [Accessed November 19, 2013].

Zheng, F. et al., 2015. Evaluation of WO2011045166A1 , Fkbp52 -- tau interaction as a novel therapeutical target for treating the neurological disorders involving tau dysfunction. *Expert Opin Ther Pat*, 25(7), pp.831–5. Available at: http://www.tandfonline.com/doi/abs/10.1517/13543776.2015.1042860?journalCode=ietp20.

Zhu, J.-H. et al., 2007. Regulation of autophagy by extracellular signal-regulated protein kinases during 1-methyl-4-phenylpyridinium-induced cell death. *The American journal of pathology*, 170(1), pp.75–86.

Available at: http://www.ncbi.nlm.nih.gov/pubmed/17200184 [Accessed October 4, 2016].

Zlotkowski, K. et al., 2013. Small-molecule mechanism of action studies in Caenorhabditis elegans. *Chembiochem : a European journal of chemical biology*, 14(17), pp.2338–44. Available at: http://www.ncbi.nlm.nih.gov/pubmed/24123757 [Accessed June 12, 2015].

Zoico, E. et al., 2010. In vitro aging of 3T3-L1 mouse adipocytes leads to altered metabolism and response to inflammation. *Biogerontology*, 11(1), pp.111–22. Available at: http://www.ncbi.nlm.nih.gov/pubmed/19526322 [Accessed October 8, 2013].